https://theses.gla.ac.uk/

Theses Digitisation:

https://www.gla.ac.uk/myglasgow/research/enlighten/theses/digitisation/

This is a digitised version of the original print thesis.

Copyright and moral rights for this work are retained by the author

A copy can be downloaded for personal non-commercial research or study, without prior permission or charge

This work cannot be reproduced or quoted extensively from without first obtaining permission in writing from the author

The content must not be changed in any way or sold commercially in any format or medium without the formal permission of the author

When referring to this work, full bibliographic details including the author, title, awarding institution and date of the thesis must be given

Enlighten: Theses
https://theses.gla.ac.uk/
research-enlighten@glasgow.ac.uk

Isotopic (^{13}C and ^{14}C) Tracers in Ecosystem Respiration

Susan Mary Lennox Fawley

Thesis submitted for the degree of

Doctor of Philosophy

UNIVERSITY
of
GLASGOW

"the Way, the Truth, the Life"

Scottish Universities Environmental Research Centre

May 2007

ProQuest Number: 10753931

All rights reserved

INFORMATION TO ALL USERS
The quality of this reproduction is dependent upon the quality of the copy submitted.

In the unlikely event that the author did not send a complete manuscript
and there are missing pages, these will be noted. Also, if material had to be removed,
a note will indicate the deletion.

ProQuest 10753931

Published by ProQuest LLC (2018). Copyright of the Dissertation is held by the Author.

All rights reserved.
This work is protected against unauthorized copying under Title 17, United States Code
Microform Edition © ProQuest LLC.

ProQuest LLC.
789 East Eisenhower Parkway
P.O. Box 1346
Ann Arbor, MI 48106 – 1346

GLASGOW
UNIVERSITY
LIBRARY:

Dedication

I dedicate this thesis to my dad, William Allan Fawley (1944-2007), this means nothing without you; and also to my gran, Mary Fraser Allan Fawley (1916-2004), she never lost faith.

'Avoid loud and aggressive persons,
they are vexatious to the spirit.
If you compare yourself with others,
you may become vain and bitter,
for always there will be greater and lesser persons than yourself...'

from '*Desiderata*' by Max Ehrmann

'The rose of all the world is not for me.
I want for my part
Only the little white rose of Scotland
That smells sharp and sweet - and breaks the heart.'

'The Little White Rose' by Hugh MacDiarmid

Abstract

Terrestrial ecosystems are expected to respond to global warming with the very real possibility that they may add to global atmospheric anthropogenic CO_2 emissions, thus exacerbating climate change. Isotopes of carbon in ecosystem respiration provide valuable information regarding the contribution of individual sources. A portable sampling system was developed (MS^3) incorporating zeolite molecular sieve, which can capture CO_2 for stable and radiocarbon analysis without contamination, fractionation or hysteresis. The sampling system and its application in studies of respiration and carbon cycling, both *in situ* and *ex situ*, has the potential to be applied in a wide range of ecosystems.

A field experiment was performed to assess the contribution of individual components of a peatland ecosystem (peatland soil and the three main plant functional groups it supported) to total peatland ecosystem respiration. Stable carbon ($\delta^{13}C$) analysis of respired CO_2 collected using Exetainers to partition respiration sources had limited use, mainly due to methodological difficulties. A laboratory peat core experiment studied the interactive effects of abiotic regulators: temperature, moisture and substrate quality. All parameters influenced soil carbon decomposition with temperature being the primary regulator of CO_2 fluxes. Interactive effects on decomposition rates were observed, with increased temperature, decreased moisture and reduced substrate quality affecting the largest Q_{10} values.

The radiocarbon signature of both ecosystem and soil respiration were successfully characterised in the field using MS^3. Modelling implied there to be a third source of respired CO_2 that contributed to total ecosystem respiration (in addition to plant and soil components). This is believed to be the first time that this third source, 'plant mediated catotelm CO_2', has been directly observed. It is estimated to contribute ~ 20 % of the total peatland ecosystem respiration flux.

Table of Contents

List of Figures

List of Tables

Acknowledgements

I thank Professor Tony Fallick for inspiring me to undertake a PhD in the first place, for his foresight in everything and for having a guiding hand throughout. I thank Dr. Mark Garnett, for without his help and encouragement from beginning to end, I would not be writing these words. I thank Dr. Nick Ostle for guidance and for always being there whenever I thought it seemed like a good idea to 'go native', as he put it (translation - give up and go back to Scotland!). I thank Phil Rowland for guidance and support in everything before and during my time at CEH Lancaster (including provision of useful wee items, such as a laptop; which was invaluable).

I would like to thank Dr. Charlotte Bryant, the academic and technical staff at the NERC Radiocarbon Laboratory, East Kilbride, for their assistance and instruction during the first year of my PhD spent there and on each return visit since. In particular I would like to thank Frank Elliott for instruction in the use of a vacuum rig and for keeping me entertained with his vast knowledge of *Lepidoptera* and their food plants during many a coffee break. A big thank you to Margaret Currie and Dr. Pauline Gulliver for their friendship and for keeping my spirits up on many an occasion when it all seemed a little too overwhelming. A big thanks also to Dr. Mike Billett, CEH Edinburgh for collaborative work carried out through the Radiocarbon Lab.

I would like to thank a number of friends and colleagues at CEH Lancaster: I thank all the girls in the admin department for ensuring that everything from orders to expenses and all else related were dealt with expediently (a special mention for Julie G, who made me feel so welcome at CEH before I had actually arrived there full time!). I would like to thank the boys in CCS for all things computer related including coming to the rescue during my many 'blonde moments'. A very special thank you to the librarians Jeanette Coward and Celia Cook who provided me with a large number of papers that the CEH collection did not hold, especially those ones that saved me a small fortune in photocopying!

For assistance with field and laboratory work I would like to say thank you to: Maria Briones, Kate Ludley, Simon Oakley, Jan Poskitt, Bruce Thomson, Angela Wakefield, Sue Ward and Simon Weldon: in particular to Jan Poskitt, Kate Ludley and Angela Wakefield who looked after incubation experiments during Christmas periods (saving me a 300 mile round trip in the process), to Sue Ward for allowing me to work alongside her in the field at Moor House NNR on her vegetation manipulation experiment, and to Bruce Thomson who collected 96 peat cores in the most awful weather conditions, when I myself was

unable to do so. Thank you also to both Dave Benham and Jack Kelly for assistance with field kit and space to work in at the SSU when required. Thanks to Ken Taylor for identification of vegetation collected at Moor House and to Tony Harrison for discussions on radiocarbon.

A number of analyses were carried out on my behalf, when either I could not be in two places at once or had not the technical knowledge to do so myself. For this I would like to thank: Helen Grant, Simon Oakley, Clive Woods, Darren Sleep and Dr. Andy Stott. In particular I would like to thank Helen Grant and Andy Stott, not only for assistance with analyses and discussions on isotope work but also for friendship extended (and in Helen's case, also a home and a cat). Special thanks also to Kate Ludley and Angela Wakefield for sharing the ups and downs of a PhD.

Thanks to a number of friends and colleagues within the Chemistry Department at the University of Glasgow: Dr. Ian Pulford and Dr. Harry Duncan, for organising a desk at which to write my thesis. Thank you to Dr. Justin Hargreaves, for information provided on zeolites. Many thanks go to all those in C5-12 (Annabelle, Basma, Christine, Clemens, Geraldine, Leena, Lidia, Margaret, Michael, Mohammed, Nicola, Paul, and Yinka) for helping to keep me sane whilst writing up!

I thank English Nature for access to Moor House National Nature Reserve. I thank NERC for funding of stable carbon isotope analyses. Finally I would like to thank: the staff at SUERC (special thanks to Margaret Kerr), the NERC Radiocarbon Lab Steering Committee for granting radiocarbon analyses that were central to my PhD, to the staff at the SUERC AMS facility, East Kilbride, for the analysis of those samples and last but not least to NERC for funding of a PhD studentship.

Author's Declaration

I declare that except where in the text reference is made to others, the presented work is that of the author. Furthermore, the work presented has not been submitted in whole or in part for any other degree. A number of results have been published elsewhere and copies can be found at the end of the thesis.

Susan M.L. Fawley

Definitions

A_0	equilibrium living activity
A_t	activity remaining after time t
Al	aluminium
ANOVA	analysis of variance
AMS	accelerator mass spectrometry
aq	aqueous
atm	atmosphere
α	kinetic fractionation factor
°C	degree Celsius
C	carbon
C_3	Calvin photosynthesis
C_4	Hatch-Slack photosynthesis
$CaCO_3$	calcium carbonate
$CaSO_4$	calcium sulphate
CAM	crassulacean acid metabolism
CCD	carbonate compensation depth
CEH	Centre for Ecology and Hydrology
CFC	chloroflurocarbon
CH_4	methane
CH_2O	carbohydrate
C_m	mass of carbon
CO	carbon monoxide
CO_2	carbon dioxide
CO_3^{2-}	carbonate
C_V	CO_2 flux
δ	relative isotope ratio
DIC	dissolved inorganic carbon
DOC	dissolved organic carbon
EA-IRMS	elemental analysis – isotope ratio mass spectrometry
E_B	binding energy
ECN	Environmental Change Network
Fe	iron
FID	flame ionisation detector
GC	gas chromatography
GPC	gas proportional counter
GPP	gross primary production
Gt	giga tonne
h	hour
H_2	hydrogen
H_2CO_3	carbonic acid
H_2O	water
HCO_3^-	bicarbonate
HNO_3	nitric acid
$h\nu$	light
IAEA	International Atomic Energy Agency
ID	inner diameter
IPCC	Intergovernmental Panel on Climate Change
IRGA	infrared gas analyser
IRMS	isotope ratio mass spectrometry
IUPAC	International Union of Pure and Applied Chemistry
k	Boltzmann constant

k	rate constant
K	degree Kelvin
keV	kilo electronvolt
KP	Keeling plot
λ	radioactive decay constant
Li	lithium
ln	natural logarithm
LHS	left hand side
LSC	liquid scintillation counter
LSD	least significant difference
m	mass
m	metre
m	molecular weight
mbar	millibar
mol	mole
MPa	mega Pascal
MS^3	molecular sieve sampling system
MSC	molecular sieve cartridge
MV	mega electronvolt
n	neutron
nm	nanometre (10^{-9} m)
N_2	nitrogen
N_2O	nitrous oxide
NaCl	sodium chloride
NaOH	sodium hydroxide
NEP	net ecosystem production
NERC	Natural Environment Research Council
NERC-RCL	Natural Environment Research Council Radiocarbon Laboratory
NNR	National Nature Reserve
NPP	net primary production
O_2	oxygen
O_3	ozone
OD	outer diameter
OH^-	hydroxyl radical
Ox	oxalic acid standard
ρ	partial pressure
p	proton
P	barometric pressure
P	probability
PAR	photosynthetically active radiation
PEP	phosphoenolpyruvate
pH	power of Hydrogen
ppb	parts per billion
ppm	parts per million
ppmv	parts per million by volume
PC	personal computer
PVC	polyvinylchloride
Q_{10}	the increase in respiration rate for every 10 °C rise in temperature
r	correlation coefficient
R	universal gas constant
RHS	right hand side
Rubisco	ribulose bisphophate carboxylase oxygenase
σ	kinetic diameter
σ	standard deviation

σ_e	standard error of the mean
SCPs	spheroidal carbonaceous particles
Si	silicon
SO_2	sulphur dioxide
SOM	soil organic matter
STP	standard temperature and pressure (273.15 K and 1 atmosphere)
SUERC	Scottish Universities Environmental Research Centre
t	time
$t_{1/2}$	half-life
T	absolute temperature (K)
TTP	two time point
TG-IRMS	trace gas – isotope ratio mass spectrometry
Tt	tera tonne
v	velocity
v	volume
VOCs	volatile organic carbons
VPDB	Vienna Pee Dee Belemnite
W m^{-2}	Watts per square metre
Zn	zinc

1 Introduction

1.1 Climate change and the greenhouse effect

1.1.1 The climate system

The climate system consists of five main components: the lithosphere, hydrosphere, biosphere, cryosphere (ice and snow) and the atmosphere. The atmosphere is where what we term as 'weather' takes place and is characterised by variations in precipitation, windiness, humidity, cloudiness and temperature.

Climate is a long-term view of the weather, and can be defined as the average (usually over 30 years) of the weather conditions. It varies from place to place depending on latitude, distance from the sea, presence or absence of mountains, vegetation and other geographical factors. Climate also varies temporally, from day to day, season-to-season (e.g. the Madden-Julian Oscillation in the tropics), year to year (e.g. the El Niño Southern Oscillation and the North Atlantic Oscillation), decade to decade (e.g. the Pacific Decadal Oscillation) and on much longer timescales such as ice ages. Statistically significant variations of the average state of the climate that persist for decades or longer are referred to as climate change.

Four and half billion years ago when the Earth was formed, the Sun was approximately 25 to 30 % less luminous than it is today. This should have meant that the Earth was encapsulated in ice and snow for in the region of 2 billion years (Sagan & Mullen, 1972), but instead, liquid water was present and the beginnings of life were apparent as much as 3.5 to possibly 4 billion years ago (Rind, 2002). This situation is what is referred to as the "faint Sun paradox", and is thought to have occurred due to high levels of greenhouse gases present in the Earth's atmosphere at that time.

1.1.2 The greenhouse effect

The greenhouse effect 'is the warming of the surface and lower atmosphere of a planet (as the Earth or Venus) that is caused by conversion of solar radiation into heat in a process involving selective transmission of short wave solar radiation by the atmosphere, its absorption by the planet's surface, and re-radiation as infrared which is absorbed and partly re-radiated back to the surface by atmospheric gases' (Merriam-Webster, 2003). In short,

the greenhouse effect refers to the presence of an atmosphere around a planet that causes a reduction in outgoing thermal radiation to space, thereby causing that planet to be warmer than it would otherwise be.

Incoming short wave radiation from the sun is absorbed by the Earth's surface and consequently raises the temperature of the surface and the air closest to it. However, not all of it is absorbed, a portion of the short wave radiation is returned back to space by reflective surfaces; land, water, ice and snow and this is known as the Earth's albedo effect. Clouds, air and atmospheric dust also reflect some of the short wave solar radiation before it reaches the Earth's surface. A portion of the short wave radiation that is absorbed by the Earth is re-emitted as long wave thermal radiation. It is this thermal radiation that is partially absorbed by greenhouse gases in the Earth's atmosphere that causes the Earth's surface and the adjacent lower atmosphere to heat up.

The Earth's atmosphere consists of clouds, aerosols, water vapour and gases. The bulk of the atmosphere is made up of nitrogen (78 % by volume) and oxygen (21 % by volume), neither of which absorb or emit thermal (long wave) radiation. What does absorb thermal radiation in the atmosphere are some of the minor trace gases that make up the remaining 1% of gases, clouds (liquid water), water vapour and some aerosols. Gases that absorb thermal radiation are referred to as 'greenhouse gases'. The change in the Earth's climate caused by a modification of the Earth's radiative balance by agents such as greenhouse gases, aerosols and clouds is referred to as radiative forcing and is measured in Watts per square metre ($W\ m^{-2}$).

1.1.3 Greenhouse gases

The main greenhouse gases concerned with radiative forcing are water vapour, carbon dioxide (CO_2), methane (CH_4), ozone (O_3) in the troposphere (not stratosphere), nitrous oxide (N_2O) and chlorofluorocarbons (CFC's). All of these gases (with the exception of CFC's) occur naturally in the atmosphere and so this phenomenon is known as the 'natural greenhouse effect'. As a direct result of the natural greenhouse effect the Earth's surface is approximately 32 °C warmer than it would otherwise be (Sarmiento & Bender, 1994). The 'enhanced greenhouse effect' is the direct anthropogenic contribution (supplied *via* burning of fossil fuels, cement production, deforestation and agricultural activities) of these gases to the Earth's atmosphere.

Water vapour is the most important greenhouse gas, largely due to its concentration rather than its heat trapping capability, and accounts for approximately 80 % of the natural greenhouse effect (Skinner & Porter, 2000), followed by the most important of the trace gases, carbon dioxide, methane, ozone and nitrous oxide respectively. Each greenhouse gas exists in varying concentrations in the Earth's atmosphere and has differing heat trapping abilities and atmospheric life spans. Although water vapour is the most important of these gases in terms of enhancing radiative forcing, it is not produced as a direct result of human activities (or at least very little relative to that transferred in the hydrological cycle). Greenhouse gases that are a direct result of anthropogenic activities include carbon dioxide, methane, nitrous oxide, ozone and chlorofluorocarbons.

Of these trace gases CO_2 is the most important and it is relative to this gas that the radiative forcing potentials of the other greenhouse gases are compared. Before the industrial revolution in the mid to late 18th century CO_2 had a concentration in the Earth's atmosphere of about 280 parts per million by volume (ppmv). Since then, CO_2 has been steadily increasing due mainly to the aforementioned anthropogenic activities. Levels of CO_2 in the atmosphere have been measured directly since 1958 (Keeling & Whorf, 2002) at Mauna Loa, Hawaii (Figure 1.1).

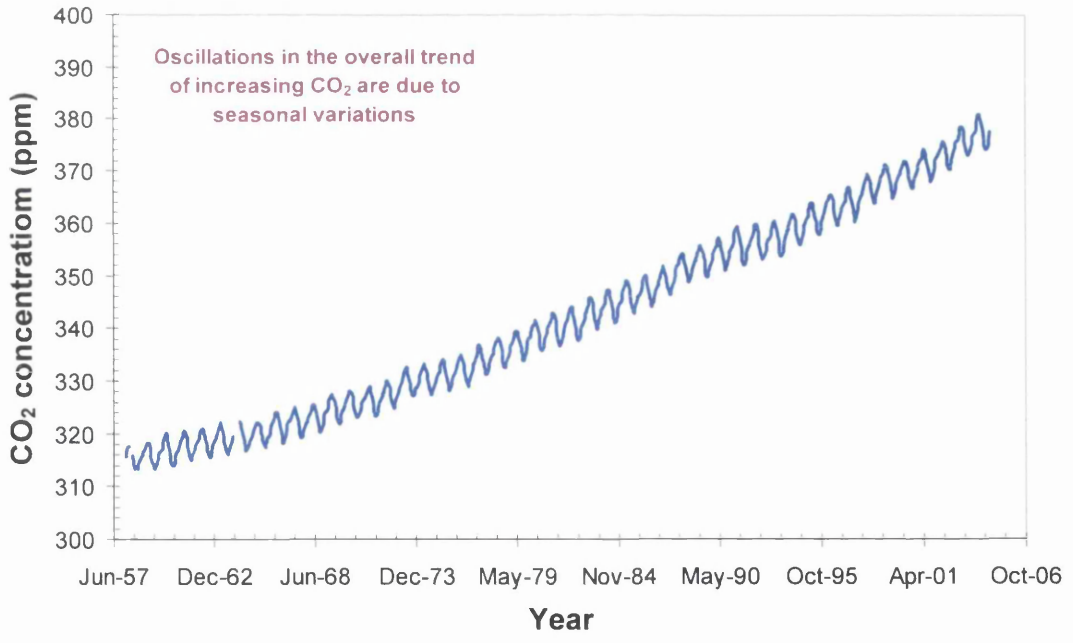

Figure 1.1 – Atmospheric CO_2 concentration measured on Mauna Loa, Hawaii since 1958. Source: C.D. Keeling and T.P. Whorf and the Carbon Dioxide Research Group, Scripps Institution of Oceanography (SIO), University of California, La Jolla, California, USA. http://cdiac.ornl.gov/ftp/trends/co2/maunaloa.co2.

It is reasonably easy to estimate the amount of fossil fuel that is burned globally as statistics on world energy consumption and production have been compiled since the early

1970's (Andres *et al.*, 2000), but less easy to quantify the effects on atmospheric CO_2 concentrations from the burning of forests and changing land use.

At present the atmospheric concentration of CO_2 is approximately 380 ppmv. As the northern hemisphere is responsible for approximately 95 % of fossil fuel burning it has a slightly higher level of CO_2 than the southern hemisphere by about 2 ppm. This small difference reflects the rapid mixing of CO_2 in the atmosphere between hemispheres. Over the years the increase in CO_2 concentration has grown in parallel with the increased consumption of fossil fuel, a fact that supports the argument that the increase in atmospheric levels of carbon dioxide is due to these emissions (Houghton, 1997).

Methane is present in the Earth's atmosphere at much lower levels in comparison to carbon dioxide. Its present concentration in the atmosphere is ~ 2 ppmv, which is, more than double its pre-industrial revolution value. The average lifespan of CH_4 in the atmosphere is 8 years. However, although it is present at much smaller levels than CO_2 it has a heat trapping ability 23 times (over a period of 100 years) that of CO_2 (IPCC, 2001) and therefore has a high radiative forcing potential. Wetlands are the main natural source of methane, due to the decomposition of organic matter under anaerobic conditions. Anthropogenic sources include the coal, gas and petroleum industries, enteric fermentation by ruminants, rice paddies, biomass burning and landfill sites.

Nitrous oxide, a minor greenhouse gas, has an atmospheric concentration of approximately 0.3 ppmv. Again, although this appears small relative to CO_2 levels, it has a much more efficient heat trapping ability at 296 times that of carbon dioxide (Harvey, 2000). The main source for nitrous oxide emission is nitrogenous fertilisers. Emissions are hard to quantify both spatially and temporally as soil water content and timing of fertiliser application have a large influence on losses. N_2O has one of the longest life spans of all the greenhouse gases at an average of 120 years.

NO_x gases (NO and NO_2) do not affect the radiative balance of the Earth directly but they are responsible for the catalysis of O_3 in the troposphere, where it is responsible for a positive radiative forcing. However, NO_x gases can also have a negative effect on the radiative balance of the Earth by reducing the lifetime of greenhouse gases such as CH_4 through increased production of the OH^- radical during NO_x breakdown (Fuglestvedt *et al.*, 1999). The lifespan of NO_x gases in the atmosphere varies from hours to days (Fuglestvedt *et al.*, 1999).

1.1.4 Clouds and aerosols: their effect on the Earth's radiation budget

Clouds are one of the most difficult greenhouse agents to quantify and they can both warm and cool the surface of the Earth. By reflecting radiation from the sun, clouds cool the Earth, but by absorbing thermal radiation from the surface and reemitting less (the tops of the clouds are cooler and hence emit less radiation) they warm the Earth's surface. Which of these two processes (warming and cooling) dominates depends on a number of parameters including: cloud droplet size, cloud height and cloud thickness.

Aerosols (small particles found in suspension in the atmosphere) are similar to greenhouse gases in that they can be produced naturally as well as anthropogenically (with the exception of CFC's). Natural sources include: sea salt, forest fires, mineral dust produced by wind erosion on arid land and aerosols produced during volcanic activity. Man-made aerosols are formed mainly from the burning of fossil fuel and biomass. Aerosols in the troposphere (lowest layer of the atmosphere) have a lifespan of only a few days, as they are very quickly washed out by rain. That said, like clouds, aerosols can both reflect and absorb solar and thermal radiation, thereby exerting a direct radiative forcing (Kaufman & Koren, 2006).

The absorption capacity of aerosols is a function of their chemical composition and the concentration of the absorbing component therein (Kaufman & Koren, 2006). The two main types of aerosols of interest are sulphate aerosols and carbonaceous aerosols. With the exception of soot (black carbon), carbonaceous and sulphate aerosols are responsible for a loss of sunlight (*via* scattering back into space) of 0.6 W m^{-2} (Haywood & Boucher, 2000) and hence have a cooling effect on the Earth (this process is now referred to as 'global dimming'). Conversely, particles of soot absorb solar radiation (especially when situated above cloud decks) and are responsible for warming the Earth's surface with a radiative forcing of 0.1 W m^{-2}.

Aerosols also have indirect effects on atmospheric radiative forcing *via* alteration of the optical properties and lifecycle of clouds (by becoming cloud condensation nuclei during the process of cloud formation). The first indirect aerosol effect occurs because aerosols allow the formation of clouds containing smaller and more numerous cloud droplets, thus making clouds brighter and hence more reflective. The formation of smaller droplets leads to the second indirect aerosol effect, reduced precipitation, thus prolonging the lifetime of clouds and causing an alteration in cloud cover (Breon, 2006).

Sulphate aerosols are produced by chemical action on sulphur dioxide (SO_2), a gas that is formed anthropogenically by burning of fossil fuels such as coal and oil and the smelting of certain metals; however, SO_2 is also formed naturally through volcanic activity and also *via* biogenic sources, in particular marine phytoplankton, emitting dimethyl sulphide. The main chemical pathways that convert SO_2 into sulphate aerosols are aqueous phase reactions with cloud droplets and gaseous phase reactions with the hydroxyl radical (OH^-). Due to the problems associated with SO_2 and acid rain, countries of the developed world have placed restrictions on its emission and so it is likely that the radiative forcing by sulphate aerosols will be much less than that associated with greenhouse gases and carbonaceous aerosols in the future (IPCC, 2001).

Carbonaceous aerosols, originating mainly from the incomplete combustion of fossil fuels and biomass (anthropogenic soot) and organic carbon aerosols produced by vegetation (natural) are much less well defined than sulphate aerosols in terms of their effect in aiding radiative forcing. Models for sulphate aerosols are very common but models for both organic and black carbon aerosols are in the early stages of development due to a lack of reliable measurements (IPCC, 2001). However, overall aerosols have a cooling effect on the Earth's surface temperature.

According to the Intergovernmental Panel on Climate Change the evidence for climate change is unequivocal (IPCC, 2001). Instrumental records began in about the mid-19th century (1861) and it is very likely that the 1990's were the warmest decade since then and 1998 the warmest year. However, it should be noted that since the publication of the last IPCC assessment report even warmer years have occurred. The global average surface temperature has increased by 0.6 ± 0.2 °C over the period of the 20th century (IPCC, 2001). Prior to the mid-19th century we have to rely on what are termed 'proxy' indicators to ascertain variations in climate.

Proxy measurements of past climate include; annual layers from laminated (varved) sediment cores, ice core paleoclimatology, geothermal information from boreholes, measurements of density and width from tree-rings (dendroclimatology) and isotopes from corals. Data from the proxy record indicates that the largest increase in temperature that has occurred in any century in the last 1000 years was in the 20th century. In addition to the proxy record, satellite data have shown that since the 1960's snow and ice cover has reduced globally by 10 % (IPCC, 2001).

Analysis of data from ice cores that extends as far back as 420,000 years suggests that the Earth's climate was characterised by glacial-interglacial cycles that lasted ~100,000 years. During these glacial-interglacial cycles atmospheric CO_2 alternated between approximately 180 and 280 ppmv, up until the time of the industrial revolution (Falkowski *et al.*, 2000). CO_2 levels are now almost 100 ppmv higher than the interglacial-maximum and rising. This rapid increase in levels of global atmospheric CO_2 since the 1850's has led to an intense scrutiny of the carbon cycle in a bid to better understand and quantify the flow of carbon to and from each of the major reservoirs within it. A more accurate understanding of the carbon cycle will help us predict how it may behave in the future.

1.2 The Global Carbon Cycle

In 1896, the Swedish chemist Arrhenius noticed the potential effects of anthropogenic activities on the carbon cycle and the subsequent impact on climate (Arrhenius, 1896). The carbon cycle (Figure 1.2) involves the flux of carbon to and from each of its four main

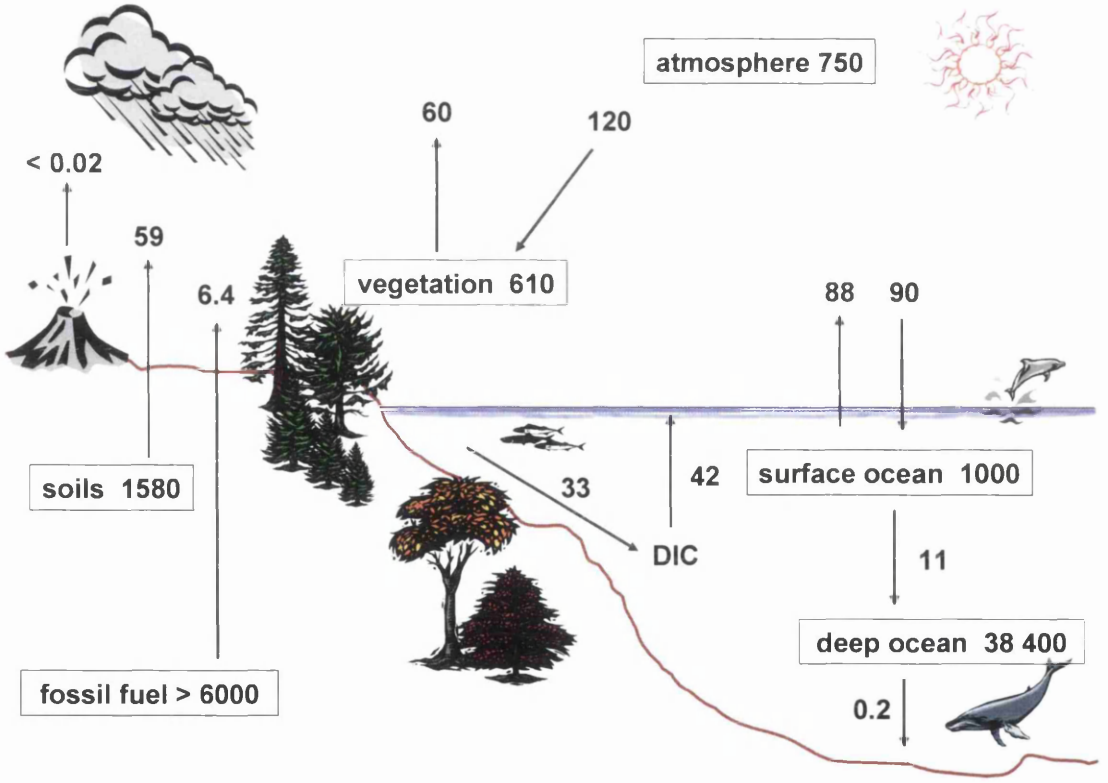

Figure 1.2 – Schematic diagram of the global carbon cycle. Estimates of carbon contained in reservoirs, pools and fluxes are given in Gt (figures are approximate as considerable variation exists in the literature as to the size of carbon pools and fluxes).

reservoirs: the atmosphere, terrestrial biosphere, lithosphere and the hydrosphere. Carbon is exchanged from one reservoir to another primarily in the form of CO_2. The lithosphere is by far the largest reservoir with greater than 75 million Gt of carbon stored, followed by

the deep oceans with nearly 40,000 Gt of carbon (Falkowski *et al.*, 2000). By comparison the terrestrial stores are quite small, with soil storing ~ 1580 Gt of carbon and land biota ~ 610 Gt of carbon (Schimel, 1995a). However the terrestrial carbon stock is approximately 3 times that of the atmosphere and any increase in carbon flux will exacerbate the loading of CO_2 in the atmosphere, thus providing a positive feedback to global warming (Jenkinson *et al.*, 1991; Raich & Schlesinger, 1992).

Of all the anthropogenic CO_2 that is released into the atmosphere only about half remains and accumulates there, the other half is taken up by the oceans and the terrestrial biosphere. For the years 1990 to 1999 the net flux of carbon from the atmosphere to the land biosphere was 1.4 Gt per year and from the atmosphere to the ocean, 1.7 Gt per year (IPCC, 2001). Volcanic CO_2 contributes only 0.22 % of anthropogenic emissions to the atmosphere on an annual basis (Williams *et al.*, 1992).

1.2.1 Ocean-atmosphere carbon flux

Atmospheric CO_2 exchanges rapidly with the Earth's terrestrial ecosystems and the oceans (Kasting *et al.*, 1988). Ninety-eight percent of the combined ocean and atmospheric inventory of carbon resides in the oceans, with an exchange rate in each direction of about 90 Gt of carbon per year (Siegenthaler & Sarmiento, 1993). On dissolution in water at the air-sea interface, CO_2 forms a weakly dissociated acid, carbonic acid (H_2CO_3), which then reacts with carbonate ions (CO_3^{2-}) to form bicarbonate (HCO_3^-).

$$\mathbf{CO_2 + H_2O \Leftrightarrow H_2CO_3} \qquad \mathbf{(1)}$$

$$\mathbf{H_2CO_3 + CO_3^{2-} \Leftrightarrow 2HCO_3^-} \qquad \mathbf{(2)}$$

CO_2 accounts for a mere 0.5 % of carbon in global mean surface water, whilst the carbonate and bicarbonate ions account for 10.7 % and 88.8 % respectively (Sarmiento & Bender, 1994). The three forms of carbon together make up the total dissolved inorganic carbon (DIC) in the oceans and amounts to 50 times that resident in the atmosphere.

Uptake of CO_2 in the oceans is relatively well understood but their capacity for uptake is not limitless. The ocean's carbonate system buffers changes in CO_2 concentration but its capacity to resist change depends on the rate of weathering of rocks and the subsequent addition of cations associated with these rocks (Falkowski *et al.*, 2000). At approximately 1 km depth, the concentration of total DIC is 12 % greater than that of the ocean surface

waters (Sarmiento & Bender, 1994) and is a result, mainly, of two independent processes, the 'biological pump' and the 'solubility pump.'

1.2.1.1 The solubility pump

Carbon dioxide, like oxygen, is more soluble in colder high latitude waters than in warmer mid latitude surface waters. Warm surface waters move towards the polar regions, where they become colder, more saline (due to the formation of sea ice in polar waters) and therefore denser. The denser water begins to sink (downwelling), taking with it the increased concentration of CO_2 dissolved in it, and sinks beneath the oceans permanent thermocline (Pulford & Flowers, 2006). These waters are then transported laterally throughout the abyssal ocean thus preventing re-equilibration with the atmosphere until eventually they re-emerge at the ocean surface again (upwelling).

This process is known as the solubility pump and acts to move large quantities of carbon from the surface to deep waters. It can take anywhere from decades to hundreds of years for these waters to re-emerge at the ocean surface in the tropics where they will once again re-equilibrate with the atmosphere. This upwelling releases large quantities of CO_2 to the atmosphere in the Equatorial regions (Sarmiento & Bender, 1994). Thermohaline circulation, and latitudinal and seasonal changes determine the efficiency of the solubility pump (Schmittner & Stocker, 1999).

1.2.1.2 The biological pump

The oceans, *via* biological processes absorb atmospheric CO_2. Phytoplankton (small microscopic plants) serve as the basis of the ocean food chain. They photosynthesise in the euphotic zone (upper 100 m of the ocean) thus removing CO_2 dissolved in seawater by converting it into organic matter. This reduces the partial pressure of carbon dioxide (ρCO_2) at the air-sea interface and consequently promotes absorption of CO_2 from the atmosphere. Similarly planktonic organisms also remove carbon from the ocean surface waters. They do so by removing carbonate ions and turning them into shells or tests of calcium carbonate ($CaCO_3$).

When these organisms die they decompose and in doing so return carbon to the ocean in the form of DIC. However, not all of the carbon is returned to the ocean. Of all the carbon fixed in the upper ocean, approximately 25 % sinks down into the deep ocean (Falkowski *et al.*, 1998) some of which is sequestered in the ocean sediments. This means that there is

a net transfer of carbon from the ocean surface to depth. This mechanism is known as the 'biological pump' and is the other process that causes the total DIC of the deep oceans to be greater than that of shallow surface waters.

As the tests sink they reach a level in the oceans where the water is undersaturated with respect to $CaCO_3$, at which point the tests begin to dissolve (due to the change in solubility). This level in the oceans is called the lysocline. At even greater ocean depths (~ 4 km in the Atlantic), lies a level of water, which contains no free $CaCO_3$. This is called the carbonate compensation depth (CCD), below which there is no accumulation of carbonate. In addition, this process causes a decrease in the partial pressure of CO_2 in the ocean and a concomitant decrease in the concentration of CO_2 in the atmosphere (Ridgwell & Zeebe, 2005). This sequence of events is driven by the fact that $CaCO_3$ possesses inverse solubility, i.e. it becomes less soluble at warmer temperatures.

If current understanding of the ocean carbon cycle is proved to be correct it is possible that in the future, the sink strength of the oceans will weaken, thus laying the burden of absorption of increased levels of atmospheric CO_2 produced by human activities on terrestrial ecosystems (Falkowski *et al.*, 2000).

1.2.2 Carbon flux between the atmosphere and the terrestrial biosphere

Unlike ocean-atmosphere carbon exchange, the land-atmosphere flow of carbon is much less well defined (due to the complex nature of terrestrial processes). The main processes by which carbon is transferred between the atmosphere and the terrestrial biosphere are photosynthesis, plant respiration (autotrophic) and soil respiration (heterotrophic). The total amount of carbon that is stored in soils and the terrestrial biosphere (2190 Gt) is approximately three times that stored in the atmosphere (750 Gt) and approximately half of the carbon cycled between the atmosphere and the Earth is done so *via* photosynthesis by land plants (Schimel, 1995a).

Some of the carbon that is fixed by photosynthesis is then lost from the vegetation pool, either through litterfall, or when a plant dies. Subsequently, this carbon is either released back to the atmosphere or sequestered (stabilised) in the soil by way of a number of mechanisms: either through various humification processes within the soil or *via* physicochemical protection. Aggregate formation in soils provides physical protection for carbon held within organic matter from decomposition in two main ways. Firstly, by

restricting both oxygen and microbe (with their accompanying enzymes) penetration into the aggregate and secondly by reducing the passage of water soluble enzymes if the aggregate has low water solubility (Davidson & Janssens, 2006). Chemical protection from decomposition comes *via* adsorption processes (both chemisorption and physisorption).

Formation of humus (humification) takes place by 2 main processes. The material that is more easily decomposed is broken down and releases compounds such as amino acids and phenolics, which have low molecular weight. These compounds then react and join together (polymerise) to form humic material (Pulford & Flowers, 2006). Low molecular weight materials in the soil can also react with more resistant organic material such as partially degraded lignin, resulting once again in humus production (Pulford & Flowers, 2006). Other mechanisms/routes for carbon loss from soil include: biogenic production of CH_4 and volatile organic carbons (VOCs) and production of dissolved organic carbon (DOC).

Plants also release carbon back to the atmosphere during respiration. About 60 Gt of carbon per year (Gt C y^{-1}) is utilised by terrestrial plants during photosynthesis and a similar amount of carbon is released *via* plant and soil respiration. In this way carbon is either sequestered or released back to the atmosphere in the form of CO_2 through soil and plant respiration processes. Recent global warming models have predicted that by the year 2050 the terrestrial biosphere will turn from sink to source (Cox *et al.*, 2000), and so the need for a better understanding of processes in the terrestrial biosphere that control carbon fluxes is of the utmost importance.

1.2.2.1 Photosynthesis and cycling of CO_2

Plants take up CO_2 from the atmosphere through pores in their leaves called stomata. The CO_2 is then directed to the photosynthetic sites in the chloroplasts of plant cells. Here, the CO_2 in the presence of light and water is converted to starch (a carbohydrate) that is used by the plant for growth of roots, leaves and wood and in the process oxygen (O_2) is released as in equation 3:

$$\mathbf{CO_2 + H_2O + energy \xrightarrow{h\nu} CH_2O + O_2} \qquad \mathbf{(3)}$$

The amount of CO_2 that is fixed from the atmosphere by plants during photosynthesis is known as gross primary production (GPP). Based on $\delta^{18}O$ measurements of CO_2 in the

atmosphere GPP has been estimated at 120 Gt C y^{-1} (Ciais *et al.*, 1997) and is stored primarily in woody material e.g. forests and savannahs.

Photosynthesis is controlled by a number of factors including nutrient availability, water availability and concentration of atmospheric CO_2. Whilst photosynthesising, plants keep their stomata open as wide as possible in order to absorb as much CO_2 as they can. However, if plants become water-stressed they will reduce their stomatal apertures in order to prevent further water loss through the evaporation of leaf water, with a subsequent reduction in photosynthesis due to less CO_2 entering the stomates. Conversely, plants will increase their rate of photosynthesis in response to a greater level of CO_2 in the surrounding air (due to a reduction in stomatal conductance) and will therefore use water much more efficiently. This process is known as CO_2 fertilisation and studies have shown an increase of between 20 and 40 % in the rate of photosynthesis by plants in response to doubled levels of CO_2 (Coleman *et al.*, 1993; Idso & Kimball, 1993).

Annual plant growth is referred to as net primary production (NPP) and is the difference between photosynthesis and autotrophic respiration and is estimated at approximately 60 Gt C y^{-1} (Ciais *et al.*, 1997). Net ecosystem production (NEP) is defined as the difference between NPP and soil respiration and represents a carbon flux to ecosystems from the atmosphere. Present atmospheric concentrations of CO_2 have not yet saturated NPP (Cao & Woodward, 1998), which means that terrestrial plants are a potential sink for increased levels of carbon added to the atmosphere. The difference between uptake and release by the terrestrial biosphere is in the order of 2 Gt C y^{-1} (Rayner *et al.*, 1999).

1.2.2.2 Respiration and cycling of CO_2

As mentioned previously, respiration is one of the mechanisms by which the flux of carbon between the terrestrial biosphere and the atmosphere is controlled, and it is essentially the reverse reaction of photosynthesis. Respiration can be subdivided into that which is autotrophic and carried out by plants and that which is heterotrophic and carried out by organisms (e.g. arthropods, bacteria, fungi, macrofauna and algae) in the soil. About half of the respiratory flux is carried out by plants themselves, whilst the other half is carried out by micro-organisms in the soil that decompose the organic material produced by plants (Grace & Rayment, 2000).

The ratio of plant respiration to plant photosynthesis is in the order of 1:2 and this is not surprising because if both mechanisms were equal there would be no net plant growth.

Whilst plant respiration is relatively well understood as regards the part it plays in the cycling of carbon, soil respiration is less so. One of the most challenging phases of the terrestrial carbon cycle scientifically, is that which is carried out below ground and soil respiration is the second largest flux of carbon (globally, 60 Gt C y^{-1}) after photosynthesis in most terrestrial ecosystems (Davidson *et al.*, 2002).

1.3 Soil respiration

A key question in climate change research is whether or not there will be a shift in the balance of carbon fluxes between reservoirs due to anthropogenic warming of the planet. Some of the earliest measurements of soil respiration (the sum of root and heterotrophic respiration) were made nearly 90 years ago (Gainey, 1919). It is now recognised that the total emission of CO_2 from soils globally, is one of the largest fluxes within the global carbon cycle. This means that small changes in fluxes of carbon from soil could exact a large influence on atmospheric concentrations of CO_2.

Total carbon within soils of the world is estimated at ~1600 Gt (Schimel, 1995a), which is twice the amount of that estimated to reside in the atmosphere (750 Gt) and more than twice that of the terrestrial biosphere (610 Gt). If current predictions are correct and there is an increase in temperature of 0.3 °C per decade for the next 60 years with an additional doubling of CO_2 concentration in the atmosphere, soils would release in the region of about 1 Gt C y^{-1} (IPCC, 2001). This substantial flux (equivalent to C release from current global deforestation) highlights the need to better understand and quantify how physical, chemical and biological processes within soil contribute to the mineralisation of soil organic carbon (which occurs mainly *via* respiration) and how the rate of carbon mineralisation is affected by changing climatic conditions.

Soil respiration is made up largely of two main components: the mineralisation of organic matter by soil micro-organisms (microbial decomposition) and root respiration (which includes respiration of microbiota in the rhizosphere). The rate at which these two components respire is dependent on a number of factors including: soil carbon substrates (plant litter inputs and root exudates), root distribution and activity, actual soil organism populations, soil temperature, soil moisture content, nutrient availability and chemical and physical properties of soil, all of which vary temporally and spatially. Chemical oxidation of carbon compounds in the soil also releases CO_2 but to a much lesser extent than the aforementioned processes. Of all these factors, it is temperature followed by hydrology that

are widely regarded as being the most critical parameters affecting the emanation of CO_2 from soil (Bowden *et al.*, 1998) and so an understanding of how these factors control soil respiration is therefore extremely important.

1.3.1 Regulation of soil respiration by temperature

The effect of temperature on NPP is relatively well known; however, when it comes to respiratory processes this is not the case, with particular regard to soil respiration. It is generally agreed that an increase in global temperature will accelerate rates of soil respiration and hence levels of atmospheric CO_2, causing enhancement of the greenhouse effect, thus leading to a positive feedback mechanism. A number of studies have demonstrated that soil respiration is influenced strongly by temperature (Fang & Moncrieff, 2001; Katterer *et al.*, 1998; Lloyd & Taylor, 1994; Sanderman *et al.*, 2003; Trumbore *et al.*, 1996), but, it is not clear exactly by how much decomposition rates will be affected and how soil biological systems may respond or adjust to such temperature increases.

The temperature dependence of soil on rates of respiration is often described by Arrhenius kinetics or by the Q_{10} value (Lloyd & Taylor, 1994). Raich and Potter (1995) demonstrated that when predicting global fluxes of CO_2 from soil, the dependence of soil biological activity to temperature, when compared to linear, quadratic or Arrhenius functions, was best described by the Q_{10} relationship. The Q_{10} value is the coefficient that describes the exponential relationship between temperature and soil organic matter decomposition and represents the increase in respiration for every 10 °C rise in temperature and it is commonly used to predict soil respiration rates. Q_{10} values for soil (mineral) range from 1.3 to 3.3 (Raich & Schlesinger, 1992) with much of the variation in values being accounted for by the inaccuracy inherent in the exponential form (Lloyd & Taylor, 1994). Through analysis of residuals, the remainder of the variation in Q_{10} values is accounted for by the systematic overestimation of respiration rates at high temperatures and underestimation of rates at low temperatures.

In addition, some researchers (1994) have found that found that for soils at low temperatures the relative sensitivity to temperature change is much greater than for warmer soils. Lloyd and Taylor (1994) found that, when moisture limitations were not an issue, a 22 % increase in respiration was produced when the temperature was increased from 0 °C to 1 °C. However, a 1-degree increase in temperature from 25 °C to 26 °C only resulted in a 5 % increase in respiration. This means that ecosystems that are associated with low

temperatures, like tundra, boreal forest, peatlands and boreal wetlands, will have the greatest respiration rate sensitivity to a rise in global temperatures. Further studies since Lloyd & Taylor (1994) have shown this to be the case. For example, in a field study of two peatland ecosystems, Chapman and Thurlow (1996) derived Q_{10} values of between 3.3 and 6.1 (soil temperatures ranged from 1 to 13 °C). Furthermore, studies of the temperature dependence of soil respiration rates at 0 °C, have obtained Q_{10} values as high as 8.0 (Kirschbaum, 1995).

However, whilst temperature may effect a strong influence on soil respiration rates, it is not the sole controlling parameter and in fact some studies have shown that there is a weak relationship between the flux of CO_2 from soil and soil temperature (Craine *et al.*, 1998; Fitter *et al.*, 1999). In addition, other research has shown that factors such as rates of C inputs to soils, diffusivity and soil water content can affect the efflux of CO_2 from soils. Furthermore, Raich & Tufekcioglu (Raich & Tufekcioglu, 2000) have stated that the rate of CO_2 efflux from soil is controlled by a number of parameters such as CO_2 production within the soil ('the true soil respiration rate'), as well as properties such as wind speed, soil pore size, air temperature and the size of the difference between the CO_2 content of the soil and the CO_2 content of the atmosphere (CO_2 concentration gradient).

In another study Liski *et al.* (2000), suggested that only the labile fraction of soil organic matter (SOM) was sensitive to temperature and that the somewhat larger stocks of older, more recalcitrant carbon were unaffected by temperature regimes. Giardana and Ryan (2000), on the other hand, suggested that temperature was not the key to SOM mineralisation rates, that carbon pool turnover times were insensitive to temperature and that in fact, it was substrate quality (see section 1.3.3) that was the key parameter that controlled soil carbon mineralisation rates. As rates of biological and chemical processes are for the most part increased as temperature rises this was greeted almost incredulously by the scientific community.

However, using the same data sets but a more sophisticated model, Knorr *et al.* (2005) discredited Giardina and Ryan's theory. Knorr *et al.* (2005) demonstrated that non-labile soil organic carbon (carbon that is resistant to oxidation) was in fact more sensitive to temperature than labile organic carbon, indicating that there may be an even stronger feedback mechanism to the atmosphere over time than currently predicted.

In addition, it should be borne in mind that some soil warming studies have indicated that increases in CO_2 efflux from soils due to temperature are only transitory (Luo *et al.*, 2001;

Melillo *et al.*, 2002). These studies demonstrated that increased soil CO_2 efflux from soils was only temporary and that after a period of time, soil respiration rates begin to fall back to rates found prior to warming. This process of change in soil respiration rates has been referred to as acclimatisation and has been found to be greater at higher temperatures (Luo *et al.*, 2001). The operation of this process could mean that the positive feedback of the terrestrial carbon cycle on the climate system would ultimately weaken.

1.3.2 Effects of soil moisture and hydrology on soil respiration

Soil water content is generally considered to be the second most important parameter (under normal soil moisture conditions), after temperature (Bowden *et al.*, 1998; Illeris *et al.*, 2004), to have an effect on soil microbes and soil respiration and its influence is relatively straightforward to understand. Effects of moisture on soil biota can generally be split into three phases (Skopp *et al.*, 1990). Firstly, where metabolic activity of soil biota increases as moisture content of a dry soil increases, followed by a phase where soils are at field capacity (the maximum amount of water a soil can hold by capillary action) and microbial activity is at its maximum or close to its maximum, and, finally where a soil is deficient in oxygen due to saturation, thus inhibiting aerobic respiration (Raich & Potter, 1995).

Orchard and Cook (1983) found an exponential relationship between soil water potential and microbial activity. They found that when the matric potential (the pressure plants need to exert in order to extract water from the soil) fell below –0.01 MPa there was a decrease in microbial respiration and attributed it to a decline in bacterial activity. On the whole, whether changing hydrology increases or decreases soil respiration depends on the hydrological status of a given soil. For example, peatland soils such as fens and bogs have been shown to respond differently to changes in water table levels with below-ground carbon flux responding in different directions (Weltzin *et al.*, 2000).

However, it should be noted that changes in hydrological status often co-vary with temperature and it is often difficult to separate confounding effects such as temperature and substrate quality, particularly under uncontrolled conditions in the field (Reichstein *et al.*, 2005). According to Raich and Potter (1995), after temperature and moisture, substrate quality and quantity are frequently considered to be the most important variables to exert control over microbial activity, and hence on soil respiration rates.

1.3.3 Carbon substrate quality, the priming effect and nutrient mineralisation

Micro-organisms in the soil play a key role in the decomposition of litter and therefore also in the cycling of nutrients within ecosystems. In a nutrient-limited environment this can mean that rates of decomposition will limit NPP. Also, a considerable component of the soil labile carbon, phosphorus and nitrogen is made up from the microbial biomass. The diversity and biomass of the microbial community in the soil is determined largely by the species and activity of the plant community, as it is the autotrophs that the microbes are dependent on for their supply of carbon (Johnson *et al.*, 2003).

Carbon is supplied to micro-organisms *via* the plant community both directly and indirectly. Indirect supply comes from root exudation, sloughing of root cells, exudation and death of mycorrhizal mycelia and *via* the death of roots and shoots. Mycorrhizal fungi supply carbon to the microbial community directly. The fact that the carbon available to micro-organisms in soil is plant-derived means that plants are one of the main controls over the carbon that the microbiota are able to release back from the soil to the atmosphere in the form of CO_2.

Löhnis (1926) discovered during the study of decomposition of green manure in legume planted soil that the addition of fresh organic residues to the soil increased mineralisation of humus nitrogen. This is thought to be as a result of increased microbial activity that responds to the readily available supply of nutrients and energy delivered by easily decomposable fresh organic matter. This process is commonly known as the 'priming effect' (Bingeman *et al.*, 1953). Evidence for this was found by Zak *et al.* (1994), who demonstrated that there is a positive linear relationship between aboveground NPP and the microbial biomass at the ecosystem level.

However, further studies have shown that addition of fresh organic residues does not always increase mineralisation, in particular when compared to additions of less easily accessible carbon e.g. cellulose, ryegrass and wheatstraw. Ryegrass, cellulose and straw are less easily decomposed due to their polymerised structure so weaker priming effects might be expected (Fontaine *et al.*, 2003). Experiments have shown that when the addition of these less easily decomposable substrates have been compared to more easily accessible carbon (e.g. glucose or fructose), little or no effect was induced on mineralisation rates (Shen & Bartha, 1997; Wu *et al.*, 1993). Furthermore, as a result of this, Fontaine *et al.* (2003) suggested that the priming effect may actually depend on soil microbial population

dynamics, as SOM mineralisation did not seem to be influenced by a change in the amount of available energy. In other words, increased soil populations were the stimulus for increased SOM mineralisation and not increased activity by a particular population.

In a 20 year study of an acidic tundra ecosystem, increased microbial activity was one mechanism postulated by Mack *et al.* (2004), to have increased mineralisation in plots that were fertilised with additions of N and P, relative to unfertilised plots. Mack *et al.* (2004) discovered that although fertilisation increased C storage in above ground woody shrub material and in standing litter, there was a net loss from the soil of 2 kg m^{-2}. Interestingly, it had been thought that micro-organisms generally only became limited by carbon availability. This finding challenged that school of thought and implied that micro-organisms were in fact limited by nutrient availability rather than carbon as suggested in other studies (Fierer *et al.*, 2003). However, although both plants and micro-organisms regulate the flow of nitrogen and carbon in terrestrial ecosystems, this relationship could well be altered by rising concentrations of CO_2 in the atmosphere.

1.3.4 Soil and microbial respiration under elevated CO_2 conditions

The response of plants and soil micro-organisms to CO_2 increases in the atmosphere is represented by the efflux of CO_2 from the soil. Most studies (of grassland, herbaceous and woody plants) have reported that under conditions of elevated CO_2, respiration rates become more rapid (Zak *et al.*, 2000) and therefore indicate a greater sequestration of carbon below ground by plants. This in turn means that there is the possibility of an alteration in the availability of plant-delivered substrate to the soil for metabolism by micro-organisms. Inferring what effect this will have on soil respiration rates is difficult due to limited understanding and the complex nature of the relationship that increased CO_2 will have on vegetation (e.g. an alteration in litter quality) and the concomitant effects on available nitrogen (by changing microbial demand) (Zak *et al.*, 2000).

In addition, increases in atmospheric CO_2 conditions often lead to an enhancement in plant growth (Morgan *et al.*, 2001; Owensby *et al.*, 1999). Biological adaptation can then occur through changes in the chemistry of plant tissue and addition of organic carbon to soils (*via* plant roots). These adaptations in conjunction with other changes e.g. feedbacks controlled by microbial processes, can have an affect on the mineralisation of organic matter (or carbon sequestration) through alteration of nutrient availability. If carbon sequestration is to take place then it is of critical importance that plant production is not hindered by

nutrient availability and also that stabilisation of new soil organic carbon into pools with relatively long turnover times must take place (Gill *et al.*, 2002).

However, in a review paper, Zak *et al.* (2000) reported that the variability found in soil respiration in response to elevated levels of CO_2 was similar to the variability found in microbial respiration. They concluded that as microbial metabolism in soil is driven by substrate availability, the variation in microbial respiration was likely due to differences in plant growth response to elevated CO_2 levels. From this they postulated that increased levels of CO_2 in the atmosphere can be mitigated to a certain extent *via* land use manipulation.

1.3.5 Soil respiration and effects of land use and vegetation type

Different land use operations have exhibited differences in CO_2 emissions from soils and between 10 and 30 % of current anthropogenic emissions have been attributed to a change from one land use type to another (IPCC, 2001). Studies have shown for example, (Lindroth *et al.*, 1998; Malhi *et al.*, 1998) that old and middle-aged forests are absorbers of CO_2 and act as a sink for increased levels of CO_2 in the atmosphere. Thus, land use has implications for carbon storage and land use strategies could have the potential to mitigate some of the negative impacts of climate change (Dale, 1997).

Mechanisms for increased storage or release of carbon are not clear, but possibilities for variations between different land use sites include: the way in which carbon is allocated (grasslands do not allocate carbon to tree rings), differences in litter production rates, root respiration and litter quality. Increased absorption could also be due to greater levels of nitrogen deposition from anthropogenic activities and CO_2 fertilisation, both of which increase photosynthesis. As photosynthesis responds positively to raised atmospheric CO_2 levels, so too will respiration rates (exponentially), both autotrophic and heterotrophic. This has led to the commonly held view that forest capacity as a sink will weaken and ultimately that they will become a source of CO_2 emissions to the atmosphere.

However, in a review paper, Raich and Tufekcioglu (2000), carried out a comparison of published studies on soil respiration rates under differing vegetation types (but in similar topographic locations and on the same soil-forming parent material) and found that vegetation type does not always have a significant effect on soil respiration rates. Sites they compared were: coniferous and broad-leaved forests, grasslands and forests, grasslands and croplands, forests and croplands and cropped and fallowed field sites. They

found that although cropped sites on average had ~ 20 % higher respiration rates than fallowed ones, there was no actual significant difference between the two (some fallowed sites were found to have greater respiration than neighbouring vegetated sites, due to higher soil temperatures).

Furthermore, no significant differences were found in respiration rates between croplands and forests or between croplands and grasslands either. However, respiration rates in grasslands were consistently found to be greater than those in forests suggesting that forests are indeed a sink for carbon and that conversion to grassland would increase levels of CO_2 efflux to the atmosphere. In addition, broad-leaved forests were found to have significantly higher respiration rates (on average 10 %) than coniferous forests.

Raich and Tufekcioglu (2000) also reported that the contribution from roots to total soil respiration can be relatively high within low temperature ecosystems such as boreal forests (between 62 and 89 %) and Arctic tundra (between 50 and 93 %). Root contribution to soil respiration in lower latitude ecosystems such as temperate forests was found to be lower, with roots within broad-leaved forests contributing between 33 and 50 % to total soil respiration, and in pine forests contributing between 35 and 62 %. The smallest contribution to soil respiration from roots was found to occur in grasslands and croplands at between 12 and 40 %. However, despite the fact that on an annual basis ~ 10 % of atmospheric carbon passes through soil on an annual basis, Raich and Tufekcioglu (2000) concluded that vegetation type actually has minimal influence on soil respiration rates and that in fact substrate quality, moisture, and temperature were more important in this regard.

According to Boone *et al.* (1998) the effects of a warmer planet on the flux of carbon from soils to the atmosphere will be determined mostly by the sensitivity of soil respiration to temperature. Relatively small changes in soil respiration induced by changes in climate could contribute a CO_2 loading to the atmosphere that is equivalent to the current annual loading contributed by fossil fuel combustion (Raich & Schlesinger, 1992). Further, they state that ultimately, the response of soil respiration to temperature is likely to be the critically important factor in determining the rate of future climate change.

However, Davidson *et al.* (2000) maintain that the important issue regarding carbon release from soils is how all of the parameters (not just temperature) that effect soil respiration interact with one another to influence the rate of decomposition of organic matter within soils. If, globally, soils begin to release more CO_2 due to rising temperatures, the terrestrial biosphere sink could saturate or even become a net source. That being the case, the focus

now for soil scientists and ecologists is on how to better quantify soil carbon pools (sizes, age and turnover times). One of the ways to do this is by measurement of soil carbon fluxes in the form of soil respiration (both primary and isotopic).

1.3.6 Techniques used in the measurement of soil respiration

Estimates of the flux of CO_2 from soils are fraught with variability, largely resulting from the different methods of measurement that are employed (Raich & Schlesinger, 1992) and consequently are a far from certain source in the global carbon cycle. However, since in some terrestrial ecosystems (e.g. temperate forests) soil respiration has been estimated at between 40 and 60 % of total ecosystem respiration (Longdoz *et al.*, 2000), it is necessary to be able to use a method of measurement that one is confident in and can rely on to give an accurate value of flux. Techniques for measuring soil CO_2 flux include eddy covariance methods (for use above and below forest canopies) and chamber-based measurements.

Ecosystem-atmosphere CO_2 exchange on short time-scales can be measured using eddy covariance, which relies on rapidly responding sensors mounted on towers to resolve the net flux of CO_2 between a patch of land and the atmosphere (Baldocchi *et al.*, 1988). When used to estimate soil respiration in forest systems, measurements are complicated by under-canopy vegetation photosynthesising and respiring. However, using eddy covariance at night, above the forest canopy, can be useful in estimating total ecosystem respiration and the method is commonly used (Janssens *et al.*, 2000). Estimates of daytime respiration rates can then be carried out by applying temperature functions to these measurements.

Soil respiration can also be measured using chamber-based techniques. This method, which has been in use for a number of decades, involves placing a chamber over the soil surface to collect respired CO_2. Chambers can essentially be used in two modes to calculate efflux of CO_2 from soil: steady state and non-steady state. More recently, these chambers have been used in conjunction with infrared gas analysers (IRGAs).

Longdoz *et al.* (2000) reported that estimates of soil respiration made using chamber-based techniques were as high or higher than total ecosystem respiration derived from nocturnal eddy covariance measurements. Problems can also arise with the eddy covariance technique, when conditions are not ideal: low wind speeds or no wind at all and also high turbulence intensities which can affect the very assumptions that eddy covariance flux measurements are based on.

Chamber-based measurements can suffer from an alteration in the CO_2 diffusion gradient as CO_2 begins to build up inside the chamber. An underestimation of flux may then occur. This effect can be minimised however if an IRGA-based chamber system is used in non-steady state mode. This allows CO_2 fluxes to be measured quickly thus minimising the time that the chamber is over the soil and hence any alteration in diffusion gradient (Boutton, 1996; Davidson *et al.*, 2000).

Focus on the efflux of CO_2 from soils has shifted recently from primary flux measurements to include additionally the isotopic flux. This is important as utilising isotopes of carbon can give us additional information about sources, rates and the age of carbon that is respired from soil. Furthermore, carbon isotopes used as tracers (both enriched and natural abundance) are used to help us better understand and predict how the Earth's carbon reservoirs will respond to future variations in climate and land use.

1.4 Carbon isotopes and isotopic theory

Atoms that have differing numbers of neutrons but the same number of protons, and hence atomic number, are called isotopes. Isotopes therefore differ in mass (although they have identical electron shell configurations lending them the same chemical properties), and also in nuclear spin (Schimel, 1993). Carbon has 3 isotopes that occur naturally on Earth: ^{12}C which makes up 98.89 % of the natural abundance of carbon atoms, ^{13}C which is a stable isotope and is present at 1.11 % (Craig, 1957) of the natural abundance, and ^{14}C which is radioactive (unstable) and occurs only one in every million million (10^{12}) atoms. In nature, variations of these natural abundances between the light (abundant) and the heavy (rare) isotopes occur and in doing so provide valuable information about the carbon cycle (Coleman & Fry, 1991). These variations occur due to two phenomena: radioactive decay and isotopic fractionation.

1.4.1 Isotopic fractionation

Urey (1947) laid the foundations for stable isotope geochemistry. He was able to demonstrate that if atoms of an element were present in more than one isotopic form during a chemical reaction that it is likely that there would be an unequal distribution of these isotopes between products and reactants, a process we now refer to as isotopic fractionation. Mass differences in the atomic nuclei of isotopes lead to fractionation and take place through physical, chemical and biological processes (Boutton, 1991b).

There are two types of isotope fractionation (O' Leary, 1981): equilibrium fractionation (sometimes referred to as thermodynamic fractionation) and kinetic fractionation. Equilibrium fractionation takes place where two phases or compounds are in chemical equilibrium with one another e.g. liquid water and gaseous water in a closed system. Differences in free energy occur in an equilibrium reaction when two identical compounds containing different isotopes react, leading to differences in the isotopic ratios between the compounds at equilibrium. The net result of this thermodynamic effect is that the heavy isotope accumulates in the form of the compound containing the stronger bonds (Schimel, 1993) .

This occurs because mass differences between molecular species containing differing isotopes have different binding energies (E_B). In general, molecules containing the heavier isotope have higher binding energies than those containing the lighter isotope, as the chemical bonding is stronger between atoms of the heavier isotope (due to the differences in their zero point energies) and as such more energy is required to break them. The heavy isotope forms a lower energy bond; it does not vibrate as rapidly. This process is known as the normal isotope effect (Mook & de Vries, No date). However, often there are exceptions to the rule, and when the opposite process takes place it is known as the inverse isotope effect, as is the case with $^{13}CO_2$ having higher vapour pressure than $^{12}CO_2$ (normally molecules containing the heavier isotope are enriched in the phase with the lowest energy i.e. in liquid water as opposed to water vapour).

Kinetic fractionation occurs where either a chemical reaction goes to completion and the two phases or compounds are completely removed from one another e.g. the evaporation of water in an open system, or along a diffusion gradient e.g. the diffusion of CO_2 from soil to the atmosphere (Cerling *et al.*, 1991). Mass difference means that molecules containing heavier isotopes will have reduced mobility because the kinetic energy of a molecule is governed by temperature:

$$\mathbf{kT = \tfrac{1}{2}mv^2} \qquad \mathbf{(4)}$$

(k = Boltzmann constant, T = absolute temperature, m = molecular mass and v = average molecular velocity). The kinetic theory of gases explains that the distribution of velocities at a given temperature will be a Maxwell-Boltzmann distribution. Molecules at a given temperature will therefore have the same average velocity.

Therefore, if mass increases, the average velocity of a given molecule must decrease in order to conserve kinetic energy (the Boltzmann constant relates temperature to energy). This necessarily means that heavier isotopes will diffuse less quickly (known as diffusive fractionation, a kinetic isotope fractionation effect) than lighter isotopes. If the diffusional fractionation process occurs in a biological system (e.g. CO_2 diffusing into plant stomates during photosynthesis) then the biological substance will become enriched in $^{12}CO_2$ and hence depleted in $^{13}CO_2$. Typically CO_2 within plant stomates is depleted by ~ 4.4 ‰ (Cerling *et al.*, 1991; Farquhar *et al.*, 1982) relative to CO_2 left behind in the atmosphere outside the stomata (but can vary due to differences in stomatal conductance).

Reduced velocity caused by mass differences also means that heavier isotopes will collide less frequently than lighter ones. This is important because the collision frequency dictates how quickly a reaction will take place and is one of the reasons why lighter isotopes are preferentially used up in a chemical reaction, e.g. the fixation of CO_2 inside plant stomata and subsequent incorporation into plant leaf material (Farquhar *et al.*, 1982). This effect is known also as chemical fractionation. In a chemical reaction such as an enzymatic reaction, there will be preferential uptake of the light isotope due to the fact that the reaction will proceed much faster with substrates that are composed of this isotope.

The size of the kinetic effect (assuming 1st order kinetics) is expressed using the discrimination coefficient or fractionation factor α, and can be derived using the following equations:

$$\alpha = k / k' \qquad (5)$$

or

$$\alpha = (R / c) / (R' / c') \qquad (6)$$

where R and R′ are the reaction rates for the heavy and light isotopes and c and c′ are the concentration of the heavy and light isotopes in the molecular species of interest (Schimel, 1993). Fractionation is highly temperature dependent, and fractionation effects are much reduced at higher temperatures (Melander, 1960).

1.4.2 Stable carbon isotopes

The distribution of the two stable carbon (^{12}C and ^{13}C) isotopes varies only very slightly around the percentages given previously (98.9 and 1.1 %), due to isotopic fractionation,

which occurs during biological, chemical and physical processes (Galimov, 1985). As measuring absolute ratios of a substance is rather difficult, an evaluation of the difference in absolute isotopic ratios between two substances (usually an unknown and a standard) is sufficient for most geochemical purposes. Furthermore, these differences are measured far more readily and precisely than absolute ratios.

Because, the values of these variations are small, they are measured relative to a standard and expressed in parts per thousand, or per mil (‰). The natural $^{13}C/^{12}C$ ratios are expressed using the delta notation, illustrated in equation 7:

$$\delta^{13}C\ (‰) = \left[\frac{(^{13}C/^{12}C)_{Sample} - (^{13}C/^{12}C)_{VPDB}}{(^{13}C/^{12}C)_{VPDB}} \right] \times 1000 \qquad (7)$$

The original standard used by Craig (1957) was a limestone fossil of a marine belemnite (*Belemnitella americana*), discovered in the Cretaceous Pee Dee formation, North America. However, this standard has since been exhausted and an internationally calibrated standard is now used (Vienna Pee Dee Belemnite – VPDB) to which all $\delta^{13}C$ values are reported (Gonfiantini, 1984). Positive values indicate that the sample is enriched in ^{13}C relative to the international standard and negative values indicate that the sample is depleted in the heavier isotope relative to the standard. The ratio of $^{13}C/^{12}C$ in a sample is measured by an Isotope Ratio Mass Spectrometer (IRMS).

To measure the $^{13}C/^{12}C$ ratio in a sample, the carbon must first be removed from its matrix and converted to CO_2 (Boutton, 1991b). A CO_2 gas sample goes through a number of stages when first introduced to the IRMS. First of all the CO_2 sample enters a dual-inlet system that copes with both standards and samples separately. Gases are then ionised by electrons emitted from a hot filament (tungsten) in the ion source. Ionised CO_2 molecules are accelerated by a magnetic field then progress to a curved flight tube that is situated within an electromagnetic field. The magnetic field resolves the ion trajectories according to their mass (heavier ions are deflected least from their flight path when passing through the magnetic field). Finally the ions are collected in Faraday cups, which neutralise the charge and in doing so create an electrical current. The current created by the different ion beams (masses 44, 45 and 46) is then amplified. Thus the $^{13}C/^{12}C$ ratio of the CO_2 sample is calculated, with a minor correction (known as the 'Craig correction') made for contributions from ^{17}O to the signal for mass 45 (Craig, 1957).

Once determined, the natural abundance ratio of isotopes of carbon in both inorganic and organic materials can be very revealing as they record information regarding the following: processes that govern material formation, the rate at which formation takes place and also prevailing environmental conditions at the time of formation. The use of these small differences in the natural abundance of carbon isotopes between the various components that make up an ecosystem are extremely valuable in quantifying and tracing sinks, sources and flux rates within the carbon cycle (Boutton, 1996).

1.4.2.1 $\delta^{13}C$ as a tracer for ecosystem processes

Typical $\delta^{13}C$ values for carbon-containing substances in the environment range from marine carbonate with a value of between 0 and 2 ‰ to C_3 plants, which have an average value of about -27 ‰ (depleted in $^{13}CO_2$ and so consequently enriched in $^{12}CO_2$). Biogenically produced methane has $\delta^{13}C$ values that range from between approximately -45 and -65 ‰ (when produced *via* aceticlastic methanogenesis) (Strapoc *et al.*, 2006). CH_4 produced *via* CO_2 reduction can be more depleted still and $\delta^{13}C$ values can range from between -70 to -110 ‰ (Strapoc *et al.*, 2006). Figure 1.3 illustrates the $^{13}C/^{12}C$ ratios for a number of terrestrial carbon sources.

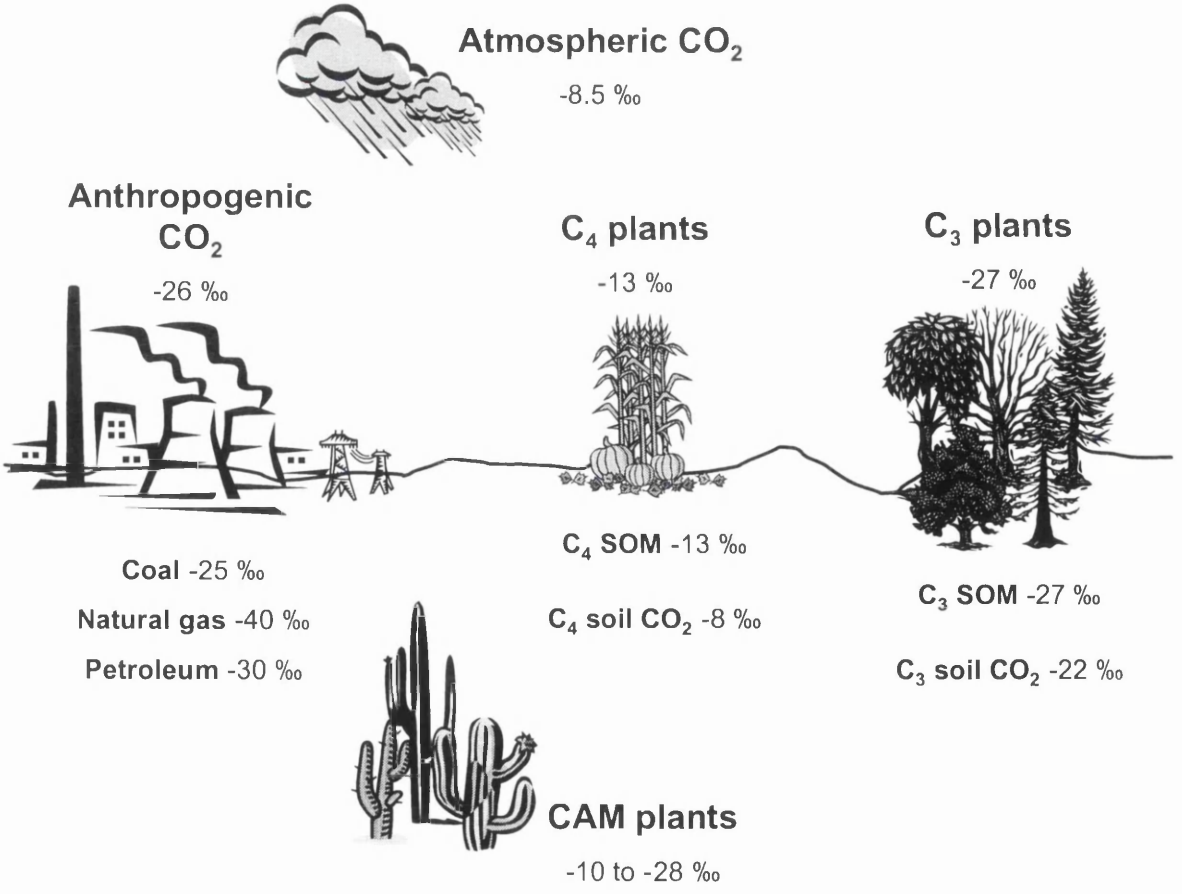

Figure 1.3 – $\delta^{13}C$ ratios of the major components in the terrestrial ecosystem. All single $\delta^{13}C$ values given are mean values. After Boutton (1996).

Plants serve as the main source of organic matter to soils, where they accumulate and are transformed by the activity of the soil biota (mostly by heterotrophic organisms) that use the organic carbon as their energy source. Because plants isotopically fractionate atmospheric CO_2 during fixation, plants and the soils derived from them have a very different $\delta^{13}C$ signature relative to that of the atmosphere. The $\delta^{13}C$ signature of soil organic matter is related to the isotopic signature of the vegetation from which it is formed (Figure 1.3) as fractionation during decomposition is considered small (Lin & Ehleringer, 1997; Nadelhoffer & Fry, 1988).

This means that stable carbon isotopes are particularly useful in providing a means to aid quantification of the contribution of individual component sources of respiration and photosynthesis that ultimately control carbon flow and fate within an ecosystem (Flanagan & Ehleringer, 1998). Furthermore, the relative contribution of specific ecosystem sources and sinks to total atmospheric CO_2 can be examined using the $\delta^{13}C$ of atmospheric CO_2, not just at local scales but also at regional and global scales (Bakwin *et al.*, 1998; Battle *et al.*, 2000; Ciais *et al.*, 1995; Ciais *et al.*, 1997; Fung *et al.*, 1997; Lloyd & Farquhar, 1994; Tans *et al.*, 1989; Tans *et al.*, 1993; Yakir & Wang, 1996).

The $\delta^{13}C$ values of CO_2 respired from vegetation are mainly determined by the average isotopic composition of the plant biomass. Soil respired CO_2, whilst having a similar isotopic signature to the organic matter it was produced from, undergoes isotopic fractionation when it leaves the soil due to diffusion. The diffusion coefficient has been calculated from isotopic theory to be around a minimum of 4.4 ‰ (Cerling *et al.*, 1991), but can be smaller as demonstrated by Davidson (1995) and Dörr and Münnich (1986). If the biospheric system being investigated is in steady state, then the $\delta^{13}C$ of CO_2 derived from the decomposition of organic matter (i.e. soil CO_2) will become enriched by +4.4 ‰. When this soil CO_2 is respired the $\delta^{13}C$ value approaches that of the organic carbon source (Cerling *et al.*, 1991; Davidon, 1995; Dörr & Münnich, 1987).

Emissions of CO_2 from bare soil surfaces can provide an insight into the dynamics of soil carbon in the short term (Rochette *et al.*, 1992). However, when plants are present the signature of total soil respiration is complicated by the production of respiration in the rhizosphere (R_{rh}), which includes respiration from living roots and feeding micro-organisms. One technique used to partition heterotrophic and autotrophic respiration is to replace one vegetation type with another e.g. replacing a C_3 crop which is growing in soil containing SOM derived from C_3 crops with a C_4 crop (Ineson *et al.*, 1996) or *vice versa*.

This technique has also been used to estimate rates of soil organic matter turnover (Bernoux *et al.*, 1998). The drawback with this method is it involves considerable soil disturbance, however the use of natural abundance radiocarbon has no such drawbacks.

1.4.3 Radiocarbon

1.4.3.1 Natural production of ^{14}C

The scientists Martin Kamen and Samuel Ruben first discovered the existence of radiocarbon in February 1940 (Gest, 2004). Radiocarbon (^{14}C) is a cosmogenic radionuclide and is produced naturally in the Earth's upper atmosphere (within a transitional region between the troposphere and the stratosphere). Galactic cosmic rays (composed mainly of high energy protons, but also some alpha particles) strike gases 12 km above the surface of the Earth, in a process known as spallation. This bombardment produces secondary particles, thermal neutrons (first discovered by Korff in 1939; (Libby, 1960)), which are travelling at slow enough speeds to be absorbed by an atomic nucleus. Some of these neutrons produced during cosmic ray showers are captured by nitrogen, finally producing radiocarbon by subsequent release of a proton (Libby, 1946),

$$^{14}N + n \rightarrow {}^{14}C + p \qquad (8)$$

(where n is a neutron and p is a proton). The presence of radiocarbon in environmental samples was first discovered by Anderson *et al.* in 1947 (Anderson *et al.*, 1947). The radiocarbon half-life of 5730 ± 40 years (Godwin, 1962) is referred to as the Cambridge half-life to distinguish it from the Libby half-life which was the first estimate of the half-life of radiocarbon, but was subsequently found to be in error (see p. 32 for further details). Cosmic ray neutrons interacting with oxygen at the Earth's surface also produce radiocarbon,

$$^{17}_{8}O\ (n, \alpha) \rightarrow {}^{14}_{6}C \qquad (9)$$

where α is an alpha particle consisting of 2 protons and 2 neutrons. Radiocarbon produced by this mechanism is referred to as *in situ* production (but accounts for only a very small fraction of the total natural ^{14}C production).

1.4.3.2 Anthropogenic perturbation of atmospheric ^{14}C

In the last century two anthropogenic effects caused a change in the natural abundance of ^{14}C in the atmosphere. The first anthropogenic effect to have altered the natural abundance of ^{14}C in the Earth's atmosphere was fossil fuel combustion. Since the beginning of the Industrial Revolution, increasing amounts of fossil fuels were required to sustain industrial progress. The addition of fossil fuel CO_2 to the atmosphere caused (and still causes today) a dilution of the natural atmospheric radiocarbon abundance because fossil fuels contain essentially no radiocarbon.

Dilution of radiocarbon in the Earth's atmosphere was first recognised by Hans Suess (1955) and is referred to as the 'Suess effect'. The 'Suess effect' began to have a significant effect on the Earth's atmosphere from around 1890. The reason fossil fuels cause a dilution of the natural radiocarbon present in the atmosphere is because they are millions of years old. Any radiocarbon fossil fuels once contained (in the plants from which they were originally formed) has decayed away (after 10 half-lives or 60 000 years, only background amounts of radiocarbon remain). Because of this, fossil fuel CO_2 and indeed CO_2 produced from carbonates or limestone (e.g. during cement production) are termed 'radiocarbon dead'.

A second anthropogenic disturbance to the ^{14}C concentration of the atmosphere was introduced during the 1950s and 60s, with the advent of thermonuclear weapons and their subsequent testing *via* detonation near the Earth's surface. The consequence of atmospheric nuclear weapons testing, which took place from ~ 1954 until 1963, when atmospheric weapons testing was banned (implementation of the Nuclear Test Ban Treaty agreed in 1963), was that the natural abundance of radiocarbon was perturbed (De Vries, 1958). In the 20^{th} century the Suess effect was somewhat obscured by the bomb effect. Figure 1.4 illustrates both the Suess effect and the 'bomb' effect on the radiocarbon concentration of the atmosphere since 1900.

The radiocarbon that was produced during nuclear weapons testing was carried up into the lowest part of the stratosphere, whereupon it was rapidly oxidised to $^{14}CO_2$ *via* ^{14}CO as an intermediary (Glasstone & Dolan, 1977). A significant quantity of the $^{14}CO_2$ injected into the stratosphere, re-entered the troposphere of the northern hemisphere, when mixing between the troposphere and the stratosphere took place during winter and spring (Holton *et al.*, 1995). Mixing between hemispheres (northern and southern) is relatively slow, and so consequently $^{14}CO2$ concentrations in the southern hemisphere lagged behind

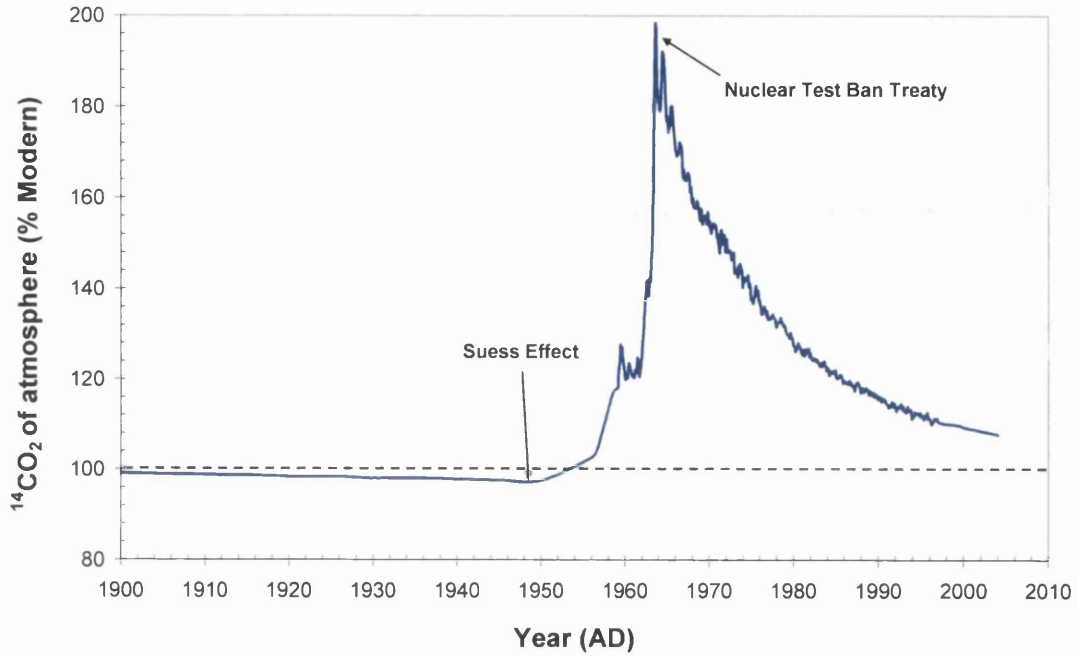

Figure 1.4 – Atmospheric $^{14}CO2$ from 1900 to 2004 based on northern hemisphere measurements. Data for 1955-2004 from Hua & Barbetti (2004) and pre 1955 from IntCal04 (Reimer *et al.*, 2004). 100 % Modern is the theoretical ^{14}C content of the atmosphere in 1950 (had there not been any Suess effect).

concentrations in the northern hemisphere for a number of years (Nydal & Lovseth, 1983) during the mid-1960's.

1.4.3.3 Measurement of ^{14}C by accelerator mass spectrometry (AMS)

The radiocarbon concentration of unknown samples has been measured in the past by liquid scintillation counting (carbon converted to benzene) and gas proportional counting (carbon converted to acetylene or CO_2) both of which detect β^- particles as ^{14}C decays to ^{14}N. However, these methods have now largely been superseded by accelerator mass spectrometry (AMS), which requires only 1 mg of carbon for analysis (as opposed to ~1 g for LSC and GPC). Furthermore, samples that have an age of more than 10 000 years can be counted within minutes (as opposed to days or weeks by LSC) and determined with a statistical precision of 0.5 % (Fifield, 1999).

An accelerator mass spectrometer is essentially a standard mass spectrometer with a particle accelerator between the ion source and the detectors. A standard mass spectrometer typically works with energies of tens of keV, whereas an AMS generally works with energies of MeV. These higher energies are necessary to resolve ^{14}C from its main interfering isobar ^{14}N and also from molecular interferences such as $^{12}CH_2$, ^{13}CH, ^{12}CD and $^{7}Li_2$ (Fifield, 1999). Samples are prepared for analysis by AMS by first converting a sample to CO_2 and thence to graphite *via* an Fe/Zn reduction reaction (Slota *et*

al., 1987). The resulting graphite powder is pressed into a small aluminium cathode, called a target, and placed in a wheel containing a number of samples alternating with a number of standards of known ^{14}C concentration.

Graphite targets are sputtered in the ion source of the AMS with caesium ions, which produces negative carbon ions (thus eliminating the major isobaric contaminant ^{14}N which does not form a stable negative ion). Negative carbon ions are subsequently focused into ion beams using lenses and magnets before entering the accelerator itself. The accelerator is referred to as a tandem accelerator as the acceleration of carbon ions occurs in two stages. First, carbon ions are accelerated towards the positive high voltage terminal called the stripper (either low pressure argon gas or very thin carbon foil), which removes electrons from the carbon atoms and produces positively charged ions (usually C^{3+} or C^{4+}). The stripper causes any molecular interferences to dissociate into their atomic components (Fifield, 1999).

In the second stage of the tandem accelerator, positively charged carbon ions become repelled from the similarly charged stripper and are accelerated further, back to ground potential. On exit from the accelerator, ions pass through a magnetic field, which resolves all ions by mass, the abundant ions e.g. $^{12}C^{4+}$ and $^{13}C^{4+}$ are collected and counted in Faraday cups. The rare element ($^{14}C^{4+}$) then enters a gas ionisation detector. In the detector analyte ions collide with the gas and the rate at which they slow down (energy loss) depends on mass and charge state and so distinguishes radiocarbon from any isobaric interferences that may have made it into the detector (nitrogen is pervasive in any vacuum system).

Having ascertained the quantity of radiocarbon in a sample, that quantity must then be calibrated relative to an international radiocarbon standard of known radiocarbon concentration.

1.4.3.4 Determination of radiocarbon age

Radiocarbon concentration of an unknown sample, like stable carbon, is measured relative to an internationally calibrated modern reference standard of known concentration, as it is extremely difficult to measure absolute radiocarbon activities. The first international radiocarbon standard was Oxalic acid (OxI). Ninety five percent of the activity of the original oxalic acid standard (calibrated in 1958) is equivalent to the theoretical ^{14}C concentration of carbon fixed from the atmosphere in 1950, had there been no Suess effect

(Stuiver & Polach, 1977). The activity of the atmosphere in 1950 was determined by measuring the ^{14}C activity of tree rings grown in 1890, that were then decay-corrected to 1950 (wood from 1890 was chosen since it was growing prior to a significant Suess effect). As only 1000 lbs of the first international standard, OxI, was originally made, it has long since been exhausted and is no longer available commercially.

The modern reference standard, currently used by most radiocarbon laboratories is Oxalic acid II. Oxalic acid II, was developed from beet molasses in 1977, and was calibrated by 121 laboratories in the early 1980's to enable its activity to be corrected to that of the OxI standard. All radiocarbon dates are reported relative to 95 % of the OxI modern reference standard (Stuiver & Polach, 1977) and hence all radiocarbon ages are reported to AD 1950.

International practice is to report radiocarbon results as conventional radiocarbon years BP (relative to 1950) and %Modern ^{14}C. Percent Modern is calculated using the following equation:

((Activity of sample) / (0.95 x Activity of OxI)) x 100 **(10)**

A conventional radiocarbon age (years) is calculated using equation 11:

-8033 ln (%Modern / 100) **(11)**

where 8033 (assuming Libby half-life) is the mean life of ^{14}C in years (Stuiver & Polach, 1977).

All conventional radiocarbon ages (and %Modern values) are normalised to a $\delta^{13}C$ of -25 ‰ (Stuiver & Polach, 1977), to take account of isotopic fractionation effects. For example, during the transition of carbon in the atmosphere (as CO_2) to carbon fixed in plant material, isotope fractionation takes place. The $\delta^{13}C$ of C_3 plants differs from C_4 plants by ~15 ‰, due to the different photosynthetic pathways utilised. Fractionation of ^{14}C is assumed to be twice that of ^{13}C (because the mass difference between ^{12}C and ^{14}C is double that between ^{12}C and ^{13}C). This necessarily means that a C_3 plant and a C_4 plant grown in the same atmosphere, at exactly the same time, will have different concentrations of radiocarbon (but they are in fact the same age). Hence normalisation by correcting to a $\delta^{13}C$ of -25 ‰ corrects for this fractionation effect.

Two additional corrections to conventional radiocarbon ages are required. Firstly, Willard Libby originally calculated the half-life ($t_{1/2}$) of radiocarbon to be 5568 ± 30 years (known

as the Libby half-life). The Libby half-life is about 3 % too low, but is still used today for reporting conventional radiocarbon ages, by international agreement. This was done to avoid confusion; as for more than a decade radiocarbon ages were published using the Libby half-life. Secondly, radiocarbon production was assumed to have been constant throughout time. However, cosmic ray radiation is deflected by anything in the Universe which has a magnetic field (hence it is difficult to ascertain the source of cosmic rays) and so variations in both the Sun's and the Earth's magnetic fields (heliomagnetic and geomagnetic modulations) lead to variations in radiocarbon production.

Today, radiocarbon ages can be corrected for both the above errors, through calibration with the record of radiocarbon reconstructed from dendrochronologically dated tree rings (e.g. IntCal04; Reimer *et al.*, 2004). Accurate measurement and calibration of the isotopic ratios of carbon in environmental samples by both IRMS and AMS provides the necessary precision required to aid elucidation of key processes within the various reservoirs and ecosystems of the global carbon cycle.

1.4.3.5 Radiocarbon in ecosystem tracer studies

The atmospheric concentration of ^{14}C almost doubled due to atmospheric nuclear weapons testing and in doing so created a tracer, on a global scale, that allows monitoring of carbon dynamics in the oceanic and terrestrial environments (Harrison *et al.*, 2000; Levin & Hesshaimer, 2000). Once produced, ^{14}C in the stratosphere rapidly oxidises (within hours) to become ^{14}CO, which has a lifetime of months, whereupon it is oxidised to $^{14}CO_2$ (Lingenfelter, 1963). As such it enters terrestrial ecosystems *via* plants during photosynthesis and is subsequently cycled through animals, micro-organisms, soils and soil organic matter. Everything that is in equilibrium with the atmosphere will have approximately the same number of radiocarbon atoms. As soon as a biological organism ceases exchange with the atmosphere (i.e. dies), the amount of ^{14}C within it begins to reduce *via* first order radioactive decay kinetics;

$$A_t = A_0 e^{-\lambda t} \qquad (12)$$

where A_0 is equal to the equilibrium living activity, A_t equals the activity remaining after time t (since death) and λ is the decay constant which is equal to the natural log of 2 (ln 2) divided by the half life (Cambridge) in years.

The rate at which the ^{14}C produced by atmospheric nuclear weapons testing is incorporated within soil's carbon reservoirs can be a useful tool for deciphering carbon turnover in soils, on timescales of decades to tens of thousands of years. For example, many studies have used radiocarbon analyses to determine rates of carbon cycling in soils (Goudriaan, 1992; Harkness *et al.*, 1986; Jenkinson *et al.*, 1992). However, soils cannot be treated as just one homogeneous carbon reservoir. It is well known that there are a number of pools of carbon within soil organic matter, all with varying turnover times ranging from fast cycling pools of a few years to very slow cycling pools of millennia (Trumbore, 2000). Furthermore, measurements of bulk soil organic matter only can lead to underestimates of carbon residence times (Trumbore, 2000), for example, due to penetration of modern carbon to depth (e.g. mobile fulvic acids).

Because of this fact, there is now increasing interest in the isotopic signature of respired CO_2 (Dioumaeva *et al.*, 2002; Gaudinski *et al.*, 2000; Schuur & Trumbore, 2006; Trumbore *et al.*, 2006; Wang *et al.*, 2000). Soil respiration and the abundance of radiocarbon in it, provides a better understanding of soil organic matter and how it is formed, stored and decomposed within soil. Carbon is continually being added to the soil pool (as deceased plant matter) and lost in the form of dissolved organic carbon (DOC) or CO_2. Therefore, one of the greatest challenges today is to determine the relative contribution of each of these pools to the overall flux of carbon, to and from terrestrial ecosystems.

Given that the terrestrial biosphere is absorbing approximately one quarter of anthropogenic CO_2 emissions (IPCC, 2001) it is imperative that we better quantify exactly how terrestrial carbon fluxes are influenced by changing climatic regulators such as temperature and moisture. This information will be used to better constrain global climate models which will allow us to predict more accurately what effect man is having, and will have, on the future of planet Earth.

The aims of this thesis project are as follows:

1. To develop a sampling system to capture isotopically representative samples of CO_2 both in the field and in the laboratory, for stable and radiocarbon analysis.

2. To use the developed method and other widely used techniques to characterise and partition peatland ecosystem respiration.

3. To evaluate the influence of abiotic drivers, such as temperature, moisture and substrate quality on the rate and stable carbon isotopic signature of peatland soil respiration fluxes.

4. To partition total ecosystem respiration into its constituent components of plant and soil respiration.

2 Development of a zeolite molecular sieve sampling system for use in isotopic (^{13}C and ^{14}C) studies of soil respiration

2.1 Introduction

Natural abundance carbon isotope tracers can be used as a means to better understand and predict how the Earth's carbon reservoirs will respond to global change (e.g. climate, land use, pollution). Differences in the $\delta^{13}C$ values of C_3 and C_4 plants and derivative soil organic matter (SOM) have been used to examine rates of decomposition and turnover of SOM on timescales of one year to hundreds of thousands of years (Boutton, 1996). Studies have also used radiocarbon analyses of bulk SOM to estimate rates of carbon cycling in a range of ecosystems (Harkness *et al.*, 1986; Harrison, 1996; Paul *et al.*, 1997; Quideau *et al.*, 2001; Richter *et al.*, 1999).

However, since SOM is composed of various pools of carbon, cycling on different timescales (i.e. from hours to millennia), bulk measurements obscure the response of specific pools to both transient and long term change. Furthermore, although measurements of ^{14}C in SOM have been used as a surrogate for soil respiration, Trumbore (2000) has suggested that this approach significantly underestimates (in the short term) CO_2 fluxes. This occurs because the soil is not a homogeneous pool of carbon and soil is composed mainly of longer lived soil organic matter (Trumbore, 2000). Consequently, there is now considerable interest in the use of ecosystem and soil respired CO_2 isotopic values to understand the role of environmental factors on the rate of organic matter decomposition and the magnitude and source of CO_2 fluxes.

Capture of CO_2 respired from soils for subsequent isotopic analysis has been achieved in the field using various methods including, cryogenic trapping (Craig, 1953), collection in evacuated flasks (Charman *et al.*, 1999) and absorption in hydroxide solutions, such as sodium hydroxide (Dörr & Münnich, 1980; Dörr & Münnich, 1986). Each of these methods has its disadvantages but common to all is the fact that they are impractical when used at remote locations in the field.

For example, absorption of CO_2 in hydroxide solutions causes an isotopic fractionation effect (Keeling, 1958) and the solutions are difficult to use in the field due to their caustic

nature. Cryogenic trapping of CO_2 in the field using liquid nitrogen (b.p. -196 °C) is potentially hazardous and may result in the condensation of atmospheric O_2 (b.p. -183 °C). This may reduce the collection efficiency of CO_2 but more importantly could result in an explosive situation on recovery of CO_2 using a vacuum rig (Bauer *et al.*, 1992).

A small number of studies have utilised zeolites (often referred to as molecular sieves – a term which was first coined by McBain (1932)) as an alternative method of CO_2 capture (Bauer *et al.*, 1992; Bol & Harkness, 1995; Gaudinski *et al.*, 2000; Koarashi *et al.*, 2002). The zeolite molecular sieve approach is easy to use and has none of the above disadvantages making it ideal for field experiments and remote area research to determine the isotopic source of ecosystem and soil respired CO_2. Furthermore, the molecular sieve material (synthetic faujasite) is re-usable and can withstand temperatures of 500 °C almost indefinitely (Barrer, 1959).

2.1.1 Zeolites

The Swedish scientist Cronstedt first discovered zeolite (stilbite) in 1756. He observed intumescence on heating and named it after the Greek words, 'zeo', which means boil and 'litho', which means stone (Zhao *et al.*, 1996). Zeolites are three-dimensional crystalline aluminosilicates of the alkali and alkaline earth elements (commonly sodium, potassium and calcium) represented by the empirical molecular formula:

$$\mathbf{M_2/nO{\cdot}Al_2O_3{\cdot}xSiO_2{\cdot}yH_2O}$$

where n is the valence of the cation and x and y are integers. Zeolites are used in the petrochemical and petroleum refining industries as ion exchangers, adsorbents and selective catalysts (Dyer, 1988; Yang, 1997).

The characteristics of zeolites (dehydrated zeolites in particular) that are of interest when partitioning an analyte gas from a mixture of gases such as the separation of CO_2 from air include: uniform molecular pore size, polarity, reversible and selective adsorption (different cationic forms of zeolite can lead to significant differences in the adsorption of a given gas), and adsorption capacity. Firstly, the three dimensional framework of the crystalline aluminosilicate structure created *via* the sharing of adjacent oxygen atoms by SiO_4 and AlO_4 tetrahedra (Breck, 1974) contains a network of uniform molecular-sized pores (0.3 to 0.8 nm (Flanigen, 1991)). This feature gives zeolites their molecular sieving property as the porous structure allows selective admittance of molecules with diameters

less than that of the pore window size, whilst those that are larger are sterically or kinetically hindered.

Secondly, the isomorphous substitution of aluminium for silicon in the crystalline lattice structure of a zeolite lends it an overall net negative charge. This negative charge is neutralised by an electrochemical equivalent of cations (Barrer, 1978) such as sodium, barium and potassium. Consequently zeolites have a high affinity for polar molecules such as H_2O and CO_2. Competitive adsorption is typically of the order: $H_2O > N_2O > NO > CO > CO_2 > N_2 > O_2 > CH_4$ (Breck, 1974) at ambient temperature and pressure. The affinity of polar molecules like CO_2 for substituted zeolites is due to an interaction between the molecule and the zeolite. In the case of CO_2 it is the interaction of its quadrupole moment with the electric field of the zeolite (Cui *et al.*, 2003) resulting in high adsorption of monolayer coverage (Siriwardane *et al.*, 2001). Furthermore, the isotherms applicable to many zeolites follow classification 'I' of IUPAC (International Union of Pure and Applied Chemistry) grouping, also known as the Langmuir type adsorption isotherm (Ruthven, 1984).

A crucial property possessed by zeolites is reversible sorption. Desorption of a gaseous adsorbate from zeolite can be effectively controlled by the application of adequate temperature or pressure (BDH, No date), otherwise a hysteretic effect may occur. Finally, zeolites possess a high adsorption capacity at ambient temperature and pressure, even at low adsorbate concentrations (BDH, No date).

2.1.2 Zeolites in isotope studies of CO_2

Zeolites that have been used in the partitioning of the trace gas CO_2 from carrier gas streams include molecular sieve type 4A (Koarashi *et al.*, 2002), a sodium aluminosilicate with an effective pore diameter of 0.42 nm, and type 13X (Bauer *et al.*, 1992; Bol & Harkness, 1995; Gaudinski *et al.*, 2000), another sodium aluminosilicate with an effective pore diameter of 0.78 nm (Flanigen, 1991). Bauer *et al.* (1992) used standards of known isotopic composition to test molecular sieve type 13X incorporated within a vacuum rig. The use of a single ^{13}C standard, however, precluded the detection of any isotopic memory effect. Two standards were used for ^{14}C, but any tests for memory effect were not reported.

Bol and Harkness (1995) carried out a method validation of their sampling system (incorporating molecular sieve type 13X) using the ^{13}C signal of atmospheric CO_2. Whilst accounting for possible isotope fractionation, this method would not have been sensitive to

test for memory effect or indeed any contamination *via* atmospheric CO_2 leaking into the sampling system. Gaudinski *et al.* (2000) made a study of the ^{14}C content of soil respiration using molecular sieve type 13X, but do not report testing of their sampling system. In another soil respiration study, Koarashi *et al.* (2002) used molecular sieve type 4A; tests were made for quantitative recovery but not for isotope fractionation or memory effect.

In this chapter the development of a sampling system intended for ecosystem respiration studies is discussed. Once developed the system underwent a rigorous analytical testing programme, executed by repeated measurement of authenticated laboratory standards to enable the detection of any atmospheric contamination, isotopic fractionation or memory effect (Hardie *et al.*, 2005).

2.2 Materials and methods

2.2.1 Molecular sieve sampling system (MS^3) design

A closed loop sampling system was designed (see Figures 2.1 and 2.2) for laboratory and

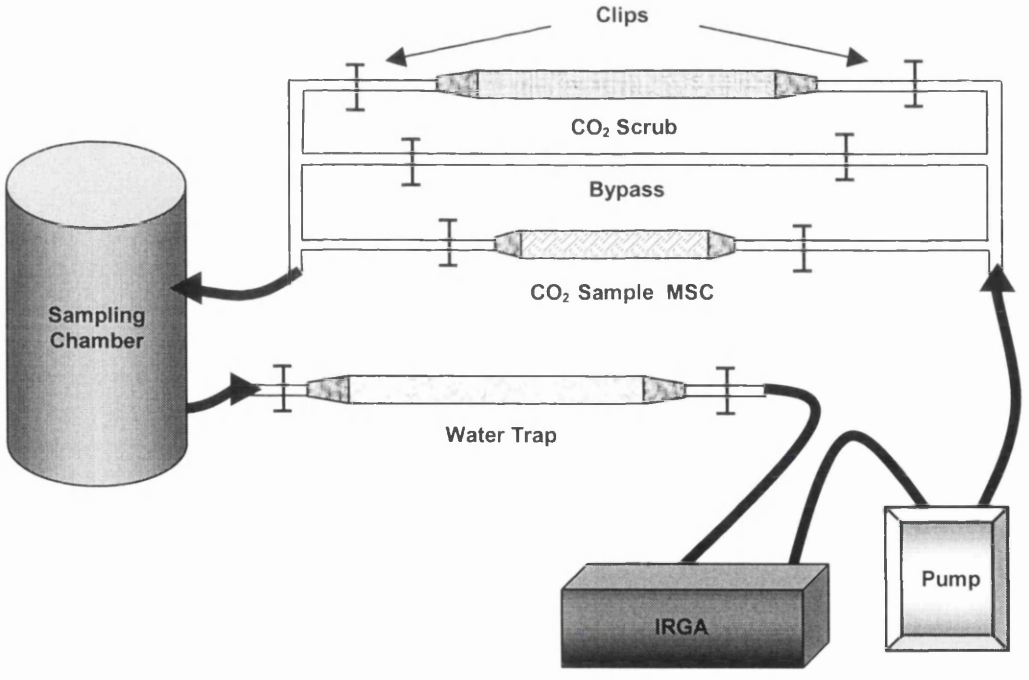

Figure 2.1 - Schematic diagram of the molecular sieve sampling system. Gas flow pathways are manipulated by opening and closing the clips. Clips removed from the CO_2 scrub (soda lime) allow atmospheric CO_2 to be removed from within the sampling chamber. Removal of clips from the bypass allows CO_2 evolution inside the chamber to be monitored, thus ensuring enough CO_2 has been respired for radiocarbon analysis. Finally, clips are removed from the MSC to capture an isotopically representative sample of the CO_2 in the chamber. IRGA = Infrared gas analyser.

field applications with elements similar to one described by Gaudinski *et al.* (2000). The sampling system incorporated the following components: a molecular sieve sampling cartridge (MSC), a CO_2 scrub, a bypass (to allow monitoring of CO_2 concentration before sampling), a water trap, a portable Infrared Gas Analyser (IRGA, PP Systems, UK), a sampling chamber, and a small battery powered pump (AeroVironment Inc., USA).

Figure 2.2 - The molecular sieve sampling system in field operation. The chamber is for demonstration purposes only.

The water trap, CO_2 scrubber and sampling cartridges were made from quartz glass and were based on an original design by Bol and Harkness (1995). Both ends of every cartridge were fitted with an auto-shutoff Quick Coupling (Colder Products Company, USA) attached with short lengths of PVC tubing (Tygon, R3603, 4.8 x 8.0 mm, Fisher Scientific, UK). WeLoc clips (Scandinavia Direct, UK) were placed across the PVC tubing between each end of the cartridge and the Quick Couplings to control gas flow into the MSC during operation. All junctions were made using T Connectors (Kartell Plastics UK Ltd., UK).

The CO_2 scrubber cartridge was filled with ~14 g of soda lime (BDH laboratory supplies, UK) and the water trap (similar quartz cartridge) filled with a desiccant, regular $CaSO_4$, Lab Grade, -10+20 Mesh (Alfa Aesar, Germany). A similar but smaller-bodied quartz cartridge was filled with 3 - 4 g of molecular sieve type 13X (1/16" pellets, BDH Laboratory supplies, UK). The contents of all three cartridges were held in place with quartz wool. During the initial development of the sampling system molecular sieve types 4A and 5A were tested before settling on the use of molecular sieve type 13X. In addition, type 3A was tested as a desiccant. The performance of all 4 zeolite types is discussed

herein with a selection of the results for the testing of molecular sieve types 4A and 13X to be found in Tables 2.2 to 2.5.

The sampling chamber (~5 litres) used for the test programme was constructed from PVC pipe and sealed at either end with nitrile rubber (LRC Products Ltd, UK). The chamber was connected to the CO_2 sampling system *via* two Quick Couplings and nylon tubing (see Figure 2.2). Gas flow pathways within the sampling system were manipulated using WeLoc clips.

2.2.2 Molecular sieve cartridge activation

To ensure that zeolite cartridges were free of contamination prior to sampling, MSCs were simultaneously heated to 500 °C using a tube furnace (Carbolite MTF 10/15, Carbolite, UK) and evacuated to 10^{-2} mbar (see Figures 2.3 and 2.4). The vacuum rig was constructed

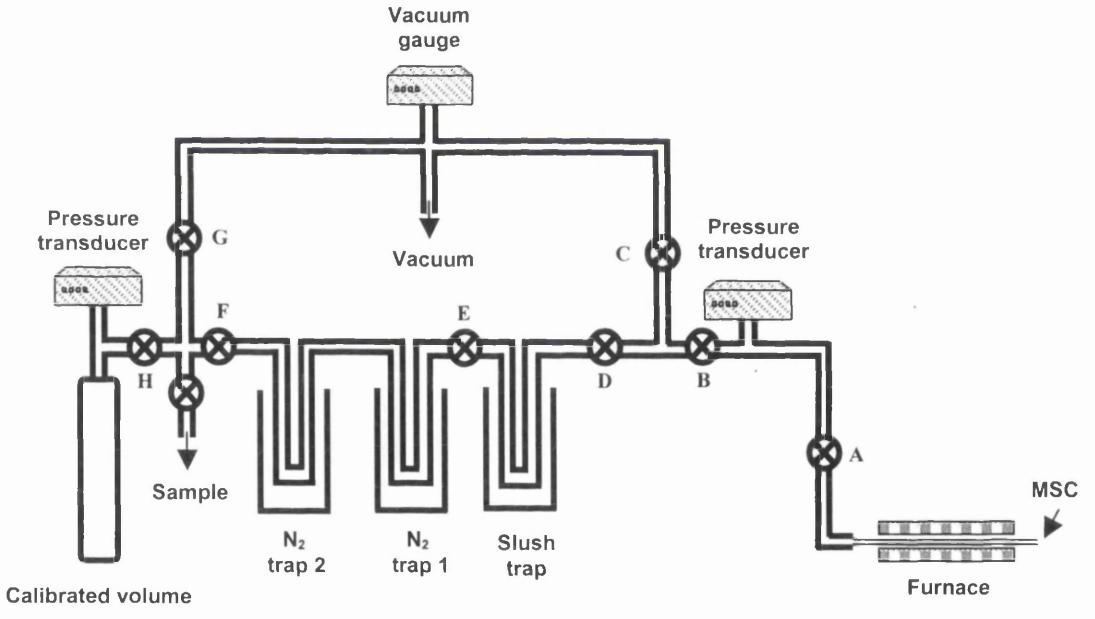

Figure 2.3 - Schematic of the vacuum rig used in the desorption of CO_2 from the MSCs. Valves are labelled with capital letters.

from 6 mm bore stainless steel tubing connected to glass traps with O-ring sealed Cajon-Torr fittings and Cajon valves purchased from Swagelock, UK. Glass traps were custom designed, and made from borosilicate glass (borosilicate is less permeable to CO_2 than quartz glass). The necessary vacuum was attained with a vacuum pump (E2M5 – Edwards, West Sussex, UK) and measured using a pressure transducer (Edwards, West Sussex, UK) and a thermocouple vacuum gauge (Javac UK Ltd, Middlesbrough, UK). The borosilicate glass calibrated volume is capable of holding up to 30 ml of purified CO_2 at standard temperature and pressure (273 K and 1013 mbar).

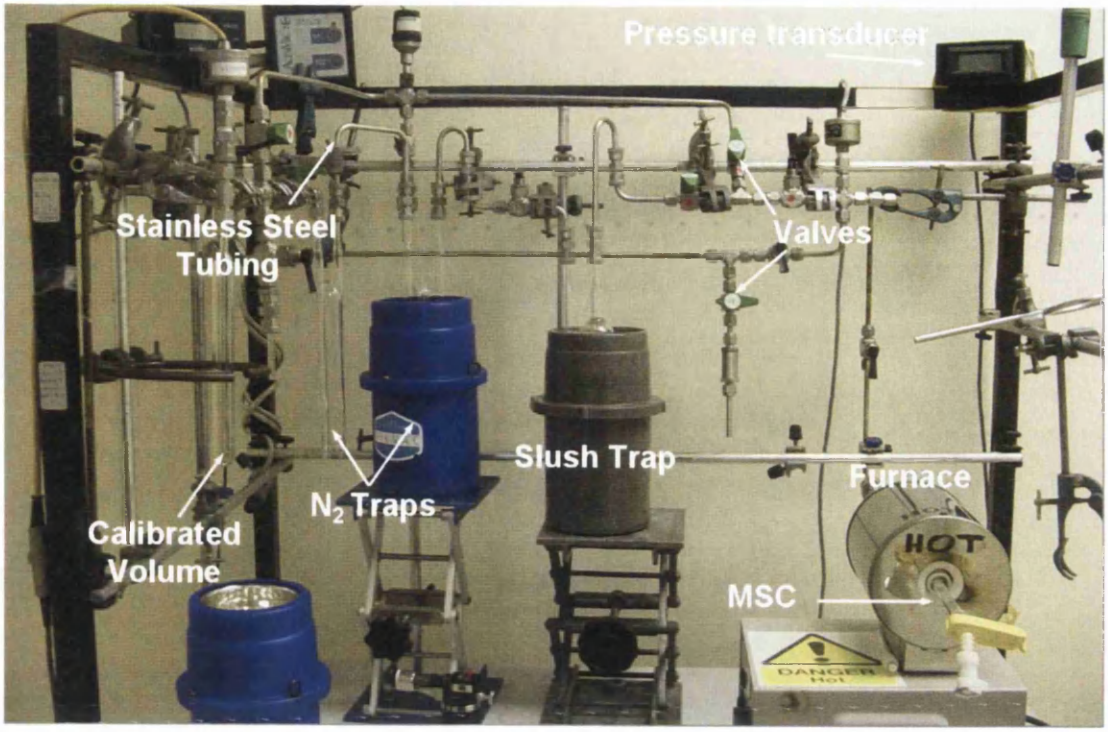

Figure 2.4 - Photograph depicting the vacuum rig and all its components used to activate and discharge MSCs.

A slush trap consisting of dry ice and industrial methylated spirit (-78 °C) and a liquid nitrogen trap (-196 °C) were used to aid desorption of any gases held on the zeolite and also to protect the pump from moisture. Each MSC was then allowed to cool to <30 °C and filled with high purity N_2 gas to just above atmospheric pressure (~1100 mbar). It was found during testing that new zeolite molecular sieve exhibited a small amount of hysteresis on first use (data not shown), therefore fresh zeolite was first purged of all gases and then flushed with CO_2 in an air stream, and recharged at 500 °C again prior to sampling.

2.2.3 Carbon dioxide sampling procedure

A scored borosilicate glass tube containing a CO_2 standard was placed into the sampling chamber and positioned inside a cylindrical protrusion in one of the nitrile rubber seals. The sampling chamber atmosphere was then circulated by the pump (flow rate, 500 ml min^{-1}) through the CO_2 scrubber cartridge and the CO_2 concentration monitored using the IRGA. The chamber was considered ready for testing when the CO_2 concentration had dropped below 10 ppm, whereupon the pathway through the CO_2 scrubber was closed and the pathway to the sample MSC was opened. This was considered as acceptable for testing purposes because all standards were of a concentration greater than 1600

ppm CO_2 when released into the sampling chamber (i.e. the residual 10 ppm CO_2 accounted for <0.6 % of the total).

The borosilicate glass tube containing a CO_2 standard was cracked within the sampling chamber, the gas pumped around the sampling system and through the MSC. The MSC was closed and sampling ceased when the sampling chamber CO_2 concentration had reduced to below 100 ppm.

2.2.4 Molecular sieve cartridge desorption procedure

The MSC was attached to the vacuum rig with both WeLoc clips still in place and dead space air removed by opening valves A, B and C (see Figure 2.3) until 10^{-2} mbar was attained whereupon all valves were closed. The MSC was then detached from the vacuum rig and the WeLoc clip removed from the front end of the cartridge to allow passage into the tube furnace. After insertion into the furnace, the clip was replaced and the MSC reattached to the rig. Valves A, B and C were opened and the vacuum rig was then pumped down to 10^{-2} mbar as far as the clip. Valves A, B and C were closed again. A slush trap and two liquid N_2 traps were activated by raising the dewar flasks around the borosilicate glass traps of the rig and valves A, B, D and E opened. The MSC was then opened to the traps and the furnace temperature raised to 500 °C.

CO_2 was collected at 500 °C under static vacuum for 20 minutes after which valves F and G were opened and any non-condensables pumped away until a vacuum of 10^{-2} mbar was achieved in the MSC. All valves were then closed and the second nitrogen trap was removed and replaced with the slush trap. The CO_2 was transferred to the calibrated volume and the pressure of the expanded gas was measured using a pressure transducer (BOC Edwards, UK) allowing the volume of CO_2 recovered to be calculated at s.t.p (standard temperature and pressure). CO_2 was subsequently aliquoted into mass spectrometry tubes and $\delta^{13}C$ ratios analysed by isotope ratio mass spectrometry (IRMS); (dual inlet, VG Optima, UK). Further sub-samples of CO_2 were flame-sealed in borosilicate glass tubes, one of which was prepared as a graphite target (Slota *et al.*, 1987) for ^{14}C measurement by accelerator mass spectrometry (AMS), by the 5 MV tandem accelerator at the Scottish Universities Environmental Research Centre (SUERC), East Kilbride, UK (Freeman *et al.*, 2004; Xu *et al.*, 2004).

2.2.5 Experimental design

A total of 8 CO_2 standards were used in the final testing programme (ranging from 8 to 11 ml), four for each of the two MSCs used (5 and 6). The range of standard volumes chosen ensured sufficient CO_2 for AMS ^{14}C analysis, duplicate IRMS analysis, and also for a sub-sample to be archived. The CO_2 standards were prepared from materials with a wide range of $\delta^{13}C$ and ^{14}C isotopic values: Carbonate, Sucrose and Barley mash (see Table 2.1).

Standard Material	$\delta^{13}C_{VPDB}$ (± 0.1 ‰)	^{14}C Concentration (%Modern ± 1σ)
Carbonate	+1.8	Background
Barley mash	-26.8	116.35 ± 0.0084 (Gulliksen & Scott, 1995)
ANU Sucrose	-10.5	150.61 ± 0.11 (Rozanski *et al.*, 1992)

Table 2.1 - $\delta^{13}C$ and ^{14}C consensus values for isotopic standards used in the analytical testing programme of the molecular sieve sampling system.

The range of $\delta^{13}C$ values from +1.8 to -26.8 ‰ allowed a stringent test of the sampling system since it covered a much greater range of values than would likely be encountered in the field. The testing programme also enabled a sensitive test for memory effect by alternating capture of standards, i.e. the difference between the Barley mash standard and the Carbonate standard for $\delta^{13}C$ analysis is 28.6 ‰.

The standards had radiocarbon concentrations ranging from 150.6 %Modern (Sucrose) to background (Carbonate). A Sucrose standard following a Carbonate standard effects a difference of ~150 %Modern and again allowed for a sensitive test of memory effect. Each of the two sets of standards were captured and recovered from both of the MSCs (5 and 6) sequentially. All values for ^{13}C are reported using the delta notation with $^{13}C/^{12}C$ variations relative to the international standard Vienna Pee Dee Belemnite (VPDB), as described by the following equation:

$$\delta^{13}C\ (‰) = \left[\frac{(^{13}C/^{12}C)_{Sample} - (^{13}C/^{12}C)_{VPDB}}{(^{13}C/^{12}C)_{VPDB}} \right] \times 1000 \qquad (1)$$

^{14}C data are reported as %Modern with samples being normalised to a $\delta^{13}C$ of -25 ‰ (Stuiver & Polach, 1977).

2.3 Results

2.3.1 Selection of tubing for the MSCs

In addition to the major changes discussed in this section, there were also some minor changes to the molecular sieve cartridge design, one of which was the type of tubing used to attach the Quick Couplings to either end of the quartz glass MSCs. The original cartridge design in use at the NERC Radiocarbon Laboratory, based on a design by Bol and Harkness (1995) utilised clear Versilic tubing (silicone) on one end of the MSCs and black Masterflex tubing (neoprene) on the other (Figure 2.5).

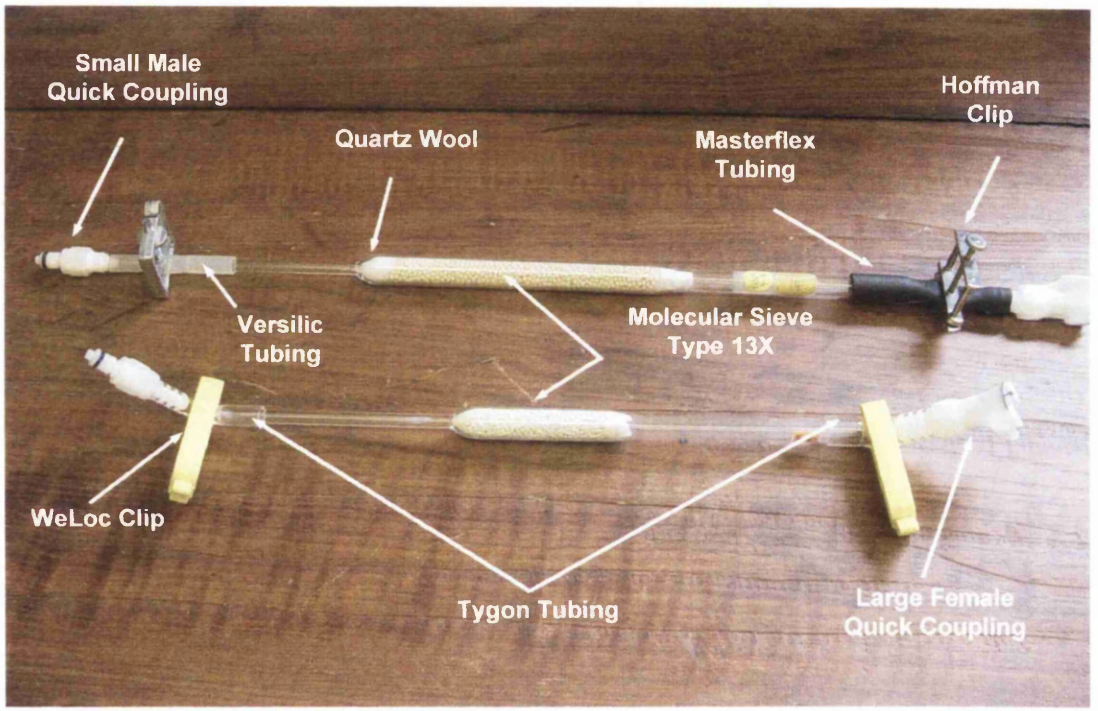

Figure 2.5 - Photograph of the original (top) and new (bottom) designs for the MSCs.

Any tubing type chosen for the final design of the MSCs had to be highly impermeable to CO_2. In order to establish permeability/impermeability, 3 x 5 cm lengths of each tubing type (Masterflex, Versilic and Tygon) were individually attached to the vacuum rig, sealed at the other end with a WeLoc clip and evacuated to 10^{-1} mbar. After one hour the pressure on the transducer was recorded. The results are shown in Figure 2.6.

Masterflex tubing performed almost as well as the Tygon tubing. The Tygon tubing recorded a mean pressure of 0.7 ± 0.6 mbar and the Masterflex tubing recorded a pressure of 1 mbar on each of the three replicated evacuation tests. The silicone tubing was much less competent at holding the same vacuum in comparison to the other tubing types. After

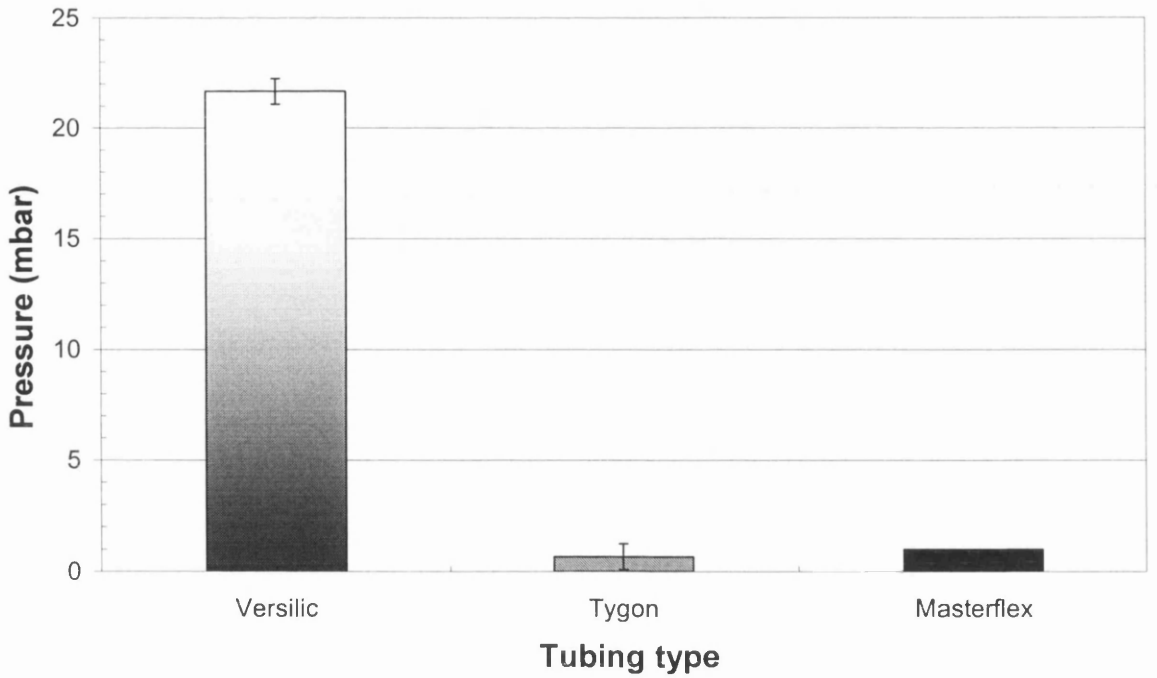

Figure 2.6 – Five cm lengths of each tubing type were attached to the vacuum rig, sealed with a clip and evacuated to 10^{-1} mbar. After 1 hour, the pressure on the transducer was recorded. Measurements are the mean of 3 replicate analyses. Error bars are 1 σ. No error bar is shown for the Masterflex tubing as the pressure recorded on the transducer was identical for each of the three evacuation tests.

one hour the mean pressure recorded on the transducer for the Versilic tubing was 21.7 ± 0.6 mbar. Tygon tubing was chosen for the final design for the MSCs due its superior impermeability and also its flexibility.

A further test was carried out in order to check whether the chosen tubing would degas any significant amount of CO_2. Three 10 cm lengths of Tygon tubing were cut up into small pieces, placed in a combustion tube, evacuated to 10^{-2} mbar and left under vacuum for 4 weeks. On cracking of the combustion tube on the vacuum rig, no CO_2 was recorded and therefore it was considered that this tubing would not degas CO_2 when MSCs were being activated or discharged.

2.3.2 Selection of molecular sieve type

During initial development of the molecular sieve sampling system, testing was undertaken at each stage using CO_2 standards of known volume and $\delta^{13}C$. A selection of these results is presented in Tables 2.2 to 2.5. These tests resulted in modifications being made to the design of the MSCs and the MSC activation and desorption procedures; the tests are described in the discussion. Results of tests on molecular sieve type 5A are not reported, as recoveries for the first 3 standards tested, were less than 25 %. Testing of this molecular sieve type was abandoned in favour of type 13X. Testing of molecular sieve type 4A was

initially undertaken in order to eliminate any potential problems that might occur through unwanted molecules such as hydrocarbons back-diffusing from the vacuum pump (Karlsson, 2002).

2.3.2.1 Molecular sieve type 4A

The results in Table 2.2 demonstrate the variability found in the $\delta^{13}C$ analyses when using

Run Order	Molecular Sieve Type	Percentage Recovery	$\delta^{13}C_{VPDB}$ (± 0.1 ‰) (Standard)	$\delta^{13}C_{VPDB}$ (± 0.1 ‰) (After capture)
Previous	4A	-	-12.5	-
1 (1)	4A	95	-12.4	-12.3
2 (1)	4A	89	- 4.0	-5.1
3 (1)	4A	96	- 27.2	-25.9
Previous	4A	-	Unknown	-
1 (2)	4A	77	- 27.5	-27.4
2 (2)	4A	78	- 12.7	-11.7
3 (2)	4A	31	- 26.9	-26.3
4 (2)	4A	96	- 26.9	-26.7
Previous	4A	-	Unknown	-
1 (3)	4A	92	- 12.5	-9.7
2 (3)	4A	64	- 26.9	-26.7
3 (3)	4A	73	- 26.9	-27.4

Table 2.2 - $\delta^{13}C$ measurements for standard gases before and after adsorption and desorption from molecular sieve sampling cartridges 1, 2 and 3 containing molecular sieve type 4A. Numbers in brackets beside the run order identify which of the 3 MSCs were used. The $\delta^{13}C$ measurements are the mean of 2 replicate analyses.

molecular sieve type 4A to capture standard gas released into the sampling chamber. Recoveries varied greatly, from between 31 and 96 %. There are only four instances in Table 2.2 where the $\delta^{13}C$ value of the recovered CO_2 was within 2 σ of the consensus value for the standard gas. Results 1 (1) and 4 (2) in Table 2.2 are within 2 σ of the consensus value. However, it is noteworthy that the previous standard was of the same $\delta^{13}C$ value and as a consequence both these results would not have been subject to changes in isotopic composition due to hysteresis.

It should be noted here that the only modifications to the original MSC design that had been made during the testing of molecular sieve type 4A were to the tubing and the type of clips used. The remainder of the modifications e.g. cartridge length, were made during the testing of molecular sieve type 13X. Therefore, some of the problems encountered with

molecular sieve type 4A may have been due to the MSC design and not the molecular sieve type itself.

2.3.2.2 Molecular sieve type 13X

Table 2.3 shows the improved quantitative recoveries and $\delta^{13}C$ measurements obtained for the CO_2 standards used to test MS^3 on first use of molecular sieve type 13X.

Run Order	Molecular Sieve Type	Percentage Recovery	$\delta^{13}C_{VPDB}$ (± 0.1 ‰) (Standard)	$\delta^{13}C_{VPDB}$ (± 0.1 ‰) (After capture)
1 (4)	13X	96	-27.0	-26.9
2 (4)	13X	66	-27.0	-26.5
3 (4)	13X	87	-27.0	-26.9
4 (4)	13X	88	-27.0	-26.8
5 (4)	13X	89	-27.0	-27.1

Table 2.3 - Quantitative recoveries and $\delta^{13}C$ measurements obtained during initial testing of molecular sieve type 13X. Standards used all had the same $\delta^{13}C$ value. Numbers in brackets beside the run order identify the MSC that was used.

Recoveries ranged between 66 and 96 %, with one standard, 2(4), failing to measure within 2 σ of the consensus value. This standard also had the lowest quantitative recovery at 66 %. Once the majority of standard recoveries and delta values were in (or close to) the desired range (between 85 and 100 % for quantitative recovery and 2 σ of the consensus values for $\delta^{13}C$), it was decided to test the MSCs and the sampling system for memory effect. This objective was achieved by alternating the $\delta^{13}C$ contents of the standards introduced to the sampling chamber and by collecting them consecutively on the same MSC. A selection of the results is shown in Table 2.4.

Run Order	Molecular Sieve Type	Percentage Recovery	$\delta^{13}C_{VPDB}$ (± 0.1 ‰) (Standard)	$\delta^{13}C_{VPDB}$ (± 0.1 ‰) (After capture)
Previous	13X	89	-27.0	-27.1
1 (4)	13X	76	-3.8	-6.4
2 (4)	13X	91	+1.8	+1.1
3 (4)	13X	85	-3.4	-1.9
4 (4)	13X	98	-27.0	-26.5

Table 2.4 - Quantitative recoveries and $\delta^{13}C$ values for CO_2 standards of varying isotopic ratio applied alternately to the same MSC (4). The $\delta^{13}C$ measurements are the mean of two replicate analyses.

The mean recovery for standards in Table 2.4 is 88 %. However, none of the standards once they had been captured by the sampling system and then purified on the vacuum rig were within 2 σ of the consensus values. The standard with a $\delta^{13}C$ value closest to the consensus value is 4(4), this is also the standard with the highest recovery at 98 %. The recovered standard that had a $\delta^{13}C$ value furthest from the consensus value is 1(4) also had the lowest recovery of all the standards contained in Table 2.4 of 76 %.

The results, in Table 2.4 show that, in general, the higher the recovery of a standard the closer the $\delta^{13}C$ ratio of the recovered CO_2 is to that of the expected value (consensus value). In addition, it can also be seen from Table 2.4 that the $\delta^{13}C$ ratio obtained for each recovered standard falls to the same side of the consensus value that the previous standard lay on. For example, in Table 2.4, the consensus value for standard 1(4) is -3.8 ‰. The value after capture for this standard is more depleted and has a $\delta^{13}C$ of -6.4 ‰, which falls to the same side of the consensus value as the previous standard captured by the MSC (-27.0 ‰). Conversely, standard 3(4) in Table 2.4 has a $\delta^{13}C$ of -3.4 ‰ similar to that of standard 1(4). The value after capture of this standard is -1.9 ‰, which is more enriched than the $\delta^{13}C$ value of the applied standard, but once again falling to the side of the consensus value that the previous standard (+1.8 ‰) lay on. This suggests that there is a carry over of CO_2 from one standard to the next, due to incomplete desorption.

2.3.3 Modifications to the original MSC design

As recoveries were not 100 % or close to 100 %, it was deduced that a small amount of hysteresis (or memory effect) was taking place. A check on the temperature variation from the outside edge of the tube furnace, to its centre, was carried out. The temperature was measured at varying distances inside the furnace using a mercury thermometer and the results are depicted in Figure 2.7.

Figure 2.7 clearly demonstrates that the temperature at the ends of the furnace was not the same as the temperature displayed on the digital readout of the furnace (500 °C). At 5 mm inside the furnace from the outer edge, the temperature recorded was approximately 200 °C cooler than that displayed on the digital readout. In fact, it was not until ~ 34 mm from the edge towards the centre of the furnace, that the temperature inside the tube reached 500 °C. It was considered at this point that incomplete desorption of CO_2 adsorbed onto molecular sieve type 13X held within the MSCs would occur unless all the molecular sieve material

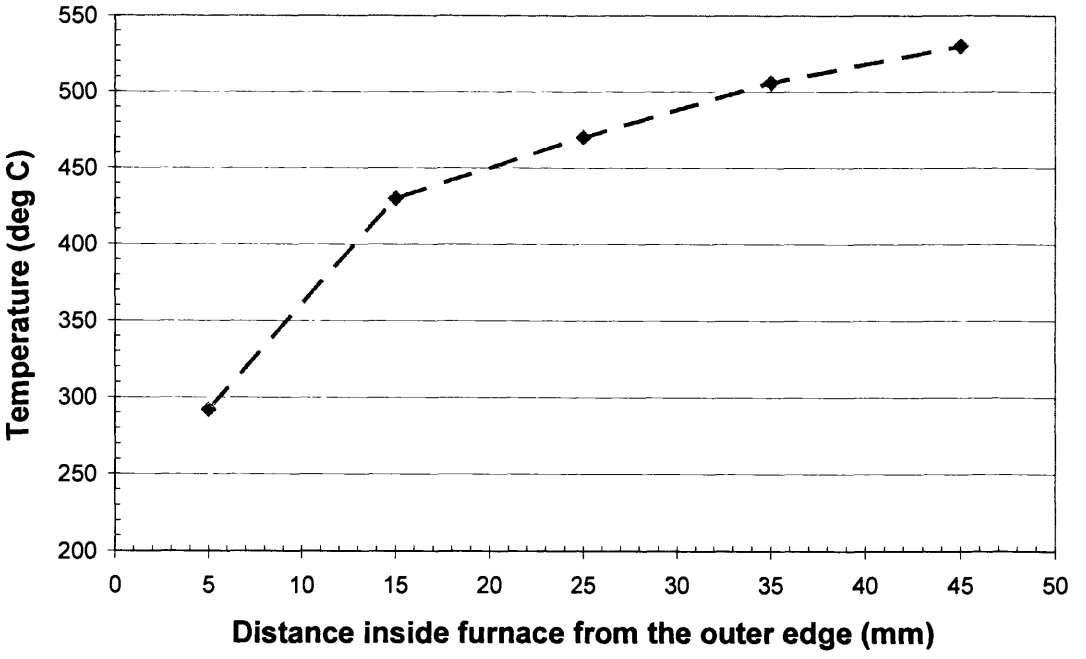

Figure 2.7 - Plot of temperature versus distance from the outer edge of the tube furnace. The temperature recorded on the digital display of the furnace was 500 °C. The total length of the tube inside the furnace was 152 mm.

was at 500 °C. The design of the quartz MSC was modified so this was the case. The length of the main body of the MSC was reduced from 150 mm to 75 mm (see Figure 2.5).

Following the modifications to the MSC design, it was important to check that the reduced volume of molecular sieve type 13X held in the new MSC design, would adsorb enough CO_2 for analysis by IRMS, AMS and also enough to be able to archive a fraction of each sample. In addition, it was important to test the time taken and volume of CO_2 adsorbed before breakthrough occurred (less than 100 % adsorption taking place). An activated MSC was attached to an air cylinder (~ 900 ppm CO_2) and the IRGA as shown in Figure 2.8.

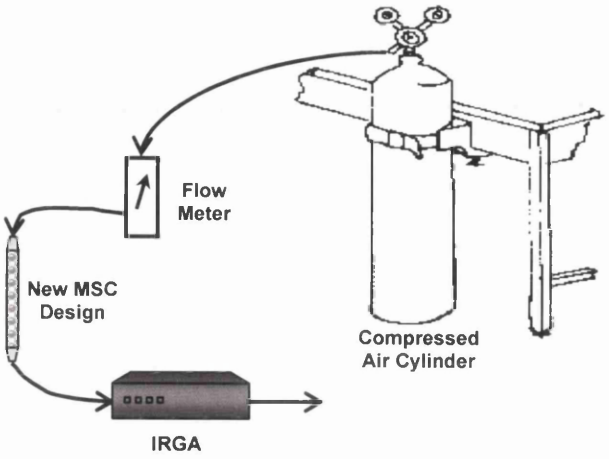

Figure 2.8 - Schematic of setup used to test the time to reach breakthrough for the new smaller MSC design.

The flow rate was set at 500 ml min^{-1} and the air from the cylinder was allowed to pass through the activated MSC. The concentration of CO_2 exiting the MSC was recorded on the IRGA and the results are depicted in Figure 2.9.

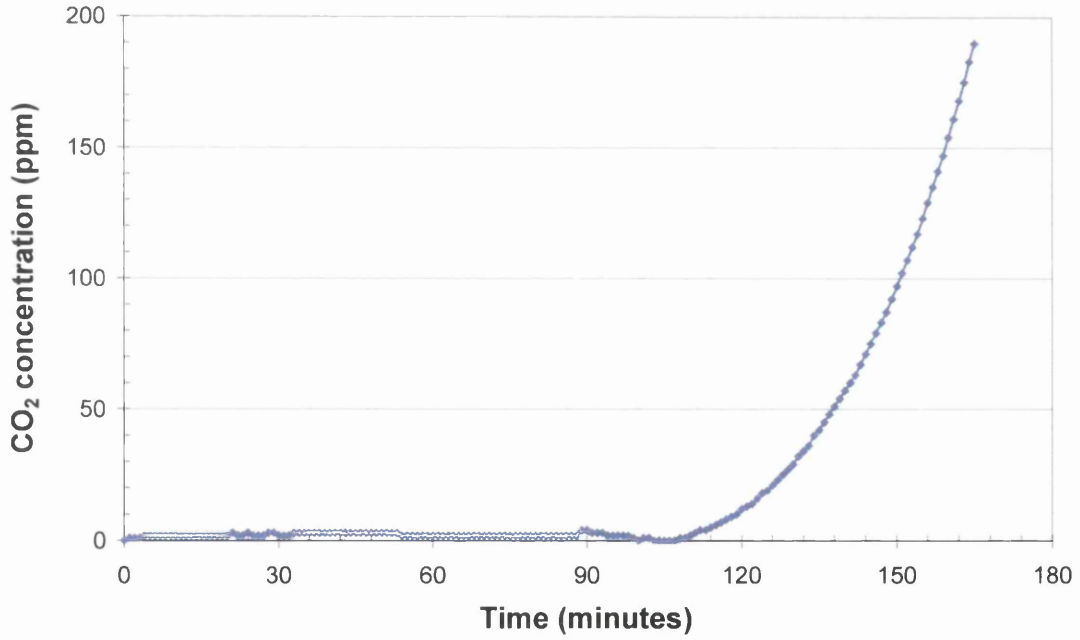

Figure 2.9 - Plot of time versus CO_2 concentration exiting the new smaller design for the MSCs.

As can be seen from Figure 2.9, the MSC removes 100 % of the CO_2 in the air stream flowing from the compressed air cylinder for ~ 111 minutes. At this point breakthrough is reached and the concentration of CO_2 rises exponentially. If the CO_2 was allowed to flow through the MSC, eventually the MSC would become completely saturated and the input to

the MSC from the cylinder (~ 900 ppm) would equal the output. The plot would then resemble something not too dissimilar to a Langmuir adsorption isotherm.

After the aforementioned checks and modifications had been made, another suite of CO_2 standards for IRMS analysis were applied to a single MSC. Again the ^{13}C content of these standards was varied alternately to check that no hysteresis was taking place. These results are displayed in Table 2.5.

Run Order	Molecular Sieve Type	Percentage Recovery	$\delta^{13}C_{VPDB}$ (± 0.1 ‰) (Standard)	$\delta^{13}C_{VPDB}$ (± 0.1 ‰) (After capture)
1 (4)	13X	100	-26.9	-27.0
2 (4)	13X	98	+1.8	+1.6
3 (4)	13X	100	-26.9	-26.6
4 (4)	13X	100	-11.5	-11.7

Table 2.5 - $\delta^{13}C$ results and quantitative recoveries for standard gases before and after adsorption and desorption from molecular sieve sampling cartridge 4, containing molecular sieve type 13X. The $\delta^{13}C$ measurements are the mean of 2 replicate analyses.

The data in Table 2.5 show that percentage recoveries for standard gases are ~100 % and $\delta^{13}C$ measurements are all within 2 σ of the standard consensus values.

2.3.4 Final test sequence results for MS^3

The results in Table 2.5 meant that a stringent testing programme (shown in Table 2.6) could be undertaken in order to fully test MS^3, the new MSCs and vacuum rig procedures. The results of the testing programme (both $\delta^{13}C$ and ^{14}C) used to evaluate the final design of the MSCs and procedures are also displayed in Table 2.6. The table shows that all $\delta^{13}C$ results are within 2 σ of the standard consensus values (see Table 2.1). The ^{14}C concentrations of the two Carbonate standards (SUERC-4181 and SUERC-4189) were higher than the usual levels obtained at the laboratory for background standards (i.e. for blanks combusted in sealed quartz tubes or processed by acid hydrolysis), but were identical at 2 σ. The remaining standards were therefore background-corrected using the mean ^{14}C concentration of these two carbonates (1.25 %Modern). With one exception, all results for the radiocarbon standards were within 2 σ of the consensus value.

Run Order	Standard Material	Publication Code	$\delta^{13}C_{VPDB}$ (± 0.1 ‰)	^{14}C Concentration (%Modern ± 1 σ)
Previous	Sucrose	-	-	-
1 (5)	Carbonate	SUERC-4181	+ 1.7	1.23 ± 0.02
2 (5)	Sucrose	SUERC-4182	- 10.7	150.59 ± 0.44
3 (5)	Barley mash	SUERC-4183	- 26.9	116.91 ± 0.36
4 (5)	Barley mash	SUERC-4187	- 26.8	116.37 ± 0.27
Previous	Carbonate	-	-	-
1 (6)	Sucrose	SUERC-4188	- 10.6	150.06 ± 0.41
2 (6)	Carbonate	SUERC-4189	+ 1.7	1.28 ± 0.02
3 (6)	Barley mash	SUERC-4191	- 26.7	114.78 ± 0.28
4 (6)	Barley mash	SUERC-4192	- 26.8	115.94 ± 0.36

Table 2.6 - $\delta^{13}C$ and ^{14}C results for standard gases after adsorption and desorption from molecular sieve sampling cartridges 5 and 6 and subsequent recovery for analysis by IRMS and AMS. Numbers in brackets beside the run order identify which of the two MSCs were used. The $\delta^{13}C$ measurements are the mean of 2 replicate analyses.

All yields were for standards captured during the testing programme were ~ 100 %.

2.4 Discussion

A number of studies have reported the use of various types of zeolite molecular sieve to capture carbon dioxide from air streams for isotope measurement (see Section 2.1.2). Of these, few present the results of tests used to verify their sampling methods. Through the development of the sampling system described in this chapter, a number of changes were made to the original MSC design and operating procedures in use at the NERC-RCL. Only when these changes were made did the sampling system deliver quantitative trapping and recovery of CO_2 with preservation of isotopic integrity.

2.4.1 Selection of molecular sieve type

During the initial development stages of the sampling system molecular sieve types 4A (pore window size 0.42 nm) and 5A (pore window size 0.49 nm, (Dyer, 1988) were tested for CO_2 capture before settling on the use of molecular sieve type 13X (pore window size 0.78 nm). The kinetic diameter[1] (σ) of CO_2 is 0.33 nm (Breck, 1974), calculated from the minimum equilibrium dimension (Pauling) of 0.37 nm (as opposed to the Lennard-Jones

[1] The kinetic (or collision) diameter of a molecule 'is the intermolecular distance of closest approach for two molecules colliding with zero initial kinetic energy' (Breck, 1974) and is used to describe the dimension of an adsorbate or probe molecule with reference to entering (or being excluded from) a pore window of a zeolite.

approach which is used to calculate σ for spherical and non-polar molecules), and so types 4A and 5A were deemed to have pore windows large enough to imbibe the CO_2 molecule. However, improved yields of CO_2 and $\delta^{13}C$ values that were much closer to standard values were obtained on initial testing of zeolite molecular sieve type 13X (Table 2.3). Consequently further testing of types 4A and 5A was abandoned.

Molecular sieve type 3A (effective pore diameter of 0.3 nm) was originally employed as a desiccant but was found to adsorb a small amount of CO_2 despite the fact that σ of this molecule is larger than the effective pore window size of the zeolite. This anomaly could be due to two phenomena: firstly the oxygen framework of a zeolite is capable of being polarised (i.e. distorted). Secondly both the zeolite framework and the adsorbate molecule are continually vibrating under the influence of temperature, the net effect of which is to create changes of ~0.04 nm in the size of the pore window (Dyer, 1988). The combined effect of these processes is the adsorption of molecules of apparently larger diameter than that of the pore windows (measured crystallographically).

2.4.2 Modifications to the original MSC design

One of the first modifications made to the MSC design was the type of clips used to seal either end of the MSCs before and after sampling and to manipulate gas flows around the sampling system. The original design by Bol and Harkness (1995) utilised stainless steel Hoffman clips. These clips are relatively heavy and unwieldy to use and in addition require care to ensure that the tubing is sealed (plates of the Hoffman clip have to be parallel). These were replaced with WeLoc clips which are much easier to use, particularly in the field, lighter and maintained the desired vacuum (10^{-2} mbar).

A minor but important modification made was to the type of tubing used to attach the Quick Couplings to both ends of the MSCs. The tubing types used on the original design were made from silicone (Versilic) and neoprene tubing (Masterflex). Silicone tubing in particular was found to be quite poor compared to Tygon (PVC) or Masterflex tubing at holding a vacuum (10^{-1} mbar) for any length of time (Figure 2.6). After just one hour, the silicone tubing had allowed the pressure on the transducer rise from 0 to 22 mbar, whereas the pressure increased by only 1 mbar (the error of the pressure transducer) using the PVC tubing. Not only did the PVC tubing outperform the silicone at keeping the desired vacuum, it allowed the MSCs to be pumped down to a superior vacuum of 10^{-2} mbar (10^{-1} mbar was the best vacuum that could be reached using silicone tubing). This also meant

that the Tygon tubing would be less permeable to atmospheric CO_2 and therefore reduced the possibility of sample contamination.

Another important modification to the MSCs was to reduce the length of the part of the quartz glass cartridge containing the zeolite molecular sieve material. Originally, this part of the MSC was the same length as the tube furnace used for desorption of CO_2 as based on the design of Bol and Harkness (1995). From their tests, Bol and Harkness (1995) reported mean CO_2 recovery rates of ~ 88 % of (although they had other evidence suggesting greater recovery rates). However, with incomplete recovery of a sample, the risk of isotopic fractionation and memory effect remains.

In the centre of a tube furnace there is a zone of uniform temperature (Carbolite, No date) which extends only to about 2.5 times the diameter of the tube measured from the outside of the furnace. Any area outside this central zone is likely to be at a lower temperature due to heat loss at the ends of the furnace (Figure 2.7). Only when the length of the main body of the MSC was reduced so that all the molecular sieve material was within the zone of uniform temperature did sample recoveries consistently reach ~100 % and isotope results agree with consensus values (Table 2.5 and Table 2.6). Prior to this modification it is possible that some CO_2 that had been desorbed at 500 °C from within the zone of temperature uniformity was re-adsorbed onto cooler zeolite outside the zone. This was confirmed by moving the tube furnace backwards and forwards around the ends of the MSC whilst the MSC was attached to the vacuum rig during discharge, which resulted in an increase in pressure registered by the vacuum gauge.

In the procedure of Bol and Harkness (1995) MSCs were prepared by heating to 500 °C and evacuating to a best vacuum of 0.05 to 0.1 torr. This vacuum was increased to 10^{-2} mbar (0.0075 torr) for both activation and sample desorption. In this study a higher vacuum ensured a sample recovery of >97 % and an isotope value consistent with the consensus values. The lower recoveries (~88 %) observed by Bol and Harkness were therefore most probably due to incomplete desorption of CO_2 from the zeolite molecular sieve.

After all modifications were made the sampling system was tested and the results are presented in Table 2.6. Since all $\delta^{13}C$ results and all but one of the ^{14}C results of the standards recovered using the system fell within 2 σ of the consensus values, the results demonstrate that the sampling system collects isotopically representative samples of CO_2 from air streams.

The ^{14}C concentration of the Carbonate background standard was observed to be higher than the usual laboratory background (blank). This was not surprising given the greater number of potentially contaminating steps involved in the capture and desorption of the Carbonate standard (e.g. large surface areas of the molecular sieve material and the sampling system). It is possible that further modifications to the system could be made to provide a lower background value. For example, the replacement of quartz glass wool within the body of the MSCs, with silver wool or glass sinters, would reduce particles or fragments getting into the vacuum rig, thereby reducing contamination potential. In addition, a superior tubing to Tygon R3603 could be investigated. Whilst this tubing holds an excellent vacuum, it deteriorates over time, and has to be replaced on a regular basis to prevent the possibility of contamination from atmospheric CO_2.

Current background levels using the MSCs are not considered to pose a particular limitation. Firstly, the ^{14}C concentrations for the two background standards were statistically identical, suggesting a constant contribution that can be used to background-correct the other results. Secondly, the system is intended for the measurement of the ^{14}C concentration of ecosystem respiration, which is likely to be modern (Gaudinski *et al.*, 2000), and therefore little affected by variations in background.

A 1 σ error of $\pm$ 0.1 ‰ is attributed to IRMS measurement of $\delta^{13}C$. The $\delta^{13}C$ results were all within 2 σ of the consensus values showing that the sampling system enabled capture, recovery and analysis of a CO_2 sample without isotopic fractionation. For ^{14}C, there may be a suggestion of a memory effect in the results presented in Table 2.6 with, for example, the ^{14}C result for SUERC-4191 falling to the side of the previous standard applied to the MSC. However, there are also instances in the results that would not indicate any memory effect, for example, the result for SUERC-4182 (150.59 % Modern) is almost exactly the same as the consensus value (150.61 % Modern), yet the previous standard applied to the MSC was a background standard (SUERC-4181).

The single result which fell outside the consensus value (SUERC-4191) could possibly be explained by a small amount of air contamination, assuming air would have a modern ^{14}C concentration of about 107 % Modern (Levin & Kromer, 2004). However, there are many examples in Table 2.6 that strongly suggest that they have not been contaminated with air. In the example of SUERC-4191, due to the amount of air required, it is likely that the contamination would also have been reflected in a detectable shift in the $\delta^{13}C$ result (which was not the case). One possible reason might be that a very small amount of atmospheric CO_2 might have entered the mass spectrometry tube whilst sub-sampling the aliquot that

was to be used for AMS measurement. If this were the case, the aliquot sampled for IRMS measurement would not be affected. Consequently, since the results from the measurement of both ^{13}C and ^{14}C concentration, for a range of different standards, fell within 2 σ error of the consensus value (with the exception of one ^{14}C result), it is considered that the developed molecular sieve sampling system provides a reliable method to collect isotopically representative samples of CO_2 from air streams.

2.5 Conclusions

A sampling system has been developed and tested (Hardie *et al.*, 2005) for the collection of CO_2 from air, which is easy to use, safe, portable and suitable for use in the laboratory or at remote locations. Results from the measurement of standards collected using the system show that it can be used reliably to capture representative samples of CO_2 for isotopic studies. Although primarily designed for use in carbon isotope studies of soil and plant respiration, the system can be used for other applications that require CO_2 collection from air. For example, by attaching the molecular sieve sampling system to a floating chamber (Figure 2.10), Billett *et al.* (2006) were able to capture CO_2 evasion from peatland streams for radiocarbon analysis. These measurements provide the first ever direct measurements of stream evaded CO_2 for radiocarbon analysis.

Figure 2.10 - Photograph of MS^3 attached to a floating chamber (Billett *et al.*, 2006), used to capture CO_2 evasion from a peatland stream in the Upper Conwy, Wales, February 2006. Photograph supplied courtesy of Dr. Mike Billett, CEH Edinburgh, UK.

3 Flux and stable isotope ($\delta^{13}C$) signature of ecosystem respiration and its constituent components

3.1 Introduction

Among the greatest uncertainties in our efforts to better constrain the global carbon cycle are potential and existing feedbacks that link processes occurring within terrestrial ecosystems (primarily photosynthesis and respiration) to global levels of atmospheric CO_2 (Pataki *et al.*, 2003). Terrestrial ecosystems contain approximately three times as much carbon as is currently resident in the atmosphere (750 Gt). Furthermore, soils, not vegetation, contain the vast majority of the terrestrial carbon stock (72%). Peatland soils are especially important as they are estimated to hold 455 Gt of carbon, a figure that is approximately equal to one third of the global soil carbon stock (Gorham, 1991). There is therefore an urgent need to accurately quantify sequestration and release of carbon from these soils in order to model and predict the potential effects that existing and future global change will have on carbon fluxes occurring within these ecosystems.

Soils within northern latitude ecosystems (e.g. boreal and subarctic soils) are subject to relatively low temperatures, with peatland soils also experiencing low oxygen contents. Both these parameters individually or interactively, lead to slow rates of decomposition and nutrient cycling that ultimately allows these systems to sequester such large amounts of carbon. In these harsh climatic environments, key ecosystem processes such as those that control carbon loss and sequestration (e.g. respiration and photosynthesis, nutrient retention and release and the formation of soil organic matter) may be very closely linked to chemical and physical factors in their surrounding environment (Wookey *et al.*, 2002). Furthermore, small changes in the environment have the potential to exact large effects on the function and structure of plant and soil systems (Wookey *et al.*, 2002) possibly resulting in an alteration of the net carbon flux.

Carbon dioxide fluxes have been measured in a wide range of ecosystems including grasslands (Norman *et al.*, 1992; Ostle *et al.*, 2000), agricultural soils (Byrne & Kiely, 2006), tropical soils (Grace *et al.*, 1995), forests (Dixon *et al.*, 1994), Arctic tundra (Wookey *et al.*, 2002) and peatlands (Alm *et al.*, 1999; Chapman & Thurlow, 1996; Moore *et al.*, 2002). Northern peatland soils are currently of particular scientific interest, not just

because they are huge reservoirs of carbon but also because it is at these high latitudes that climatic warming is expected to have the greatest impact (IPCC, 2001).

Flux measurements allow quantification of changes in carbon storage/release taking place within an ecosystem; however, they do not allow partitioning of overall observed ecosystem flux into its individual component source fluxes (e.g. autotrophic and heterotrophic respiration). To identify and quantify the contribution to total ecosystem respiration of individual component sources we can use isotopic measurements (Charman *et al.*, 1999; Dawson *et al.*, 2002; Hemming *et al.*, 2005; Kuzyakov, 2006; Ostle *et al.*, 2000; Staddon, 2004; Wookey *et al.*, 2002; Yakir & Sternberg, 2000).

Carbon has two stable isotopes, ^{12}C, which makes up approximately 98.89 % of all naturally occurring carbon atoms and ^{13}C, which makes up 1.11 %. During photosynthesis carbon undergoes isotope fractionation by way of a number of physical and chemical processes (e.g. diffusion and carboxylation). This fractionation leads to plant matter being depleted in $^{13}CO_2$ relative to the atmosphere, with the $\delta^{13}C$ of plant material ranging from ~ -9 to ~ -32 ‰ (Boutton, 1991a), depending on which photosynthetic pathway has been utilised (C_3, C_4 or CAM).

Isotope measurements have an advantage over many other partitioning techniques because they can be used *in situ* (isotope measurements effect minimal disturbance) as well as *ex situ*. Isotope techniques that are used in the partitioning of ecosystem respiration include: continuous labelling, pulse labelling, repeated pulse labelling and natural abundance methods using either ^{13}C or ^{14}C as a tracer (Hanson *et al.*, 2000). However, natural abundance techniques require there to be a significant difference in the isotopic composition of the sinks and sources in question (Dawson *et al.*, 2002).

Consequently, studies have generally been confined to investigating the natural difference in $\delta^{13}C$ values of organic matter derived from C_3 (c. -27 ‰) and C_4 (c. -15 ‰) plants in order to source the origin of soil respired CO_2 in the field (Ineson *et al.*, 1996; Rochette & Flanagan, 1997; Rochette *et al.*, 1999; Trumbore *et al.*, 1995). Experiments exploiting the large difference in $\delta^{13}C$ between the two different photosynthetic pathways are usually carried out on soils that have been subjected to land use conversion (e.g. the cutting down of tropical forest to make way for agricultural crops) or crop rotation (e.g. a maize crop (C_4) planted on soil that formerly held C_3 crops).

Plants metabolise leaf substrates e.g. glucose and release the carbon as CO_2. This CO_2 may or may not be enriched in ^{13}C relative to the respiratory substrate used but does leave a distinct imprint on the atmosphere due to the fact that plants respire CO_2 that has a carbon isotope composition that is depleted relative to that of the atmosphere ($\delta^{13}C = \sim -8.5$ ‰ (Hemming *et al.*, 2005)). Recent evidence suggests that there are large enough variations between ecosystem respiration sources such that differences in the $\delta^{13}C$ values are measurable, thus allowing collective respiration sources within total ecosystem respiration to be partitioned (Tu & Dawson, 2005). For example, Ghashghaie *et al.* (2001) demonstrated that respired CO_2 had a carbon isotope composition that was enriched by several per mil compared to bulk leaf material and indeed enriched relative to sucrose, the most ^{13}C-enriched leaf metabolite. Ghashghaie *et al.* (2003) postulate that, to conserve mass, this enrichment in ^{13}C could be due to lipid formation, as respiration and lipid formation are both closely related biochemical systems. Ghashghaie *et al.* (2001) also demonstrated that the $\delta^{13}C$ value of respired CO_2 varies from species to species and also under changing environmental conditions where the same substrate (e.g. sucrose) is used as the source for respiration.

Finally, any change in the species composition of an ecosystem (e.g. due to climate change) could have a knock-on effect on the ecosystem's carbon sink-source function, as plant community composition directly and indirectly affects fluxes of carbon within an ecosystem (as they are the primary producers). For example, species composition determines the fundamental input of carbon (both production and carbon isotope composition) to an ecosystem. Secondly, species composition (and hence substrate quality) also plays an important role in determining carbon release from a system (Swift *et al.*, 1979). Therefore, a shift from species that are easily decomposed by the microbial soil community to species that are more difficult to breakdown could lead to an increase in C stored in the soil.

It is therefore of vital importance to quantify the contribution of individual plant species to carbon cycling within an individual ecosystem in addition to the soil contribution. With this in mind, the specific aims of this investigation were threefold. The first aim was to determine the contribution of different plant types (monocots, ericoids and bryophytes) to total ecosystem respiration. Secondly, to examine the role that plant community composition plays in the stable carbon isotope composition of natural abundance CO_2. Finally, to attempt to quantify and partition *in situ*, total peatland ecosystem respiration

into its individual heterotrophic and autotrophic components (i.e. plant and soil respiration).

The hypotheses for this investigation were as follows:

1. Peatland CO_2 fluxes are influenced by the presence or absence of different plant functional types (shrubs, mosses or monocots).

2. The presence or absence of specific plant functional types alters the net $\delta^{13}C$ signature of peatland ecosystem respiration.

3. That peat respiration is more depleted than plant respiration.

To test our hypotheses respired carbon dioxide was captured from a plant species removal experiment (see section 3.2.2) established within a peatland ecosystem and the CO_2 concentration and stable carbon isotope composition of fluxes analysed by GC and IRMS respectively. The measurements were then combined to investigate the second and third aims by utilising an established ecosystem carbon flux approach (i.e. Keeling plot) and mass balance in a two-end member system. In addition to respiration, samples of vegetation and soil were collected for $\delta^{13}C$ determination (i.e. to characterise the substrates utilised for respiration).

3.2 Materials and methods

3.2.1 Site Description

Moor House National Nature Reserve (UK National Grid ref. NY70 30 – Figure 3.1) was chosen as the study site, an area of blanket bog moorland considered to be representative of British upland terrain (Heal & Smith, 1978). Glacial till underlies a range of soil types (Garnett, 1998), the most dominant soil type in the Reserve being blanket bog, which is thought to have begun accumulating around 7500 years ago (Heal & Smith, 1978). Moor House peat is classified as oligo-fibrous (Avery, 1980) and forms a part of the Winter Hill soil series (Carroll *et al.*, 1979). The lowest part of the Reserve rests at a height of 290 m above sea level, rising to a maximum altitude of 848 m. The western region of the Reserve is characterised by steep slopes and extensive upland grassland while the eastern side is covered with blanket bog and associated vegetation species e.g. *Sphagnum* spp. (moss), *Calluna vulgaris* (heather) and *Eriophorum vaginatum* (cotton grass) (Eddy *et al.*, 1969).

Figure 3.1 - The eastern side of Moor House National Nature Reserve, northern Pennines.

Current mean annual precipitation for the Reserve is 2016 mm and mean annual temperature is 5.3 °C (at a height of 550 m) with climate falling into the subarctic oceanic classification (Evans *et al.*, 1999). The blanket bog at Moor House is mostly ombrotrophic (systems in which nutrients and water are supplied mainly *via* rainfall) and the length of the growing season (defined as days on which the mean diel temperature is > 5.6 °C) is approximately 180 days (Heal & Smith, 1978). Temperature is critical for vegetation production as new growth rarely begins until 5.6 °C is reached (Perkins *et al.*, 1978).

Studies first began at Moor House with the installation of a weather station in the 1930s (Manley, 1936) and since then the Reserve has had a long history of research. Studies performed at Moor House have been many and diverse and include investigations into: vegetation type (Eddy *et al.*, 1969), vegetation productivity (Forrest & Smith, 1975), nutrient dynamics (Harrison & Harkness, 1994), dissolved organic matter (Tipping *et al.*, 1999), hydrology (Conway & Millar, 1960), microbiology (Latter *et al.*, 1967), the effects of burning (Garnett *et al.*, 2000) and sheep grazing (Rawes, 1981) combined, on water table depth (Worrall *et al.*, 2007). In addition, the Reserve is part of the UK Environmental Change Network (ECN) and as such has been and continues to be used to obtain long-term datasets through the monitoring of a wide range of ecological variables identified as being of major environmental importance (Sykes & Lane, 1997).

All samples in this investigation (CO_2, vegetation and soil) were taken from an experimental site within the Reserve - Hard Hill (NY735 335 – Figure 3.2) - an area characterised by gentle slopes with typical blanket bog/moorland vegetation. The site

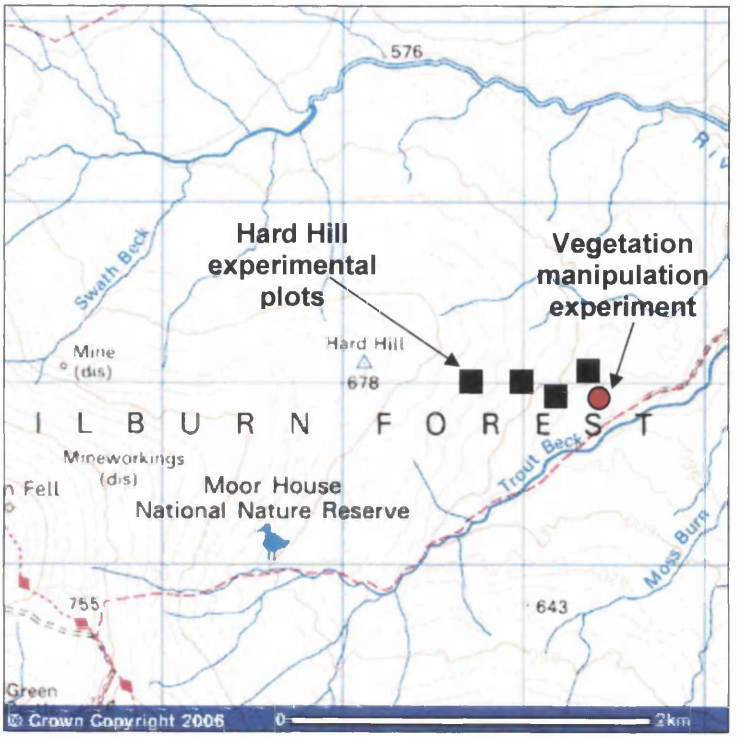

Figure 3.2 - Ordnance survey map showing the Hard Hill site (National Grid ref. NY735 335) within Moor House NNR. The long-term experimental plots at this site are marked by squares. A red circle marks the vegetation manipulation experiment (next to Block A). Map reproduced by kind permission of Ordnance Survey. © Crown Copyright NC/06/60264.

chosen for the experimental work in this chapter was directly adjacent to Block A (Figure 3.2) which rests at an altitude of 590 m (1935 feet). A full description of the long-term burning and grazing experiments, set up at this site in 1954, is detailed in Garnett (1998) and Ward (2006). The site chosen had not previously been used for experimental work but some light grazing would have taken place. This particular site was selected because plant species cover was homogeneous. Plant community composition included *Sphagnum* spp., *Calluna vulgaris* and *Eriophorum vaginatum* (the predominant monocot). The average peat depth at the Hard Hill site is approximately 1 to 2 metres (Garnett, 1998).

3.2.2 Previous carbon isotope studies at Moor House NNR

Of all the soil types present within Moor House NNR, the blanket peat (as opposed to soil types such as brown podzols and stagnohumic gleysols) contains by far and away the largest volume of organic carbon (Garnett, 1998; Garnett *et al.*, 2001). One of the most comprehensive carbon isotope studies performed on the blanket peat was carried out at the Hard Hill site by Garnett and Stevenson (2004). Garnett and Stevenson (2004) used the radiocarbon bomb spike of the 1950s and 60s to date the surface layers of the blanket peat as surface layers are considered to have high temporal resolution, relative to deeper layers (due to the fact that they have not undergone as much decay or compaction).

In addition, Garnett and Stevenson (2004) attempted to validate their method (radiocarbon dating of plant macrofossils extracted from the peat and matching them with the atmospheric $^{14}CO_2$ record) by comparison with independent chronological markers such as layers rich in charcoal (produced during burning events) and spheroidal carbonaceous particles (SCPs). SCPs are produced during incomplete combustion of fossil fuels such as oil and coal and can be used as a chronological marker because increases in their occurrence in the peat profile have been shown to reflect local variations in industrialisation (Wik & Renberg, 1996).

The study by Garnett and Stevenson (2004) demonstrated that by calibrating the ^{14}C dates of the surface peat with the atmospheric $^{14}CO_2$ record (e.g. Levin & Kromer, 2004), the ^{14}C chronology compared well and was in 'broad agreement' with the charcoal derived chronologies. However, it was also shown that the concentration of radiocarbon in the peat did not exactly match the atmospheric $^{14}CO_2$ record. It was suggested that this may have been due to contamination of plant macrofossils with SCPs (which adhere well to *Sphagnum* macrofossils (Punning & Alliksaar, 1997), thereby causing a dilution of the radiocarbon signal), or to differences in the incorporation of plant material during peat growth or possibly to site disturbance.

Another study, the first of its kind in the UK, investigated soil carbon storage (using traditional methods such as % loss on ignition to determine % organic matter) and soil carbon turnover (that utilised more novel techniques such as radiocarbon measurement), was carried out by Harrison and Harkness (1994) in the early 1990s. Harrison and Harkness (1994) investigated soil carbon storage along an altitudinal sequence (on the Western slopes of Great Dun Fell, Moor House NNR) over which the mean annual temperature varied by 2 °C. Soil cores were removed from the surface layers of peat (peaty podzols and peaty gleys) with vegetation left intact, at several points along a transect, and divided into three sections (litter, 0-2 cm and 2-5 cm).

Harrison and Harkness (1994) showed that soil carbon and organic matter storage increased by a factor of 2 over the altitudinal range they investigated (~ 450-750 m), thus demonstrating that upland soils store considerably larger amounts of carbon in comparison to lowland soils. Radiocarbon analyses revealed that the mean residence time of carbon in these soils ranged from between 5 and 40 years in the litter layer to between 360 and 1750 years for the 2-5 cm layer; the litter layers being younger due to continued input from above ground plant production. Furthermore it was shown that the greatest carbon turnover

rates occurred in the litter layer, with turnover rates decreasing markedly with increasing depth from the surface.

Harrison and Harkness (1994) also demonstrated that the age of soil organic matter increased with altitude (although there were some deviations within both soil types at the 500-550 m sampling point). In addition, it was shown that carbon turnover rates within the litter layer and the two soil layers (0-2 and 2-5 cm) decreased with increasing altitude. Finally, Harrison and Harkness (1994) concluded from this study, that much of the carbon that was stored just a few cm below the peatland surface was old and stable, but, they suggested that environmental changes such as erosion, land use change and in particular increases in temperature caused by climate change, could lead to loss of this carbon to the atmosphere.

Other studies within Moor House NNR have included an examination of the effect of climatic regulators on leaching of organic matter from acidic soils, such as those found on the slopes of Great Dun Fell (Tipping *et al.*, 1999). This three-year study involved transplanting soil cores removed from near the summit of Great Dun Fell to three sites further down the hillside, all of which were subject to lower temperatures and smaller volumes of precipitation. Tipping *et al.* (1999) demonstrated that soil cores subjected to warmer and drier conditions *via* translocation, released significantly more dissolved organic carbon (DOC) from peaty gley horizons (but not from the micropodzols or brown earths; possibly due to adsorption of dissolved organic matter onto mineral surfaces). However, stable and radiocarbon analysis of the DOC (Tipping *et al.*, 1999) revealed that heating had negligible effects on carbon isotope values, except for the possibility of stimulating release of some older carbon from within brown earth soils.

One of the dominant above and belowground faunal species in moorland ecosystems is the enchytraeid (a worm commonly found in acid soils), an organism that is involved in soil decomposition. The feeding behaviour of the enchytraeid and its response to climate change is important as enchytraeid populations in upland soils have been shown to be effected by both changes in moisture and temperature (Briones *et al.*, 1997). Furthermore, increases in soil CO_2 flux have been positively correlated to increases in enchytraeid biomass (Briones *et al.*, 2004). In a study involving soil cores extracted from both the Great Dun Fell and Hard Hill sites, Briones and Ineson (2002) used radiocarbon to examine the feeding habits of the enchytraeid and demonstrated that enchytraeids assimilated soil carbon components with a mean age of 5 to 10 years old relative to the time of fixation from the atmosphere. In addition Briones and Ineson (2002) also showed

that warming led to a change in the radiocarbon content of the enchytraeids food source, indicating that the enchytraeids may have been decomposing differently aged pools of carbon within the soil.

Finally, Bol *et al.*, (1999) examined the natural variation in carbon isotope distributions within a range of soil types (podzols, brown podzols and stagnohumic gleysols) at Moor House. This study demonstrated that in general there was an increase in both the ^{13}C content and the ^{14}C age with depth. In addition, Bol *et al.*, (1999) found that there was a significant correlation between the dominant pedogenic features within each soil type and carbon isotope variation. Bol *et al.*, (1999) suggested that this finding indicated that the carbon isotope composition (^{12}C, ^{13}C and ^{14}C) of SOM was significantly affected by soil forming processes.

The aforementioned studies have concentrated on isotope analyses of various soil types and soil organisms inside Moor House NNR, with particular regard to the potential impacts of climate change. This study will build on the excellent work that has been carried out previously, with the focus being on plant species composition. This is important as expected future changes in climate (IPCC, 2001) may alter the plant species make up of this moorland site; thus influencing the ecosystem sink-source function.

3.2.3 Experimental design

A Latin square design was established with five vegetation manipulation treatments (Table 3.1) replicated five times (Figure 3.3) in September of 2003 by Sue Ward (Ward, 2006).

Treatment No.	Treatment Name	Treatment Description
1	Ecosystem	All peatland vegetation left intact
2	Soil	All peatland vegetation removed
3	No shrubs	Ericoid sub-shrubs removed
4	No monocots	Graminoids and sedges removed
5	No mosses	Bryophytes removed

Table 3.1 - Description of the 5 experimental treatments.

Each individual treatment plot measured 50 cm by 50 cm and was situated within a larger 'buffer' square of dimensions 1.5 m x 1.5 m allowing a 1 m break between each of the treatment squares. The five treatments (Table 3.1) established were as follows: selective removal of graminoids and sedges (monocots), ericoids, bryophytes, or, all vegetation cleared (used to define soil respiration) or no vegetation removal (i.e. ecosystem respiration). The roots within the soil plots were left in place in order to minimise soil

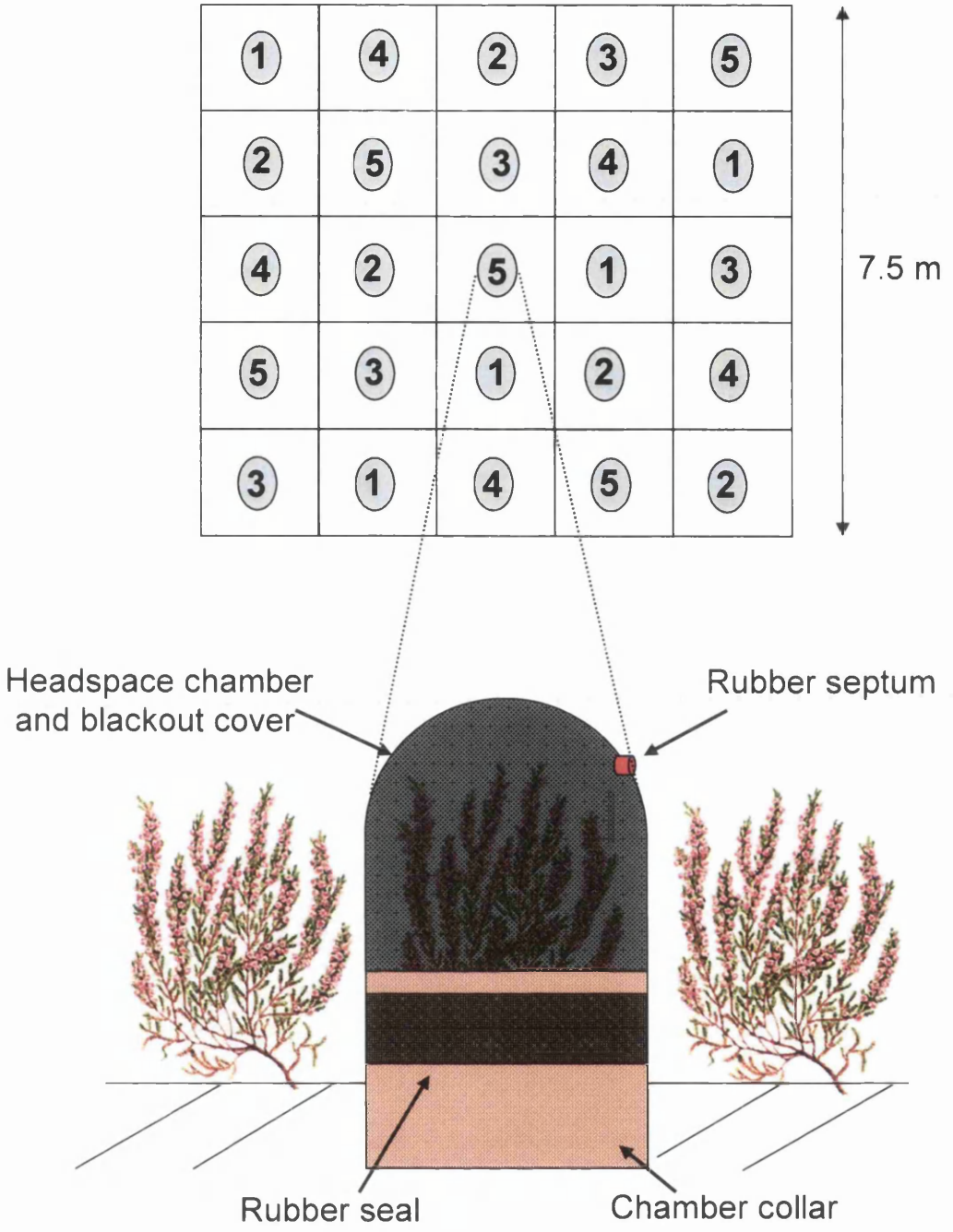

Figure 3.3 - The 5 x 5 Latin square vegetation manipulation experiment at the Hard Hill site. The 5 treatments are represented by a number (Table 3.1). Enlargement depicts peatland respiration chambers designed and tested by Sue Ward (Ward, 2006). Blackout covers were placed over chambers when measuring respiration fluxes.

disturbance. All soil plots were covered with a black muslin-like piece of cloth that allowed water to percolate through but not sunlight. As this experiment was set up 21 months before sampling (May 2005) it allowed ample time for the faster cycling (<1 year) pools of carbon (e.g. root exudates) to decompose within the soil plots. Plots were regularly gardened (monthly) to remove any unwanted species that may have grown within each treatment plot.

Collars for static sampling chambers were constructed from PVC and measured 30 cm in diameter (covering a surface area of 0.071 m^2) and 20 cm depth. Bedding in of collars took place 12 months after selective vegetation removal. Special moorland flux (gross and net) chambers were developed and tested by Sue Ward (Ward, 2006) and attached to chamber collars by means of a rubber seal (Figure 3.3). Chamber blackout covers used during collection of all respiration samples were also designed and tested by Sue Ward (Ward, 2006).

3.2.4 Gas sample collection

Respired CO_2 from each of the treatment plots was captured using a static chamber approach (Heikkinen *et al.*, 2002; Nykänen *et al.*, 2003; Rochette & Flanagan, 1997) under non-steady state conditions. Flux calculations made using static chambers require a closed system. A system that remains open may give misleading flux measurements. However the closed static chamber system is subject to certain caveats e.g. porous soil and roots underneath the chamber collars could result in respiration escaping from within a sampling chamber. With this in mind it was decided to use measurements from chambers where CO_2 concentrations increased monotonically with time and where $\delta^{13}C$ values decreased monotonically with time. If these criteria were not met, it was deemed likely that the chambers were not closed systems and therefore they were removed from mean flux measurements. Chambers that did meet the criteria were considered to be closed systems but it should be noted that the possibility exists that they were not.

Samples of CO_2 taken during a series of time-trials showed that ecosystem respiration build-up within static chambers was linear between 400 and 4000 ppm (Ward, 2006). On commencement of sampling (12^{th} of May 2005), each flux chamber was attached to a chamber collar with the rubber seal (Figure 3.3). The blackout cover was placed over the chamber and a 20 ml sample of gas was removed from the chamber headspace (time point zero). Gas samples were withdrawn from the chamber through a Suba-seal rubber septum (Scientific Laboratory Supplies Ltd, Nottingham, UK), inserted into the PVC chamber (Figure 3.3). Further 20 ml samples of gas were removed from the headspace of all 25 static sampling chambers at a further 5 time points. Headspace gas was removed from chambers using a gastight syringe (Alltech, Carnforth, UK) fitted with a hypodermic syringe needle (16 mm, 25 gauge - Fisher Scientific, Leicester, UK). Samples were then transferred to pre-evacuated (10^{-1} mbar) 12 ml Exetainers (flat bottomed soda glass vials - Labco Ltd, Wycombe, UK) fitted with screw caps that incorporated pierceable rubber septa (see Appendix i for Exetainer testing).

A total of six samples of gas were removed from chambers over a time course of three hours (between 12 and 3 pm) in order to obtain enough samples for a Keeling plot (to estimate $\delta^{13}C$ of source respiration - see section 3.2.8). Air and soil temperatures were recorded during the sampling period using 'Tinyview' temperature loggers (Gemini data loggers, Chichester, UK). On return to the laboratory, the lids of all Exetainer vials containing gas samples were dipped in hot wax and allowed to cool (an extra step carried out as a precaution to ensure the isotopic integrity of each gas sample was preserved). Samples were stored at ~ 20 °C prior to analysis.

3.2.5 Soil and vegetation collection

Samples of peat and peatland vegetation were collected on the same day as respiration samples were obtained. Ideally samples of peat would have been removed from within the individual chamber collars to ascertain whether each of the individual treatments had an effect on the $\delta^{13}C$ of the soil. This was not possible as further experiments were to be carried out, but it was deemed unlikely that an effect caused by the vegetation treatment would be detected in the peat. Cores of peat were removed from an area directly adjacent to the experiment using a stainless steel corer (4.7 x 4.9 x 100 cm) designed to minimise compaction (Cuttle & Malcolm, 1979). The corer was carefully removed from the peat profile and the top 10 cm of each core was placed into labelled plastic bags and kept in a cool box until arrival at CEH Lancaster whereupon samples were frozen until required for analysis.

Tens of grams of live biomass (*Sphagnum* spp., *Calluna vulgaris* and *Eriophorum vaginatum*) were collected from around the Latin square and placed in labelled bags and stored in a cool box until return to CEH Lancaster. All vegetation samples were frozen until required for analysis.

3.2.6 Preparation of soil and vegetation for analysis

Immediately prior to analysis, peat samples were removed from their individual bags and placed in a pre-weighed foil tray. Trays containing peat samples were weighed once more and oven dried at 70 °C until a constant weight. Once dried, samples were ground and homogenised using a pestle and mortar. Sub-samples (up to 2 g) were then ground to a fine homogeneous powder using a liquid nitrogen cooled impact grinding mill (Glen Creston, Crewe, UK). The action of the impactor in the freezer mill in conjunction with the low

temperature created by the liqiuid nitrogen allowed sample material to be ground to an ultra fine powder.

All vegetation samples were treated in the same way as peat samples. After grinding to a fine homogeneous powder sub-samples of vegetation species and soil were placed into individual screwcap vials and sent to the NERC Life Sciences Stable Isotope Facility, CEH Lancaster, for $\delta^{13}C$ analysis by EA-IRMS (Elemental Analysis – Isotope Ratio Mass Spectrometry).

3.2.7 Analysis of soil and vegetation samples

Sub-samples of powdered vegetation and soil were dried again at 70 °C and approximately 2 mg were placed into 6 x 4 mm tin capsules (Elemental Microanalysis Ltd, Okehampton, Devon UK) and sealed. The capsules were loaded into the autosampler of an Elemental Analyser (Eurovector, Milano, Italy), which was coupled in-line to a Micromass Isoprime Stable Isotope Mass Spectrometer (Micromass, Manchester, UK). Reference standards of known isotopic and elemental composition were included after every tenth sample during the run. Internal precision was better than ± 0.2 ‰ (1 σ) for $\delta^{13}C$. All EA-IRMS analyses were performed by Darren Sleep.

Isotopic data are reported using the delta notation with $^{13}C/^{12}C$ variations relative to the international standard Vienna Pee Dee Belemnite (VPDB), as described by the following equation:

$$\delta^{13}C\ (‰) = [(R_{sample} / R_{standard}) - 1] \times 1000 \qquad (1)$$

where R is the ratio (absolute) of the isotopes being compared and differences in the ratio between a standard and sample are reported in parts per thousand or per mil (‰). For carbon, $R = {}^{13}C^{16}O^{16}O/{}^{12}C^{16}O^{16}O$. The delta values are calculated from the measured mass ratios (46/44 and 45/44) of a sample and a carbon dioxide standard gas (Craig, 1957). As the primary standard (calcium carbonate from a belemnite of the Pee Dee formation) originally used by Craig (1953; 1957) has now been exhausted, the standard currently used is an internationally calibrated one, Vienna Pee Dee Belemnite (VPDB).

3.2.8 Gas sample analysis

Carbon dioxide concentrations were analysed by gas chromatography. The Gas chromatograph (GC) used was a Perkin Elmer Autosystem XL fitted with a flame ionisation detector (FID; set at 275 °C) and a methaniser. Injector temperature was 150 °C. Gases in the sample were separated on a 4 m long column using Porapak QS (50-80 mesh) as the stationary phase. Column temperature was 45 °C with the N_2 carrier gas flow rate set at 20 ml min^{-1}. Approximately 1 ml of sample was withdrawn from each Exetainer using a gastight syringe (Hamilton, Reno, Nevada) and placed directly into the injection port of the GC. A certified CO_2 gas standard (541 ppm – BOC, UK) was used to calibrate detector response at the beginning, during and end of every sample run. The GC was interfaced to a PC that processed GC output using Perkin Elmer TurboChrom Software, version 6.1. The run time was 6 minutes with CO_2 eluting at ~5 minutes. As the GC was equipped with a methaniser, concomitant CH_4 concentrations were also measured. Methane data is not discussed further but is available for reference in Appendix ii.

CO_2 fluxes for each of the 5 treatments were converted from ppm min^{-1} to units of mg CO_2-C m^{-2} h^{-1}. An example of the conversion is given below. The volume of each headspace chamber was 33 Litres.

3.2.8.1 Conversion of a concentration (ppm) of CO_2 to a mass of CO_2-C

One mole of a substance when converted to a gas has a volume of 22.4 litres at standard temperature and pressure (s.t.p. 273.15 K and 1013 mbar),

1 mole C = 12 g

when combusted in O_2 this carbon has a volume of 22.4 litres (CO_2-C)

$\therefore$ 1 ml = 12 g / 22 400 ml = 5.36×10^{-4} g.

with a headspace volume of 33 litres,

1 ppm CO_2 = 0.033 ml

and so 1 ppm headspace CO_2 is equivalent to:

0.033 x 0.536 mg = 0.018 mg.

Once the calculated ppm values were converted to mg CO_2-C, the surface area inside each chamber was taken into account (0.071 m^2). The flux in mg of CO_2-C was then multiplied by (1 / 0.071) to convert the flux inside the chamber to a flux per square metre. All treatment plots had additional air space within chamber collars to be accounted for. Four measurements were taken (at 90 degrees from one another) from the top of each chamber collar to the surface of the peat. The mean depth was used to calculate the volume of headspace inside each chamber collar. This volume was then added to the volume of the flux chamber lids and factored into flux calculations.

The $\delta^{13}C$ of CO_2 stored in Exetainers was determined by trace gas – isotope ratio mass spectrometry (TG-IRMS). That is to say, an isotope ratio mass spectrometer (Micromass, Manchester, UK) was coupled to a Micromass Isoprime trace gas pre-concentration unit (Micromass, Manchester, UK). One hundred microlitres of gas was removed from each Exetainer and injected with a gas tight syringe into the TG-IRMS. The sample was then diverted through a trap filled with magnesium perchlorate to remove water, after which the CO_2 was cryogenically concentrated in a dewar of liquid nitrogen. Prior to entering the IRMS the CO_2 was separated from other non-condensable gases on a 30 m gas chromatography capillary column filled with Pora plot Q. Reference standards of known isotopic composition were included after every fifteenth sample during analysis. Internal precision was better than ± 0.3 ‰ at 1 σ for $\delta^{13}C$.

3.2.9 $\delta^{13}C$ determination of source respired CO_2

To identify and quantify the contribution and isotopic composition of carbon fluxes between the atmosphere, the ecosystem and individual ecosystem components, firstly respired CO_2 was captured over a time period when the concentration was constantly changing. Then, having measured the concentration and stable carbon isotope value of the samples (by GC and IRMS), we utilised the Keeling plot technique, the basis of which is conservation of mass (Pataki *et al.*, 2003), to estimate the carbon isotope composition of source respiration.

This will now be described in more detail, illustrated *via* a number of equations, and using as an example a sample removed at a single point in time from a respiration chamber:

$$C_T = C_1 + C_2 \qquad (2)$$

where C_T is the concentration of chamber CO_2 measured at any time (t), C_1 is the amount of CO_2 added to the chamber by ecosystem respiration sources (which increases with increasing t) and C_2 is the background or atmospheric CO_2 concentration (which remains constant but decreases relative to C_T as C_1 increases). Incorporating the stable carbon isotope value of CO_2 into equation 2 we get,

$$\delta_T C_T = \delta_1 C_1 + \delta_2 C_2 \quad (3)$$

where δ_T is the stable carbon isotope value of CO_2 measured in the chamber at time t, δ_1 is the carbon isotope value of source respired CO_2 and δ_2 is the isotopic signature of the background (or atmospheric) CO_2. We assume δ_1 and δ_2 are constant with time, as is C_2. Substituting equation 2 (where C_1 becomes $C_T - C_2$) into equation 3 gives,

$$\delta_T C_T = \delta_1 (C_T - C_2) + \delta_2 C_2 \quad (4)$$

$$= C_T \delta_1 + C_2 (\delta_2 - \delta_1) \quad (5)$$

$$\therefore \delta_T = \delta_1 + \frac{C_2 (\delta_2 - \delta_1)}{C_T} \quad (6)$$

This is the equation of a straight line ($y = c + mx$), where $y = \delta_T$, $x = 1 / C_T$ and since δ_1 and $(\delta_2 - \delta_1)$ are constant, the gradient is $C_2 (\delta_2 - \delta_1)$ and the intercept is δ_1. This is illustrated pictorially in Figure 3.4 and was first demonstrated by Keeling (1958) in a study

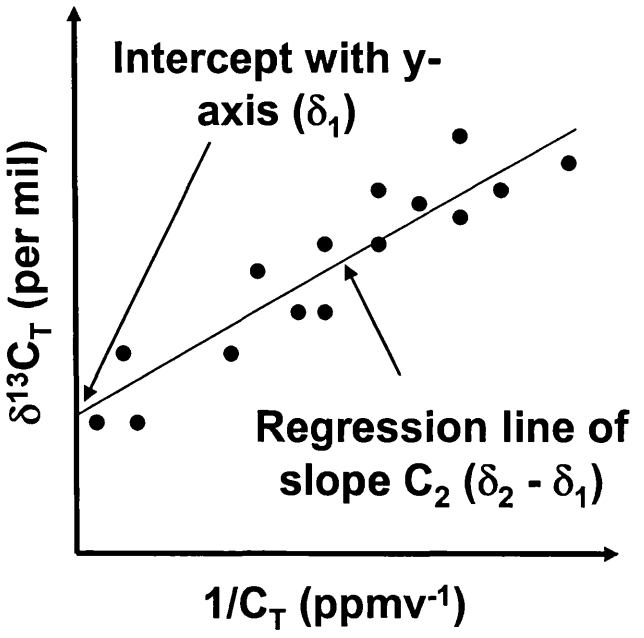

Figure 3.4 - Illustration of a Keeling plot. As variation in the $\delta^{13}C$ of carbon dioxide is proportional to the reciprocal of carbon dioxide concentration, the intercept of a linear regression with the y-axis is an estimate of the $\delta^{13}C$ signature of source CO_2, the concentration of which is changing with time.

of 'the concentration and isotopic abundances of atmospheric carbon dioxide in rural areas'. Keeling demonstrated that carbon isotope ratio variations were proportional to the inverse of the molar carbon dioxide concentration. The intercept of the linear regression with the y-axis being the estimate of the $\delta^{13}C$ of source respired CO_2.

3.2.10 Statistical analysis

All statistical analyses were performed using the statistical software package Minitab, Release 15 (Minitab, Inc., USA). An F-test was first performed on the data to check for equality of variances. Differences between treatments were subsequently examined by a two-sample t-test.

3.3 Results

Soil and air temperatures were recorded on the day of sampling (see appendix iii). Mean air temperature during sampling was 13 °C and mean soil temperature was 5.4 °C.

3.3.1 $\delta^{13}C$ of bulk soil and vegetation

All $\delta^{13}C$ data for the atmosphere, soil and vegetation are collated and displayed in Table 3.2. Monocots were the most enriched of the vegetation species, having a $\delta^{13}C$ of -26.1 ‰,

Parameter	$\delta^{13}C$ (per mil)	% C
Calluna vulgaris	-28.2	54.9
Sphagnum spp	-29.0	51.4
Eriophorum vaginatum	-26.1	50.3
Soil	-27.5 ± 0.2	50.1
Atmosphere 1m above canopy	-10.8 ± 1.2	0.039

Table 3.2 - $\delta^{13}C$ of the atmosphere (n = 3), bulk soil (n = 5) and vegetation on the day of sampling. Soil $\delta^{13}C$ is for the top 10 cm of the profile only. Only one measurement was carried out for each of the plant species and so no estimate of the error is given. However, analytical precision was ± 0.3 ‰.

~ 3 ‰ more enriched than the bryophytes. The atmosphere 1 m above the canopy had a $\delta^{13}C$ value of -10.8 ‰, a value that is slightly more depleted than would be expected (~ -8.5 ‰; Hemming *et al.* 2005) presumably due to the incorporation of ecosystem respiration on the free atmosphere 1 m above the canopy. The fact that the concentration of CO_2 in the atmosphere was generally in excess of 390 ppm (current atmosphere is ~ 380 ppm CO_2) provides more evidence for this assumption.

3.3.2 Respiration fluxes and Keeling plots

There follows a suite of graphs that depict CO_2 concentrations and the carbon isotope values ($\delta^{13}C$) of CO_2 captured from each of the treatments within the experimental Latin square (depicted in Figure 3.3) during the six point time series performed in May 2005. All errors quoted are ± 1 standard error. The scale is chosen so as to be identical to that required for equivalent plots across all five treatments.

3.3.2.1 Fluxes and $\delta^{13}C$ of respired CO_2 from the 'soil' treatment

All respiration rates for the soil treatment (Figure 3.5) were linear with r^2 values between 0.83 and 0.99 for all 5 chambers, significant at the 95 % level.

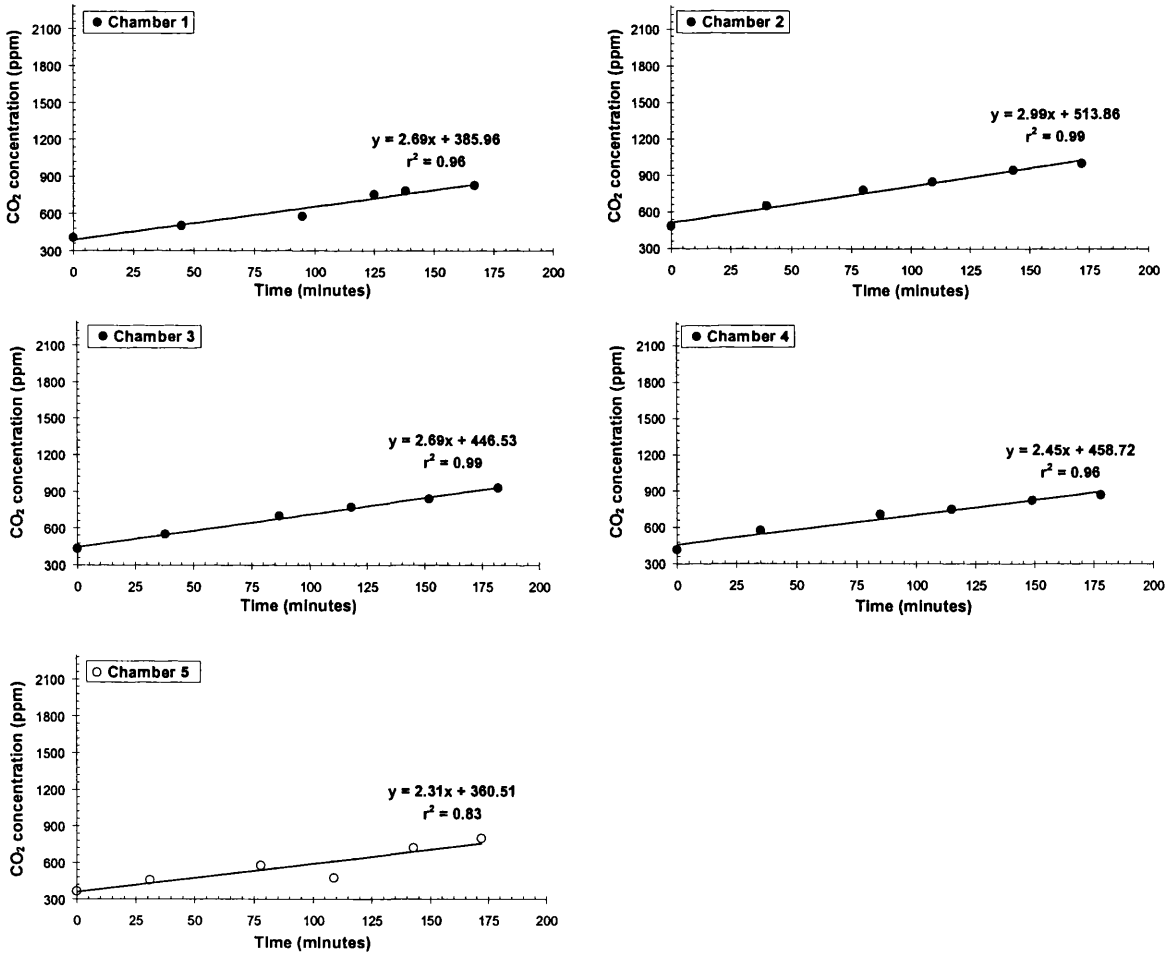

Figure 3.5 - CO_2 concentration within five chambers used to capture respired CO_2 from the 'soil' treatment. Open symbols represent a chamber that did not fulfil flux criteria. Error bars not shown as they are smaller than the symbols. Depth to which each chamber collar extended below peatland surface: chamber 1 – 7.5 cm, chamber 2 – 11 cm, chamber 3 – 5 cm, chamber 4 – 10 cm and chamber 5 – 9 cm.

The maximum CO_2 concentration reached in any one chamber was ~ 1003 ppm and the maximum respired within the 3 hour period was 519 ppm (chamber 1). The rate of CO_2

production in all five 'soil' respiration chambers is linear and the production rates range between 2.31 and 2.99 ppm min^{-1} (139 and 179 ppm h^{-1}). The r^2 values indicate that there was a clear relationship between respiration build-up and time, four of the chambers having an r^2 value ≥ 0.96 ($P > 0.99$) and one equal to 0.83 ($P > 0.95$).

Figure 3.6 illustrates the $\delta^{13}C$ of soil respiration fluxes with time (top) and also the 'soil'

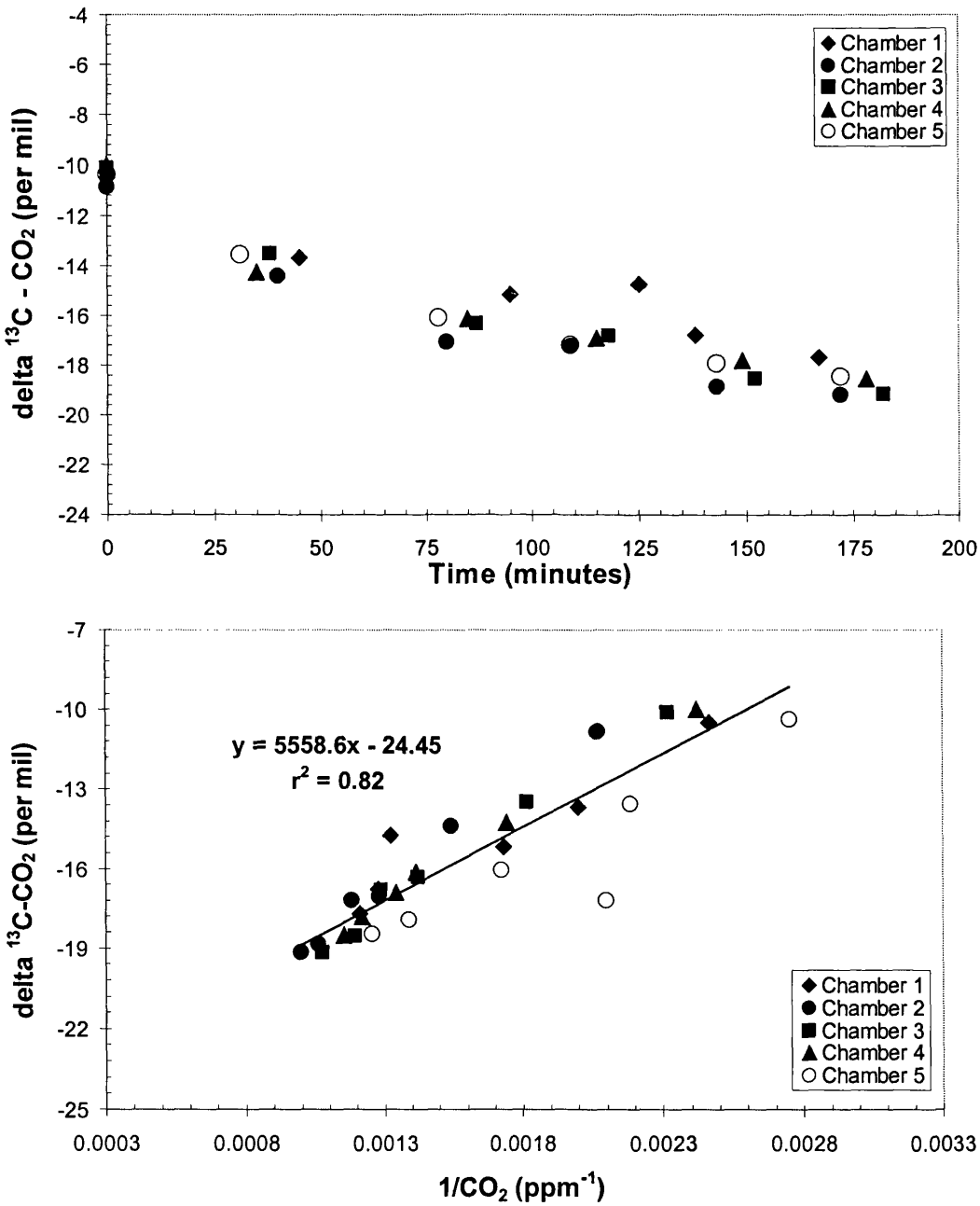

Figure 3.6 – Top - $\delta^{13}C$ of CO_2 captured from five 'soil' plots at each of the six sampling points. Bottom - Keeling plot of 'soil' respiration. Open symbols depict the chambers where the concentration of source CO_2 did not monotonically increase with time.

treatment Keeling plot (bottom). The data in the plot in Figure 3.6 (top) show a clear trend of depletion in the isotope value of chamber CO_2 with time in each of the four chambers that demonstrated a monotonic increase in CO_2 concentration. The Keeling plot shows that

the extrapolated intercept with the y-axis (estimate of source CO_2) from a linear regression of the data is –24.5 ± 0.8 ‰. An r^2 value of 0.82 indicates that there is a good correlation between the $\delta^{13}C$ of soil respiration and the reciprocal of soil respiration concentration ($P > 0.99$).

However, one chamber failed to meet the monotonically increasing flux criteria. A new Keeling plot was performed (Figure 3.7) to establish whether there was a difference in the

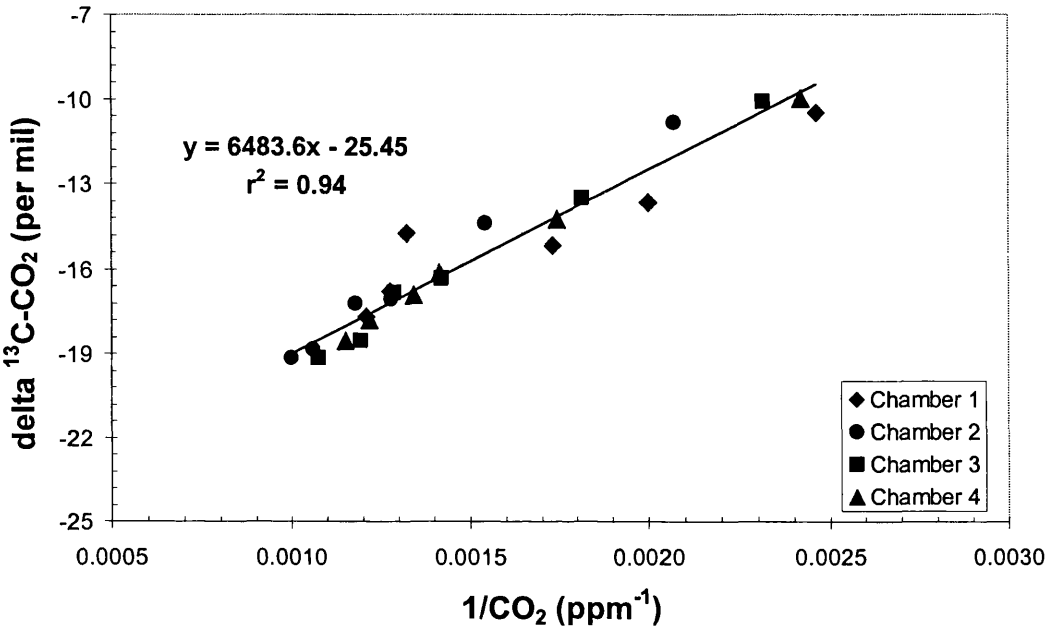

Figure 3.7 - Keeling plot of data from the 'soil' treatment with the data from chamber five removed (where there was no monotonic increase in CO_2 concentration with time).

estimate of the $\delta^{13}C$ value of source CO_2. With chamber 5 removed from the new Keeling plot, the r^2 value for the regression increased from 0.82 to 0.94 ($P > 0.99$). The new estimate for source respired CO_2 is more depleted by 1.0 ‰ at -25.5 ± 0.6 ‰.

3.3.2.2 Fluxes and $\delta^{13}C$ of respired CO_2 for the 'ecosystem' treatment

Figure 3.8 illustrates respiration fluxes from the 'ecosystem' treatment. From Figure 3.8, one can clearly see that there was very little increase in CO_2 concentration with time, within any of the five respiration chambers. The maximum concentration reached in any one chamber was 698 ppm (chamber 2). Chambers 4 and 5 show a decrease in CO_2 production with time and contain less CO_2 at the end of the time series than at the beginning. Figure 3.9 (top) illustrates the time series data plotted versus the isotopic data for the same concentration measurements depicted in Figure 3.8. All of the chambers for this treatment demonstrated a depletion in the stable carbon isotopic composition of chamber CO_2 after the first sample was taken at time 0. After the second sample was

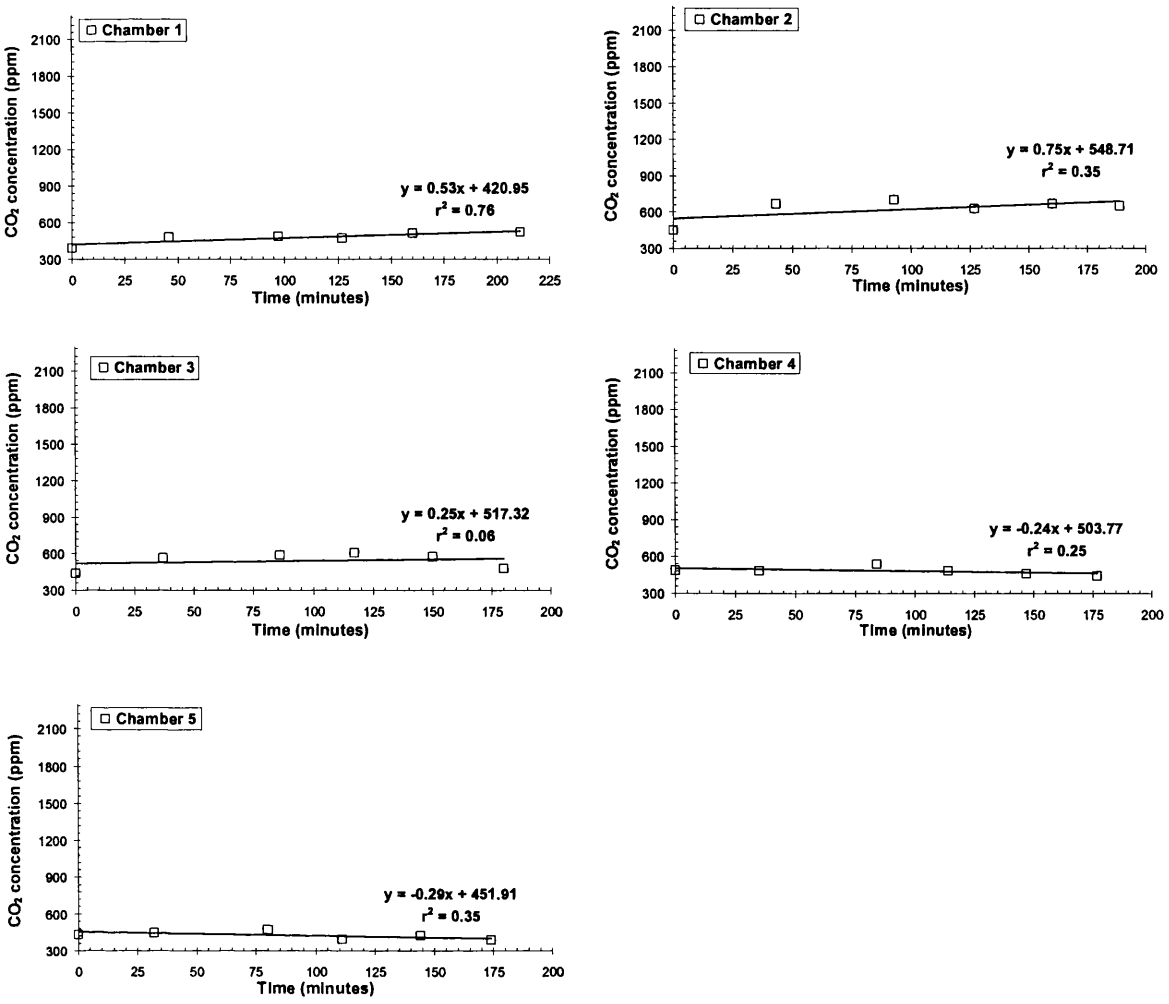

Figure 3.8 – CO_2 concentration within five chambers used to capture respired CO_2 from the 'ecosystem' treatment. Open symbols represent chambers that did not fulfil the flux criteria. Error bars not shown as they are smaller than the symbols. Depth to which each chamber collar extended below peatland surface: chamber 1 – 2 cm, chamber 2 – 3 cm, chamber 3 – 2 cm, chamber 4 – 4 cm and chamber 5 – 5cm.

removed from each chamber the carbon isotope value of subsequent samples remained much the same, with the maximum difference in the $\delta^{13}C$ value of CO_2 collected from within each chamber (after time point 1) being 0.9 ‰ (chamber 3 – between time point 2 and time point 3).

The sample with the most depleted $\delta^{13}C$ value was found in chamber 2 (time point 2), having a value of -16.4 ‰. As mentioned above, this sample also had the highest CO_2 concentration out of the 30 analysed for this treatment. Of the five chambers that collected respired CO_2, none met the criteria (section 3.2.3) for use in flux calculations and so were considered to be open systems. However, as a Keeling plot takes account of any air in gas samples removed from chambers, the data is presented in a Keeling plot (Figure 3.9 -

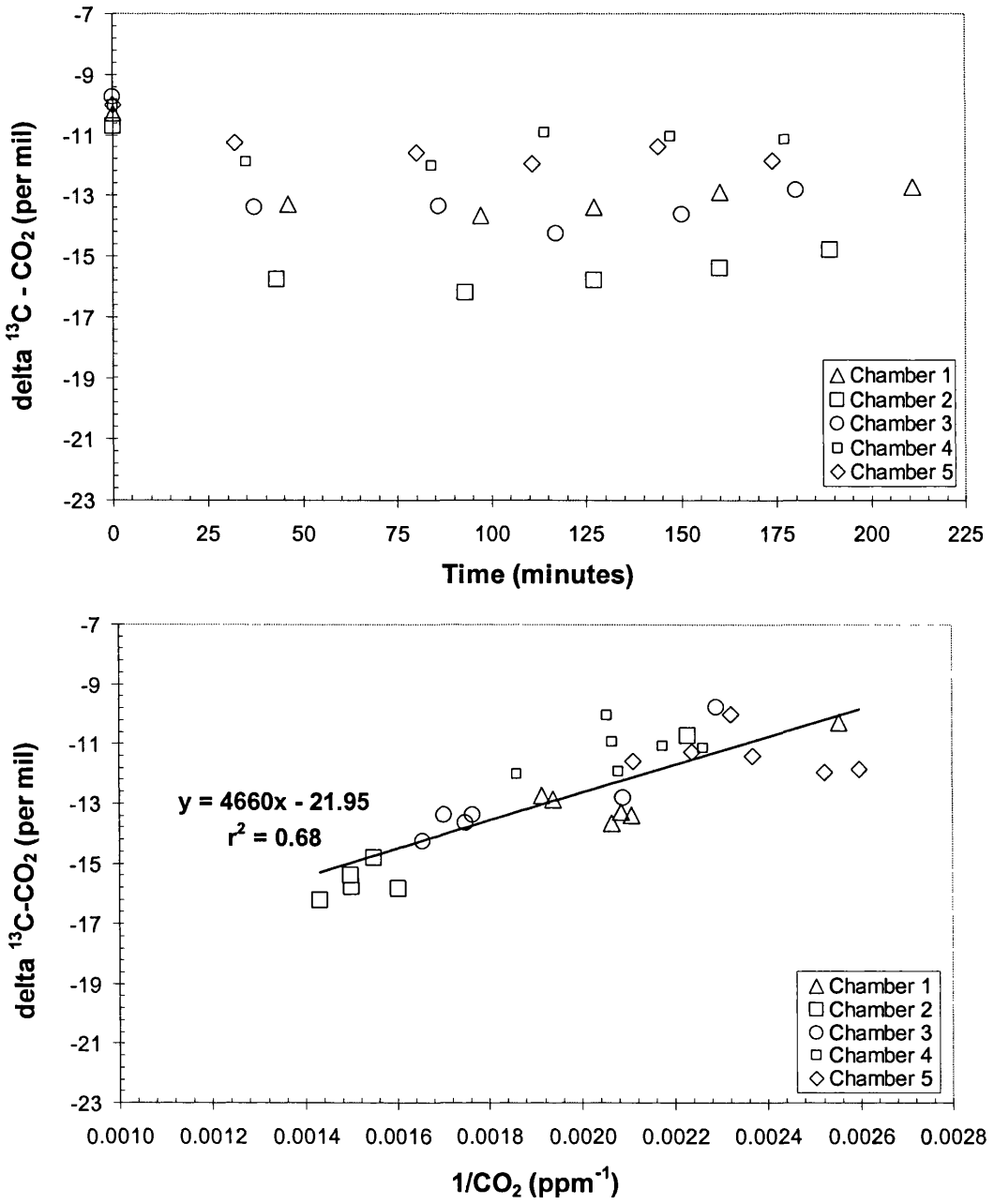

Figure 3.9 - Top - $\delta^{13}C$ of 'ecosystem' respiration fluxes at each of the six sampling points within five peatland respiration chambers. Open symbols depict the chambers where the carbon isotope value of chamber CO_2 did not monotonically decrease with time. Bottom - Keeling plot of 'ecosystem' respiration.

bottom). The estimate of the $\delta^{13}C$ signature of 'ecosystem' respiration given by the linear regression is -22.0 ± 1.2 ‰. The regression of the data is significant at the 95 % level.

3.3.2.3 Fluxes and $\delta^{13}C$ of respired CO_2 from the 'no shrubs' treatment

Respiration rates within all 5 chambers illustrated in Figure 3.10 were linear, with all r^2

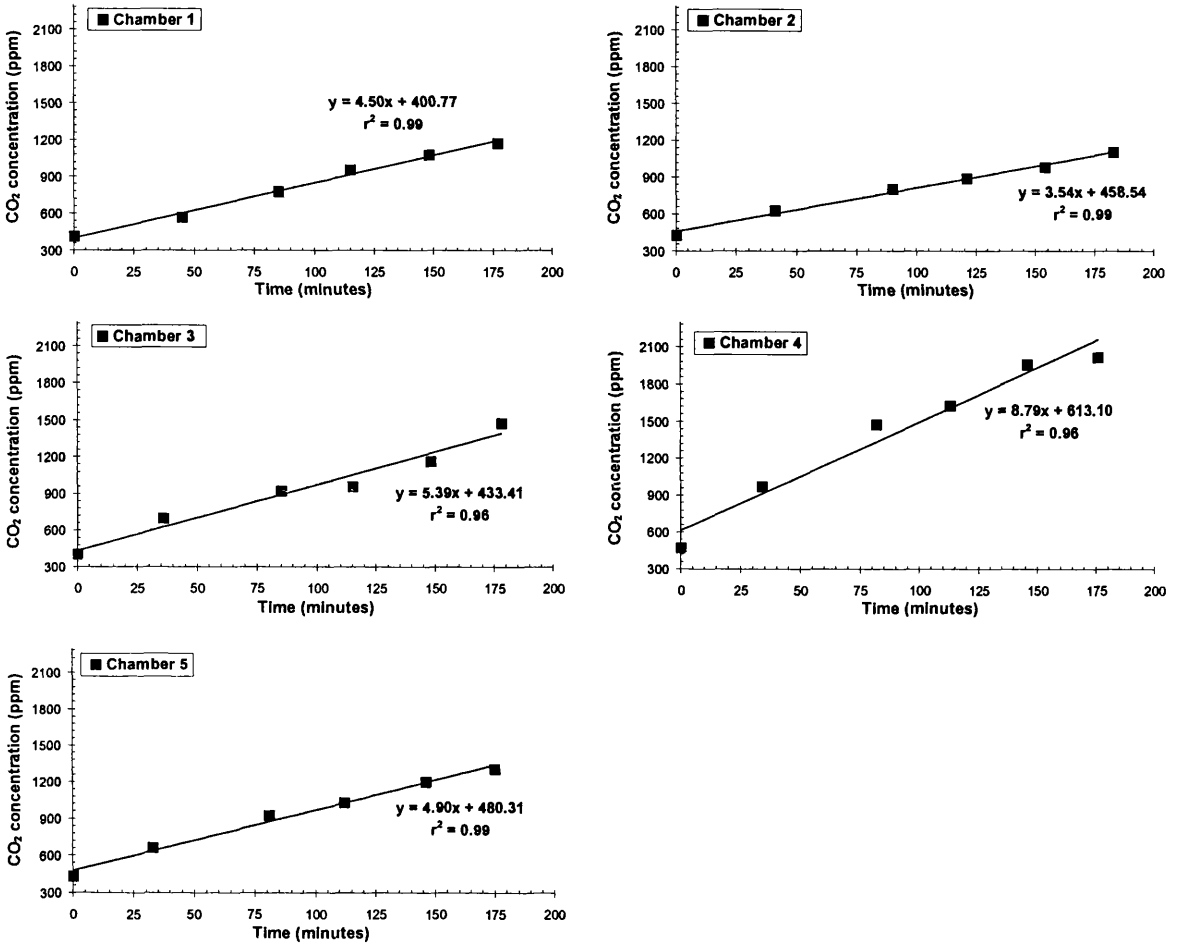

Figure 3.10 - CO_2 concentration within five chambers used to capture respired CO_2 from the 'no shrubs' treatment. Error bars not shown as they are smaller than the symbols. Depth to which each chamber extended below peatland surface: chamber 1 – 6.5 cm, chamber 2 – 3 cm, chamber 3 – 8 cm, chamber 4 – 8 cm and chamber 5 – 8 cm.

values ≥ 0.96 which is significant at the 99 % level. Production was variable and ranged between 3.5 and 8.8 ppm min^{-1}. The maximum CO_2 concentration reached in any one chamber (4) was 2018 ppm, ~ twice the maximum produced in any of the 'soil' treatment chambers over a similar time period. The mean flux for the 'no shrubs' treatment was 327 ± 53 ppm h^{-1} with no plateau in concentration being reached within the sampling timeframe. The shrub removal treatment had the second highest CO_2 production rate of all 5 treatments. All treatment chambers met the concentration criterion to be included in mean flux measurements.

Figure 3.11 (top) shows that the CO_2 produced within each of the 5 treatment chambers became more depleted in ^{13}C over time. Two obvious outliers were removed from the Keeling plot regression, increasing the r^2 from 0.87 to 0.97. The linear regression of the

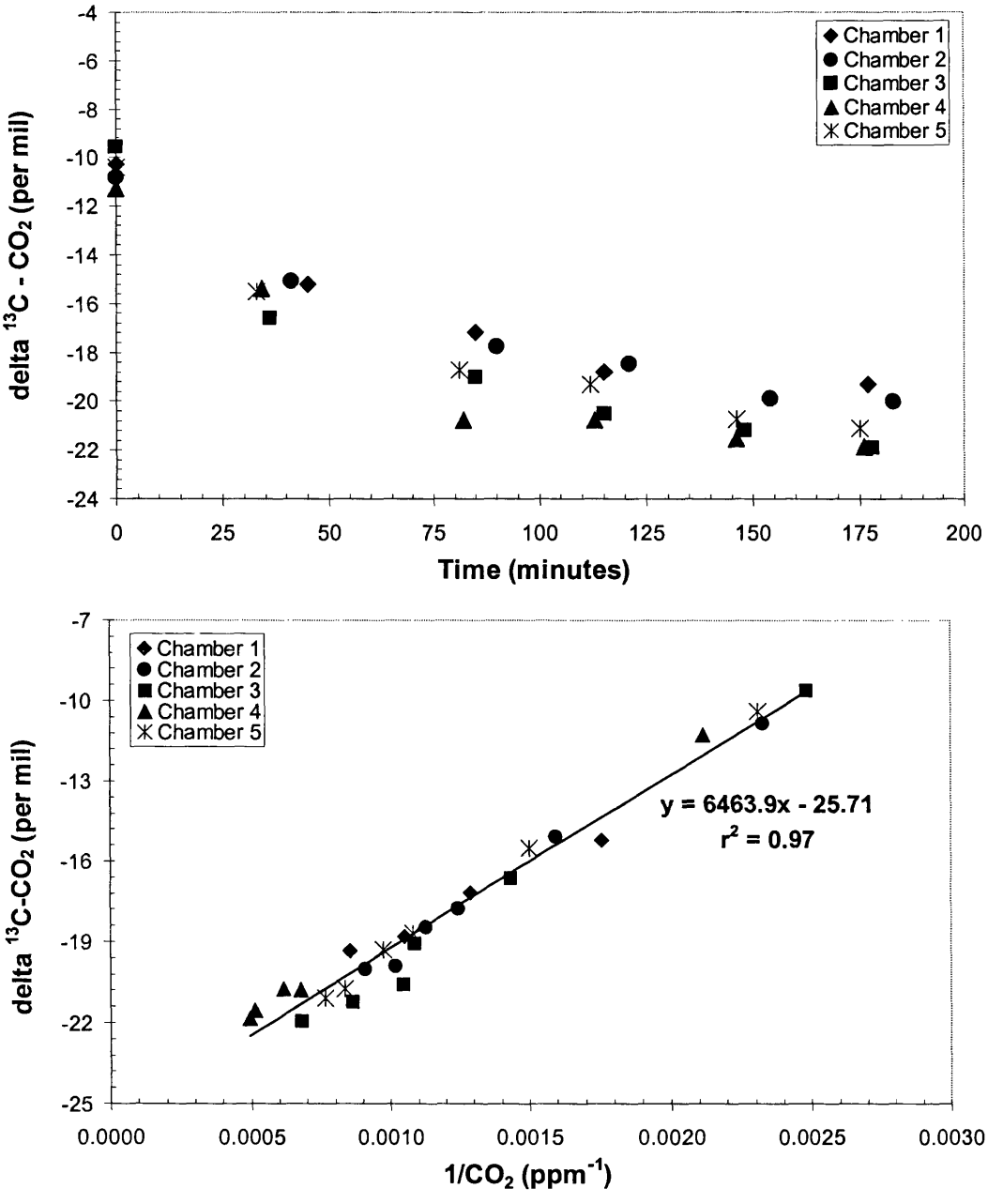

Figure 3.11 - Top - $\delta^{13}C$ of respiration fluxes from the 'no shrubs' treatment at each of the six sampling points within five peatland respiration chambers. Bottom - Keeling plot of the data measured in 5 respiration chambers under the shrub removal treatment.

data in the Keeling plot indicates that there is a very good correlation ($P > 0.999$) between the $\delta^{13}C$ values of CO_2 respired from the 'no shrubs' treatment and the reciprocal of the CO_2 concentration. The $\delta^{13}C$ value for respired CO_2 emitted from the 'no shrubs' treatment (estimated from the Keeling plot) is -25.7 ± 0.6 ‰.

3.3.2.4 Fluxes and $\delta^{13}C$ of respired CO_2 from the 'no monocots' treatment

Figure 3.12 illustrates the respiration fluxes for the 'no monocots' treatment.

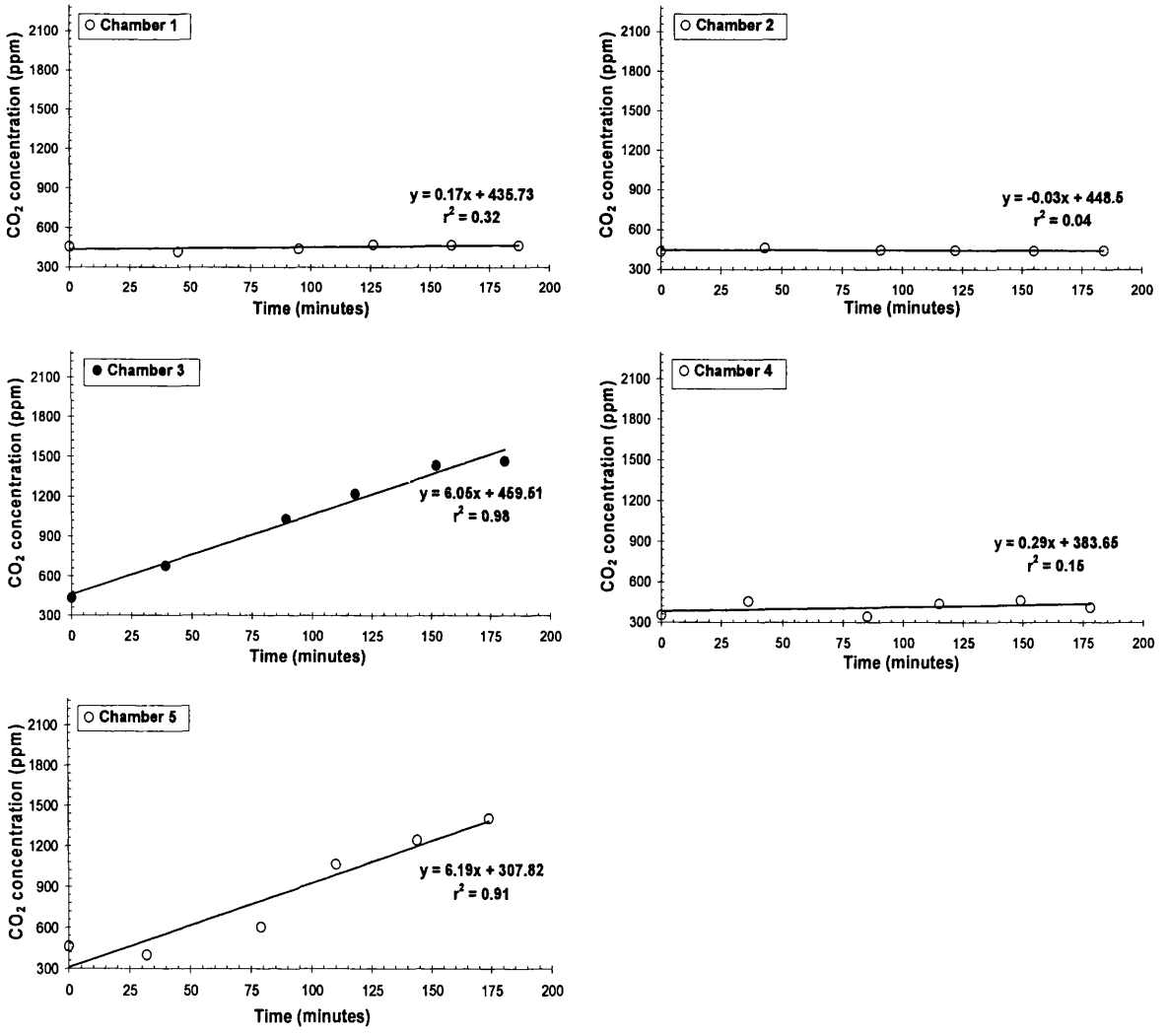

Figure 3.12 - CO_2 concentration within five chambers used to capture respired CO_2 from the 'no monocots' treatment. Open symbols represent chambers that did not fulfil the flux criteria. Error bars not shown as they are smaller than the symbols. Depth to which each chamber collar extended below peatland surface: chamber 1 – 1.5 cm, chamber 2 – 1 cm, chamber 3 – 8 cm, chamber 4 – 4 cm and chamber 5 – 7 cm.

Some of the time series data for this treatment demonstrated a linear increase in CO_2, whilst in others there is no significant increase in CO_2 concentration. Three chambers appear to have minimal to no build up in CO_2 concentration, with production rates ranging from 0.17 to 0.15 ppm min^{-1} in chambers 1 and 4 respectively. Chamber 2 showed a slight decrease in CO_2 production from time zero. Chambers 3 and 5 however, show linear rates of CO_2 increase of between 6.05 and 6.15 ppm min^{-1}, with the maximum concentration reached being 1466 ppm over the 3 hour period in chamber 3. However, only chamber 3 meets the concentration criteria.

A plot of the isotope data with time, for this treatment (Figure 3.13 - top), shows that there

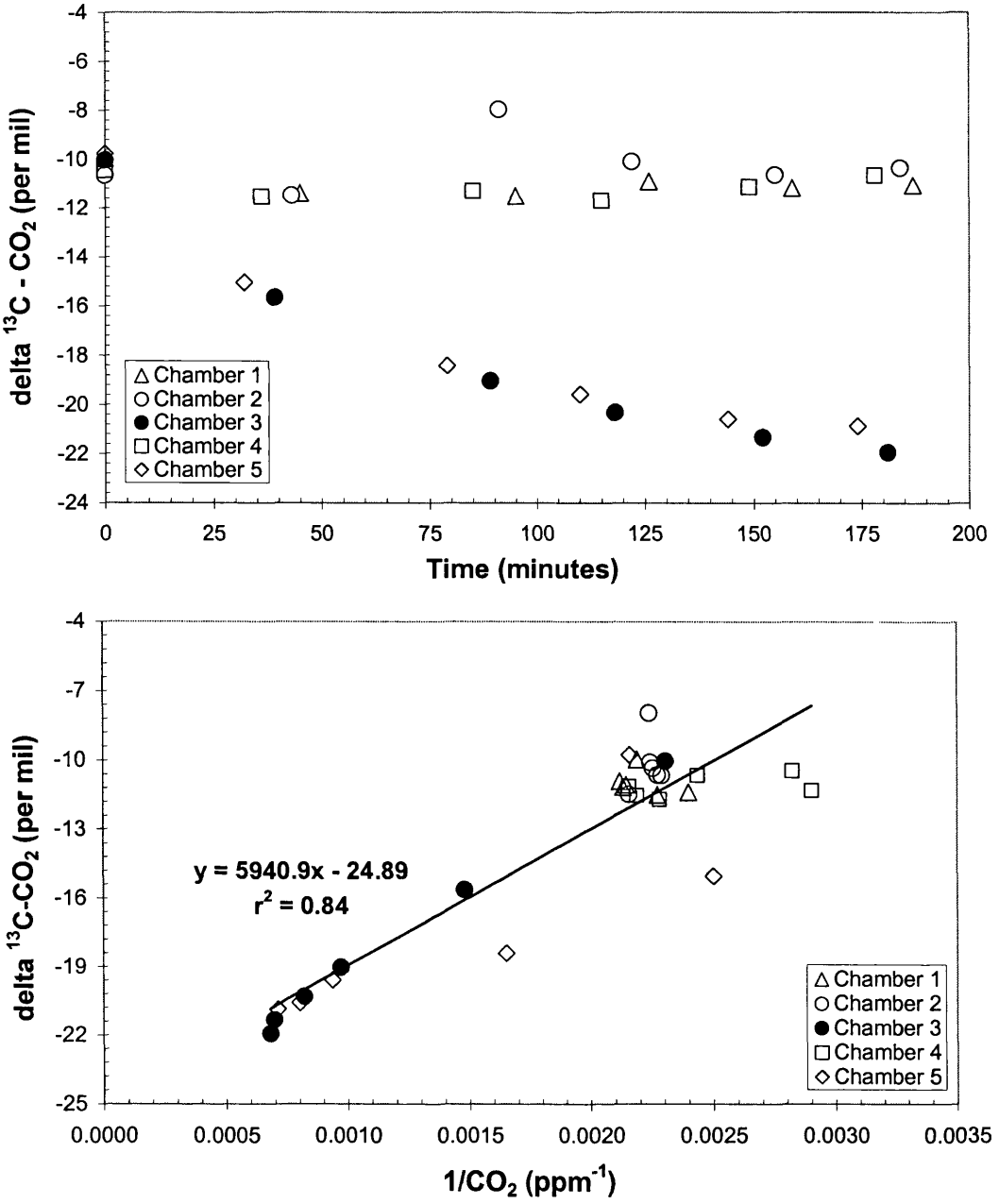

Figure 3.13 – Top - $\delta^{13}C$ of respiration fluxes at each of the six sampling points within five peatland respiration chambers where the monocots had been removed. Bottom - Keeling plot of data under the monocot removal treatment. Open symbols indicate the chambers where the concentration of respired CO_2 did not monotonically increase with time.

is little or no change in the $\delta^{13}C$ value of CO_2 collected from three of the five chambers (1, 2 and 4), the same chambers, where there is either no increase or very little increase in CO_2 concentration during the sampling period (Figure 3.12). However, two chambers clearly demonstrate that the stable carbon isotope value of captured CO_2 became more depleted with time.

Despite the fact that only 2 chambers appeared to capture respired CO_2 from this treatment and only 1 chamber met the concentration criteria, when the data were entered into a Keeling plot, the linear regression was rather well constrained ($r^2 = 0.84$, $P > 0.999$). The estimate of $\delta^{13}C$ for this treatment from the Keeling plot in Figure 3.13 is -24.9 ± 1.0 ‰.

A revised estimate is obtained when only the data from chamber 3 is entered into a Keeling plot (Figure 3.14). The estimate for the $\delta^{13}C$ value of source respired CO_2 for the 'no

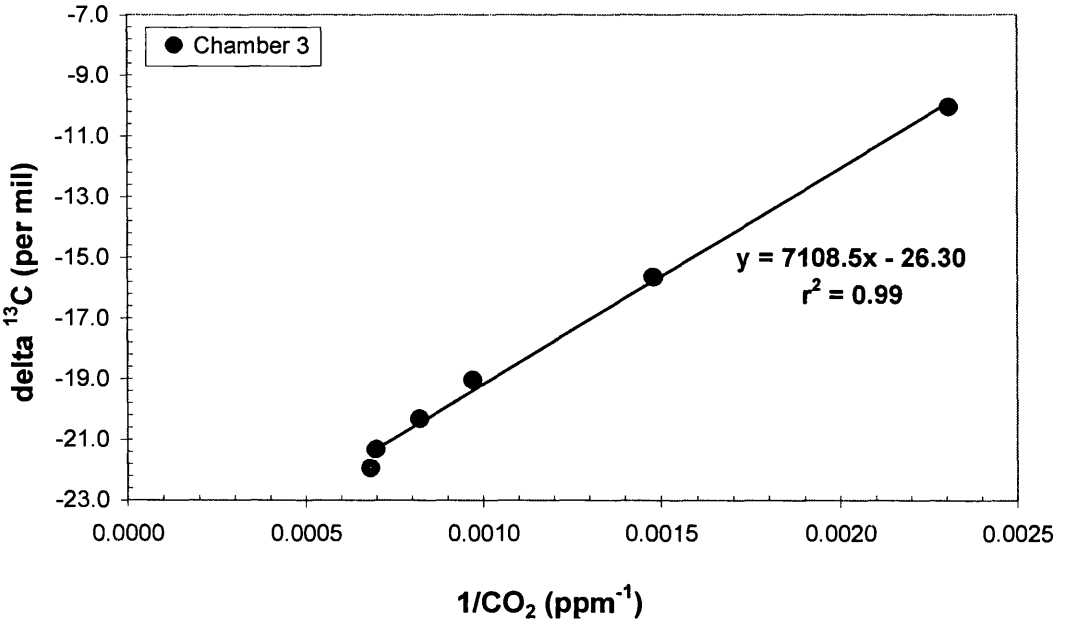

Figure 3.14 - Keeling plot of data from the 'no monocots' treatment with the chambers removed that did not meet the specified flux criterion.

monocots' treatment became lower (relative to the estimate gained in Figure 3.13) at -26.3 ± 0.3 ‰ ($P > 0.999$).

3.3.2.5 Fluxes and $\delta^{13}C$ of respired CO_2 from the 'no moss' treatment

Figure 3.15 illustrates respiration fluxes for the 'no moss' treatment. Within chambers 2 and 5 in Figure 3.15 there was no evidence of an increase in CO_2 concentration. Chambers 1, 3 and 4 had CO_2 production rates of between 0.51 and 1.34 ppm min^{-1}. The maximum concentration reached in any one chamber was 702 ppm (chamber 3, time point 4) ~ 300 ppm less than the highest CO_2 concentration found in the 'soil' treatment and ~ 1300 ppm less than the highest CO_2 concentration reached in the 'no shrubs' treatment. Monotonically increasing CO_2 concentration did not take place in any of the 5 'no moss' treatment chambers.

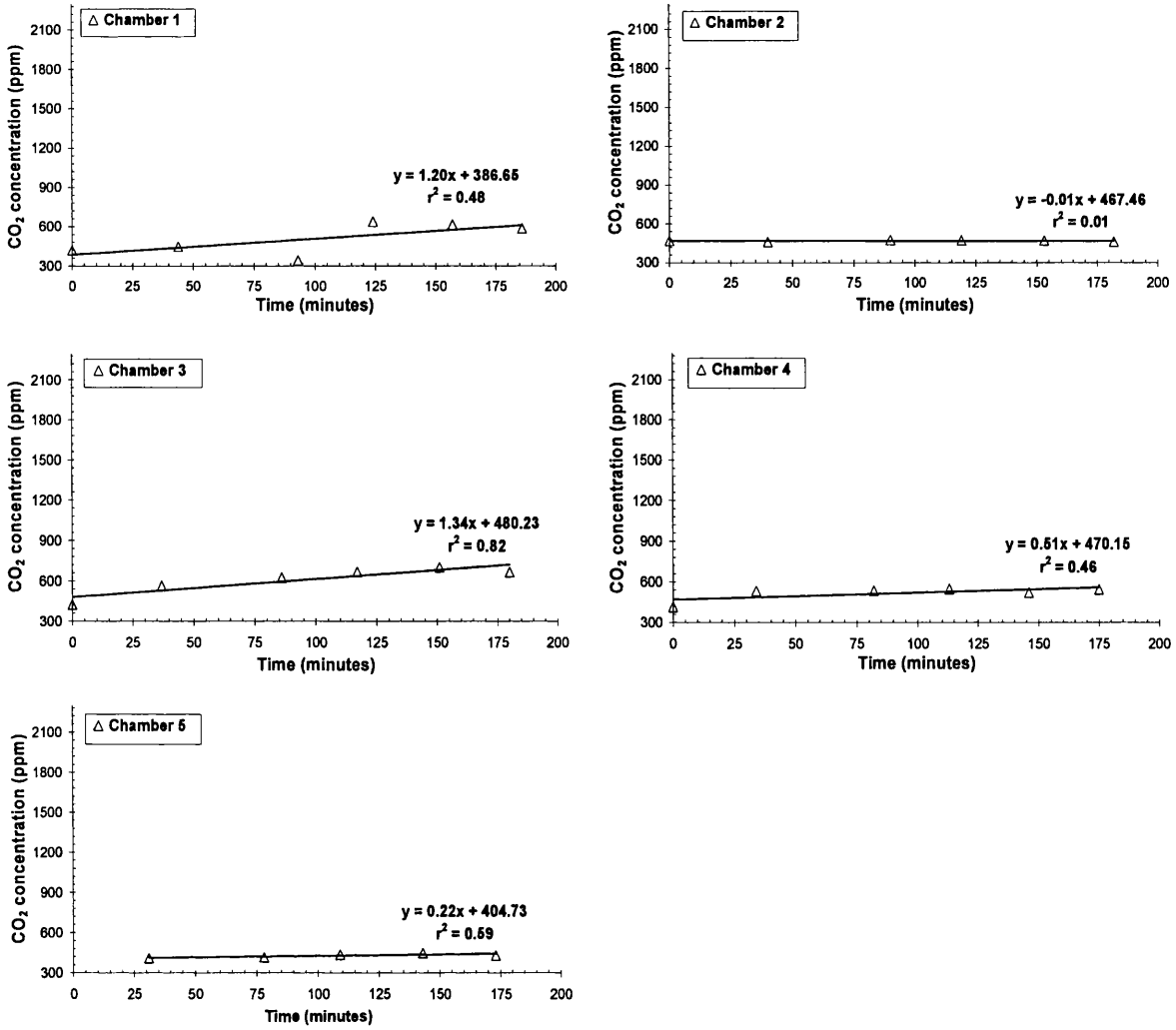

Figure 3.15 – CO_2 concentration within five respiration chambers in which all the bryophytes had been removed. Open symbols represent chambers that did not fulfil the flux criteria. Error bars are not shown as they are smaller than the symbols. Depth to which each chamber collar extended below peatland surface: chamber 1 – 2 cm, chamber 2 – 3 cm, chamber 3 – 5 cm, chamber 4 – 6 cm and chamber 5 – 3 cm.

Furthermore, it can be seen from Figure 3.16 (top) that CO_2 captured from within the same five chambers did not demonstrate much change in stable carbon isotope composition, as the $\delta^{13}C$ value of CO_2 captured for analysis was close to that of the contemporary atmosphere. This is consistent with the data in Figure 3.15, where most of the treatments showed little or no increase in CO_2 concentration throughout the time course. If there was an increase in CO_2 concentration due to respiration being added to these chambers (from soil and vegetation) we would expect to see a concomitant reduction in the $\delta^{13}C$ value with time.

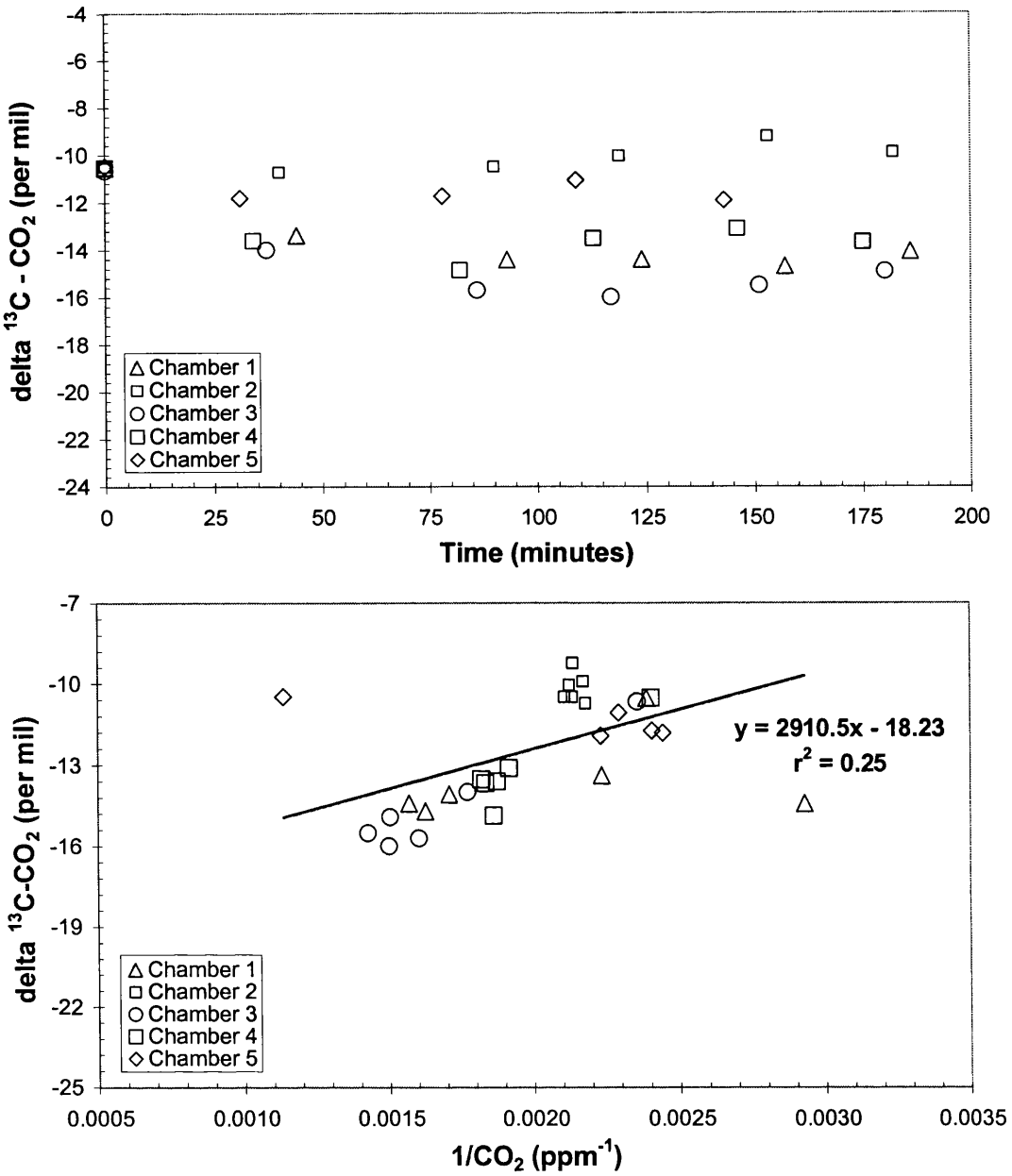

Figure 3.16 – Top - $\delta^{13}C$ of respiration collected from the 'no moss' treatment at each of the six sampling points within each of the five chambers. Bottom - Keeling plot illustrating respired CO_2 from the moss removal treatment. Open symbols indicate chambers where the $\delta^{13}C$ signature of respired CO_2 did not monotonically decrease with time.

Figure 3.16 (bottom) depicts all the CO_2 data from the 'no moss' treatment entered into a Keeling plot. Using this approach, the estimated $\delta^{13}C$ value for ecosystem respiration excluding mosses is -18.2 ± 1.9 ‰. However the r^2 value is only 0.25 and is not statistically significant ($P < 0.95$), thus the intercept of the linear regression cannot be considered as a reliable estimate of the $\delta^{13}C$ value of source respiration for this particular treatment.

3.4 Discussion

Respiration fluxes were measured from 5 different vegetation removal treatments, each treatment being replicated 5 times, on the 12th May, 2005. It is obvious from the results section, when studying individual fluxes within chambers in conjunction with the concomitant carbon isotope data that a number of chambers were not closed systems. This was clearly demonstrated by measurement of CO_2 within chambers where there was minimal or no increase in respired CO_2 with time. In addition, the isotope data for the same CO_2 concentration measurements provided further evidence that they were in fact acting like open systems. It was expected that each CO_2 sample removed from these chambers would become increasingly more depleted in ^{13}C during the course of a sampling (due to the addition of isotopically depleted CO_2 respired from both plants and soil). Instead, the CO_2 collected from these chambers retained an isotopic value close to the $\delta^{13}C$ value of CO_2 collected from 1 m above the canopy (atmospheric CO_2).

There are a number of possible explanations for the lack of respired CO_2 in the chambers that were acting as open systems. One reason could be that no respiration took place. However, this is considered unlikely, as even during winter when respiration rates are slower than during the growing season, an increase in chamber CO_2 concentration would be expected (Ward, 2006). If photosynthetic processes had been occurring within some chambers (i.e. due to some light penetration through the chamber black-out covers), then this could also be an explanation for the lack of increase in respired CO_2 concentration. Again, this is deemed unlikely as the chamber blackout covers were tested with a photosynthetically active radiation (PAR) sensor (Ward, 2006) before use in the field. Furthermore, if photosynthesis was occurring, it is likely that a substantial negative flux would have been observed in the treatment chambers that contained vegetation (due to uptake during photosynthesis).

A more likely explanation could be due to the nature of the ecosystem itself and the problems it poses when using standard ecosystem respiration chambers to capture CO_2 in the field. All chambers were tested for collection of respired CO_2 without loss of sample (Ward, 2006) and are therefore not considered to be a potential source of error in this experiment. However, the collars that house respiration chambers in the field have to be sunk far enough into the peat to ensure that no respired CO_2 can escape from underneath to the atmosphere. If loss of respired CO_2 were to take place, then the concentration and isotopic integrity of collected samples would be compromised.

In a study on chamber artefacts and biases Davidson *et al.* (2002) pointed out that the depth to which chamber collars should be inserted into a profile will depend on the porosity of the soil, which in turn is dependent on soil water content and texture. Davidson *et al.* (2002) recommended that in forest soils chamber collars should be sunk to a depth of at least 9 cm for soils of high porosity. Of the five chambers that collected respiration from the 'no monocots' treatment, only 2 chambers demonstrated an increase in CO_2 concentration (3 and 5). The collars for these chambers were sunk to a minimum of 7 cm below the peatland surface. The maximum depth for the remaining three chamber collars was 4 cm. This may indicate, that these collars were not making an air tight seal with the surface peat (despite being less porous than a well drained forest soil), thus explaining the apparent lack of respired CO_2 within these chambers.

However, respiration chambers for two treatments ('soil' and 'no shrubs') performed very well, with 9 out of 10 chambers making the specified flux criteria (these chambers all had monotonically increasing CO_2 concentrations with time). In addition, the r^2 values were $\geq$ 0.83 ($P > 0.95$) for all 9 chambers and ≥ 0.96 ($P > 0.99$) for 8 out of the 9 chambers. These treatments had one thing in common, which was that the ericoid sub-shrubs had been removed. It is considered that the presence of shrub roots underneath chamber collars had an effect on how deep chamber collars extended beneath the surface peat when being bedded in at the beginning of the experiment. Therefore, it is thought likely that the presence of shrub roots is responsible for loss of respired CO_2 from many of the treatment chambers.

Furthermore, it is concluded that these chambers were being flushed with atmospheric CO_2, the severity of which depending on how near to the peatland surface the bottom of each individual chamber collar extended to. Consequently, any chambers that did not demonstrate monotonically increasing CO_2 concentrations in conjunction with decreasing $\delta^{13}C$ values were eliminated from mean CO_2 flux calculations.

3.4.1 Mean respiration fluxes

CO_2 fluxes for each treatment chamber that met the criteria specified in section 3.2.3 were averaged and expressed as mg CO_2-C m^{-2} h^{-1} (Figure 3.17). Of the 5 treatments only 3 met the flux criteria, with the 'no monocots' treatment having the highest flux rate at 90.4 mg CO_2-C m^{-2} h^{-1} (however only one out of five replicates made the flux criteria for this treatment). Samples of CO_2 removed from each of the five 'no shrubs' treatment chambers demonstrated monotonically increasing CO_2 concentrations and therefore met the specified

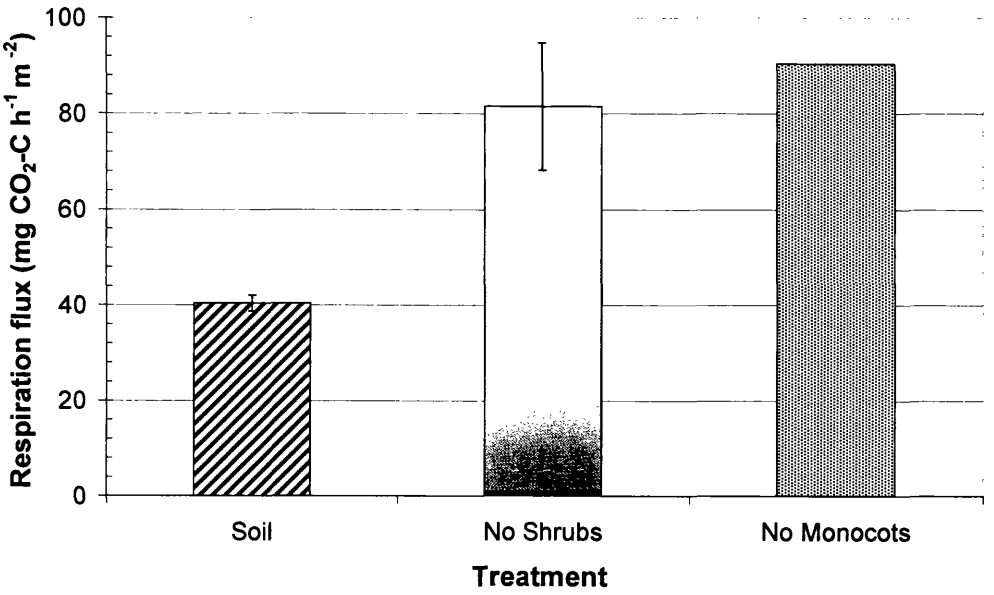

Figure 3.17 - Mean CO_2 flux (± 1 σ_e) for the 3 treatments that met the specified flux criteria. 'Soil' (n = 4), 'No shrubs' (n = 5), 'no monocots' (n = 1). Error bars where shown are ± 1 σ_e.

flux criteria. This treatment had the second highest CO_2 flux rate at 81.5 ± 13.3 mg CO_2-C m^{-2} h^{-1}. The 'soil' treatment flux rate was the mean of four replicates and had a flux approximately half that of the other two treatments at 40.4 mg CO_2-C m^{-2} h^{-1}.

3.4.2 Isotopic signature ($\delta^{13}C$) of peatland soil and vegetation

The isotopic signature of peatland vegetation (Table 3.2) growing at the Hard Hill site was typical of that found for C_3 plants, i.e. $\delta^{13}C$ values were within the range between -22 and -31 ‰ (Boutton, 1996). The $\delta^{13}C$ value of bulk soil reflected the photosynthetic pathway of these C_3 plants, as would be expected due to the fact that the main organic input to the soil is plant litter (Boutton, 1991a). In a Swiss ombrotrophic bog, Menot and Burns (2001) found $\delta^{13}C$ values for *Eriophorum vaginatum, Calluna vulgaris* and *Sphagnum* spp that ranged from -24.5 to -26.0 ‰, -28.5 to -30 ‰ and -23.0 to -28.0 ‰ respectively. These values are broadly similar to what was found for the same plant species at the Hard Hill site.

Eriophorum vaginatum was found to be between 2 and 3 ‰ more enriched in ^{13}C than *Calluna vulgaris* shoots and *Sphagnum* respectively and is likely due to differences in photosynthetic processes between the species. For example, *Sphagnum* chloroplasts are surrounded by hyaline cells that are filled with water; thus resistance to CO_2 diffusion differs fundamentally between non-vascular (bryophytes) and vascular plants (sedges and ericoids) (Menot & Burns, 2001). As CO_2 diffuses approximately ten thousand times

slower in water than in air (Wild, 1981), the presence of hyaline cells might be expected to cause *Sphagnum* to have the lowest $\delta^{13}C$ values.

In addition, *Sphagnum* of all the peatland vegetation functional groups, sits closest to the peat surface. As such, *Sphagnum* is likely to be exposed to a larger percentage of soil respired CO_2 than say *Calluna vulgaris* (which is surrounded by a more turbulent and well mixed atmosphere, being situated relatively high in the vegetation canopy). If this depleted CO_2 is fixed by *Sphagnum* spp, this would also lead to lower $\delta^{13}C$ values. For example, in an Irish peat bog, Price *et al.* (1997) found relatively low $\delta^{13}C$ values for *S. cuspidatum* and suggested that this was due to the incorporation of a proportion of soil respired CO_2 during fixation *via* photosynthesis (i.e. CO_2 recycling).

3.4.3 Summary of fluxes (both primary and isotopic)

Table 3.3 presents a summary of the mean respiration fluxes and estimates of the isotopic signature for each treatment calculated *via* the Keeling plot technique.

Treatment	Mean Flux (mg CO_2-C m^{-2} h^{-1})	$\delta^{13}C$ source (‰ ± 1 σ_e) - KP	$\delta^{13}C$ source (‰ ± 1 σ_e) – TTP
Soil	40.4 ± 1.7	-24.5 ± 0.8	-26.2 ± 0.6
No shrubs	81.5 ± 13.3	-25.7 ± 0.6	-25.8 ± 0.4
No monocots	90.4	-26.3 ± 0.3	-26.9

Table 3.3 – Mean respiration fluxes and estimated $\delta^{13}C$ values for CO_2 respired from each treatment (± 1 σ_e). KP = Keeling plot, TTP = two time points. There is no estimate of the uncertainty for the 'no monocots' flux and $\delta^{13}C$ value *via* the two time point approach as only 1 replicate met the flux criteria. 'Soil' treatment (n = 4), 'No shrubs' treatment (n = 5), 'no monocots' treatment (n = 1).

Mean respiration fluxes ranged from 40.4 to 81.5 mg CO_2-C m^{-2} h^{-1} with the highest mean flux produced by the 'no shrubs' treatment (only one chamber measured a flux for the 'no monocots' treatment and so is not considered to be a mean flux). The smallest CO_2 production rate was produced by the 'soil' treatment, having a mean value of 40.4 ± 1.7 mg CO_2-C m^{-2} h^{-1}. This 'soil' flux measured was approximately 45 % of the single 'no monocots' treatment and approximately half of the mean flux for the 'no shrubs' treatment.

In addition to estimating the $\delta^{13}C$ signature of respired CO_2 for all treatments using the Keeling plot approach, it was decided to establish whether a similar value could be derived for each treatment using only two time points from each set of time series data that met the flux criteria (i.e. entering the concentration and isotopic data from these two time points into a mass balance equation). This was done in order to determine whether reliable

estimates could be obtained for the $\delta^{13}C$ value of source respired CO_2 using fewer samples than that required for a Keeling plot. For example, as would be the case during an incubation experiment (see Chapter 4) where much smaller respiration collection chambers are used. Results calculated using the two time point approach are also presented in Table 3.3.

The $\delta^{13}C$ values of source respiration calculated by the Keeling plot technique and the two time point approach were identical at 2 σ_e for all treatments. Mean $\delta^{13}C$ values for source respired CO_2 were generally lower for the two time point calculation than those estimated using the Keeling plot approach, but not significantly so at 2 σ_e. This suggests that reliable estimates can be obtained for the stable carbon isotope composition of source respiration using the two time point approach.

3.4.4 Statistical analysis

3.4.4.1 Fluxes of respired CO_2

To investigate whether there were any significant differences between the 'soil' treatment and the 'no shrubs' treatment an F test (tests for equality of variances) was performed on the flux of respired CO_2 for each treatment. As variances were unequal ($F_{4,3} = 80.02$) at the 5 % probability level, it was considered appropriate to perform a two-sample t-test with unequal variances (i.e. non-pooled t-test or Welch's t-test). According to this test, on the day of sampling, respired CO_2 from the 'no shrubs' treatment was significantly greater than the 'soil' treatment ($P > 0.95$). The 'no monocots' treatment was not compared as one of the requirements for performing an ANOVA (to compare 3 treatments or more) is that you have a minimum of two replicates (but preferably three) for each treatment.

3.4.5 Carbon isotope composition ($\delta^{13}C$) of respired CO_2

It is clear from Table 3.3 that using natural abundance $\delta^{13}C$ values to partition ecosystem respiration into that of different plant functional types or to partition plant and soil respiration is not possible with the method employed here; all calculated $\delta^{13}C$ values were statistically identical at 2 σ_e. Furthermore, using selected statistical tests, it was still not possible to find a significant difference between the two treatments. There are a number of possible reasons for this to be the case.

Firstly, it is possible that there were no differences between plant functional groups in the stable carbon isotope composition of respired CO_2 or, alternatively, the differences were not large enough to be detected. However, assuming there were differences, there are a number of possible reasons why they were not detected, e.g. the method of CO_2 collection used in this study may be unsuitable for trapping respiration from a peatland ecosystem (due to sample loss). Another reason could be that the size of sample removed from chambers was inadequate. A 20 ml sample of air removed from a 33 000 ml headspace chamber (0.06 %) may not be completely representative of CO_2 within the chamber. This is unlikely however, as headspace gas was well mixed by pumping the chamber atmosphere with the syringe three times before removing a sample.

Other problems may arise when using the Keeling plot technique. For example, a drawback with the Keeling plot approach in that the extrapolated intercept of the linear regression is several per mil away from that gained in the actual measurements (Yakir & Sternberg, 2000). This means that errors (even small ones) in the measurement of either the concentration or the isotopic signature of respired CO_2 may lead to a large error (*via* extrapolation) in the estimate of source CO_2 from the Keeling plot intercept.

3.5 Conclusion

The aim of this study was to investigate the contribution of various components of a peatland ecosystem (e.g. soil, monocots, bryophytes and ericoid sub-shrubs) to total ecosystem respiration and hence determine their role in carbon loss from the system. However, due to the physical nature of the ecosystem itself, measuring fluxes proved to be difficult and many flux chambers did not perform as required. This is attributed to the presence of shrub roots beneath chamber collars, which prevented an airtight seal between chamber collar and the peat surface.

For future studies of primary fluxes and isotopic signatures of source respiration within peatland ecosystems it is recommended that all chamber collars are inserted to a minimum depth of 10 cm below the peatland surface in order to avoid flushing of chambers and loss of respired CO_2. Furthermore, if ericoid sub-shrubs are to be included within a chamber collar, a careful search should be made to find plots where shrub roots originate from directly below the peatland surface and not laterally positioned with respect to respiration chambers (to avoid the presence of shrub roots underneath chamber collars). This may be extremely difficult to carry out satisfactorily because it is the nature of the growth of the *Calluna vulgaris* species to grow laterally as well as horizontally. Furthermore, a thorough

search was in fact performed before placement of chamber collars for this experiment (Ostle, personal communication). An additional drawback to performing a thorough search could be considerable site disturbance. However, if this careful site selection is not carried out, it is worth noting that chamber collars that are sunk to depth in the peat, may cut off roots, and in doing so will likely cause vegetation to senesce (Davidson *et al.*, 2002), with particular regard in this respect to shrubs.

A further aim of this study was to ascertain whether ecosystem sources could be distinguished isotopically using stable ($^{13}C/^{12}C$) isotopes and this aim was achieved. It is concluded that it is not possible (using the technique employed here) to partition peatland ecosystem respiration into that of different plant functional groups using natural abundance stable isotopes, as all sources proved to be statistically identical at 2 σ_e. It is suggested that an isotopic label (e.g. ^{13}C) may be of more use in this regard (Ward, 2006).

However, although it was not possible to partition ecosystem respiration into its individual component sources using the stable carbon natural abundance technique, it is considered that a reliable estimate for the isotopic signature of source respiration can be calculated from only two time points that are significantly different (in CO_2 concentration and $\delta^{13}C$). This will be particularly useful for incubation experiments where CO_2 is normally collected in much smaller respiration chambers (where only a limited number of sub-samples can be taken) to that used in the field.

4 Abiotic drivers and their interactive effect on the isotopic ($\delta^{13}C$) signature and flux of soil CO_2

4.1 Introduction

Soils contain the largest reservoir of carbon in the terrestrial biosphere with an estimated 1.6 Tt of stored carbon (Schimel, 1995a). This constitutes more than twice the stock of carbon held within terrestrial vegetation, and more than twice that presently resident in the atmosphere. Furthermore, peatland ecosystems in particular occupy approximately 3 % of the terrestrial land surface but are estimated to store a third of all terrestrial carbon stocks (Gorham, 1991). However, it should be said that the previous statement is indicative only, as there has been considerable variation in quantitative estimates of peatland area (Clymo *et al.*, 1998). Peat is formed from the accumulated remains of dead plants that are in varying stages of decomposition (Clymo, 1983). Its rate of formation or decomposition is controlled primarily by temperature and hydrology but also to a lesser extent by factors such as substrate quality and nutrient availability. The surface layers of a peatland and their associated vegetation are referred to as the acrotelm (Ingram, 1978).

Conditions in the acrotelm can vary between aerobic and anoxic depending on the position of the water table (which is regulated by precipitation, run-off, downward percolation and evapotranspiration) (Pearce & Clymo, 2001). The lowest point to which the water table drops during a dry growing season forms the base of the acrotelm and also the top of the catotelm (the 'true accumulator' of carbon within a peatland (Clymo *et al.*, 1998)) where permanently waterlogged and anoxic conditions persist. Both climate and land use change will influence soil carbon 'source' function (particularly for peatlands) with the potential to further increase atmospheric CO_2 levels as a result of feedback responses (Cox *et al.*, 2000; IPCC, 2001) to warming and hydrology.

Stores of soil carbon are predicted to respond to climatic change, as it has been proven that soil organic matter (SOM) decomposition rates respond to varying moisture and temperature regimes (Parton *et al.*, 1987; Schimel *et al.*, 1994). For example, concomitant with a 1 °C rise in temperature, soils globally have been predicted to release between 10 and 30 Pg of carbon to the atmosphere (Schimel *et al.*, 1994). To understand just how much and for how long carbon is stored in soils, it is of critical importance that we determine the residence time and effluxes of SOM carbon and identify the effects of the

regulatory processes involved. Many factors influence carbon flux from soils, including; soil parameters (both physical and chemical), temperature, pH, nutrient availability, hydrology and substrate quality. However it is temperature, followed by soil moisture content (under normal soil moisture conditions) (Bowden *et al.*, 1998) which are considered to be the primary regulators of CO_2 fluxes to and from soils, and also the terrestrial ecosystems in which they are situated.

Respiration in plants sharply increases with temperature (Lloyd & Taylor, 1994) and it is generally agreed that soil respiration (microbial decomposition of organic matter) will also increase with rising temperatures (caused by climate change). This has been demonstrated in a range of different ecosystems e.g. boreal forest (Dioumaeva *et al.*, 2002), peatlands (Chapman & Thurlow, 1998), Arctic tundra (Biasi *et al.*, 2005) and temperate forest soil (Bowden *et al.*, 1998). However, there is considerable debate in the literature as to how much carbon (through the mineralisation of organic matter stimulated by climatic drivers) could potentially be released to the atmosphere from soils, and hence this uncertainty extends to predictions (*via* modelling) of feedbacks to climate change (Giardina & Ryan, 2000; Knorr *et al.*, 2005).

For example, soil respiration response to increases in temperature is often described by the Q_{10} value (ratio of two soil respiration rates separated by a 10 °C difference in temperature). Kohlmaier *et al.* (1990) showed, using a modelling approach that included both net primary production and soil respiration responses to temperature, that for a Q_{10} of 2.0 for soil respiration, productivity overcame the increase in decomposition *via* soil respiration. However when the Q_{10} for soil respiration rose to between 2.5 and 3.0, the opposite was true, with increased CO_2 fluxes from soil respiration being in excess of the negative feedback response through the CO_2 fertilisation effect.

Other studies have shown that different soil organic matter fractions may have a differential response to rises in temperature. For example, Liski *et al.* (1999) suggested that the somewhat larger stocks of older, more recalcitrant carbon were unaffected by temperature regimes and that only the labile fraction of soil organic matter (SOM) was sensitive to temperature. On the other hand, Giardana *et al.* (2000) suggested that carbon pool turnover times were insensitive to temperature and that, in fact, it was substrate quality that was the key parameter that controlled soil carbon mineralisation rates and not temperature. However, Knorr *et al.* (2005) showed that not only was carbon in SOM sensitive to temperature but, further, that the non-labile fraction of SOM was more

sensitive than the labile fraction. This study used exactly the same data as Giardana *et al.* (2000) but incorporated it into a more sophisticated model.

Of even greater importance than studying soil organic matter response to the individual effects of soil moisture and temperature is to study their interactive effects (Davidson *et al.*, 2000). Soil water content is regulated by evapotranspiration, which is in turn controlled by temperature. Temperature, therefore, affects decomposition rates not only directly but also indirectly by controlling soil moisture. Hydrology can affect the decomposition of organic matter in a number of ways; either directly, by controlling the amount of moisture supplied to decomposer organisms used as a medium for tissue growth and facilitating the activity of aquatic organisms (e.g. protozoa or nematodes), or indirectly by affecting other factors such as aeration or pH (Swift *et al.*, 1979).

An excess of soil water found in saturated or waterlogged soils e.g. peatlands, will reduce decomposition due to the soil being anaerobic. Anaerobic decomposition proceeds much more slowly than aerobic decomposition (Clymo *et al.*, 1998) and occurs within waterlogged peat as a consequence of the much reduced diffusion rate of O_2 in water than in air. Reduced rates of SOM decomposition also occur at the opposite moisture extreme. Tropical soils that are dry for long periods undergo slow decomposition processes due to microbes being either physiologically stressed or inactive.

Decomposition is inhibited in this case due to very little moisture being present and what is often requires too large a matric potential to be extracted (matric potential is a measure of the availability of water in the soil to plants; it is measured as the suction or tension pressure, in pascals, required to extract water). Furthermore, decreased moisture results in reduced mobility of soluble substrates (used for assimilation by microbes) and also in reduced diffusion of extracellular enzymes produced by microbes for the breakdown of organic matter (Davidson *et al.*, 2006a). These two processes proceed much more quickly and efficiently as the film of water within soil increases. Therefore, reduced moisture conditions that lead to drought stress can lead to decreased microbial respiration within the soil (Skopp *et al.*, 1990).

However, high latitude peatlands are not moisture limited, and are in fact quite the reverse, being waterlogged for long periods throughout the year. Soil respiration fluxes in these ecosystems are limited by both reduced diffusion of O_2 in water (10,000 times slower than in air; ((Wild, 1981)) and low temperatures. The predicted scenario for these soils is that they will get warmer and drier, both of which effects have been shown to increase CO_2

fluxes in peatlands (Alm *et al.*, 1999; Martikainen *et al.*, 1995; Silvola *et al.*, 1996). Thus, temperature effects throughout a growing season can be confounded by variations in soil moisture (Davidson *et al.*, 2006a).

In addition to the interactive effects of temperature and moisture there is also the possibility of acclimation of soil carbon decomposition processes to rising temperatures. Recently, soil warming studies have shown that the response of efflux of CO_2 from soils, due to a temperature increase, decreases with time (Luo *et al.*, 2001; Melillo *et al.*, 2002) and eventually returns to rates similar to those that occurred before warming took place. This could lead to an overestimate of soil carbon fluxes in global carbon budget models if this so-called acclimation is ignored (Eliasson *et al.*, 2005). According to the IPCC (2001) it is at high latitudes, where a large portion of global soil carbon is stored, that global warming is expected to be the most pronounced. Therefore, these soils may be in danger of shifting from sinks for atmospheric CO_2 to sources. At the very least, the sink capacity of northern latitude soils may be diminished, thereby adding to the current CO_2 loading of the atmosphere (Gorham, 1991) and exacerbating further climate change.

The relative contribution of specific sources and sinks to the total atmospheric CO_2 concentration can be examined using the stable carbon isotopic composition, $\delta^{13}C$, of atmospheric CO_2, at global, regional and local scales (Bakwin *et al.*, 1998; Battle *et al.*, 2000; Ciais *et al.*, 1995; Fung *et al.*, 1997; Lloyd & Farquhar, 1994; Tans *et al.*, 1989; Tans *et al.*, 1993; Yakir & Wang, 1996). Further, the isotopic signature of soil respiration can be measured in order to elucidate substrate metabolised by microbes (Amundson *et al.*, 1998; Santruckova *et al.*, 2000). Studies of the isotopic signature of respired CO_2 and its variation due to temperature and moisture are few, but they do demonstrate however, that older and more recalcitrant carbon is mineralised effectively at raised temperatures and soil water contents (Andrews *et al.*, 2000; Biasi *et al.*, 2005; Bol *et al.*, 2003; Fessenden & Ehleringer, 2003; Lai *et al.*, 2004; McDowell *et al.*, 2004).

Understanding the response of soil respiration to climatic regulators is vital, particularly in light of current models of global warming scenarios (Cox *et al.*, 2000). Currently, simulation models use a single fixed value (Q_{10}) to describe the response of soil respiration to increases in temperature (Boone *et al.*, 1998). However, the exponential function described by the Q_{10} value, not only varies over different ranges in temperature but also varies between different ecosystems (Boone *et al.*, 1998). Furthermore, in a warmer world respiratory processes are thought to outweigh the negative feedback provided by an increase in assimilatory processes (Kirschbaum, 2000) which are subject to limitation by

nutrient supply and light. In this chapter the response of incubated peat cores to the interactive effects of both hydrology and temperature are investigated. Incubating cores under controlled laboratory conditions allows the separation of the individual effects from the interactive effects of moisture, temperature and substrate quality that co-vary in the field. Field studies are subject to a number of systematic problems, and substrate depletion is of particular importance. However, there are no such problems with laboratory based studies (Kirschbaum, 2006) as abiotic parameters such as temperature and moisture can be controlled, thus preventing them from co-varying.

The main objectives of this experiment were to determine the temperature sensitivity of peatland soil respiration (Q_{10}) in response to the individual and interactive influences of soil moisture and organic matter quality. A further objective was to establish whether the respiratory Q_{10} response from these incubated cores was transient (i.e. is there any acclimation to temperature of soil respiration with time?).

The main hypotheses for this investigation are as follows:

1) That increased temperature and reduced soil moisture both individually and interactively increase respiratory CO_2 fluxes (simulation of interactive climatic drivers).

2) The $\delta^{13}C$ value of carbon fluxes will be higher at elevated temperatures, due to increased decomposition (or mobilisation) of previously recalcitrant organic matter that is more enriched in ^{13}C.

3) That the $\delta^{13}C$ value of carbon dioxide fluxes will be higher, the further down the profile peat is removed from, due to increased contribution from ^{13}C enriched organic matter with depth.

4) That increased fluxes of soil carbon will be transient either due to acclimation or to labile substrate limitation.

To investigate these hypotheses, an incubation study was executed that involved taking flux measurements, both primary and isotopic, from incubated peat cores. Peat cores were collected from an ombrotrophic blanket bog (Hard Hill, Moor House NNR). It is generally accepted that high quality organic matter is more readily decomposed by microbiota than more recalcitrant compounds such as lignin. This applies to fresh litter and also to recently

formed organic matter which are normally expected to be of a higher quality than older, more decomposed organic matter within which the components that are more labile have already been metabolised (Aerts, 1997; Berg, 2000). Therefore, to simulate differences in substrate quality/availability peat cores were extracted from three different depths in the peat profile. Cores were then incubated at three temperatures and two moisture levels in order to simulate the effects of interactive climate drivers.

4.2 Materials and methods

4.2.1 Experimental design

To examine the interactive effects of hydrology, temperature and substrate quality, cores of blanket peat were incubated in the dark at three different temperatures (5, 10 and 15 °C) for 116 days. These temperatures fell within the normal annual range of soil temperatures found at the Moor House field site (for site description see section 3.2.1). Indeed, Ineson *et al.* (1998) reported monthly mean soil temperatures at 2 cm depth ranging from 0 to 15 °C at nearby locations to the Hard Hill site within Moor House NNR. Two soil moisture levels were chosen: 50 and 100 % field capacity. However, 100 % field capacity does not represent saturation (i.e. water-logging), but rather the maximum amount of water the soil can hold by capillary action. In addition, cores were taken at each of 3 depths in the profile to examine the effect of substrate quality/availability on decomposition. Peat was collected as intact cores in order to minimise disturbance (i.e. as opposed to drying, sieving and homogenising the soil).

4.2.2 Sample collection

Ninety-six peat cores were taken using plastic soil pipe, 10 cm in length and 3 cm in diameter with a 2 mm thick wall, from the Hard Hill site at Moor House NNR. Vegetation was removed from the peatland surface after which soil pipe was cut into the peat. Cores, retained in the soil pipe, were carefully extracted from the profile and placed into clear plastic bags, which were labelled and stored in cool boxes until returned to the laboratory at CEH Lancaster.

Once collected, ninety of the cores were placed into plastic 1.8 L microcosms (Figure 4.1), (Lock & Lock containers, Lakeland Ltd., Windermere, UK). These microcosms had airtight clip-on lids with a rubber septum (Suba seal, Scientific Laboratory Supplies Ltd,

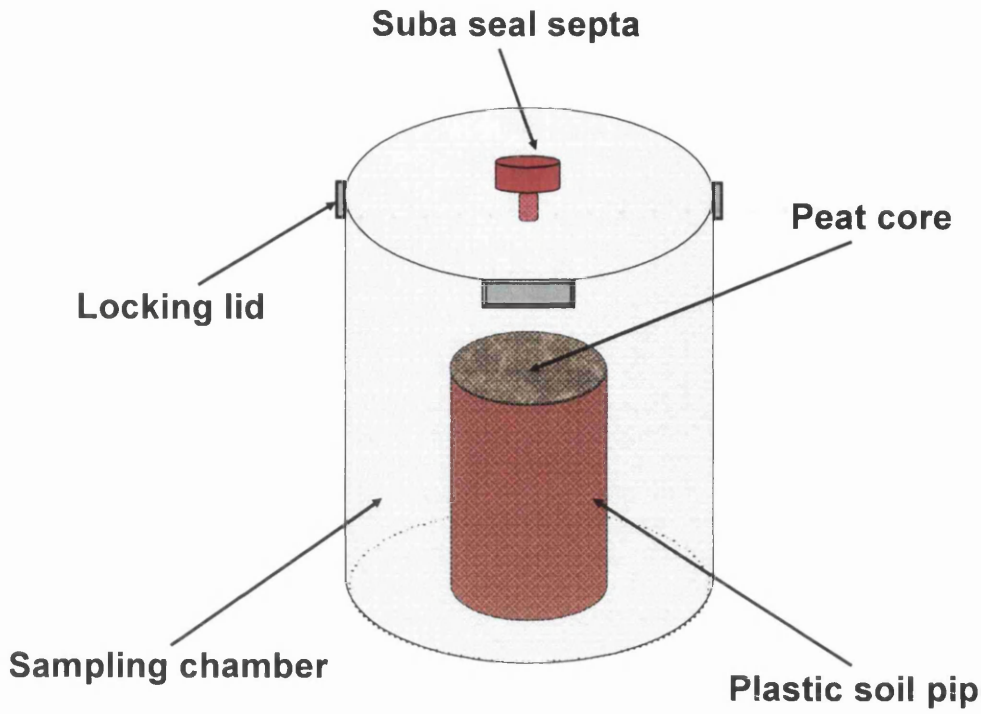

Figure 4.1 – Schematic diagram of a peat core being incubated in a plastic microcosm. Lids were removed between flux measurements.

Nottingham, UK) in the lid to allow gas sampling during incubation. The six remaining peat cores were used to measure % moisture, % carbon and bulk $\delta^{13}C$ signature prior to incubation (see section 4.2.3).

4.2.3 Laboratory incubation

All cores were weighed at field capacity (deionised water was added to cores until they could retain no more by capillary action) and placed inside plastic microcosms Figure 4.1). Ninety cores were divided into 3 groups of thirty, for each of the 3 depths in the profile that they had been extracted from. Each set of thirty was then further subdivided into 3 groups of 10 for each of the three incubation temperatures. Finally, each subset of 10 cores were divided into two groups of 5, to be incubated at the two treatment hydrology regimes, 50 and 100 % field capacity. Finally, each of the 3 interactive effects was replicated 5 times to give a total of 90:

3 depths x 3 temperatures x 2 soil moisture contents x 5 replicates = 90 cores.

All cores were initially stored at 20 °C. This allowed half of the cores to dry out to the desired 50 % field capacity water content. The remaining cores (100 % field capacity) were also stored at 20 °C during this time (to maintain the same conditions for all cores) and had their moisture level maintained by regular addition of deionised water. Six trial

cores were taken at the field site to establish the soil moisture content of peat at the Hard Hill site. Soil extracted from the surface layers (0 – 30 cm) at the Hard Hill site was found to contain ~ 90 % water.

Fifty percent of field capacity was calculated by first deducting the weight of the soil pipe from each of the cores when they were weighed at 100 % field capacity. Ninety percent of that weight was then calculated (weight moisture) and divided by 2, to get 50 % field moisture. This weight was then added to the dry weight of the peat core (10 % of the core weight at field capacity). This then became the target weight that the 50 % field capacity treatment cores had to dry out to. Once the 50 % field capacity cores had reached their target weight all ninety cores were transferred to each of the 3 incubation rooms maintained at 5, 10 and 15 °C (referred to subsequently as day 1 of the incubation).

4.2.4 Soil respiration measurements

4.2.4.1 Linearity test of respiration flux

Initial respiration measurements were carried out on cores incubated at 15 °C to establish a timeframe within which soil respiration was linear and also to ensure that CO_2 fluxes from cores had settled down to a base level after initial disturbance. Three surface cores (0-10 cm) held at 15 °C and 100 % field capacity were incubated for ~ 3 days. Gas samples were removed from the microcosms at time 0 and after, at a further 10 time points, and placed into evacuated Exetainers. Once the linearity test had been performed (results can be found in Appendix iv), the ninety incubated peat cores were sampled on four different occasions; days 34, 41, 84 and 116.

4.2.4.2 Sampling respired CO_2 from microcosms for $\delta^{13}C$ analysis using Exetainers

At the beginning of each sampling, the lid of each airtight microcosm was closed and a 5 ml sample of headspace gas was removed using a gastight syringe, and placed immediately into an evacuated (10^{-1} mbar) 3 ml Exetainer. After a given time period, a second sample was withdrawn from the chamber and placed into another evacuated Exetainer. All Exetainers containing gas samples were stored in the incubation room in which they had been sampled until required for analysis (to eliminate the possibility of compromising sample integrity by creating pressurisation effects).

Carbon dioxide concentrations were measured by Gas Chromatography using a Perkin Elmer Autosystem XL gas chromatograph equipped with an FID. The GC was interfaced to a PC equipped with TurboChrom software that integrated GC output. Gas samples (1 ml) were injected by means of a headspace autosampler (Hi Tech Applications, UK). CO_2 concentrations were calculated relative to peak areas acquired by injecting standards of known concentration, i.e. CO_2 – 541 ppm (BOC, UK). Detector responses were calibrated at the beginning, during and end of each sample run on a daily basis, in order to account for any machine drift during a run.

4.2.4.3 Conversion of CO_2 concentration (ppm) to a mass of CO_2-C per g soil

The headspace of the chamber (chamber volume – volume of peat core) was then taken into account by multiplying the concentration of CO_2 produced in the chamber (ppm) by the headspace volume (V) in litres (l):

$$\mathbf{ppm \ x \ V = ppmv \ CO_2 \ or \ \mu l \ CO_2 \ l^{-1}} \qquad \mathbf{(1)}$$

To convert this volume to a mass of CO_2-C, the Ideal gas law equation was used to take account of the different pressure that a fixed mass of CO_2-C would create at different temperatures:

$$\mathbf{C_m = (C_V \ x \ m \ x \ P) \ / \ (R \ x \ T)} \qquad \mathbf{(2)}$$

where C_m is the mass of carbon respired in the chamber ($\mu g \ CO_2$-C l^{-1}), C_V is the flux of CO_2 in the chamber ($\mu l \ CO_2 \ l^{-1}$), m is the molecular weight of the species of interest (12 μg CO_2-C/$\mu mol \ CO_2$), P is the barometric pressure in atmospheres (atm), R is the universal gas constant in units of 1 atm K^{-1} mol^{-1} (0.0820575) and T is the absolute temperature (incubation) in Kelvin. The mass of CO_2-C at the start of the incubation is deducted from the mass at the end, to acquire the total mass of CO_2-C respired during the period of incubation. This mass is converted to a flux by dividing by the incubation period in hours. Finally the flux is divided by the dry weight of the peat core to get a flux of CO_2-C respired per gram of soil ($\mu g \ CO_2$-C g $soil^{-1}$ h^{-1}).

4.2.4.4 Determination of soil sensitivity to temperature (Q_{10})

Q_{10} values were calculated (Kirschbaum, 1995; Leifeld & Fuhrer, 2005) for fluxes produced by cores extracted from each of the three profile depths and under the two

moisture treatments across the experimental range of temperatures using the following equation:

$$Q_{10} = (k_2 / k_1)^{10/(T_2 - T_1)} \quad (3)$$

where k_2 and k_1 are rate constants for the process under investigation (in this case k_1 and k_2 are production rates of CO_2) and T_1 and T_2 are the temperatures (Kelvin) that the process is observed at. Thus the Q_{10} values are based on instantaneous CO_2 production rates as opposed to being calculated *via* decay rate constants (Leifeld & Fuhrer, 2005).

4.2.4.5 $\delta^{13}C$ determination of source respired CO_2

Determination of the $\delta^{13}C$ values for samples of respired CO_2 was carried out by TG-IRMS. Samples were injected by way of a gas tight syringe, into the trace gas CO_2 preconcentrator. Water was removed by routing through a magnesium perchlorate trap prior to introduction to the chromatographic column. The chromatographic column separated any nitrous oxide in the sample from CO_2, before finally admitting the gas to the mass spectrometer (Micromass Isoprime, Micromass, UK) *via* an open split. Sample runs were 11 minutes long and reference standards were injected at the start of each run and subsequently after every 15 samples. Internal precision was better than ± 0.3 ‰ for $\delta^{13}C$. For full details of the method see Chapter 3, section 3.2.7. All values for ^{13}C are reported using the delta notation with $^{13}C/^{12}C$ variations relative to the international standard Vienna Pee Dee Belemnite (VPDB), as described by equation 4:

$$\delta^{13}C\ (‰) = [(R_{sample} / R_{standard}) - 1] \times 1000 \quad (4)$$

The stable carbon isotope composition of source respired CO_2 was determined by entering the concentration data at time 0 (atmospheric CO_2: $Conc^n_{Start}$) and time point 1 ($Conc^n_{Final}$: atmospheric + biologically produced CO_2), along with the $\delta^{13}C$ value of CO_2 measured at both these time points ($\delta^{13}C_{Start}$ and $\delta^{13}C_{Final}$) into a mass balance equation as follows:

$$\delta^{13}C_{Source} = \frac{(\delta^{13}C_{Final} \times Conc^n_{Final}) - (\delta^{13}C_{Start} \times Conc^n_{Start})}{Conc^n_{Source}} \quad (5)$$

The concentration of source respired CO_2 ($Conc^n_{Source}$) is calculated by subtracting the starting CO_2 concentration from the CO_2 concentration at time point 1.

4.2.5 $\delta^{13}C$ analysis of respired CO_2 using MS^3

After the final sampling of $\delta^{13}C$ values using Exetainers had been performed, respired CO_2 was collected for $\delta^{13}C$ analysis by attaching the molecular sieve sampling system (see Chapter 2; Hardie *et al.*, 2005) to each of a number of selected microcosms (Figure 4.2).

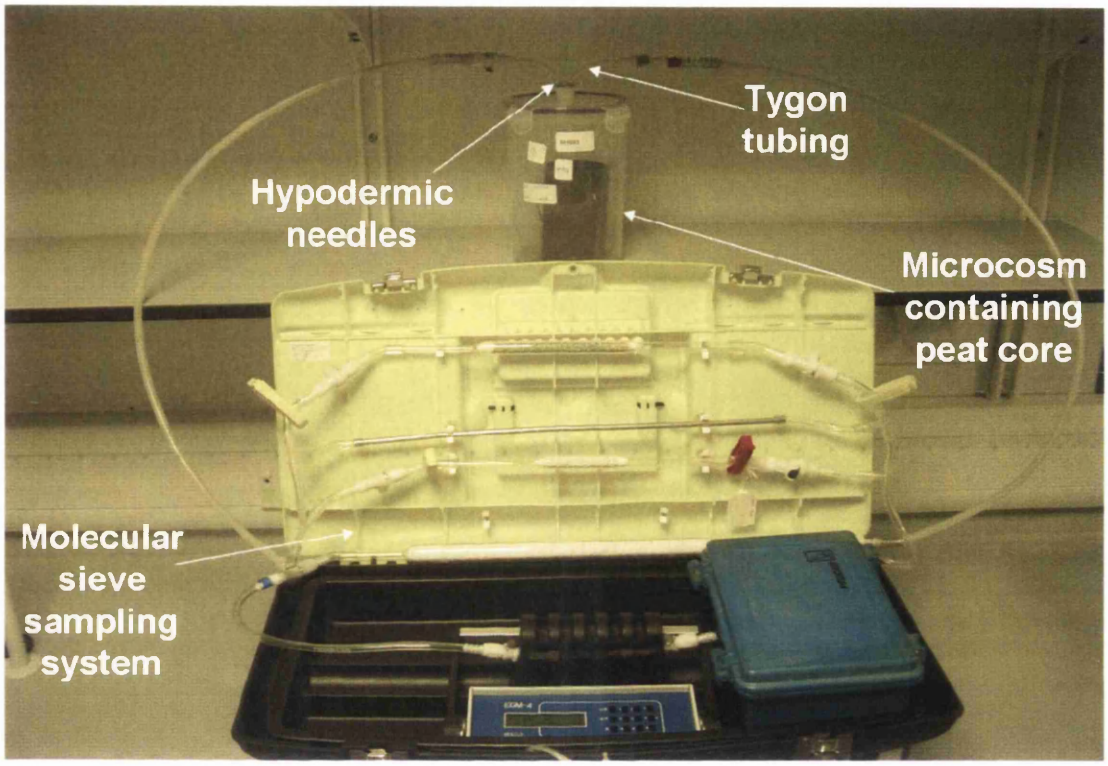

Figure 4.2 – Annotated photograph of the molecular sieve sampling system attached to a microcosm containing a peat core.

This experiment was performed to ascertain whether MS^3 could be used successfully to capture respired CO_2 from an incubation study. Although it was not envisaged that samples from this project would be ^{14}C dated, this test would demonstrate whether samples for ^{14}C analysis could be obtained in this way.

Two Quick couplings (Colder Products Company, USA) were attached with clear plastic tubing (Tygon, R3603, 4.8 x 8.0 mm, Fisher Scientific, UK) to hypodermic syringe needles (38 mm, 21 gauge - Fisher Scientific, Leicester, UK) placed into the septum of each microcosm. A 6 cm piece of 2 mm bore plastic tubing was attached to one of the hypodermic needles to facilitate good air circulation within the chamber, thus preventing air streaking from one needle across to the other when the pump was switched on.

Respired CO_2 was collected at 5 and 15 °C from all 3 depths under the 100 % field capacity treatment but from only three of the five replicates. Each microcosm was sealed

and atmospheric CO_2 removed (< 10 ppm residual left) by routing through the sodalime trap. A sufficient volume of CO_2 (3-10 ml) was then allowed to evolve before being collected on individual molecular sieve cartridges (MSCs). Once the respired CO_2 had been collected, all MSCs were returned to the NERC RCL in East Kilbride, where respired CO_2 was recovered on a vacuum rig (Hardie *et al.*, 2005).

Before sampling the incubation chambers with MS^3, evacuation tests were performed to ascertain whether there was the possibility of contamination from atmospheric CO_2 leaking into the chambers once they had been scrubbed below 10 ppm. These tests showed that insignificant amounts of atmospheric CO_2 entered the microcosms and so were considered to be reliable for capturing CO_2 from incubated cores without loss of sample.

4.2.6 Carbon isotope ($\delta^{13}C$) analysis of bulk peat

Five replicate cores from each of the three depths in the profile were oven dried at 70 °C until a constant weight, after which they were ground with a pestle and mortar. Soil was further homogenised and reduced to a fine powder by use of a nitrogen grinding mill (for full details see Chapter 3, section 3.2.5). The stable carbon isotopic signature of bulk peat was then analysed using EA-IRMS (elemental analysis – isotope ratio mass spectrometry). All EA-IRMS analyses were performed by Darren Sleep.

4.3 Results

Prior to sampling all 90 treatment cores, three cores incubated at 15 °C were sampled periodically over the course of 3 days. This was carried out to establish a period over which CO_2 fluxes were linear (to minimise diffusion gradient effects on respired CO_2 fluxes). Results can be found in Appendix 4.

4.3.1 Respiration fluxes and Q_{10} values

4.3.1.1 Day 34 of the incubation

Figure 4.3 illustrates respiration fluxes produced by all cores on day 34 of the incubation.

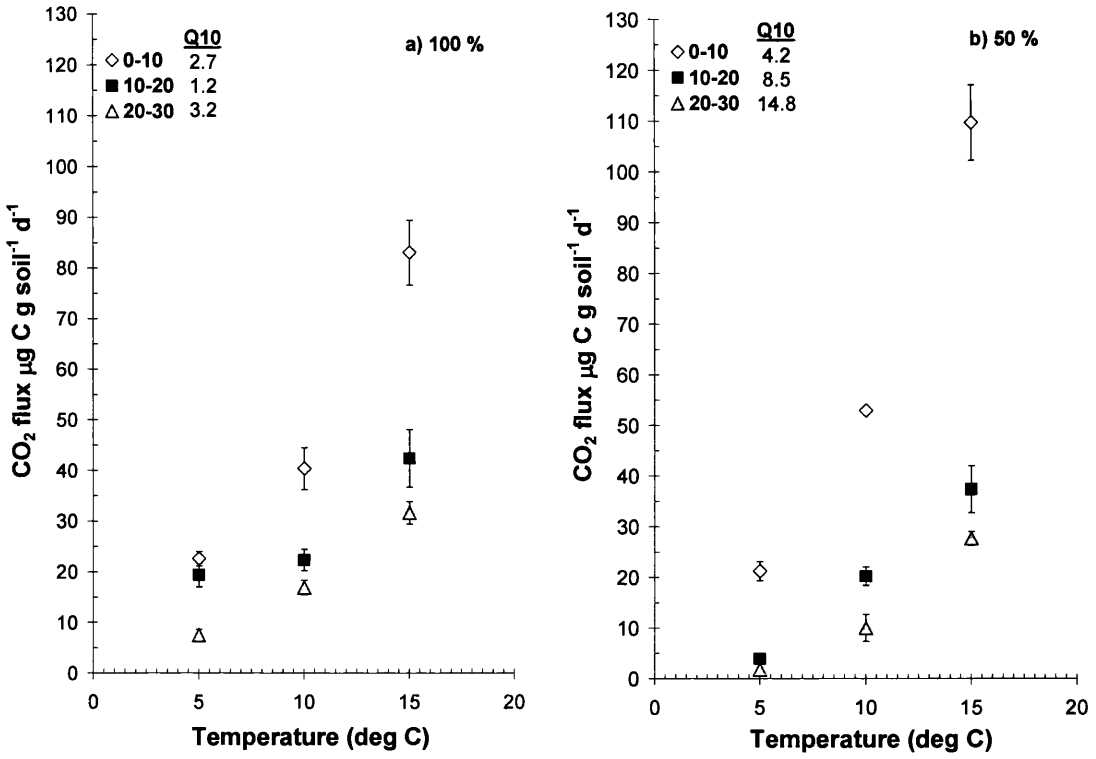

Figure 4.3 – Respiration fluxes and Q_{10} values for all cores sampled on day 34. Error bars are ± 1 σ_e. a) cores incubated at field capacity. b) cores incubated at 50 % field capacity. Error bars are ± σ_e and ones that are not visible are smaller than the symbols. n = 5 for all points except: 10-20 cm depth, 5 °C – 50 % field capacity (n = 4) and 20-30 cm depth, 5 °C – 50 % field capacity (n = 3).

This was the first respiration sampling performed on all 90 cores. The number of replicates (n) equals five unless otherwise stated (where n < 5 was due to either Exetainer failure or insufficient respired CO_2). Cores incubated at 15 °C produced the largest fluxes. This was true for all depths and both moisture levels, as would be expected. Within a single temperature treatment, the largest fluxes were found to emanate from the 0-10 cm depth followed by the 10-20 cm depth and the smallest flux measured was produced by the lowest depth increment (20-30 cm). This was also true for both moisture treatments.

Fluxes from the 0-10 cm increment ranged from 21.2 ± 1.87 at 5 °C (50 % field capacity) to 109.7 ± 7.4 µg C g soil^{-1} d^{-1} at 15 °C (50 % field capacity). The 20-30 cm depth increment produced the smallest flux, ranging from 1.8 ± 0.5 µg C g soil^{-1} d^{-1} for the cores held at 50 % field capacity and 5 °C, to 31.7 ± 2.2 µg C g soil^{-1} d^{-1} for the cores held at 100 % field capacity and 15 °C. Q_{10} values on day 34 ranged from 1.2 to 14.8, with the highest Q_{10} values being measured in the 50 % field capacity treatment. The 20-30 cm depth was most sensitive to an increase in respiration rate for every 10 °C rise in temperature (for both moisture levels) as can be seen from the Q_{10} values in Figure 4.3. Respiration rates

produced at 10 and 15 °C under both moisture treatments differ by more than 1 σ_e at all depths.

4.3.1.2 Day 41 of the incubation

Figure 4.4 illustrates CO_2 fluxes for the cores sampled on day 41 of the experiment. Once

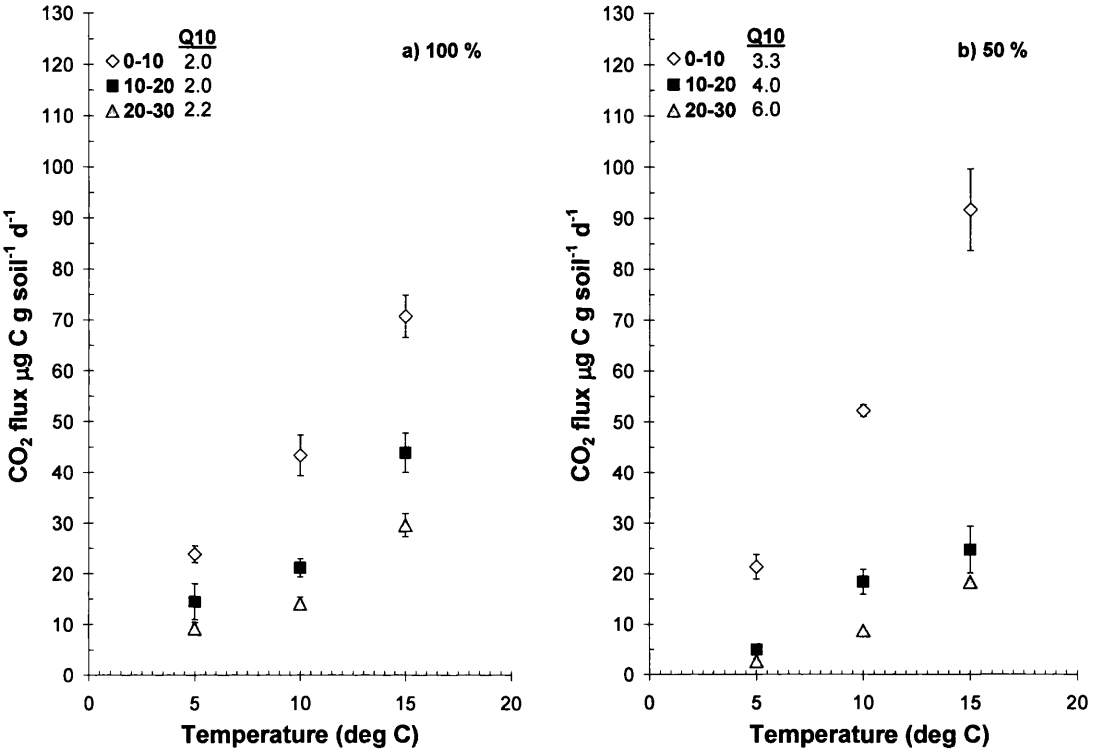

Figure 4.4 - Respiration fluxes and Q_{10} values for all cores sampled on day 41. Error bars are ± 1 σ_e. a) cores incubated at field capacity. b) cores incubated at 50 % field capacity. Error bars are ± 1 σ_e and ones that are not visible are smaller than the symbols. n = 5 for all treatments.

again the fastest respiration rate was produced by the 50 % field capacity level treatment at 15 °C (91.7 ± 8.0 µg C g soil^{-1} d^{-1}). The smallest flux produced was at 5 °C, by the 20-30 cm depth increment, but this time it was observed in the 50 % field capacity treatment (2.6 ± 0.4 µg C g soil^{-1} d^{-1}) and not the 100 % field capacity treatment, which produced a flux more than three times as large at 9.2 ± 1.2 µg C g soil^{-1} d^{-1}. Respiration rates produced at 15 °C under 100 % field capacity differ by more than 2 σ_e at all depths. The smallest Q_{10} values were produced by the 100 % field capacity treatment, covering a relatively small range of between 2.0 and 2.2. A larger range and greater sensitivity to temperature increase was calculated for the 50 % field capacity treatment, having Q_{10} values of between 3.3 for the top 10 cm and 6.0 for the bottom 10 cm depth.

4.3.1.3 Day 84 of the incubation

Figure 4.5 illustrates the fluxes and Q_{10} values for day 84 of the incubation, the third and

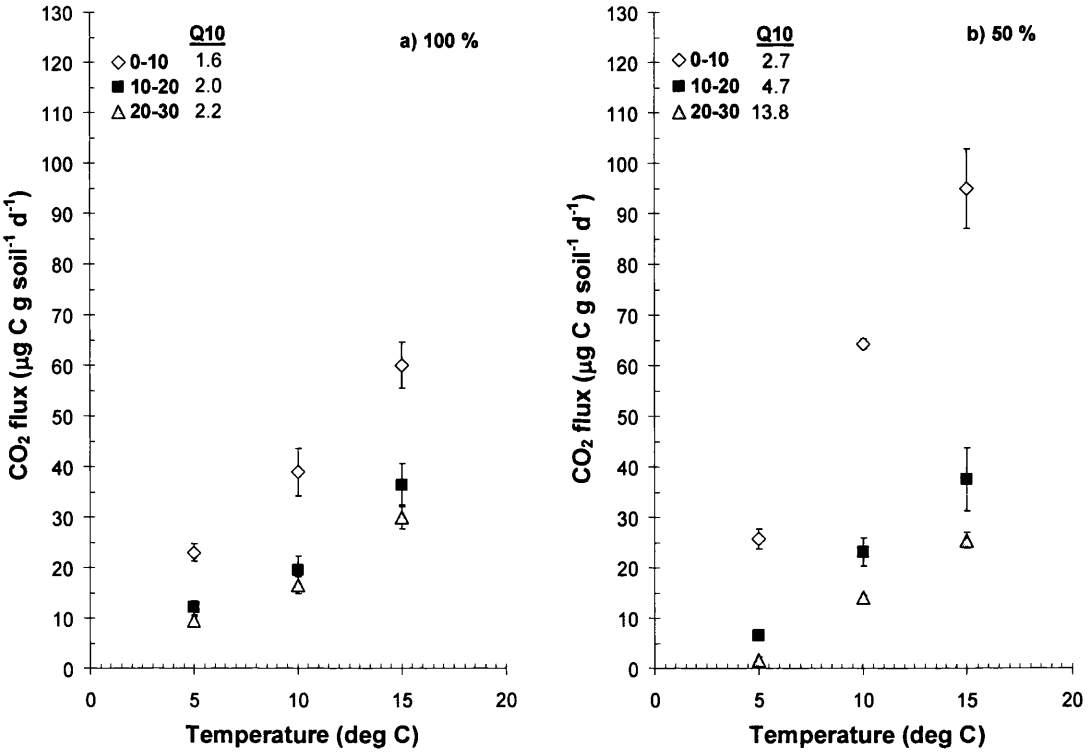

Figure 4.5 - Respiration fluxes and Q_{10} values for all cores sampled on day 84. Error bars are ± 1 σ_e. a) cores incubated at field capacity. b) cores incubated at 50 % field capacity. Error bars are ± 1 σ_e and ones that are not visible are smaller than the symbols. n = 5 for all treatments except: 100 % field capacity, 5 °C, 20-30 cm (n = 4).

penultimate flux sampling of the incubation. Fluxes follow a similar pattern to the previous two samplings. Smallest respiration rates were produced by the 5 °C treatment. At 20-30 cm depth and 50 % field capacity the measured flux was 1.7 ± 0.6 µg C g soil^{-1} d^{-1} (the smallest flux measured for the entire incubation), but was within 1 σ_e of the same flux measured on days 34 and 41. The largest flux was again produced by the 0-10 cm cores incubated at 15 °C and 50 % field capacity (94.9 ± 7.9 µg C g soil^{-1} d^{-1}), a value that is also within 1 σ_e of the same flux measured on days 34 and 41 of the incubation. Respiration rates produced by the 0-10 cm cores at 5, 10 and 15 °C differ by more than 2 σ_e for both moisture treatments.

Q_{10} values were smallest for the 100 % field capacity treatment and ranged from 1.6 for the 0-10 cm depth to 2.2 in the 20-30 cm depth increment. Q_{10} values for the 50 % field capacity treatment ranged more widely. The smallest sensitivity to temperature increase was found to occur in the top 10 cm having a Q_{10} value of 2.7. The highest Q_{10} value of

13.8 occurred in the 20-30 cm depth, a value close to that calculated on day 34 (14.8) for the same depth increment.

4.3.1.4 Day 116 of the incubation

Figure 4.6 displays the CO_2 fluxes for day 116 of the incubation. This was the final

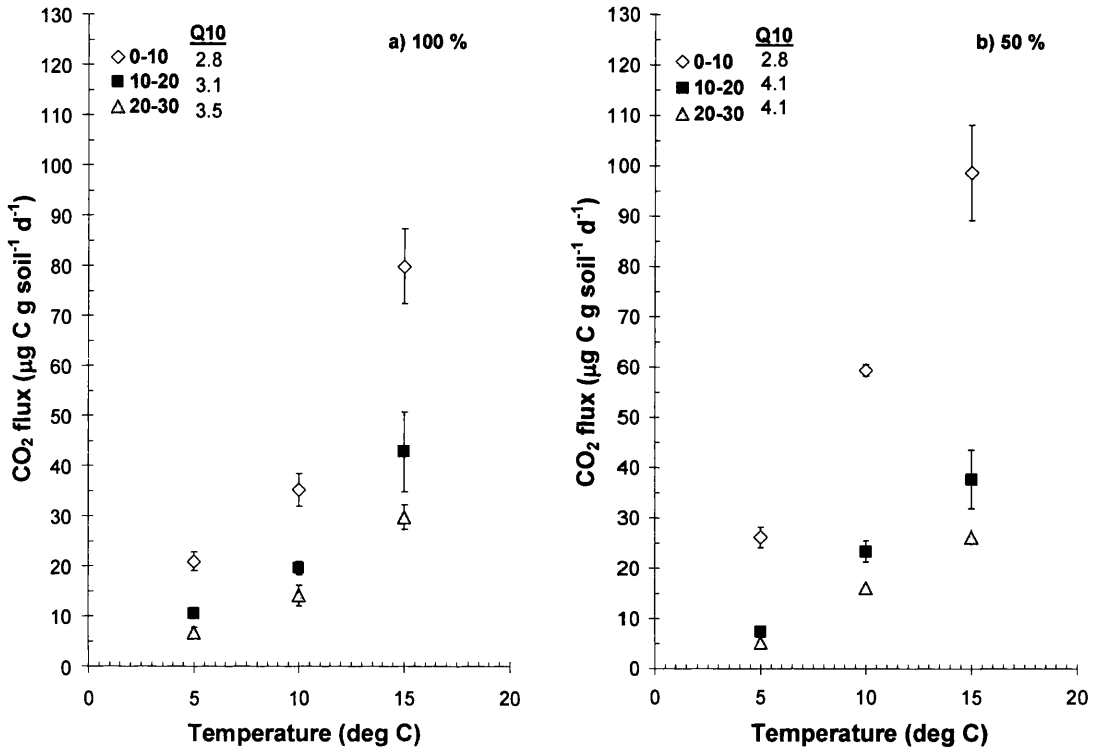

Figure 4.6 - Respiration fluxes and Q_{10} values for all cores sampled on day 116. Error bars are ± 1 σ_e. a) cores incubated at field capacity. b) cores incubated at 50 % field capacity. Error bars are ± 1 σ_e and ones that are not visible are smaller than the symbols. n = 5 for all treatments.

sampling of all 90 cores for $\delta^{13}C$ analysis using the Exetainer method. The smallest flux on day 116 was produced by the 20-30 cm cores incubated at 5°C and 50 % field capacity (5.2 ± 0.3 µg C g soil^{-1} d^{-1}). However this was the highest flux produced by these cores during the116 day incubation period and in addition was statistically different from the three other sampling dates at 2 σ_e. The largest flux produced was 98.7 ± 9.5 µg C g soil^{-1} d^{-1} from the surface cores incubated at 15 °C and 50 % field capacity. Respiration rates produced by the 0-10 cm depth increment at 5, 10 and 15 °C differ by more than 2 σ_e for both moisture levels.

Under the 50 % field capacity treatment only those cores from the 10-20 and 20-30 cm depths incubated at 5 °C produced fluxes that overlap at 1 σ_e. Q_{10} values for day 166

shown in Figure 4.6 range from 2.8 to 3.5 for the 100 % field capacity cores. This sampling produced the smallest range of Q_{10} values for the 50 % field capacity cores, for the duration of the incubation. Values ranged from 2.8 in the surface 10 cm to 4.1 for both the 10-20 and 20-30 cm increments. A Q_{10} of 4.1 for the 20-30 cm depth cores was the smallest value gained for these cores during the 116-day period.

4.3.1.5 Summary of flux data over the course of the incubation period

Figure 4.7 illustrates mean CO_2 fluxes measured on each of the 4 sampling occasions for

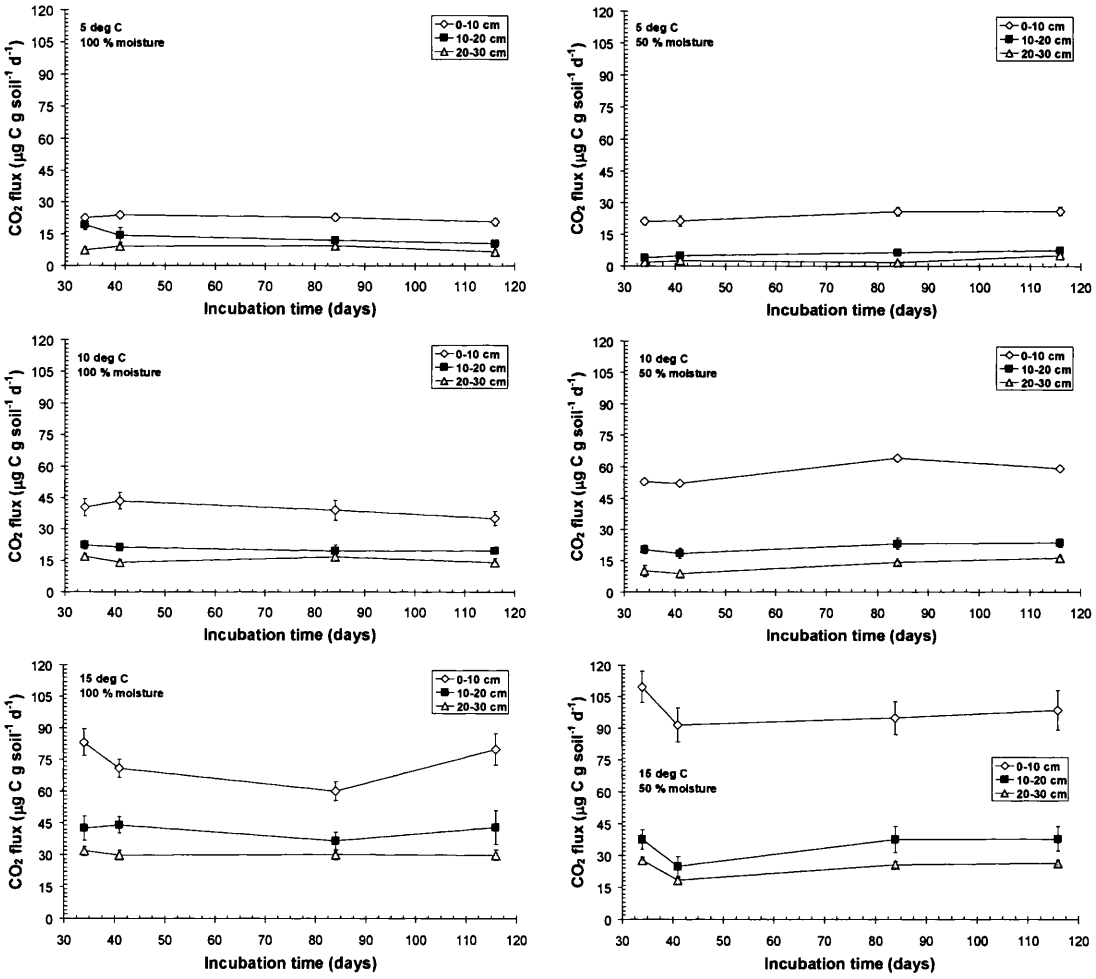

Figure 4.7 – Temporal plots of mean respiration fluxes for the 116-day incubation period. The 100 % moisture treatments are on the LHS of the figure and 50 % moisture treatments to the RHS. Error bars that are not visible are smaller than the symbols.

all treatments. The figures clearly show that fluxes for all temperature, moisture and depth treatments followed a similar pattern throughout the course of the incubation. The highest temperature treatment (15 °C) always produced the largest fluxes at all depths under both moisture regimes. Within one single temperature treatment, the largest flux always occurred in the depth increment closest to the peat surface, i.e. the 0-10 cm increment. In

addition, fluxes produced by the 10-20 cm cores were higher than those at the 20-30 cm depth, although not always significantly so at 2 σ_e.

Respiration fluxes produced at 5 °C (all depths) remained reasonably constant during the 116-day period with most of the fluxes being within 1 σ_e of one another. This was also true for fluxes at 10 and 15 °C. However, there were some differences in fluxes produced by cores extracted from the same depth in the profile but under different moisture conditions. Fluxes produced from the 0-10 cm depth stored at 10 °C, under 50 % field capacity conditions were greater at 2 σ_e than those produced under the 100 % field capacity treatment on all sampling days (except day 41 where they differed by just 1 σ_e).At 15 °C fluxes produced by the 50 % field capacity treatment were again greater than at 100 % field capacity. However, only the flux (15 °C) produced on day 84 was significantly greater at 2 σ_e. The largest standard errors calculated for all flux measurements were for the 15 °C treatment, suggesting that the error is related to a percentage of the flux.

Q_{10} values mostly increased with depth or were the same, with one exception (10-20 cm, 100 % field capacity, on day 34), where the calculated Q_{10} value was the smallest for any depth over the 116-day period. In addition, Q_{10} values were largest for the 20-30 cm depth increment under both moisture treatments. The cores incubated at 50 % field capacity were more sensitive to temperature increase than those at 100 % field capacity. All calculated Q_{10} values (12) for the 50 % field capacity treatment were greater than those at 100 % field capacity, with the exception of one where both treatments had exactly the same Q_{10} value (0-10 cm increment on day 116).

4.3.2 Mean respiration fluxes

Fluxes produced on each of the 4 sampling occasions were averaged and are displayed in Figure 4.8. Figure 4.8 shows very clearly the effects of temperature, substrate quality (depth) and soil moisture content over the 116-day incubation period. The same distinct pattern of increasing flux with increasing temperature can be seen at all 3 depths and for both moisture treatments. Furthermore, fluxes produced at the same temperature (either 5, 10 or 15 °C) decrease significantly (at 1 σ_e) with increasing depth from the surface (for both moisture levels) i.e. the deeper in the profile the peat was extracted from, the smaller the fluxes produced.

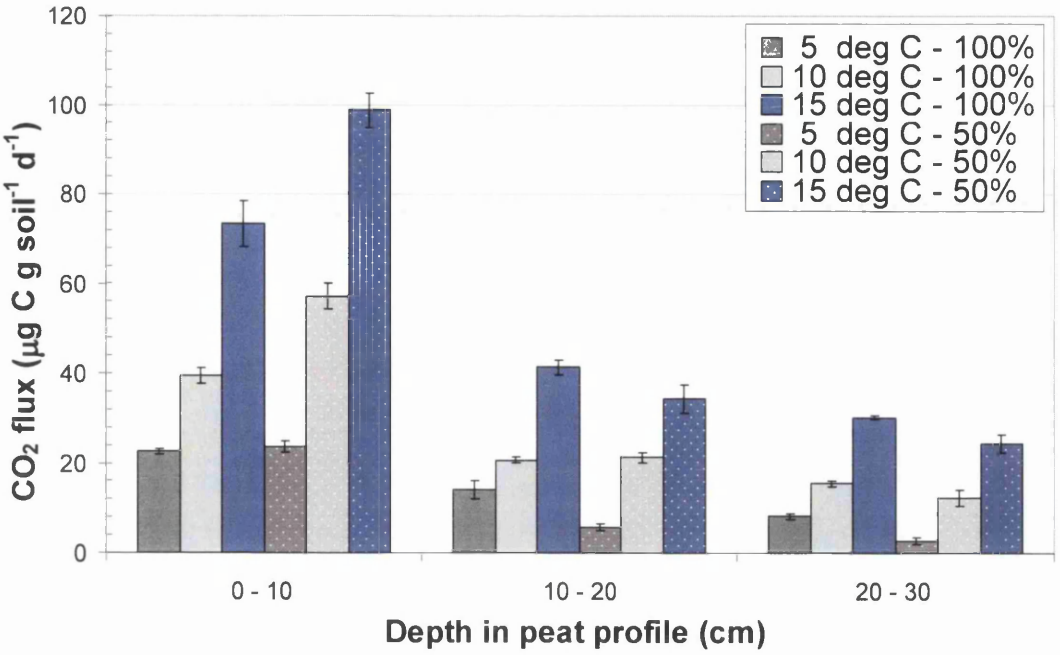

Figure 4.8 – Mean respiration flux for each depth, temperature and moisture level for the entire 116-day incubation period. n = 4 for all data points. Error bars are 1 σ_e.

The largest flux produced at 0-10 cm was from the 15 °C treatment at 50 % field capacity (98.8 ± 3.9 µg C g soil^{-1} d^{-1}) and was the highest of all the treatments. This was significantly higher at 2 σ_e than the flux produced at 15 °C and 100 % field capacity. At 10 °C fluxes were again larger from the 50 % field capacity treatment at 2 σ_e than those produced at field capacity. However, at 5 °C and 0-10 cm, respiration fluxes were the same at 1 σ_e for both moisture treatments. Fluxes produced at 15 °C were at least twice that at 5 °C for both 100 and 50 % field capacity, the smallest flux being 22.6 ± 0.78 µg C g soil^{-1} d^{-1} (100 % field capacity).

Mean respiration fluxes from 10-20 cm depth ranged from between 51 and 59 % of the equivalent flux at 0-10 cm for the 100 % field capacity treatment to 24 and 37 % of the 50 % field capacity treatment. The highest flux (41.4 ± 1.7 µg C g soil^{-1} d^{-1}) was produced again by the 15 °C treatment but unlike the 0-10 cm depth, the flux was greater from the field capacity cores than those incubated at 50 % field capacity. There was a significant increase in flux at 2 σ_e from cores stored at 5 °C and 1 σ_e for cores stored at 15 °C (100 % field capacity) relative to the same fluxes produced by cores maintained at 50 % field capacity. There was no significant difference in fluxes produced by cores stored at 10 °C under the two moisture treatments.

Cores from the 20-30 cm depth in the profile produced the smallest fluxes of the incubation relative to equivalent fluxes at 0-10 and 10-20 cm depths. Respired CO_2

produced by cores incubated at 5 and 15 °C were significantly greater at 2 σ_e, for the 100 % field capacity treatment compared to fluxes from the 50 % field capacity treatment. Mean fluxes ranged from 2.8 ± 0.8 to 24.5 ± 2.1 μg C g soil^{-1} d^{-1} for the 50 % field capacity treatment to between 8.2 ± 0.8 and 30.3 ± 0.5 μg C g soil^{-1} d^{-1} for the 100 % field capacity treatment. Under 100 % field capacity conditions fluxes produced at 20-30 cm depth (5 °C) were 42 % of those produced by the 0-10 cm depth. Similarly, at 50 % field capacity, fluxes from 20-30 cm were 12 % of those produced by the 0-10 cm depth.

4.3.3 $\delta^{13}C$, % carbon and % moisture of bulk peat

Table 4.1 summarises the results for analyses performed on bulk peat from the 3 treatment

Depth (cm)	$\delta^{13}C_{VPDB}$ (‰) ± 1 σ_e	% carbon ± 1 σ_e	% moisture capacity ± 1 σ_e
0-10	-27.5 ± 0.1	51.3 ± 0.3	90.5 ± 0.2
10-20	-26.6 ± 0.1	52.0 ± 0.3	89.1 ± 0.2
20-30	-26.5 ± 0.1	53.7 ± 0.3	89.0 ± 0.2

Table 4.1 – Mean values for % carbon, % moisture and $\delta^{13}C$ of bulk peat extracted from 3 different depths in the profile at the Hard Hill site. All cores were analysed after being incubated at 15 °C (100 % field capacity) for 116 days, n = 5 for $\delta^{13}C$, % carbon at each depth, n = 30 for % moisture at each depth.

depths (0-10, 10-20 and 20-30 cm). The $\delta^{13}C$ value for the surface 10 cm of peat is similar to that found for vegetation at the site (see Chapter 3). At 10-20 and 20-30 cm the $\delta^{13}C$ value of bulk peat becomes more enriched at 1 σ_e relative to the surface 10 cm, but is still in the normal range of values for surface peat.

Percent carbon ranged from 51.3 to 53.7, typical for peat from an ombrotrophic blanket bog, as was % moisture content (typically ~ 90 %). Two cores extracted from each depth in the profile were analysed for $\delta^{13}C$, % carbon and % moisture directly after being removed from the field. All measured parameters were identical at 1 σ_e to those featured in Table 4.1, as were % nitrogen and % phosphorus (data not shown).

4.3.4 $\delta^{13}C$ determination of respired CO_2 using the Exetainer method

The isotopic signature of respired CO_2 from each peat core using the Exetainer method was calculated by utilising an isotopic mass balance approach (see section 4.2.4.5). All values are the mean of 5 replicates unless stated otherwise.

4.3.4.1 Stable carbon isotope values for respired CO_2 on day 41

The $\delta^{13}C$ values for respired CO_2 emitted from both moisture treatments on day 41 of the incubation are shown in Figure 4.9. Values ranged from -21.0 ± 0.9 ‰ to -29.2 ± 0.6 ‰

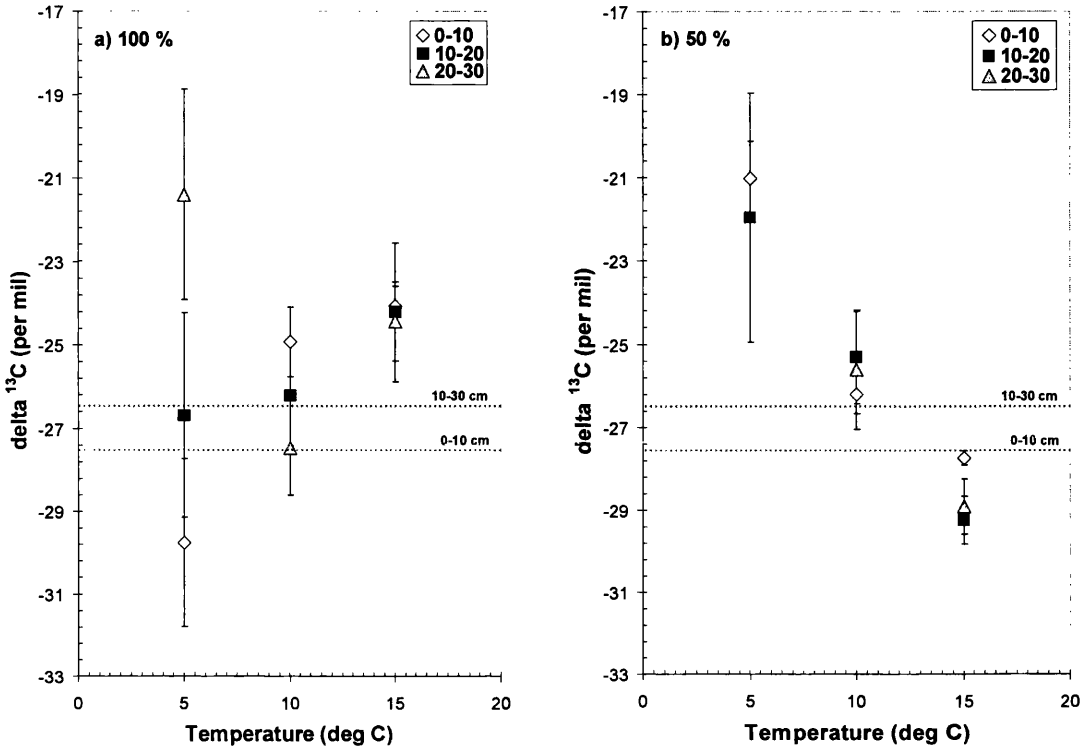

Figure 4.9 – $\delta^{13}C$ values of respired CO_2 from 3 depths in the profile and at 3 varying temperatures on day 41 of the incubation. a) cores incubated at 100 % field capacity. b) cores incubated at 50 % field capacity. Error bars are ± 1 σ_e. n = 5 for all treatments except: 50 % field capacity, 5 °C, 20-30 cm, (n = 0), 50 % field capacity, 10 °C, 20-30 cm, (n = 4) and 100 % field capacity, 5 °C, 20-30 cm (n = 4). Dotted lines illustrate the $\delta^{13}C$ values for the bulk peat.

under the 50 % field capacity treatment and similarly from -21.4 ± 2.5 ‰ to -29.8 ± 2.0 ‰ under the 100 % field capacity treatment. The largest standard errors on calculated $\delta^{13}C$ values for respired CO_2 were for the cores incubated at 5 °C, and this was true for both moisture treatments.

Stable carbon isotope values of soil respiration produced under the 100 % field capacity treatment (20-30 cm) demonstrated no clear pattern with depth. $\delta^{13}C$ values at 10 and 15 °C (100 % field capacity) became lower with increasing depth from the surface but at 15 °C there was no difference at 1 σ_e. Respired CO_2 produced by the 0-10 and 10-20 cm depth cores, under 50 % field capacity were more depleted at 2 σ_e at 15 °C than at 10 °C. $\delta^{13}C$ values of respired CO_2 produced at 10 °C (50 % field capacity regime) were statistically indistinguishable at 1 σ_e for all depths. At 15 °C (50 % field capacity) the 0-10

cm depth increment produced CO_2 that was slightly enriched in ^{13}C (but not significantly so), relative to the 2 depth increments beneath it in the profile.

4.3.4.2 Stable carbon isotope values for respired CO_2 on day 84

Figure 4.10 illustrates the calculated $\delta^{13}C$ values for respired CO_2 from all treatments on

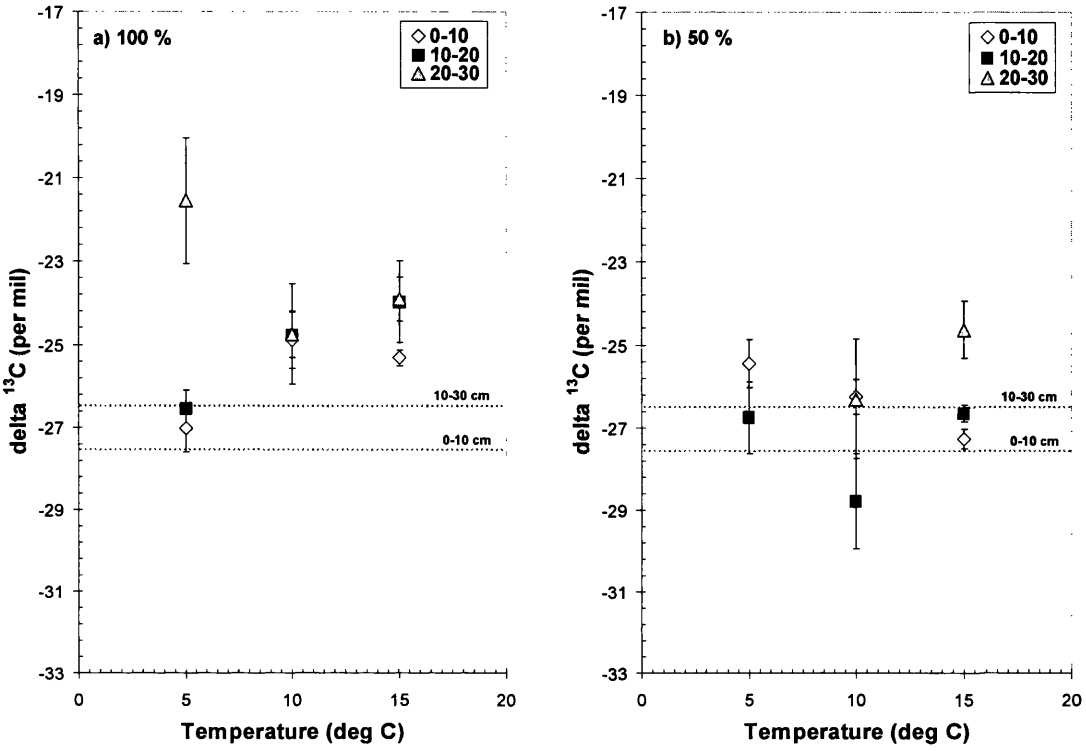

Figure 4.10 - $\delta^{13}C$ values for respired CO_2 produced at 3 depths in the profile and at 3 varying temperatures on day 84 of the incubation. a) cores incubated at 100 % field capacity. b) cores incubated at 50 % field capacity. Error bars are ± 1 σ_e. n = 5 for all treatments except: 50 % field capacity, 5 °C, 20-30 cm, (n = 0), 100 % field capacity, 10 °C, 10-20 cm (n = 4). Dotted lines illustrate the $\delta^{13}C$ values for the bulk peat.

day 84 of the incubation. Under the 50 % field capacity regime, cores from a depth of 20-30 cm incubated at 5 °C produced only small volumes of CO_2 (mean value 20 ppm). Consequently, $\delta^{13}C$ values calculated by mass balance ranged from +14.3 to -406.7 ‰, with a mean value of -100.6 ‰. As the individual and mean calculated signatures for this depth are well out of the range of values for the $\delta^{13}C$ of bulk soil, no mean value is given for this treatment in Figure 4.10.

Measured $\delta^{13}C$ values under the 50 % field capacity regime were between -24.6 ± 0.7 ‰ and -28.8 ± 1.2 ‰. This was the smallest range in $\delta^{13}C$ values produced by the two different moisture regimes. Cores incubated at 100 % field capacity produced a slightly larger range in $\delta^{13}C$ values of between -21.5 ± 0.5 ‰ to -27.0 ± 0.6 ‰ with the most

enriched value occurring at a depth of 20-30 cm (5 °C). At 10 °C (100 % field capacity) the stable carbon isotope value of respired CO_2 was identical at 1 σ_e for all depths.

In addition, under the same moisture regime the $\delta^{13}C$ value of CO_2 produced by cores incubated at 15 °C was indistinguishable from CO_2 produced at comparable depths at 10 °C. At 15 °C, CO_2 produced by the top 10 cm was isotopically more depleted in ^{13}C (but not significantly so) than that produced by the 10-20 and 20-30 cm depth increments. Under the 100 % field capacity regime, the only treatment cores to differ in stable carbon isotope value by 2 σ_e from all other treatments were the cores from 20-30 cm, stored at 5 °C. These particular cores also produced the least depleted values for respired CO_2 on day 41. However, the 5 °C cores produced rather small volumes of CO_2 relative to that produced at 10 and 15 °C and the apparent enrichment of respiration from the 5 °C cores may be due to this phenomenon.

At 5 and 10 °C (all depths), treatments under the 50 % field capacity were indistinguishable at 1 σ_e. However at 15 °C the opposite was true. The $\delta^{13}C$ value of respired CO_2 from the 0-10 cm depth in the profile was distinguishable from the 10-20 cm depth at 1 σ_e only, but statistically more enriched at 2 σ_e relative to the 20-30 cm depth. The smallest standard errors for calculated $\delta^{13}C$ values were for those cores incubated at 15 °C.

4.3.4.3 Stable carbon isotope values for respired CO_2 on day 116

Figure 4.11 depicts the $\delta^{13}C$ values of respired CO_2 for both moisture treatments on day 116 of the incubation. For this final sampling using Exetainers, cores incubated at 5 °C were incubated for 4 times longer than the cores incubated at 15 °C and 5 times longer than the cores at 10 °C. This was because previous samplings produced insufficient respired CO_2 (respiration produced was on the limit of detection) by the 20-30 cm depth cores incubated at 5 °C and 50 % field capacity to calculate a $\delta^{13}C$ signature that was considered reliable (no mean value was obtained for this treatment on days 41 and 84). This is likely due to error propagation on the small volumes of CO_2 produced and consequently there was little difference (if any) in the $\delta^{13}C$ of CO_2 captured at the beginning and end of the incubation period.

The stable carbon isotope values of respired CO_2 on day 116 produced the least variation of the three sampling occasions particularly under the 100 % field capacity treatment. At

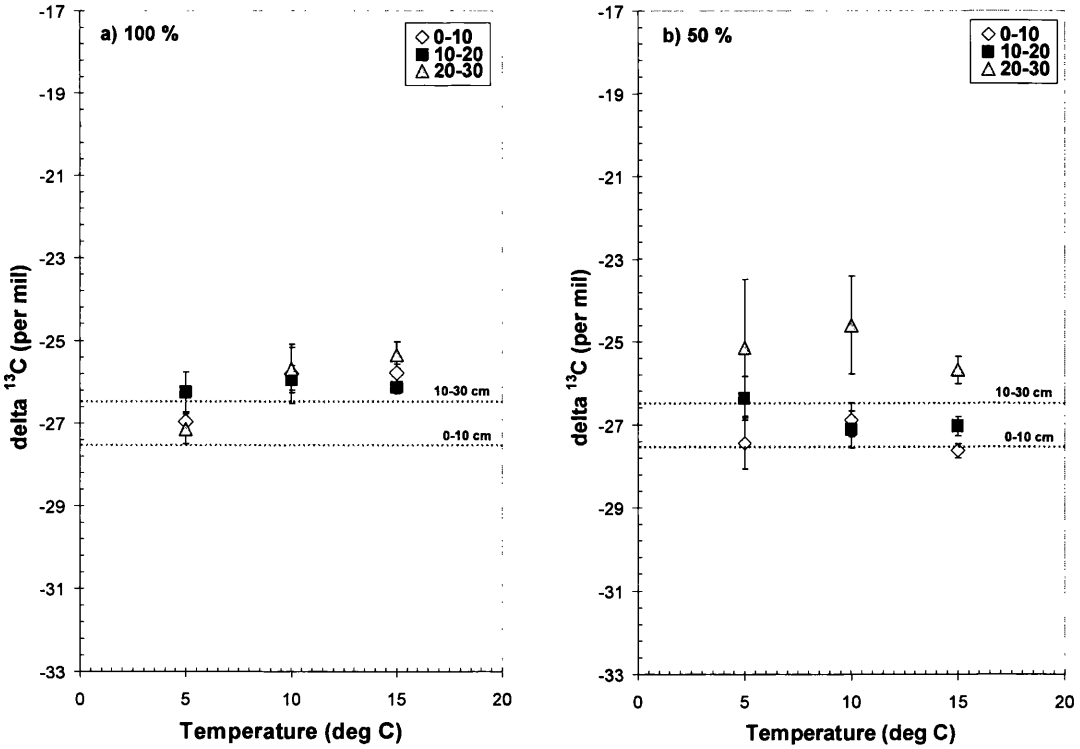

Figure 4.11 - $\delta^{13}C$ values of respired CO_2 produced from 3 depths in the profile and at 3 varying temperatures on day 116 of the incubation. a) cores incubated at 100 % field capacity. b) cores incubated at 50 % field capacity. Error bars are ± 1 σ_e. n = 5 for all treatments except: 50 % field capacity, 5 °C, 20-30 cm, (n = 4). Dotted lines illustrate $\delta^{13}C$ values for the bulk peat.

5 °C (100 % field capacity) there is no difference in the stable carbon isotope composition of respired CO_2 produced at all three depths and this is also true for $\delta^{13}C$ values at 10 °C. At 15 °C, the respired CO_2 produced by the 20-30 cm increment is slightly enriched in ^{13}C relative to the 10-20 cm increment but not significantly so.

At 50 % field capacity there was a little more variation in the $\delta^{13}C$ values of respired CO_2 than at field capacity. The effect of incubating the 5 °C cores for a longer time period can clearly be seen, with standard errors on the calculated $\delta^{13}C$ values being the smallest for the entire experiment. At 5 °C (50 % field capacity), there is no difference in the stable carbon isotope composition of respired CO_2 with depth, as all are inseparable at 1 σ_e. At 10 °C, respired CO_2 produced by the 20-30 cm depth is more enriched in ^{13}C than the remaining two depths (but not significantly so). However, at 15 °C the $\delta^{13}C$ values of CO_2 respired from each different depth is distinguishable from the other depths at 1 σ_e, suggesting an enrichment in ^{13}C with increasing depth from the surface.

4.3.5 Carbon isotope values ($\delta^{13}C$) of respired CO_2 using MS^3

Results for $\delta^{13}C$ analysis of respired CO_2 collected from cores incubated at 5 and 15 °C using MS^3 are presented in Figure 4.12a. $\delta^{13}C$ values for CO_2 collected from the same

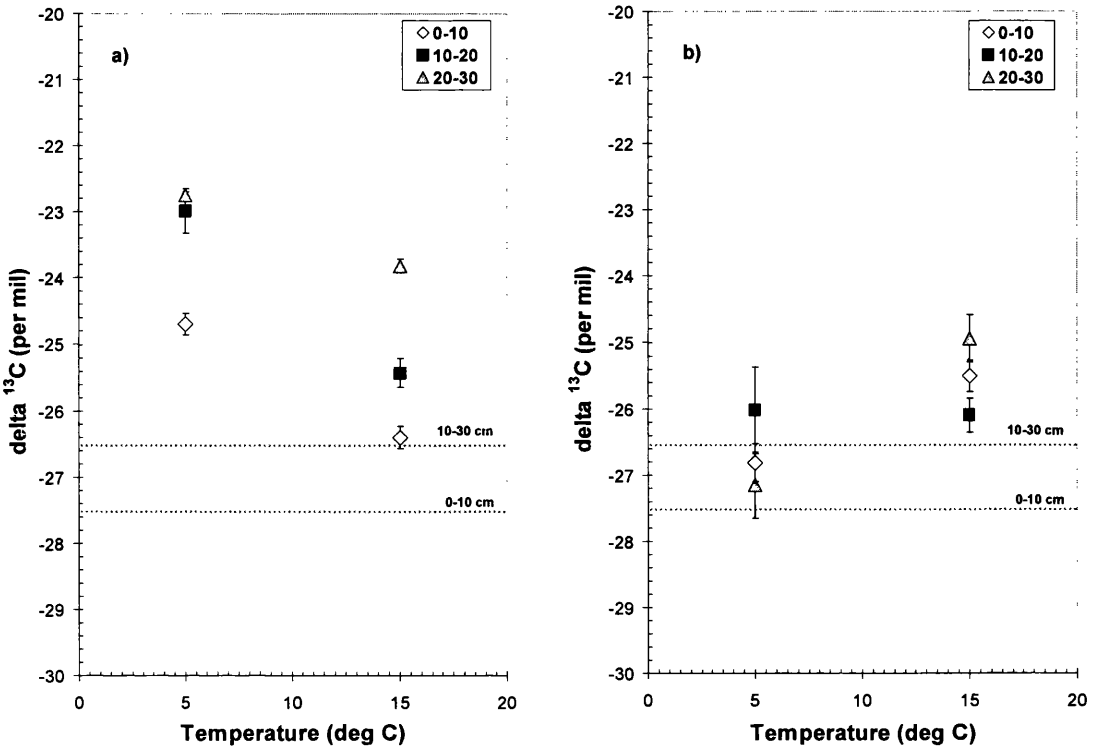

Figure 4.12 – a) $\delta^{13}C$ of respired CO_2 from cores incubated at 5 and 15 °C under 100 % field capacity (n = 3) collected using MS^3. b) $\delta^{13}C$ of respired CO_2 from cores incubated at 5 and 15 °C under 100 % field capacity (n = 3) collected using Exetainers on day 116 of the incubation. Error bars are 1 σ_e. Dotted lines illustrate the $\delta^{13}C$ values of bulk peat.

cores on day 116 of the incubation, using the Exetainer method, are presented again (but using only 3 of the 5 replicates – the same cores that were sampled using MS^3) in Figure 4.12b for comparison. From Figure 4.12a it is clear that the stable isotopic signature of respired CO_2 becomes more enriched in ^{13}C with increasing depth from the peat surface. Furthermore, respiration also becomes enriched ^{13}C with decreasing temperature. The $\delta^{13}C$ values for cores incubated at 5 °C, ranges from -24.7 ± 0.2 ‰ in the top 10 cm to -22.7 ± 0.04 ‰ in the 20-30 cm depth increment, a difference of 2 ‰.

At 15 °C, respired CO_2 becomes more depleted in ^{13}C for all depths, relative to that at 5 °C. Respired CO_2 produced by the 0-10 cm increment at 15 °C has a $\delta^{13}C$ value of -26.4 ± 0.2 ‰, a value that is 1.7 ‰ more depleted than the respired CO_2 produced by the same depth increment at 5 °C. The $\delta^{13}C$ value obtained for the 20-30 cm depth increment is also more depleted in ^{13}C at 15 °C than at 5 °C (-22.7 ± 0.04 ‰) but this time only by ~ 1 ‰.

At 15 °C, the $\delta^{13}C$ value of respired CO_2 is statistically distinguishable for all depths by at least 2 σ_e. At 5 °C the 0-10 cm depth increment produced respired CO_2 that is statistically more depleted in ^{13}C than that produced by the 10-20 and 20-30 cm depths. However the bottom two 10 cm increments produced CO_2 with the same stable carbon isotope value at 1 σ_e.

Respiration captured using the Exetainer method (Figure 4.12b) does not demonstrate the same clear pattern of ^{13}C enrichment with increasing depth from the surface or with decreasing temperature. Respired CO_2 produced by the 0-10 and 10-20 cm depth increments could not be distinguished by 1 σ_e, either at 5 or 15 °C. At 15 °C respiration sampled from these depths was statistically the most enriched in ^{13}C at 1 σ_e. In addition, respiration produced from these two depths was more enriched in ^{13}C than the similar depth increments under the 5 °C temperature treatment.

There are significant differences in the $\delta^{13}C$ value of respired CO_2 when comparing CO_2 respired from the same treatments but using different the two different techniques (Exetainer and MS^3). At 5 °C, CO_2 captured by MS^3 is between 2.1 and 4.5 ‰ more enriched in ^{13}C than CO_2 captured from the same treatments using the Exetainer method. Similarly, CO_2 captured from the 10-20 and the 20-30 cm cores at 15 °C is between 0.7 and 1.1 ‰ more enriched in ^{13}C when captured by MS^3.

4.4 Discussion

The aim of this study was to investigate the effects of temperature, moisture and substrate quality on the rate and isotopic signature of soil respiration fluxes, in a controlled environment, as these factors often co-vary in the field (Kirschbaum, 2006), and in doing so can confound interpretation of results.

4.4.1 The effect of climatic drivers on CO_2 production rates

Clear treatment effects were observed on rates of CO_2 production and it was established that temperature increased soil respiration rates from peat extracted from all 3 depths in the profile and under both moisture regimes at both 10 and 15 °C relative to those produced at 5 °C. Furthermore, fluxes were significantly higher from the 0-10 cm depth increment compared to those produced from the two depths lower in the profile under all treatments

(with one exception out of the 24 flux measurements performed at this depth) and is likely due to the presence of a greater amount of more labile carbon in the surface 10 cm.

Percent moisture had a significant effect on CO_2 production, but was not as clearly defined as the temperature effect. For the surface 10 cm, the 50 % field capacity treatment caused a significant increase (at 2 σ_e) in CO_2 fluxes produced by cores incubated at 10 and 15 °C, relative to those from the 100 % field capacity treatment. However at 5 °C, CO_2 fluxes from both moisture treatments were identical at 1 σ_e. This suggests that microbial populations present at this depth in the profile, which are responsible for carbon mineralisation at higher temperatures, were inhibited by increased moisture. Since at 5 °C, CO_2 production rates in the top 10 cm were identical at 1 σ_e, it is concluded that soil moisture would need to reach less than 50 % to begin having an effect on microbial activity through moisture stress at this temperature.

CO_2 production rates from both 10-20 and 20-30 cm depths produced a different pattern to that at 0-10 cm under the two different moisture regimes. CO_2 production from the 20-30 cm depth was significantly higher for the 100 % field capacity treatment than the 50 % field capacity treatment, at all temperatures. At 10-20 cm depth, a similar effect was found for fluxes produced at 5 and 15 °C, but at 10 °C fluxes produced from the two moisture treatments were identical at 1 σ_e. This suggests that the effect soil moisture content had on fluxes produced in the surface 10 cm (inhibiting microbial soil carbon mineralization) was acting in reverse at lower depths in the profile.

For most of the year, the 10-20 and 20-30 cm depths in the profile will be submerged by the water table and so it is possible that microbial populations existing at these depths in the profile are more water tolerant than those that exist in the top 10 cm of the peat profile. For example, in a study of forest soil respiration, Monson *et al.* (2006) demonstrated that reductions in the depth of the winter snowpack (causing decreases in insulation and therefore colder soil temperatures) reduced soil respiration rates, citing the cause as a 'unique microbial community' that functioned within a narrow range of soil temperatures that were below zero.

Rates of respired CO_2 were significantly affected by substrate quality (using increasing depth as an analogue for decreasing substrate quality), as demonstrated by mean fluxes featured in Figure 4.8. Fluxes at all temperatures decreased (by at least 1 σ_e) with increasing depth in the profile under both moisture regimes. As respiration fluxes did not

show a systematic decline throughout the 116-day incubation period, loss of labile carbon substrate or indeed temperature acclimation were not considered to be an issue in this study, unlike in a number of other studies (Gu *et al.*, 2004; Kirschbaum, 2004; Nicolardot *et al.*, 1994).

4.4.2 Temperature sensitivity (Q_{10}) of SOM decomposition

Table 4.2 summarises the Q_{10} values for CO_2 production derived from treatments on the 4

Depth (cm)	% field capacity	Day 34	Day 41	Day 84	Day 116	Mean ± σ_e
0-10	**100**	2.7	2.0	1.6	2.8	**2.3 ± 0.3**
10-20	**100**	1.2	2.0	2.0	3.1	**2.1 ± 0.4**
20-30	**100**	3.2	2.2	2.2	3.5	**2.8 ± 0.3**
0-10	**50**	4.2	3.3	2.7	2.8	**3.3 ± 0.3**
10-20	**50**	8.5	4.0	4.7	4.1	**5.3 ± 1.1**
20-30	**50**	14.8	6.0	13.8	4.1	**9.7 ± 2.7**

Table 4.2 – Q_{10} values derived for CO_2 fluxes from 3 depths in the profile and at 2 varying moisture regimes.

sampling occasions. Mean Q_{10} values for the entire incubation period are also given. Large Q_{10} values correspond to small fluxes produced during incubation of cores at 5 °C. This effect has been observed in other studies attempting to determine the temperature response of various soil organic matter fractions e.g. Leifeld & Fuhrer (2005).

4.4.2.1 Decomposition under 100 % field capacity conditions

Under the 100 % field capacity treatment, mean Q_{10} values for all depths ranged from 2.1 ± 0.4 to 2.8 ± 0.3 and are in a similar range to those observed by Fierer *et al.* (2003) on the study of CO_2 efflux (under varying moisture conditions) from surface soil horizons of a Californian soil profile. These results suggest that soil organic matter decomposition and therefore CO_2 production would take place 2 to 3 times as fast for every 10 °C rise in temperature. However, the Q_{10} values obtained for the 100 % field capacity treatment were identical at 1 σ_e, demonstrating that the temperature response of CO_2 production at each of the different depths in the profile is the same. Furthermore, the similarity of the experimentally derived Q_{10} values indicates that old more resistant SOM has the same temperature sensitivity to decomposition as more easily decomposed, labile carbon stocks (when soil moisture is at field capacity).

Similar results have been found in other studies investigating the temperature sensitivity of SOM decomposition. For example, during an incubation study on the temperature dependence of SOM decomposition of forest soil, removed from different soil horizons (surface and deeper), Fang *et al.* (2005) found no statistical difference between allegedly labile and more recalcitrant stocks of carbon. Furthermore, in a study amalgamating the temperature sensitivity of organic carbon decomposition in forest mineral soils from 82 sites across the globe, Giardina & Ryan (2000) concluded that the sensitivity of decomposition to temperature was constant and that carbon loss from these soils would not be affected by increased temperature alone.

Both the aforementioned studies are not without caveats however. In the study carried out by Giardina & Ryan (2000), the soil carbon pool was treated as a single homogeneous reservoir, thus not taking into consideration the fact that soil is composed of many different fractions of carbon cycling on widely varying timescales (Gaudinski *et al.*, 2000). The method used by Fang *et al.* (2005) involved considerable disturbance of the soil (i.e. the soil was passed through a 2 mm sieve and air dried before any flux measurements were performed). This method can result in the breaking up of stable soil aggregates that afford, to carbon that is locked within them, physical protection from biotic and abiotic degradation. Thus, sieving soil might result in a flush of more labile carbon being released and made available to the microbiota for decomposition, hence masking true soil decomposition rates.

4.4.2.2 Decomposition under 50 % field capacity conditions

Q_{10} values for the three depths in the profile incubated under 50 % field capacity ranged from 3.3 ± 0.3 in the surface 10 cm, to 9.7 ± 2.7 for the bottom 10 cm. A Q_{10} value of 9.7 is high but not unique. During an incubation study of the temperature sensitivity of decomposition of Scottish peat from 15 sites, Chapman and Thurlow (1998) obtained Q_{10} values of between 2.2 and 19. Our finding suggests that the temperature sensitivity of soil carbon decomposition from depth increases when drier soil conditions persist. Furthermore, in an incubation study of monoliths of subarctic heath dominated by dwarf shrubs, Illeris *et al.* (2004) found that the temperature sensitivity of decomposition was dependent on the level of soil moisture.

In contrast to the results at field capacity, Q_{10} values obtained under 50 % field capacity conditions demonstrate a significant increase in temperature sensitivity, with decreasing substrate quality (assuming decreasing substrate quality is analogous to increasing depth

from the peat surface). This finding indicates that older, more recalcitrant organic matter is in fact more temperature sensitive than labile carbon pools, when moisture is taken into consideration. This result, although in direct contrast to studies such as Liski *et al.* (1999) who found that the decomposition of old soil organic matter is tolerant of temperature, conforms to kinetic theory.

For example, Svante Arrhenius observed that a Q_{10} value of 2 or 3 cannot arise solely through an increase in the frequency of molecular collisions during a reaction, that in fact for every 10 °C rise in temperature, molecular collisions only increase by approximately 1.5 % (Davidson & Janssens, 2006). Furthermore, Bosatta and Ågren (1999) argued that older SOM should have higher temperature sensitivity to decomposition because the decomposition of more complex substrates requires a larger number of steps. In addition, if the substrate available for decomposition is not limiting (i.e. substrate is not exhausted or depleted during an incubation for example, as in this study), then the temperature sensitivity of a reaction should be even greater, due to the fact that raised temperatures provides the necessary activation energy to allow increased substrate decomposition (Davidson & Janssens, 2006).

4.4.3 Determination of the $\delta^{13}C$ value of soil respired CO_2

4.4.3.1 The Exetainer method utilising mass balance

$\delta^{13}C$ of soil had a similar signature to vegetation at the site, which is not surprising as plants are the main source of carbon to most soils (Amundson *et al.*, 1998). The stable isotope values of respired CO_2 produced at each depth, had similar $\delta^{13}C$ values to that of the bulk soil (-27.5 ‰ for 0-10 cm and –26.5‰ for 10-30 cm) except on day 41 where values derived for fluxes at 5 °C were relatively depleted in ^{13}C at ~ -29 ‰ (0-10 cm) or enriched in ^{13}C at ~ -21 ‰ (20-30 cm). However, these values are deemed to be unreliable due to the extremely small fluxes produced at this temperature, and hence the large standard errors produced on mean values (see Figure 4.9).

The values derived for the $\delta^{13}C$ of respired CO_2 on day 84 showed less variation than on day 41, with most $\delta^{13}C$ values for all depths, temperatures and moisture levels being in a much smaller range of between ~ -24 and -27 ‰. These values reflect the $\delta^{13}C$ signature of the bulk peat (-26.5 to -27.5 ‰), although the higher values may indicate some fractionation during decomposition. The only fluxes that could be differentiated by their

stable carbon isotope values, at all depths on day 84, were those produced at 15 °C under 50 % field capacity. However, only the 20-30 cm depth increment was statistically more enriched at 2 σ_e.

The $\delta^{13}C$ value of CO_2 produced from the three different depths on day 116, under 100 % field capacity conditions ranged from ~ -26 to -27 ‰ at 5 °C and between ~ -25 to -26 ‰ at 15 °C, again reflecting the stable isotope signature of the soil carbon substrate from which the CO_2 was produced. No significant differences in $\delta^{13}C$ values at 5 or 15 °C could be identified at corresponding depths. Although respired CO_2 had a similar $\delta^{13}C$ value to the bulk peat, there was no clear pattern of enrichment (or depletion) in ^{13}C with depth, at either 5 or 15 °C.

4.4.3.2 The molecular sieve sampling system method

Using the MS^3 method, the $\delta^{13}C$ values of respired CO_2 produced by cores incubated at 100 % field capacity conditions, showed a clear pattern of enrichment in ^{13}C with depth (Figure 4.12a) at both 5 and 15 °C and therefore reflect the ^{13}C enrichment evident in the bulk soil with depth (Table 4.1). A similar pattern in ^{13}C enrichment with depth was also observed at 5 °C, although the values from the two lower depths in the profile could not be distinguished at 1 σ_e. One reason $\delta^{13}C$ values may have become enriched in ^{13}C with depth partly due to the peat being formed from vegetation that grew in an atmosphere more enriched in ^{13}C (before addition of isotopically depleted CO_2 produced during fossil fuel combustion).

Another reason might be due to changes in the stable carbon isotope ratio of organic matter that exists in the soil caused through discrimination by the heterotrophic population during organic matter decomposition (Ågren *et al.*, 1996). CO_2 produced at 15 °C was significantly more depleted in ^{13}C than at 5 °C when comparing fluxes from the same depths. This could be due to mineralisation of more resistant organic material, at higher temperatures, such as lignin which is more depleted in ^{13}C (Benner *et al.*, 1987). In addition, the $\delta^{13}C$ value of CO_2 captured at 5 °C using MS^3 was higher than the $\delta^{13}C$ values for bulk peat, particularly at 20-30 cm, where the difference between the respired CO_2 and the substrate was almost 4 ‰; this phenomenon could reflect isotope fractionation during decomposition.

$\delta^{13}C$ values for CO_2 captured by the two different methodological approaches (MS^3 and Exetainer) were significantly different at all depths, and in addition, were always more depleted in ^{13}C when using the Exetainer method (except for the surface 10 cm at 15 °C). The difference in the $\delta^{13}C$ value of respired CO_2 obtained using the two different methods reached a maximum of 4.5 ‰. This was found to occur when CO_2 was produced by the 20-30 cm depth increment at 5 °C; differences are attributed to the small volumes of CO_2 produced at this temperature. Four different measurements are made of each sample of respired CO_2 collected, when utilising the Exetainer method, two concentration measurements analysed by gas chromatography and two isotope measurements performed by isotope ratio mass spectrometry. Consequently, differences between the two methods could also be attributed to the propagation of error involved when utilising the Exetainer method.

An example of this is given in Figure 4.13, which illustrates what affect the analytical error

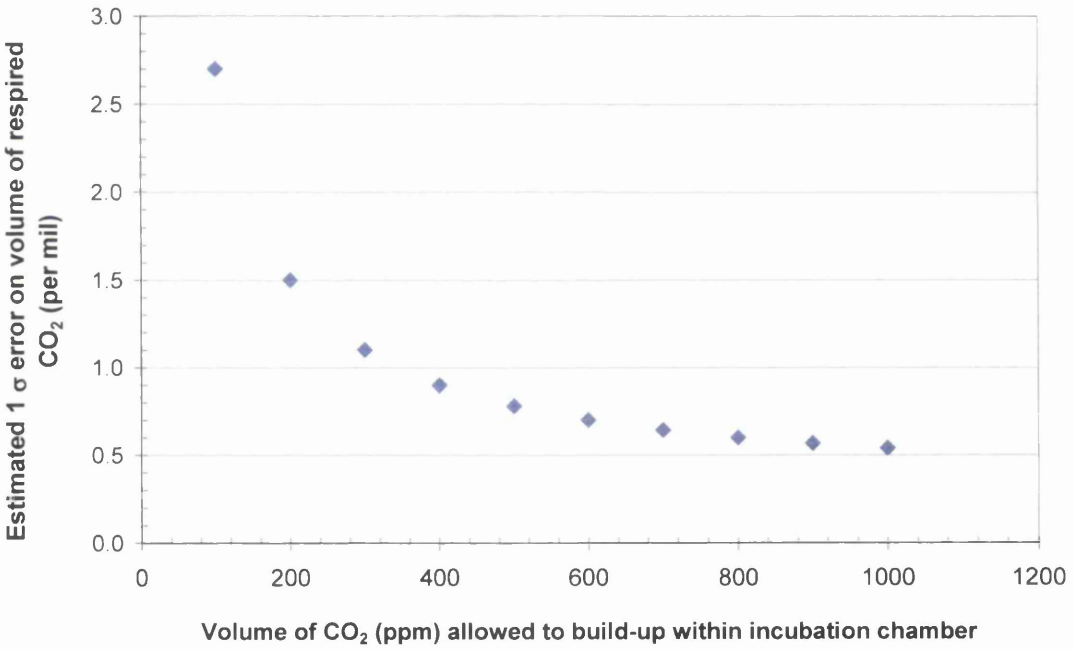

Figure 4.13 - Estimated 1 σ error on calculated $\delta^{13}C$ value of respired CO_2, derived using 0.3 ‰ error on the $\delta^{13}C$ measurement, assuming different levels of respired CO_2.

of the TG-IRMS measurement (0.3 ‰) has on different volumes of respired CO_2. If the starting $\delta^{13}C$ value of CO_2 contained within in an incubation chamber were -15 ‰ and the final $\delta^{13}C$ value after incubation were -18 ‰, the maximum difference between these two values that could be obtained when taking the analytical error into consideration, would be -14.7 and -18.3 ‰. When these values are entered into a mass balance equation along with

the volume of respired CO_2, an error on the value obtained (using -15 and -18 ‰) for the $\delta^{13}C$ values of respired CO_2 can be calculated.

The plot in Figure 4.13 clearly shows that unless the CO_2 evolved within an incubation chamber is > 400 ppm, then based on the analytical error for the $\delta^{13}C$ measurement, the propagated error on the estimate for the $\delta^{13}C$ value of source respired CO_2 is > 1 ‰. However, by scrubbing atmospheric CO_2 from the chambers using MS^3 and then using it to collect respired CO_2, only one measurement for $\delta^{13}C$ is required. This may explain some of the differences between $\delta^{13}C$ values arrived at for source respired CO_2, on comparison of the two sampling techniques.

4.5 Conclusion

Miko Kirschbaum (2000) pointed out that studies of the temperature dependence of soil organic matter decomposition have largely been performed on more easily decomposed, labile material. However, as Kirschbaum (2000) further states, the long term effect of soil warming will largely be determined by the mineralisation of older, more recalcitrant material (as it comprises approximately 90 % of the soil organic matter pool). This study, performed on peat extracted from different depths (as an analogue for decreasing substrate quality) of an ombrotrophic bog profile demonstrates that the sensitivity of soil organic matter decomposition is linked not just to temperature but also to soil moisture content and substrate quality/availability. In addition, the temperature sensitivity of older more recalcitrant organic matter was found to be greater than more labile soil organic carbon (when combined with reduced soil moisture), and is in agreement with recent modelling predictions (Knorr *et al.*, 2005).

Fluxes of respired CO_2 were, as hypothesised (hypothesis 1 – page 99), significantly higher for each 5 °C rise in temperature for both moisture treatments and at all depths with one exception (the flux from the 10-20 cm cores incubated at 10 °C and 100 % field capacity were statistically ($P > 0.95$) identical to those produced at 5 °C from the same depth under the same moisture treatment). In addition, fluxes of CO_2 were greater with increased substrate quality, i.e. under the same temperature treatment or moisture level, fluxes were higher at 10-20 cm than they were at 20-30 cm, although not always significantly. Furthermore, fluxes at 0-10 cm were significantly higher than those produced at 10-20 and 20-30 cm for all treatments, both temperature and moisture.

The increased carbon dioxide flux hypothesised (hypothesis 1 – page 99) to take place due to the interactive effect of increased temperature and decreased soil moisture was found to take place only in the top 10 cm of the profile. Further down the profile, highest fluxes were found to come from cores incubated at higher temperatures and 100 % moisture conditions. There was no evidence of transient effects due to acclimation or substrate loss on soil respiration rates up to 116 days (hypothesis 4 – page 99). This may have been due either to the fact that the incubation period was relatively short (~ 4 months), but equivalent to the growing season at the site, or that as peat soils are usually composed of ~ 50 % carbon, soil carbon substrate did not become limiting.

These findings were facilitated by the use of the Exetainer technique, which was a quick and successful method, by which to determine CO_2 fluxes and concomitant Q_{10} values. The error on flux and $\delta^{13}C$ measurements was greatly reduced when a minimum of 200 ppm respired CO_2 was collected, and it is recommended that no less than this concentration (but preferably > 400 ppm) is collected for future incubation experiments undertaken where the same analytical precision of $\delta^{13}C$ measurement is involved (0.3 ‰). However, the use of this technique to distinguish between different sources being mineralised in the peat profile *via* measurement of the $\delta^{13}C$ of respired CO_2 is not possible under 100 % field capacity conditions. It is suggested that chambers used for future incubations should be scrubbed of atmospheric CO_2 before samples are removed for $\delta^{13}C$ analysis *via* this technique. Although more time consuming, this would eliminate the need for mass balance and thus reduce the uncertainty on the estimate of $\delta^{13}C$ for respired CO_2, possibly leading to partitioning of different carbon sources being mineralised within the soil.

The use of the molecular sieve sampling system to distinguish different sources of carbon in respired CO_2 is appropriate, in most instances (the stable carbon isotope values of respired CO_2 produced by the 10-20 and 20-30 cm depths were identical, as was the bulk peat from the same depths). In this study, differentiation of carbon sources was achieved at 15 °C, but at 5 °C, only respiration from the surface 10 cm was clearly distinguished from lower depths in the profile. $\delta^{13}C$ values gained for soil respired CO_2 using MS^3 suggest that either fractionation occurs during the decomposition of organic matter or there is a switch in the source of carbon (to one more depleted in ^{13}C) at higher temperatures, as has been demonstrated by other studies (Biasi *et al.*, 2005; Bol *et al.*, 2003).

If there was a switch (shown by MS^3 data only) in sources used for mineralisation then, this was contrary to what was hypothesised, in that respired CO_2 became more depleted in

^{13}C at higher temperatures as opposed to enriched in ^{13}C. The observed effect in the $\delta^{13}C$ values of respired CO_2 is very likely due to the decomposition of more recalcitrant material such as lignin and cellulose which are more depleted in ^{13}C (Benner *et al.*, 1987) than the more readily decomposed compounds in the soil such as sugars and lipids. The $\delta^{13}C$ values of respired CO_2 from different depths in the profile (where distinguishable at 2 σ_e – by MS^3 only), as hypothesised, became more enriched with depth. This could reflect the enrichment in ^{13}C of the bulk peat with depth.

However, whilst microbes may be accessing different sources of carbon under different temperature treatments, this cannot be clearly determined for all depths using measurements of $\delta^{13}C$. In this respect, the use of radiocarbon may provide more detailed information (i.e. age) of the soil carbon pools that are being accessed by the heterotrophic soil population. It has been demonstrated that capturing respired CO_2 using MS^3 may be a viable method with which to do this (i.e. it has been demonstrated that MS^3 can be used to capture respired CO_2 produced during an incubation experiment, and has shown that it can successfully capture CO_2 for $\delta^{13}C$ analysis). It is thought likely that MS^3 will also prove successful at capturing respired CO_2 during an incubation experiment for ^{14}C analysis.

Finally, this study has shown that if temperatures rise within northern latitudes as predicted (IPCC, 2001) with an expected concomitant lowering in water table levels, then an increase in flux from soil to the atmosphere will occur, decreasing soil carbon storage. In addition, the further water tables fall, and the more aerated these peatland soils become, the faster this carbon loss to the atmosphere will become. This was demonstrated by the increased sensitivity of older soil organic matter decomposition to increased temperature, with depth from the surface of the profile.

5 Quantifying and partitioning sources of CO_2 in peatland ecosystem respiration using 'bomb' ^{14}C as a tracer

5.1 Introduction

The rapid increase in atmospheric CO_2 concentration and the associated rise in temperature (IPCC, 2001) have led to the need for a more accurate understanding of the global carbon cycle. Experiments have shown that the photosynthetic response of vegetation to raised levels of atmospheric CO_2 (700 ppm), has been found to increase gross primary production (GPP) by as much as 40-60 % and many studies have shown that response mechanisms are well understood (Norby *et al.*, 2005). However, the net response has been estimated to be much smaller than the response of GPP at between 16 and 17 % (Mooney *et al.*, 1999). It is expected that the increase in net primary production (NPP) with rising CO_2 levels will easily and rapidly be overcome by a greater release of carbon from soils due to increased temperatures and changing hydrology, thus placing soil and its response to climate change at the centre of terrestrial carbon cycling research.

Furthermore, as has been mentioned in previous chapters, soils contain the largest reservoir of carbon in the terrestrial biosphere, with an estimated storage capacity of 1.6 Tt (Schimel, 1995a). Because this huge store of carbon is more than double that of the atmosphere (0.75 Tt), a small change in the 'sink-source' function of soil could potentially have a considerable impact on the CO_2 loading of the atmosphere. Recent climate models have predicted that the current soil carbon sink will go into decline and eventually become a source of carbon, thus leading to an acceleration of the enhanced anthropogenic greenhouse effect through increased levels of atmospheric CO_2 (Cox *et al.*, 2000). In addition, peatlands are at particularly high risk of losing carbon to the atmosphere as these ecosystems exist mainly at high latitudes (Gorham, 1991) where global warming is predicted to have the most pronounced effect (IPCC, 2001).

Carbon isotopes (both stable and radioactive) have become powerful tools in the quest to elucidate terrestrial carbon cycling dynamics (Alm *et al.*, 1999; Amundson *et al.*, 1998; Dawson *et al.*, 2002; Ehleringer *et al.*, 2000; Harrison *et al.*, 2000; Ladyman & Harkness, 1980; Longdoz *et al.*, 2000; Trumbore *et al.*, 1996). The use of variations in the natural abundance of stable carbon isotope ratios in ecosystem respiration provides valuable

information on sources of respired carbon within the terrestrial biosphere (Dawson *et al.*, 2002). This technique requires that sources and sinks have contrasting isotopic signatures with a large enough variation in ratios to be detected (Dawson *et al.*, 2002).

For example, the natural difference in $\delta^{13}C$ signatures of respiration produced from organic matter derived from C_3 (c. -27 ‰) and C_4 (c. -15 ‰) plants has been used to source the origin of soil respired CO_2 in the field (Rochette *et al.*, 1999). However, there are no C_4 plants occurring at the study site (Hard Hill, Moor House NNR) employed in this thesis investigation (most C_4 species are confined to subtropical and tropical climates). Therefore the C_3/C_4 isotope technique is not a method that could be utilised in the partitioning of soil respiration from plant respiration.

Attempts to partition soil respiration using natural abundance techniques within an ecosystem that utilises only a single photosynthetic pathway is much more difficult to achieve (e.g. Chapter 3), relative to the C_3/C_4 technique, requiring a difference of ~ 5 ‰ between sources (Staddon, 2004). Partitioning CO_2 sources within these ecosystems into their individual component sources is possibly more easily undertaken by the application of an enriched stable isotope tracer, as has been successfully carried out in other studies e.g. in peatlands (Ward, 2006) and grasslands (Ostle *et al.*, 2000). An alternative to this approach is to utilise 'bomb' produced radiocarbon as a tracer.

In almost doubling the atmosphere's concentration of radiocarbon, thermonuclear weapons testing in the 1950's and 60's (Figure 1.4, Chapter 1) produced a valuable tracer in the quest to understand and quantify soil carbon dynamics (Harkness *et al.*, 1986). The advantage over other techniques (e.g. root exclusion and component integration), of utilising this 'bomb' ^{14}C as a continuous isotopic label, is that there is no disturbance of the soil-root-microbe system. Additionally, 'bomb' ^{14}C can be used to resolve soil carbon dynamics on annual to decadal timescales. However, as SOM is made up of various pools of carbon, cycling on widely different timescales e.g. days to millennia, measurements of bulk SOM (at a single time point) alone provide limited information regarding rates of carbon cycling.

Furthermore, measurements of ^{14}C in SOM only, tend to underestimate soil CO_2 fluxes (Trumbore, 2000). For example, one of the most serious sources of error in dating peat deposits is considered to be the translocation of modern carbon to depth *via* plant roots (Nilsson *et al.*, 2001). As plant roots can extend up to 2.3 m in depth (Saarinen, 1996) in some fens and since > 90 % of recently fixed carbon can be translocated to the root system

(Wallén, 1986), the translocation of recently photosynthesised carbon to depth has the potential to have a considerable impact on the age of bulk peat and hence on carbon accumulation/cycling rates.

Measurements of ^{14}C activities in soil CO_2 have been employed as a means to age carbon substrates being decomposed and returned to the atmosphere as respiration (Aravena *et al.*, 1993; Charman *et al.*, 1994). Also, a number of studies have been carried out using measurements of ^{14}C in soil organic matter (SOM) and soil respired CO_2 in order to determine the origin of respired carbon (Charman *et al.*, 1999; Gaudinski *et al.*, 2000; Koarashi *et al.*, 2002; Trumbore, 2000; Wookey *et al.*, 2002), and were first carried out by Dörr and Münnich in the 1980's (Dörr & Münnich, 1980; 1986). There are few published studies investigating the ^{14}C signature of CO_2 evolved from the surface of a peatland, an exception being Jungner *et al.* (1995) who suggested that CO_2 emitted from a peat bog was ~ 100 %Modern but they did not measure it directly.

Stores of soil carbon are predicted to respond to climatic change as it has been shown that SOM decomposition rates respond to varying moisture and temperature regimes (Parton *et al.*, 1987; Schimel *et al.*, 1994). For example, soils globally are predicted to release between 10 and 30 Pg of carbon to the atmosphere, with only a 1 °C rise in temperature (Schimel *et al.*, 1994). Considering peatlands are such a large source of carbon and with the current concerns over global warming in mind, there is an urgent need to better quantify carbon cycling rates in these ecosystems. The use of natural abundance and 'bomb' ^{14}C signatures of respired CO_2 in conjunction with the ^{14}C signature of SOM, dissolved organic carbon (DOC) and plant tissues as carbon tracers offers a means to do this.

Furthermore, to better understand and quantify how much carbon can be stored in soils and for how long, it is of critical importance that we determine the residence time and effluxes of SOM carbon and identify the regulatory processes involved (Trumbore, 2000). Therefore, the aim of this study was first, to characterise the isotopic signature (^{14}C) of respired CO_2 from an upland blanket peat as a means to quantify the different ecosystem CO_2 sources (i.e. plant and soil respiration). CO_2 evolved from plots cleared of vegetation can be used to define 'soil' respiration and respired CO_2 from vegetated control plots was used to represent 'ecosystem' respiration. In addition, respired CO_2 was captured from plots at times of differing hydrology (i.e. low and high water table) to investigate how the age of soil respired CO_2 varied with changing hydrology.

Secondly, it is necessary to characterise the ^{14}C signature of all substrates within the peatland ecosystem that could be utilised for respiration i.e. SOM, plant leaf material, DOC and atmospheric CO_2. Radiocarbon analyses of these samples should provide a means with which to differentiate between the two sources of respiration i.e. plant versus soil respiration. Few studies of peatland carbon dynamics have investigated the spatial variation in ^{14}C content and accumulation rates in surface organic matter layers (Charman *et al.*, 1999), largely due to the prohibitive costs of radiocarbon analysis. For example, in palaeoecological studies it is common for ^{14}C values of material obtained from a single peat core to be taken as representative of the entire peatland; Barber *et al.* (1998) provide one of the few investigations of spatial variability in peat palaeoecological records. However, peat accumulation (i.e. rate of depth increase) and carbon accumulation rates in peat are known to be greatly affected by a range of biotic and abiotic factors which themselves may vary over short distances and in time (Clymo *et al.*, 1998).

For example, DOC can be a source of labile carbon for soil organisms that are involved in decomposition. Charman *et al.* (1999) and references within, have shown that CO_2 can have a consistently younger ^{14}C age than the surrounding peat from the same depth, sometimes by at least 1000 years. However, these studies were performed on peat from deep layers, below the zone of water table fluctuation and greatest CO_2 production. Studies have suggested (Clymo, 1984) that due to anaerobic conditions within the catotelm, decomposition processes occur much more slowly and the relative contribution from this source to soil CO_2 efflux is minimal.

It has been suggested by Jungner *et al.* (1995) that peatland vegetation recycles soil respiration and that the ^{14}C signature of plant species is affected by this phenomenon. Low growing bryophytes in particular are likely to have ^{14}C signatures that reflect a contribution from soil respiration, due to the fact that there is less mixing lower down in the vegetation canopy. For example, in a study of the ^{14}C activity of peat, Jungner *et al.* (1995) found that samples of *Sphagnum fuscum* collected from a Finnish bog had fixed soil respired CO_2 and they estimated this fixation to be 20 % of total carbon uptake.

Recycling of soil respired CO_2 clearly has implications for ^{14}C dating of peat macrofossils, a technique which commonly advocates the use of *Sphagnum* spp as representing the actual age of the surrounding peat matrix (Nilsson *et al.*, 2001). Conversely, the actively photosynthesising leaves of the species *Calluna vulgaris* are more likely to have a similar ^{14}C signature to the atmosphere as they are situated towards the top of the vegetation canopy and the atmosphere in which they are growing is well mixed due to a greater

degree of turbulence. However, the use of parts of *Calluna vulgaris* as a plant macrofossil for use in ^{14}C dating is not without problems. For example Hobbs and Gimingham (1987) found that some heath species such as *Calluna vulgaris* can survive for at least 25 to 30 years.

Therefore, the primary objective of this chapter is to focus on biological transformations of carbon in soils in an upland peatland environment with specific emphasis on using carbon isotope tracers as a means to:

1. Characterise the isotopic signature (both ^{13}C and ^{14}C) of respired CO_2 emanating from a peatland ecosystem.

2. Partition ecosystem respiration into its soil and plant components.

3. Determine the effects of hydrology on the age and rate of peat respired CO_2.

4. Determine the spatial variability of ^{14}C in the surface layers of peat both laterally and horizontally.

5. Examine the contribution of 'labile' dissolved organic carbon (DOC) to peat respiration.

The hypotheses are:

1. That plant respiration is derived from the current year's photosynthate (Trumbore, 2000) and therefore should have a ^{14}C signature close to that of the contemporary atmosphere.

2. That soil respired CO_2 will be older than plant respired CO_2 due to the decomposition of both older DOC and SOM in the soil.

3. That the ^{14}C signal of respired carbon will change with water table depth because the zone of greatest decompositional activity is always above the level of the water table.

4. That carbon in DOC will be younger than the bulk peat that encompasses it (Charman *et al.*, 1999).

5. That from the surface to a certain level in the profile, despite bulk peat getting older with depth, it will also become more enriched in radiocarbon due to incorporation of bomb $^{14}CO_2$; i.e. it is expected that the atmospheric ^{14}C bomb spike will be visible in the peat.

6. That peatland vegetation will have a ^{14}C signature close to that of the contemporary atmosphere with the possibility that bryophytes may be slightly enriched in ^{14}C due to the incorporation of soil respired CO_2 (Jungner *et al.*, 1995).

The development of understanding will require the application of carbon isotope tracer approaches and a meaningful framework for interpretation. In this way mass-balance and ecosystem carbon budgets can be estimated. Radiocarbon signals in soil respiration should provide an improved understanding of the climatic regulators that control decomposition of carbon in the soil and its subsequent loss to the atmosphere as CO_2. Information gained will be used to establish the importance of climatic regulators on the peatland CO_2 'sink-source' function.

5.2 Materials and methods

5.2.1 Experimental design

To characterise the isotopic signature (^{14}C) of respired CO_2 and attempt to quantify, individually, the proportions of soil respiration and plant respiration that together make up total ecosystem respiration (i.e. plant and soil respiration), plots consisting of two replicated treatments (see Figure 5.1) were established within Moor House NNR (Hard

Figure 5.1 – Photographs depicting an 'ecosystem' plot with the peatland vegetation left intact and a 'soil' plot with all the vegetation removed.

Hill site – see section 3.2.1 for a site description). Three 50 x 50 cm square areas of peat surface were cleared of vegetation, in September of 2003, by Sue Ward (these were the same plots used for experimental work in Chapter 3).

Collars for these plots were bedded in ~ 6 months after vegetation removal, in March 2004. Plant roots were left in place in order to minimise soil disturbance. PVC soil pipe (30 cm in diameter) was cut into 20 cm lengths and bedded in to the vegetation free plots 6 months after vegetation removal, by circumscribing with a knife. The soil pipe served as bases (called 'collars') on which to house static gas sampling chambers (Heikkinen *et al.*, 2002; Nykänen *et al.*, 2003). Respiration chambers were attached to collars with the aid of a black rubber seal. CO_2 produced from these plots represented 'soil' respiration.

Three more treatment plots of similar size to the 'soil' plots were marked out, and all peatland vegetation was left intact. To capture 'ecosystem' respiration, PVC soil pipe, similar to that used for the 'soil' plots was bedded in to the peat surface in June 2005, taking care to ensure that the vegetation was as undisturbed as possible. Collars were inserted into the peat surface by at least 10 cm. However, within 3 weeks, all the *Calluna* within these plots had senesced. New 'ecosystem' plots were chosen and collars bedded in by Jan Poskitt, in July 2005. Peat from exposed and eroded areas near the experimental site at Hard Hill was collected and banked up around the outside of the 'ecosystem' chamber collars in order to create an airtight seal. Respired CO_2 from these plots represented 'ecosystem' respiration, i.e. plant and soil respiration.

5.2.2 Respiration chamber and scrubbing system design

Respiration chambers were made from the same lengths of soil pipe (20 cm) as described above. Circular lids were cut from PVC sheeting and attached to the soil pipe. A hole was drilled in each chamber lid and fitted with a Suba seal septum (Scientific Laboratory Supplies Ltd, Nottingham, UK) before being covered with reflective foil (to minimise heating effects in the chambers). A black rubber seal similar to that used to attach chambers to collars was placed around the chamber lid to make an airtight seal (Figure 5.2). Two additional holes were drilled into the sides of each respiration chamber, one towards the top of the chamber and one towards the bottom on the opposite side of the chamber (see Figure 5.2) to accommodate Quick couplings (Colder Products Company, USA) with which to attach the molecular sieve sampling system (Chapter 2; (Hardie *et al.*, 2005)) and a CO_2 scrubbing system (Figure 5.2). The chamber volume was 13.9 litres.

Figure 5.2 – Photographs illustrating the respiration chamber design (LHS) and the scrubbing system used to remove atmospheric CO_2 from all chambers before capture of respired CO_2 (RHS).

A scrubbing system was designed that removed moisture from the chamber atmosphere (to protect the pump) followed by atmospheric CO_2 removal from the respiration chamber headspace, prior to sample collection from each of the treatment plots. The scrubbing system consisted of three parts; a 3 l min^{-1} diaphragm pump (D3SE, Charles Austen pumps Ltd., UK) housed in a protective waterproof plastic case (Peli 1120, PeliProducts, California, USA) wired to a 12 V rechargeable battery, a water trap and a CO_2 scrub (both traps were constructed from borosilicate glass).

The CO_2 scrub cartridge design is illustrated in Figure 2.5 of Chapter 2, and was the original molecular sieve cartridge design, first used by Bol and Harkness (1995). This cartridge was filled with indicating sodalime (BDH laboratory supplies, UK) held in place by quartz glass wool. A similar but larger design quartz glass cartridge was constructed for drying chamber air (Figure 5.3) and filled with Drierite, a desiccant, Lab Grade, -10+20

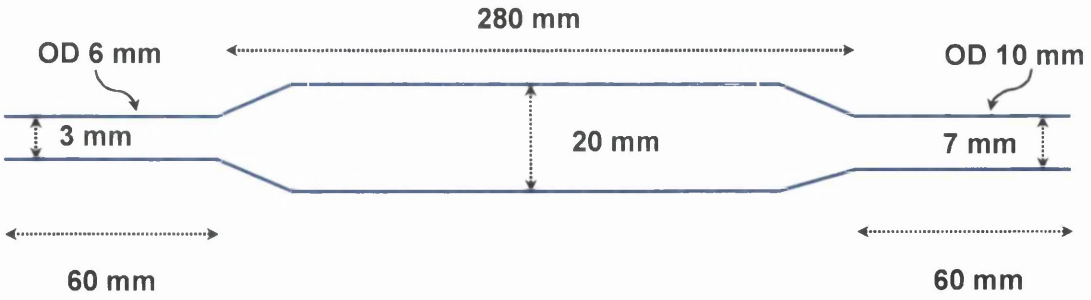

Figure 5.3 – Schematic diagram of the quartz glass cartridge (giving dimensions in mm) used for the water trap. ID = inner diameter. OD = outer diameter.

Mesh (Alfa Aesar, Germany), held in place with quartz glass wool. In addition to protecting the pump, the water trap also prevented any reaction of moisture with the sodalime. Auto-shutoff Quick Couplings were attached to either end of both the CO_2 scrub and water trap with short lengths of PVC tubing (Tygon, R3603, 4.8 x 8.0 mm, Fisher

Scientific, UK). The cartridges were attached to both the pump and the respiration chamber by way of two Quick Couplings. Airflow was reduced to ~ 2.5 l min^{-1} when the cartridges were connected in line with the pump.

5.2.3 CO_2 collection from treatment plots and the contemporary atmosphere

Air and soil temperatures were recorded during sampling periods using 'Tinyview' temperature loggers (Gemini data loggers, Chichester, UK). Temperature probes were also placed inside each chamber to monitor the temperature of the chamber atmosphere during sample collection. Before capture of respiration samples took place, each chamber was first scrubbed of atmospheric CO_2 (Gaudinski *et al.*, 2000). This was done by attaching the scrubbing system to each chamber followed by switching on the pump (Figure 5.2). The chamber atmosphere was scrubbed of CO_2 for one hour (equivalent to a minimum of 7 chamber volumes for each treatment plot), after which the scrubbing system was detached and the molecular sieve sampling system (MS^3) was connected in line to the respiration chamber (Figure 5.4). The chamber atmosphere was circulated around the bypass of MS^3

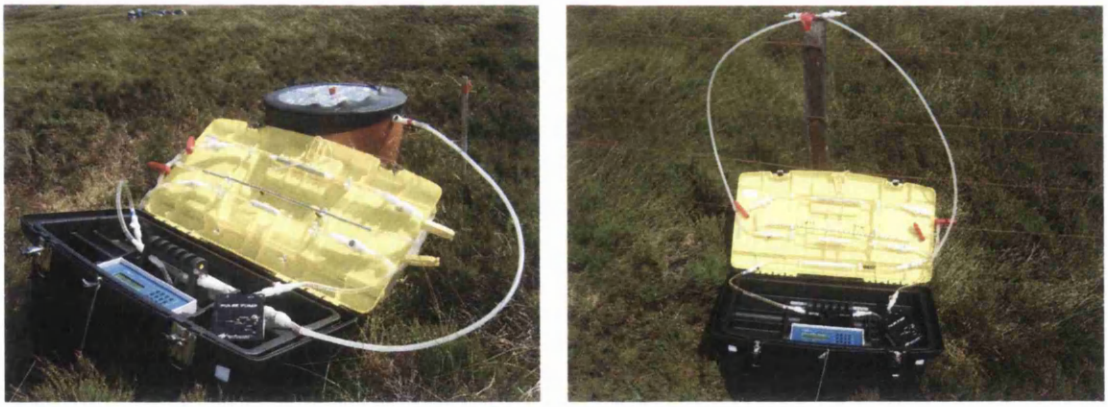

Figure 5.4 – Photographs illustrating MS^3 capturing CO_2 from an 'ecosystem' treatment chamber (LHS) and from the atmosphere (RHS), 1 m above the peatland surface.

(refer to Figure 2.1, Chapter 2 for more detail) and the CO_2 concentration in the chamber was monitored using the IRGA. Both the CO_2 concentration and the time were recorded.

MS^3 was detached from the chamber and respired CO_2 was allowed to build-up. Between 7 and 10 ml of CO_2 was the volume allowed to build up within each chamber before collection on a molecular sieve cartridge (MSC). This volume ensured enough respired carbon for three aliquots to be made: one for ^{14}C analysis, one for $\delta^{13}C$ analysis and one for a sample to be archived (as a back-up). After it was estimated that enough CO_2 had built up within each chamber, the sampling system was reattached and the CO_2 content monitored

by routing the chamber atmosphere around the bypass. When the required volume of CO_2 had built up in the respiration chamber it was trapped using MS^3.

The time and chamber CO_2 concentration were recorded once again (in order to establish how much respiration had been produced in a given time period i.e. a flux). The pathway to the bypass was then closed and the pathway to the MSC opened by removing the WeLoc clips. Respired CO_2 was then circulated from the chamber onto the MSC and the decrease in chamber CO_2 monitored on the IRGA. After the sample was collected, the WeLoc clips were replaced on either end of the MSC before it was detached from MS^3. The MSC was then labelled with the date, treatment plot number and estimated volume of CO_2.

As a backup to CO_2 measurements collated by the IRGA, 20 ml samples of chamber gas were removed from each chamber through the Suba seal septum after scrubbing had taken place. Another 20 ml sample was taken when CO_2 in the chamber had reached the target CO_2 concentration. These samples were taken using a gas tight syringe and placed immediately into evacuated (10^{-1} mbar) Exetainers, for CO_2 concentration analysis by GC and $\delta^{13}C$ analysis by TG-IRMS.

The sampling operation described above was repeated for every respiration sample collected from each of the treatment plots. Respired CO_2 was collected from all treatment plots in August 2005 when the water table was close to the peatland surface and again in September 2005 when the water table was a few cm lower. A number of sampling trips were made in June, July, August and September of 2005, in an attempt to capture respiration when the water table was between 10 and 20 cm lower than the peatland surface, but this aim was not achieved. In addition to respiration samples, CO_2 from the open atmosphere was collected from approximately 1 m above the canopy, using the molecular sieve sampling system (Figure 5.4), in order to characterise the radiocarbon signature of the contemporary atmosphere. One sample was collected in August and one in September, both being taken on the same day that treatment plots were sampled for respired CO_2.

5.2.4 Collection of bulk peat and vegetation

After all respiration samples had been collected, a 16 cm core was removed from the profile within each of the 6 treatment plots (3 'soil' and 3 'ecosystem'). Cores of peat were removed using a stainless steel corer (4.7 x 4.9 x 100 cm) designed to minimise compaction (Cuttle & Malcolm, 1979). The corer was carefully removed from the profile

and the top 16 cm of each core was subdivided into 4 cm increments (0-4, 4-8, 8-12 and 12-16 cm) using a sharp knife. Each 4 cm depth increment was placed into a clear plastic bag and labelled. Each labelled plastic bag was placed into a cool box and stored with ice packs until arrival at the NERC Radiocarbon Laboratory, whereupon samples were refrigerated at 4 °C until required for analysis.

Tens of grams of bryophytes were removed from the 'ecosystem' plots and placed into labelled plastic bags. In addition, tens of grams of shoots and flowers (the current year's growth) from *Calluna vulgaris* were also collected. Vegetation samples were placed into clear plastic bags, labelled and stored in a cool box until arrival at the NERC Radiocarbon Laboratory. Nitrile gloves were worn during the collection of all peat and vegetation samples to prevent contamination.

5.2.5 Extraction and preparation of DOC for radiocarbon analysis

Samples of dissolved organic matter were extracted from each 4 cm increment of one core from each of the two treatment ('soil' and 'ecosystem') plots. Before DOC was extracted from the cores, all glassware was acid washed in 5M HNO_3. In addition, all spatulas and forceps used were heated with a flame until red-hot before handling materials. Gloves were worn at all times during the DOC extraction procedure. The extracting solution used was 1 mM NaCl (prepared using Analar NaCl). A 500 ml centrifuge bottle was weighed on a top pan balance and each 4 cm field-moist sample of peat was rolled into a shape that allowed it to fit into the centrifuge bottle without touching the sides. The centrifuge bottles containing the peat were then reweighed before adding approximately 300 ml of the extracting solution. All bottles were placed on a shaker (170 Motions min^{-1}) for one hour. All bottles were then weighed again before being placed in a centrifuge. This was done to ensure the centrifuge was balanced by placing sample bottles of similar weight opposite one another in the rotor arm (to within 2-3 g). All samples were centrifuged for 1 hour at 9000 rpm and 10 °C before being filtered.

An ashed 0.7 μm glass fibre (GF/F) filter (which had previously been heated in a muffle furnace for 3 hours at 600 °C) was weighed and placed on the support plate of the filtration apparatus (Buchner). The filter reservoir flange was then secured with clips to the support plate and the centrifuged supernatant was carefully decanted into the filtration apparatus. The filtrate was then transferred into a rotary evaporation flask and evaporated down to approximately 5 ml using a rotary evaporator. The remaining liquid was then quantitatively transferred (using a Pasteur pipette) from the rotary flask to a small, pre-weighed, labelled

glass beaker. The beaker was then covered with a small ashed filter, which was secured with an elastic band.

All beakers were immediately placed into a freezer for one hour prior to being freeze dried. The freeze drier was switched on and allowed to reach its operational temperature (-50 °C). Sample beakers were then removed from the freezer and cooled in liquid N_2 for a few minutes before being placed into the freeze drier. All samples were freeze dried to a constant weight. The dried DOC was then weighed and placed into combustion tubes with silver foil and copper oxide, before being evacuated, sealed and then combusted in the muffle furnace at 900 °C.

5.2.6 Preparation of vegetation and bulk peat for ^{14}C analysis

Samples of vegetation were washed in distilled water and dried in a vacuum oven at 40 °C. Dried samples were then homogenised and weighed on an analytical balance. Weighed sub-samples were then placed into silica quartz glass combustion tubes with silver foil and copper oxide. All tubes were evacuated on a vacuum line, flame sealed and combusted at 900 °C in a muffle furnace to convert all the organic matter to CO_2 gas.

Each 4 cm increment of peat was placed in a pre-weighed silica evaporation dish and re-weighed before being dried at 85 °C to a constant weight. Samples were then homogenised by grinding to a powder using a pestle and mortar. Sub-samples of powdered peat were weighed before being combusted with pure oxygen in a high-pressure combustion bomb. All sample combustions carried out in the bomb were performed by Frank Elliott. Finally, three sub-samples were transferred to glass tubes, two being flame sealed for graphitisation and accelerator mass spectrometry (AMS) analysis and an archive. One sub-sample was transferred to a mass spectrometry tube for $\delta^{13}C$ analysis.

5.2.6.1 Determination of peat and C accumulation rates

Rates of peat accumulation were calculated for the different cores using the depth in the profiles where levels of ^{14}C first exceeded 100 %Modern as a chronological reference point. This fixed point represents the deepest layer that contains unequivocal evidence of bomb ^{14}C. Therefore it was considered that peat formed when atmospheric ^{14}C levels first exceeded 100 %Modern (~AD 1955) was contained within this 4 cm layer. Annual peat accumulation rate (cm yr^{-1}) was calculated, by dividing the depth of the peat slice containing the 100 %Modern layer by 50 (number of years for peat accumulation between

AD 1955 and the sampling date). It should be added here that the peak in atmospheric $^{14}CO_2$ concentration (1963) could also have been used as a chronological reference layer. However it was felt that this point in time would not be as clearly defined as the 100 %Modern reference point. Before thermonuclear weapons testing began in the 1950s and 60s, the atmospheric $^{14}CO_2$ concentration had never risen above 100 %Modern and therefore was considered to be the most unambiguous reference point.

Carbon accumulation rates (g m^{-2} yr^{-1}) were calculated using the same 100 %Modern reference layer, dividing the total carbon accumulated (g) above the reference layer by the 50-year accumulation period. Since a very coarse sampling resolution was used, only maximum and minimum values for both these rates were calculated. These were based on the range of depth and carbon mass values represented by the 4 cm slices of peat containing the reference layer.

5.2.7 Desorption and purification of respired CO_2 from MSCs

Using the same procedure as described in Chapter 2 and Hardie *et al.* (2005), CO_2 captured on each molecular sieve cartridge was desorbed onto a vacuum line using a tube furnace set at 500 °C. Once on the vacuum line, CO_2 was cryogenically purified using a slush trap (-78 °C) and two liquid N_2 (-196 °C) traps, first under static collection for a period of 20 minutes and finally under dynamic collection (until a vacuum of 10^{-2} mbar was attained). The pressure of the purified CO_2 was measured using a pressure transducer (BOC Edwards, UK) and the volume of CO_2 calculated. Two sub-samples of purified CO_2 were then flame sealed into glass tubes, one for conversion to graphite before ^{14}C analysis by AMS, and one to be archived. A further sub-sample was transferred to a mass spectrometry tube for $\delta^{13}C$ analysis by IRMS.

5.2.8 Determination of sample $\delta^{13}C$ and ^{14}C

A sub-sample of CO_2 from each treatment sample (respiration, vegetation, DOC and bulk peat) was prepared as a graphite target *via* an Fe/Zn reduction reaction (Slota *et al.*, 1987). All CO_2 reductions to graphite were performed by Callum Murray. Graphite powder from each sample was then pressed into individual aluminium targets before being analysed for ^{14}C by AMS using the 5 MV tandem accelerator (Xu *et al.*, 2004) at the AMS facility, Scottish Universities Environmental Research Centre (SUERC), East Kilbride, UK. Further CO_2 sub-samples were analysed for $\delta^{13}C$ by IRMS (dual inlet, VG Optima,

Micromass, UK). All concentrations for ^{13}C are reported using the delta notation with $^{13}C/^{12}C$ variations relative to the international standard Vienna Pee Dee Belemnite (VPDB) (Craig, 1957), as described by the following equation:

$$\delta^{13}C\ (‰) = \left[\frac{(^{13}C/^{12}C)_{Sample} - (^{13}C/^{12}C)_{VPDB}}{(^{13}C/^{12}C)_{VPDB}} \right] \times 1000 \qquad (1)$$

^{14}C data are expressed as %Modern with samples having been normalised to a $\delta^{13}C$ of -25 ‰ (Stuiver & Polach, 1977).

5.2.9 Determination of the contribution of plant respiration to total ecosystem respiration

'Ecosystem' and 'soil' respiration fluxes and the radiocarbon concentration of these fluxes were measured directly from each of the two replicated treatment plots. Plant respiration, flux, $\delta^{13}C$ and ^{14}C content, were determined using a mass balance approach as demonstrated by the following equations:

$$\Delta_{eco} \times F_{eco} = (\Delta_{plant} \times F_{plant}) + (\Delta_{soil} \times F_{soil}) \qquad (2)$$

where Δ_{eco} (or alternatively $\delta^{13}C$) is the ^{14}C signature of respired CO_2 from the 'ecosystem' treatment, F_{eco} is the total CO_2 flux produced by the 'ecosystem' treatment, Δ_{soil} is the ^{14}C signature of CO_2 produced by the 'soil' treatment and F_{soil} is the CO_2 flux produced by the 'soil' treatment. F_{plant} is calculated by deducting the CO_2 flux produced by the 'soil' treatment from that produced by the 'ecosystem' treatment. The Δ_{plant} (or $\delta^{13}C$) can then be calculated by rearranging equation 1 as follows:

$$\Delta_{plant} = ((\Delta_{eco} \times F_{eco}) - (\Delta_{soil} \times F_{soil})) / (F_{eco} - F_{soil}) \qquad (3)$$

where F_{plant} is $F_{eco} - F_{soil}$.

5.3 Results

Air and soil temperatures were recorded on each sampling date. Whilst atmospheric temperature fluctuated throughout the day (between 13 and 19 °C) during sampling (August and September 2005), soil temperature remained constant at 11.5 °C both in August and in September.

5.3.1 ^{14}C and $\delta^{13}C$ of peatland vegetation and atmospheric CO_2

The carbon isotope results for peatland vegetation and atmospheric CO_2 are given in Table 5.1.

Publication code (SUERC-)	Sample Identifier	^{14}C Enrichment (%Modern ± 1 σ)	$\delta^{13}C$ (‰) ± 0.1
8516	*Calluna vulgaris* shoots	106.21 ± 0.31	-27.8
8517	*Calluna vulgaris* flowers	106.60 ± 0.25	-27.5
8518	*Hypnum jutlandicum*	107.53 ± 0.32	-30.5
8520	*Sphagnum capillifolium*	106.49 ± 0.32	-30.4
8115	Atmospheric CO_2 - Aug	106.98 ± 0.30	-8.9
8124	Atmospheric CO_2 - Sep	106.00 ± 0.33	-8.8

Table 5.1 – ^{14}C and $\delta^{13}C$ of peatland vegetation. Also given is the ^{14}C and $\delta^{13}C$ of atmospheric CO_2 in both August and September 2005 (sampled from 1 m above the peatland surface. 1 σ = 1 standard deviation (analytical error).

Figure 5.5 graphically displays the results for the ^{14}C content of vegetation collected in September of 2005 and also the ^{14}C content of atmospheric CO_2 collected in both August and September 2005.

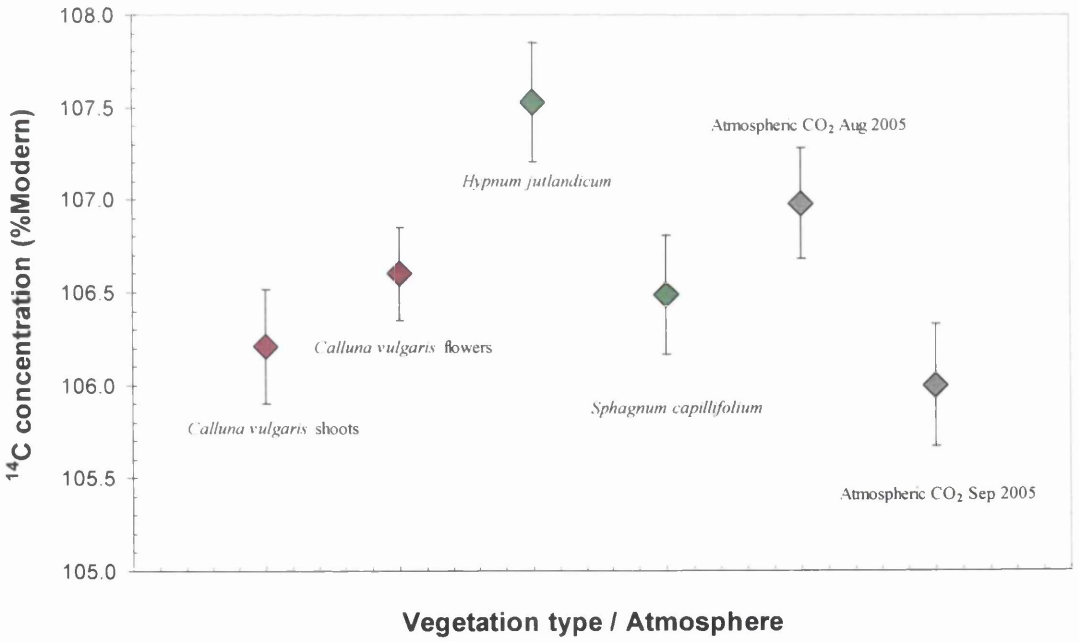

Figure 5.5 – ^{14}C concentration in peatland vegetation and atmospheric CO_2 (n = 1). Error bars are ± 1 σ. 1 σ = 1 standard deviation (analytical error).

^{14}C concentrations of peatland vegetation sampled in September of 2005, ranged from 106.2 ± 0.31 to 107.5 ± 0.30 %Modern. *Sphagnum capillifolium* and *Calluna vulgaris* shoots and flowers were statistically identical in ^{14}C concentration at 1 σ.

The bryophyte *Hypnum jutlandicum* was the most enriched in ^{14}C of the 4 vegetation samples, having a ^{14}C concentration of 107.5 ± 0.32 %Modern. However, this value is identical at 2 σ to the ^{14}C content of both the *Sphagnum* and the *Calluna vulgaris* samples. Furthermore, all vegetation ^{14}C concentrations were within 2 σ of the contemporary atmosphere in August and September 2005. The radiocarbon concentration of the atmosphere in August of 2005 (107.0 ± 0.30 %Modern) was enriched relative to atmospheric CO_2 sampled in September of 2005 but not significantly so at 2 σ.

$\delta^{13}C$ values for *Calluna vulgaris* samples ranged from -27.5 to -27.8 ± 0.1 ‰ for flowers and shoots respectively (Figure 5.6). Both samples of *Calluna vulgaris* were statistically

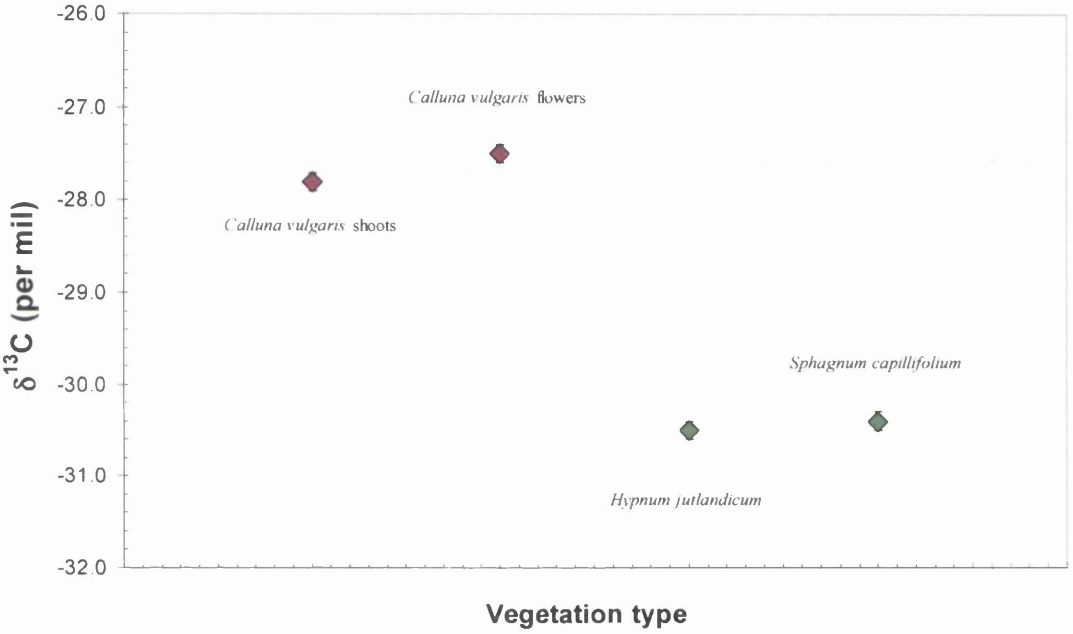

Figure 5.6 - $\delta^{13}C$ values for peatland vegetation (n = 1). Error bars are ± 1 σ. 1 σ = standard deviation (analytical error) for $\delta^{13}C$ analyses.

more enriched in ^{13}C at 2 σ than both the *Hypnum* and *Sphagnum* samples (-30.4 and -30.5 ‰). $\delta^{13}C$ values for the vegetation samples are within a similar range to that measured in May 2005 (Chapter 3, Table 3.2), although the bryophytes collected in September 2005 are statistically more depleted in ^{13}C at 2 σ, than those sampled in May. Atmospheric CO_2 in August of 2005 had a $\delta^{13}C$ value of -8.9 ‰, which was statistically identical to the $\delta^{13}C$ value of the atmosphere in September (-8.8 ‰).

5.3.2 Bulk density, % carbon and carbon isotope results of bulk peat

A single core was extracted from each of the three 'ecosystem' plots and each of the three 'soil' plots giving a total of six cores. Each sampled core was divided into 4 cm sections (0-4, 4-8, 8-12 and 12-16 cm) before analysis. Table 5.2 provides the percentage carbon,

Sample Identifier (Core - depth)	Publication Code (SUERC-)	Bulk Density (g cm^{-3})	% Carbon	$\delta^{13}C$ (‰) ± 0.1	^{14}C Enrichment %Modern (± 1 σ)
Eco 1 - 0-4 cm	9398	0.050	48.9	-29.8	113.48 ± 0.40
Eco 1 - 4-8 cm	9399	0.106	47.8	-28.5	115.05 ± 0.40
Eco 1 - 8-12 cm	9400	0.114	47.1	-25.9	99.50 ± 0.35
Eco 1 - 12-16 cm	9401	0.094	47.7	-26.6	98.42 ± 0.31
Eco 2 - 0-4 cm	8521	0.080	47.5	-28.8	116.50 ± 0.35
Eco 2 - 4-8 cm	8522	0.132	49.4	-27.8	130.42 ± 0.30
Eco 2 - 8-12 cm	8523	0.106	47.6	-27.0	105.75 ± 0.25
Eco 2 - 12-16 cm	8527	0.143	49.2	-26.4	95.62 ± 0.28
Eco 3 - 0-4 cm	9404	0.045	48.0	-30.2	111.74 ± 0.39
Eco 3 - 4-8 cm	9405	0.065	46.7	-28.6	114.98 ± 0.41
Eco 3 - 8-12 cm	9406	0.087	44.6	-26.9	125.80 ± 0.45
Eco 3 -12-16 cm	9407	0.076	48.1	-28.0	122.15 ± 0.43
Soil 1 - 0-4 cm	9408	0.086	48.3	-29.2	113.98 ± 0.40
Soil 1 - 4-8 cm	9409	0.138	49.6	-28.7	109.37 ± 0.33
Soil 1 - 8-12 cm	9411	0.101	48.4	-27.6	98.61 ± 0.35
Soil 1 - 12-16 cm	9414	0.107	49.7	-27.7	96.89 ± 0.34
Soil 2 - 0-4 cm	9415	0.038	46.2	-28.0	118.40 ± 0.38
Soil 2 - 4-8 cm	9416	0.079	48.3	-26.9	127.35 ± 0.45
Soil 2 - 8-12 cm	9417	0.095	46.4	-28.3	114.05 ± 0.40
Soil 2 - 12-16 cm	9418	0.101	47.8	-25.9	95.22 ± 0.33
Soil 3 - 0-4 cm	8528	0.084	45.2	-28.3	119.68 ± 0.36
Soil 3 - 4-8 cm	8529	0.109	46.6	-27.2	104.59 ± 0.31
Soil 3 - 8-12 cm	8531	0.097	46.2	-27.4	96.41 ± 0.29
Soil 3 - 12-16 cm	8532	0.096	48.9	-27.2	96.66 ± 0.25

Table 5.2 - Carbon isotope, bulk density and % carbon results of bulk peat. Eco = plots where peatland vegetation was left intact. Soil = plots where all peatland vegetation was removed. 1 σ = 1 standard deviation (analytical error).

bulk density and carbon isotope results. Carbon content for all samples was around 45-50 %, typical for ombrotrophic blanket peat. Bulk density was also typical of upland peat (Clymo, 1983) and ranged from ~0.04 g cm^{-3} to ~0.14 g cm^{-3}, with lowest values

occurring in surface samples. There were no significant differences in either carbon content (%) or bulk density between the 'ecosystem' and 'soil' cores.

The results for both $\delta^{13}C$ and ^{14}C at each 4 cm depth increment are illustrated graphically in Figure 5.7. Radiocarbon concentrations vary widely from pre-bomb to post-bomb values

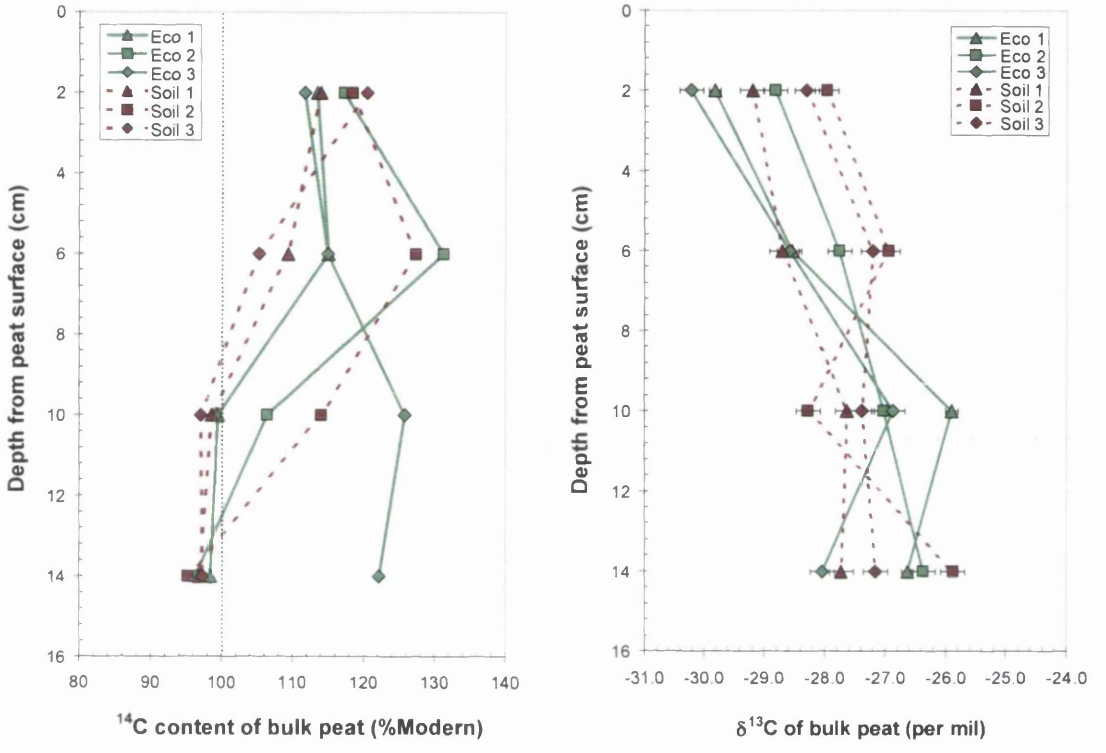

Figure 5.7 – ^{14}C and $\delta^{13}C$ values for bulk peat extracted from the surface 16 cm of each of the two treatments ('soil' and 'ecosystem'). n = 3 for all points. Eco = 'ecosystem' treatment. Soil = 'soil' treatment.

in all cases with the exception of one core ('ecosystem' 3) where bomb ^{14}C is evident throughout the entire 16 cm of the profile. Furthermore, despite their close proximity in the field, the profiles of radiocarbon content with depth demonstrated considerable variation between cores. In the remainder of the peat cores the lowest radiocarbon concentrations were found in the deepest (12-16 cm) layer.

The range in ^{14}C content of the peat was depth dependent. For example, the radiocarbon content in the surface layer varied only between ~110 and ~120 %Modern, whereas the 4-8 cm layer ranged from ~105 to ~130 %Modern. In the deepest layer, radiocarbon content in 5 of the 6 profiles ranged from ~95 to ~99 %Modern, although again, core 'ecosystem' 3 was distinct, having a radiocarbon concentration of 122 %Modern at this depth. There were no obvious differences in the profile of radiocarbon content under the two different treatments ('ecosystem' and 'soil').

$\delta^{13}C$ values for bulk peat (Figure 5.7) ranged from -30.2 ‰ in the surface layer (0-4 cm) of core 'ecosystem' 3 to -25.9 ‰ in the lowest depth increment (12-16 cm) of core 'soil' 3 and also in the 8-12 cm depth increment of core 'ecosystem' 1. In the main, bulk peat from each of the 16 cm cores demonstrated an enrichment in ^{13}C with depth from the surface 4 cm to the lowest layer in the profile (12-16 cm).

Table 5.3 presents the calculated values of peat accumulation rate (annual rate of depth

Core Identifier	Depth containing the 100 %Modern reference layer (cm)	Peat accumulation rate (cm yr^{-1})	Carbon accumulation rate (g C m^{-2} yr^{-1})
Eco 1	4-8	0.08 - 0.16	19.6 - 60.0
Eco 2	8-12	0.16 - 0.24	82.6 - 123.0
Eco 3	>16	>0.32	>72.6
Soil 1	4-8	0.08 - 0.16	33.2 - 88.0
Soil 2	8-12	0.16 - 0.24	44.6 - 79.8
Soil 3	4-8	0.08 - 0.16	30.4 - 71.0

Table 5.3 - Calculated ranges of peat accumulation and carbon accumulation rate above the 100 %Modern reference layer (i.e. for the last ~50 years). Eco = plots where peatland vegetation was left intact. Soil = plots where all peatland vegetation was removed.

increase in cm yr^{-1}) and carbon accumulation rate (g m^{-2} yr^{-1}). Peat accumulation rates ranged from ~0.08 to 0.24 cm yr^{-1} for most sites, although core 'ecosystem' 3 had an average accumulation rate of more than 0.32 cm yr^{-1} above the reference layer. Due to the coarse 4 cm sampling resolution, the ranges of carbon accumulation rates for each core were large, and the overall range was ~20 to ~125 g C m^{-2} yr^{-1}. There were no significant differences between the two treatments for peat accumulation and carbon accumulation rate as ranges overlapped.

5.3.3 ^{14}C and $\delta^{13}C$ of dissolved organic carbon (DOC)

One core from each of the two treatments underwent extraction of DOC with a weak (1 mM) NaCl solution. All carbon isotope results for DOC extractions are presented in Table 5.4. Graphical illustrations of ^{14}C concentrations and $\delta^{13}C$ values for DOC extracted from each of the two treatment cores are presented in Figures 5.8 and 5.9 respectively. Radiocarbon concentrations of DOC extracted from each of the 4 cm increments were all

Publication code (SUERC-)	Sample Identifier	^{14}C Enrichment (%Modern ± 1 σ)	$\delta^{13}C$ (‰) ± 0.1
8125	Eco 2 - 0-4 cm	112.64 ± 0.31	-27.9
8126	Eco 2 - 4-8 cm	121.57 ± 0.33	-27.1
8129	Eco 2 - 8-12 cm	112.38 ± 0.35	-27.1
8131	Eco 2 - 12-16 cm	101.61 ± 0.27	-26.7
8132	Soil 3 - 0-4 cm	117.63 ± 0.32	-27.9
8133	Soil 3 - 4-8 cm	110.76 ± 0.34	-27.4
8134	Soil 3 - 8-12 cm	103.23 ± 0.31	-26.4
8136	Soil 3 -12-16 cm	99.66 ± 0.30	-26.0

Table 5.4 – ^{14}C and $\delta^{13}C$ of DOC extracted from core 'ecosystem' 2 and core 'soil' 3. Eco = 'ecosystem' treatment. Soil = 'soil' treatment.

post-bomb except for one depth increment (soil, 12-16 cm) which was 99.66 ± 0.30 %Modern. The 'ecosystem' DOC became more enriched in ^{14}C below the surface 4 cm,

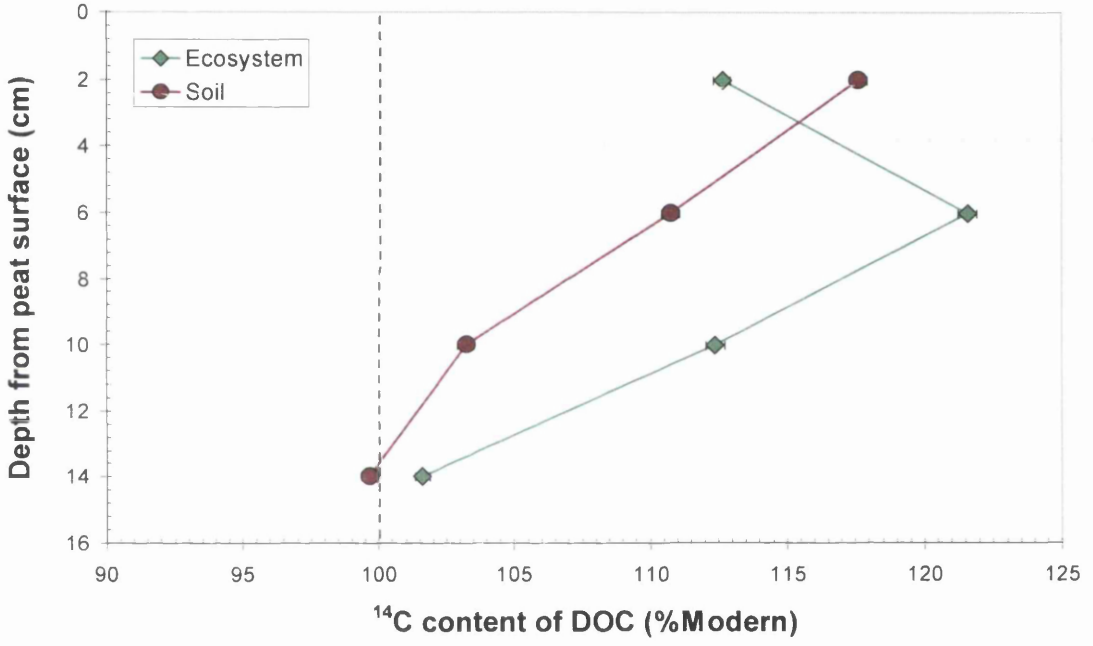

Figure 5.8 - ^{14}C concentration of DOC extracted from bulk peat removed from the top 16 cm of one core from each of the two treatments ('soil' and 'ecosystem'). Error bars are ± 1 σ (analytical error). n= 1 for each data point.

with DOC extracted from the 4-8 cm depth increment containing the most ^{14}C at 121.57 ± 0.33 %Modern. This is the peak in ^{14}C for this treatment after which ^{14}C becomes depleted with depth. DOC extracted from the surface 4 cm of the 'soil' treatment contained the most radiocarbon for this treatment core at 117.63 ± 0.32 %Modern, significantly less at 2 σ than the ^{14}C content of the 4-8 cm depth increment of the 'ecosystem' treatment. DOC from the 'ecosystem' treatment was statistically enriched in ^{14}C, by more than 2 σ relative to the 'soil' treatment, for the lowest three depth increments (4-8, 8-12 and 12-16 cm).

However, the opposite was true for the surface 4 cm, where the DOC extracted from the 'soil' treatment was significantly enriched by more than 2 σ relative to the 'ecosystem' treatment.

$\delta^{13}C$ values for DOC (Figure 5.9) extracted from the 'soil' treatment ranged from -27.9 ±

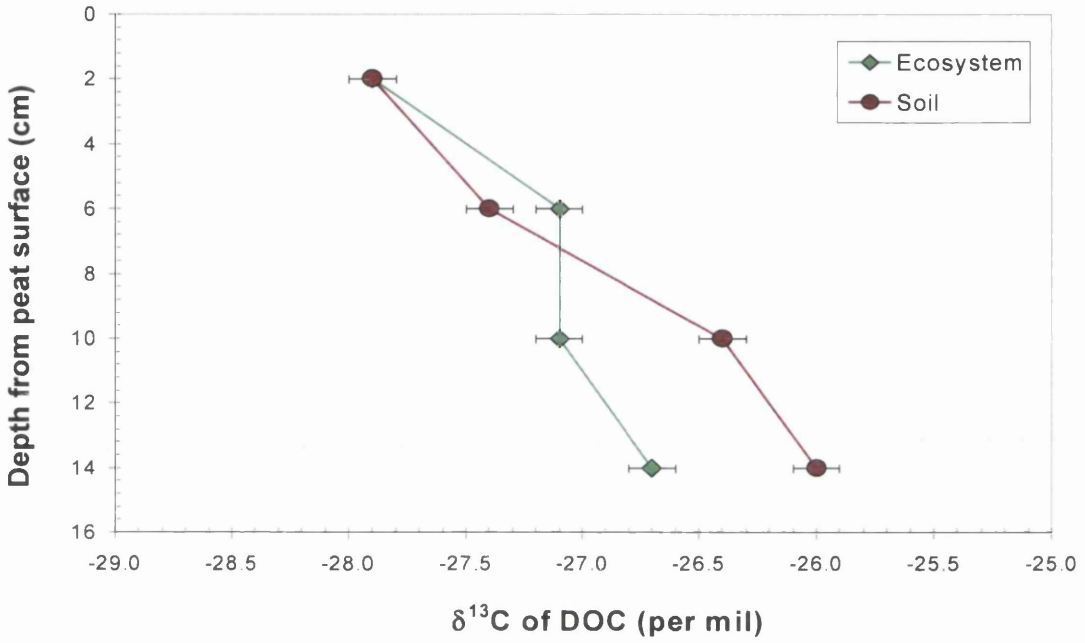

Figure 5.9 - $\delta^{13}C$ values for DOC extracted from bulk peat extracted from one core from each of the two treatments ('soil' and 'ecosystem'). Error bars are ± 1 σ (analytical error). n = 1 for each data point.

0.1 ‰ in the surface 4 cm, becoming more enriched with depth, to -26.0 ± 0.1 ‰ in the 12-16 cm depth increment, a difference of 1.9 ‰ from top to bottom. The 4-8 and 8-12 cm increments become significantly enriched in ^{13}C, at 2 σ, relative to the depths directly above in the profile. However, the lowest two depths (8-12 and 12-16 cm) are statistically the same at 2 σ. $\delta^{13}C$ values for DOC extracted from the 'ecosystem' treatment ranges from -27.9 ‰ in the surface 4 cm (identical to DOC from the same depth for the 'soil' treatment) to -26.7 ‰ in the bottom 4 cm, a range of 1.2 ‰. The DOC extracted from the 8-12 and 12-16 cm depth increments was significantly more enriched (> 2 σ) in ^{13}C in the 'soil' treatment than for the 'ecosystem' treatment. There was no significant difference between treatments for the top 8 cm of the profile.

5.3.4 Respiration fluxes

Mean respiration fluxes for the 'soil' and 'ecosystem' plots for August and September of 2005 are illustrated in Figure 5.10. The highest mean respiration rates were produced by

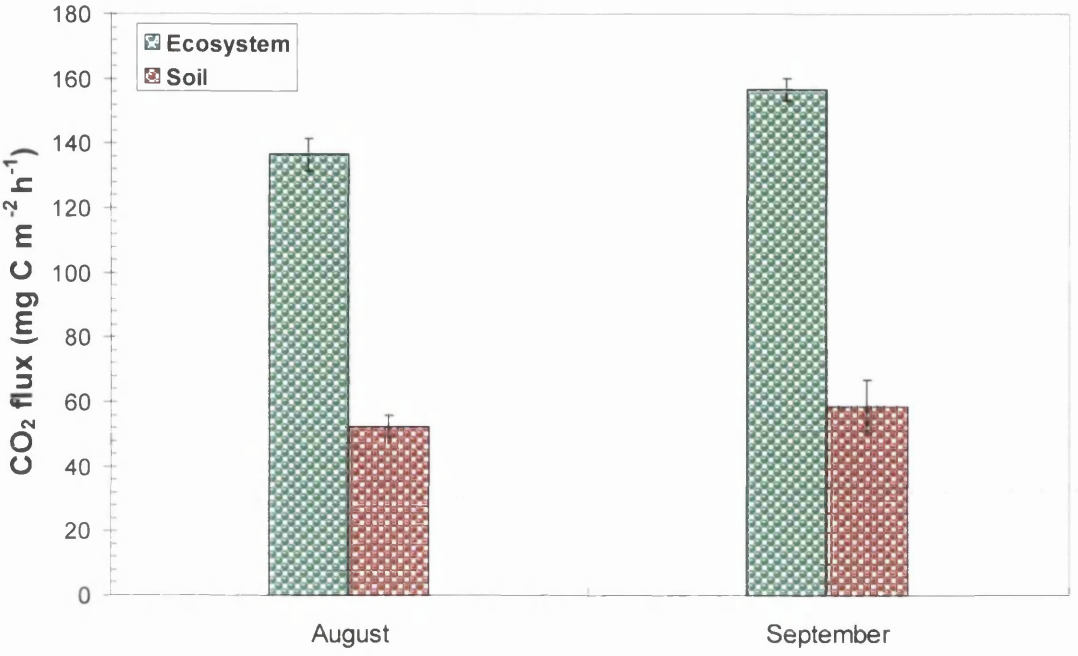

Figure 5.10 – Mean respiration fluxes measured in August and September 2005. n = 3 for all measurements except in September where n = 2 for the 'ecosystem' plots. Mean water table depth for 'ecosystem' plots in August -3.1 cm, in September -6.4 cm and for the 'soil' plots in August -1.8 cm and in September -5.6 cm. Error bars are 1 σ_e.

the 'ecosystem' plots, with the highest flux taking place in September at 156.8 ± 5.0 mg C m^{-2} h^{-1}. Rates of respired CO_2 produced by the 'soil' plots were approximately 38.5 and 37.5 % of those produced by the 'ecosystem' plots in August and September respectively. In August the mean flux produced by the 'soil' treatment plots was 52.5 ± 3.2 mg C m^{-2} h^{-1} and in September 58.8 ± 8.2 mg C m^{-2} h^{-1}. In addition, the respiration fluxes produced in August and September by the 'soil' treatment were 30.0 and 45.5 % higher than the mean flux produced by the 'soil' treatment in May 2005 (Chapter 3, section 3.4.3).

One chamber was eliminated from mean flux measurements ('ecosystem' 3 in September). This was due to the fact that the flux measured in this chamber was 19 % of the mean flux of the remaining two 'ecosystem' plots in September and 22 % of the mean 'ecosystem' flux in August. In addition, the $\delta^{13}C$ value obtained for respired CO_2 collected from this chamber was 8.2 ‰ higher than the average $\delta^{13}C$ value obtained for the remaining two 'ecosystem' chambers sampled on the same day. The flux produced was therefore deemed unreliable as it seemed likely, given the flux rate and the $\delta^{13}C$ values for the respired CO_2

that there was contamination from atmospheric CO_2. Therefore the data for this chamber were removed from further analysis.

Figure 5.11 illustrates respiration fluxes plotted versus water table depth relative to the

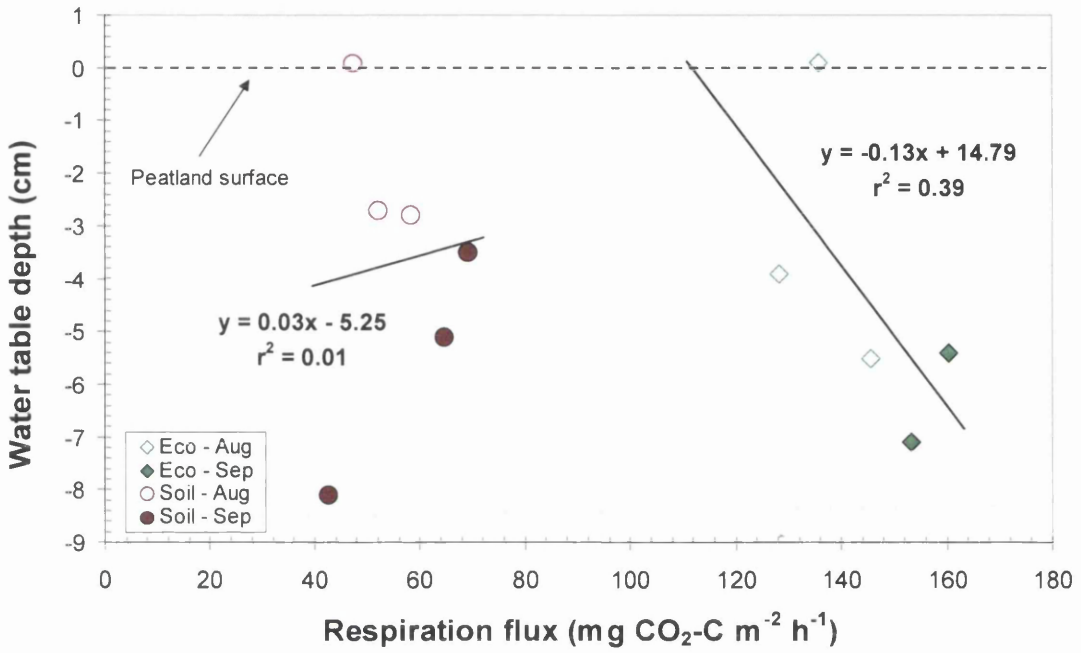

Figure 5.11 – Fluxes produced in the 'ecosystem' and 'soil' plots during August and September 2005, plotted versus water table depth. Eco = 'ecosystem' treatment.

peatland surface. The r^2 value for fluxes produced by the soil treatment is not significant ($P < 0.95$). Similarly for the ecosystem plots the r^2 value is not significant statistically ($P < 0.95$).

5.3.5 ^{14}C and $\delta^{13}C$ values of respired CO_2

Results for respired CO_2 from the treatment plots in August and September are given in Table 5.5. In addition, the results for ^{14}C and $\delta^{13}C$ were averaged and results plotted in Figures 5.12 and 5.13 respectively. The mean ^{14}C content of the contemporary atmosphere for August and September of 2005 was 106.5 %Modern and is given as a reference in Figure 5.12 (dashed line). 'Ecosystem' respired CO_2 was very slightly enriched relative to the atmosphere and ranged between 106.95 and 106.99 %Modern but was not significantly different at $> 1\ \sigma_e$.

'Soil' respired CO_2 was significantly enriched at $> 2\ \sigma_e$ relative to both the contemporary atmosphere and 'ecosystem' respiration (for both months) and ranged from 114.9 ± 0.18

Publication code (SUERC-)	Sample Identifier	^{14}C Enrichment (%Modern ± 1 σ)	$\delta^{13}C$ (‰) ± 0.1
8109	Eco 1 - August	107.07 ± 0.33	-22.5
8110	Eco 2 - August	107.29 ± 0.34	-20.3
8111	Eco 3 - August	106.49 ± 0.31	-19.7
8112	Soil 1 - August	114.59 ± 0.38	-27.1
8113	Soil 2 - August	115.09 ± 0.35	-27.8
8114	Soil 3 - August	115.14 ± 0.35	-27.4
8116	Eco 1 - September	106.44 ± 0.33	-23.6
8119	Eco 2 - September	106.62 ± 0.33	-22.8
8120	Eco 3 - September	107.92 ± 0.34	-15.0
8121	Soil 1 - September	115.94 ± 0.39	-26.8
8122	Soil 2 - September	115.87 ± 0.39	-28.0
8123	Soil 3 - September	116.25 ± 0.39	-27.1

Table 5.5 – ^{14}C and $\delta^{13}C$ for respired CO_2 from treatment plots in August and September 2005. 1 σ = 1 standard deviation. Eco = 'ecosystem' treatment.

%Modern in August to 116.0 ± 0.12 %Modern in September. In addition, soil respired CO_2 was significantly enriched in radiocarbon (> 2 σ) in September relative to the ^{14}C content of respired CO_2 produced in August.

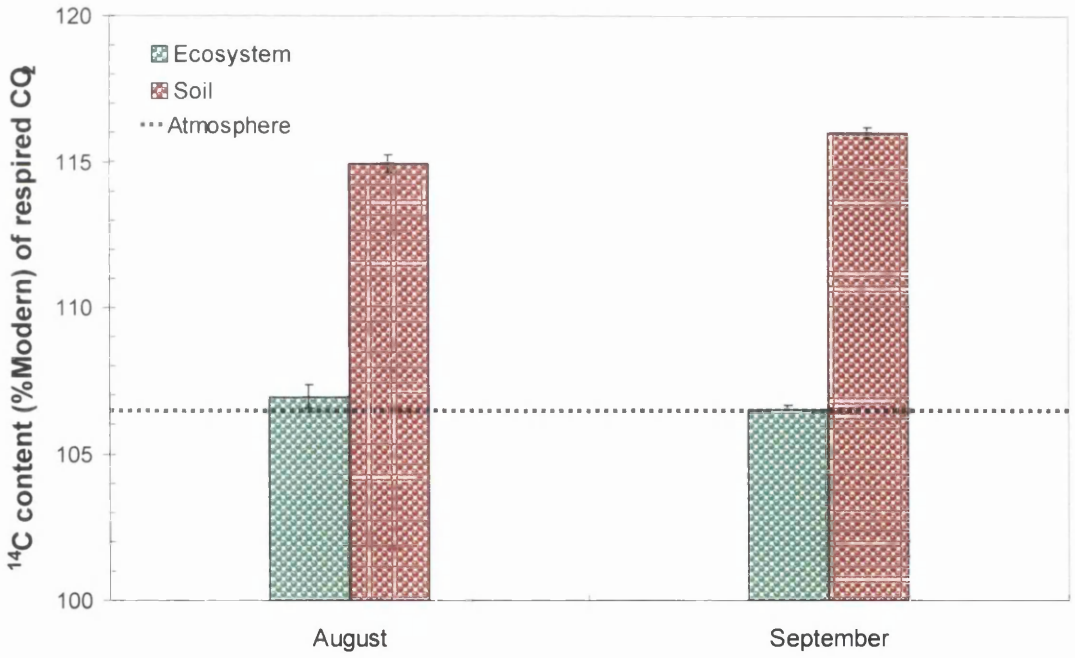

Figure 5.12 – ^{14}C concentration of respired CO_2 from the two treatment plots in August and September 2005. n = 3, except for the 'ecosystem' treatment in September where n = 2. Error bars are ± 1 σ_e. Mean water table depth for the 'ecosystem' plots in August was -3.1 cm, in September -6.4 cm and for the 'soil' plots in August -1.8 cm and in September -5.6 cm.

Figure 5.13 illustrates the $\delta^{13}C$ values of respired CO_2 for both treatments in August and September. The $\delta^{13}C$ of 'soil' respired CO_2 was depleted in ^{13}C relative to the 'ecosystem' treatment and ranged from -27.3 ± 0.6 ‰ in September to -27.4 ± 0.4 ‰ in August, both being statistically identical at 1 σ. 'Ecosystem' respired CO_2 was significantly more enriched in ^{13}C than 'soil' respired CO_2 at 2 σ, ranging from -20.8 ± 1.5 in August to

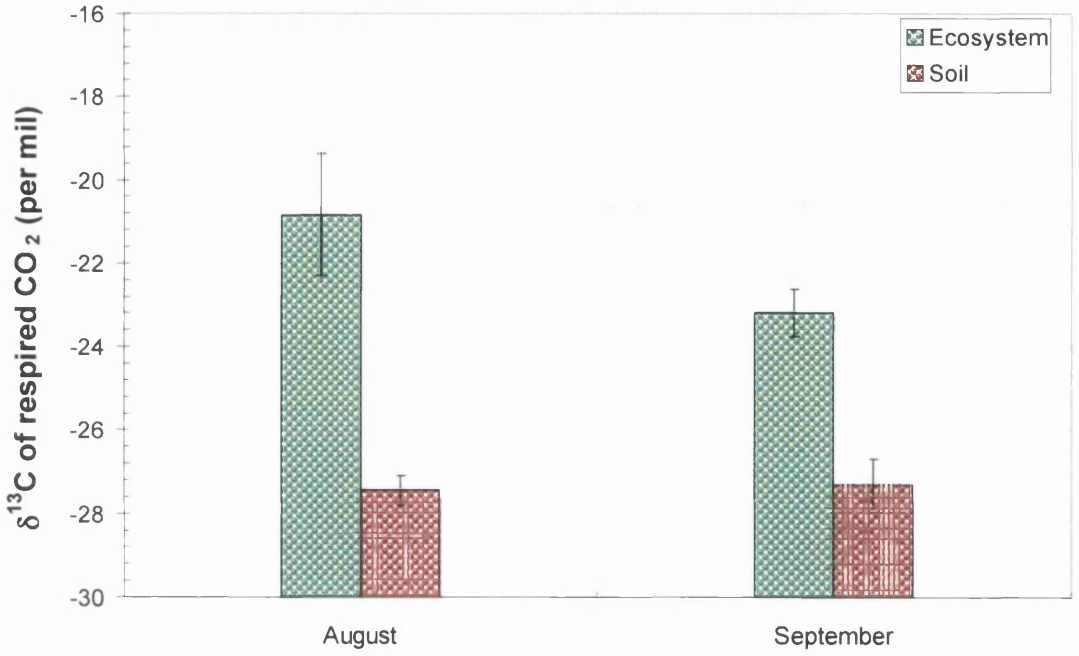

Figure 5.13 - $\delta^{13}C$ of respired CO_2 from the two treatment plots in August and September 2005. n = 3, except for the 'ecosystem' treatment in September where n = 2. Error bars are ± 1 σ_e. Mean water table depth for 'ecosystem' plots in August was -3.1 cm, in September -6.4 cm and for the 'soil' plots in August -1.8 cm and in September -5.6 cm.

-23.2 ± 0.6 ‰ in September. To ascertain whether water table height had a significant influence on the radiocarbon signature of respired CO_2, the water table height within each treatment plot was plotted versus the ^{14}C signature of the respired CO_2 from the same plot and is illustrated in Figure 5.14. The r^2 values derived from linear regression of the data for

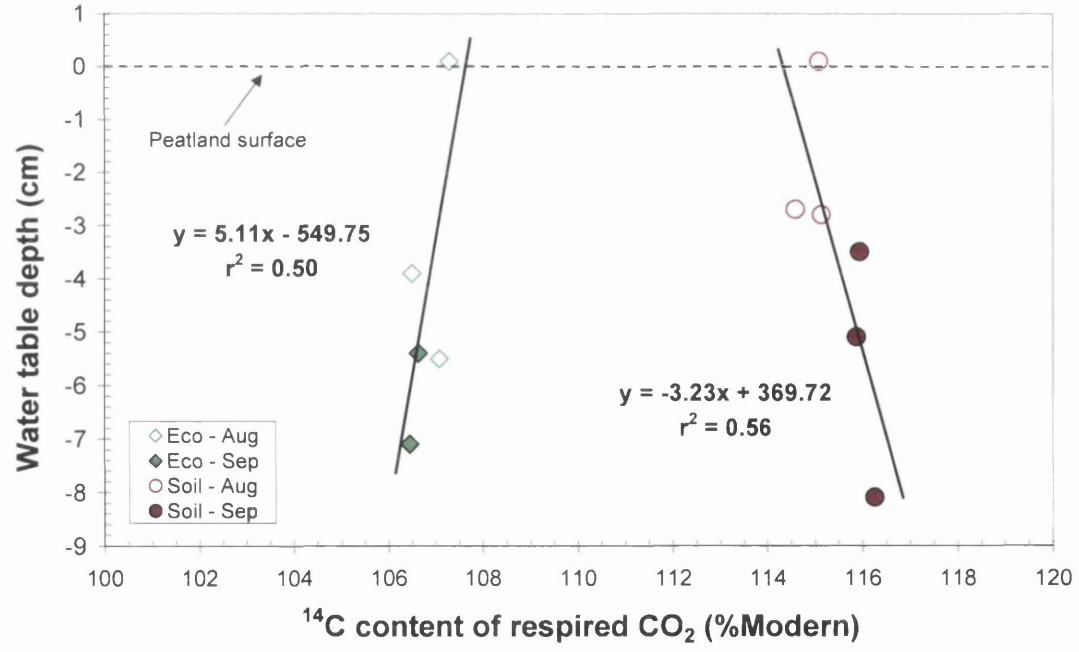

Figure 5.14 – The ^{14}C signature of respired CO_2 produced from both treatments plotted versus water table height relative to the peatland surface. Eco = 'ecosystem' treatment. Soil = 'soil' treatment.

both the 'soil' and the 'ecosystem' treatment are not statistically significant ($P < 0.95$), and therefore there is no significant effect of water table depth on the radiocarbon signature of respired CO_2 from either treatment.

5.4 Discussion

The aim of this study was to investigate the isotopic signature, both $\delta^{13}C$ and ^{14}C, of respired CO_2 from a peatland ecosystem and further to quantify the contribution of individual component sources i.e. soil and plant respiration to total ecosystem respiration. In addition, potential sources of respired CO_2 (e.g. bulk peat, DOC, atmospheric CO_2 and ecosystem vegetation) were characterised as to their $\delta^{13}C$ and ^{14}C content.

5.4.1 Isotopic signature of peatland vegetation

The ^{14}C signature of peatland vegetation was measured in order to firstly verify that vegetation was representative of contemporary atmospheric CO_2 and further, to determine the ^{14}C signature of inputs to the peatland carbon pool during the year of sampling. Several studies have suggested that peatland vegetation such as *Sphagnum* recycles soil-respired CO_2 based on stable (Price *et al.*, 1997; Proctor *et al.*, 1992) and radiocarbon analyses (Jungner *et al.*, 1995; Turetsky & Wieder, 1999). In addition, in an Amazonian forest ecosystem, recycling of soil-respired carbon was found to be significant (Martinelli *et al.*, 1991). Furthermore, it has been demonstrated that methane produced by peat bogs has been recycled by *Sphagnum* after oxidation to CO_2. In a study using stable carbon isotopes, labelled methane was oxidised to CO_2 (by methanotrophic bacteria) and subsequently found to contribute 10-15 % of the total *Sphagnum* carbon source (Raghoebarsing *et al.*, 2005). At the Hard Hill site it was considered that of all the vegetation species present, moss was the most likely plant functional group to recycle CO_2 because of its situation within the vegetation canopy (less turbulence will occur due to shelter from other accompanying peatland vegetation species).

The radiocarbon content of all peatland vegetation sampled in September 2005 was statistically the same (at $< 2\ \sigma$) as the contemporary atmosphere in which they were growing. Of the four vegetation samples collected the bryophyte species *Hypnum jutlandicum* was the most enriched in ^{14}C but was not significantly different to the other plant species analysed. The mean ^{14}C value for the 4 vegetation samples was 106.71 ± 0.30 %Modern, statistically identical to the mean atmospheric ^{14}C content (106.49 ± 0.32

%Modern) measured in August and September of the same year (using MS^3). This is compared to an extrapolated atmospheric value at Schauinsland (Levin & Kromer, 2004) of 105.8 ± 0.4 %Modern (calculated from a starting value of 106.6 %Modern recorded at Schauinsland in the summer of 2003, with an estimated yearly reduction in atmospheric ^{14}C content of 0.4 %Modern (Levin & Hesshaimer, 2000) due to the addition of fossil fuel CO_2 and uptake by the various reservoirs of the carbon cycle). Although the atmospheric ^{14}C concentration is slightly enriched at Hard Hill, it is statistically identical to the extrapolated value for Schauinsland in the summer of 2005.

Nilsson *et al.* (2001) obtained similar results to those reported here, in a study of the ^{14}C content of *Sphagnum* spp., finding no significant differences in the ^{14}C content of three different *Sphagnum* species that colonised carpets, lawns and hummocks. In addition, Nilsson *et al.* (2001) also found no significant differences between the ^{14}C content of the contemporary atmosphere and sampled *Sphagnum* spp. However these results are in contrast to a study of a Finnish bog where Tolonen *et al.* (1993) found that *Sphagnum* re-fixed approximately 20 % of CO_2 released from deep peat.

In the present study there were significant differences in the $\delta^{13}C$ of vegetation, both relative to the atmosphere and between plant functional types. The bryophytes and the vascular plant *Calluna vulgaris* were both statistically depleted in ^{13}C by -18.8 and -21.6 ‰ respectively, relative to the contemporary atmosphere (-8.9 ‰). These values are typical of the isotopic fractionation of CO_2 that occurs during photosynthesis by C_3 plants (Boutton, 1991a). The stable isotopic signature of *Sphagnum* sampled in September was 1.5 ‰ more depleted in ^{13}C than the *Sphagnum* sampled in May (see Chapter 3) and was significantly different at greater than 2 σ.

Conversely, the $\delta^{13}C$ values for *Calluna vulgaris* in September were very slightly enriched in ^{13}C (0.5 ‰) relative to the *Calluna* collected in May but not significantly so. In addition, the bryophytes *Hypnum jutlandicum* and *Sphagnum capillifolium* collected in September were significantly depleted in ^{13}C relative to the shoots and flowers of *Calluna vulgaris* by ~ 3 ‰. The difference in $\delta^{13}C$ values are likely due to differences in photosynthetic pathways between the vascular and non-vascular plant species (see section 3.4.2 for more detail) that cause different diffusion resistances to CO_2 (Menot & Burns, 2001).

5.4.2 Isotopic signature ($\delta^{13}C$ and ^{14}C) of bulk peat

A study of the variation (both spatial and temporal) in the $\delta^{13}C$ values and ^{14}C content of bulk peat was made by removing peat cores from both the 'ecosystem' and 'soil' treatment plots and was performed with the additional aim of understanding how important bulk peat was as a source of respired CO_2 from both the 'soil' and 'ecosystem' treatments. Furthermore, an assessment of recent carbon accumulation rates could be made (although vertical resolution was compromised in order to ascertain the extent of the spatial variation of carbon isotopes at the experimental site).

$\delta^{13}C$ values for bulk peat under the two different treatments increased with depth. The maximum enrichment found to occur from the surface 4 cm to the bottom 12-16 cm depth increment was 2.1 and 2.4 ‰ under the 'soil' and 'ecosystem' treatments respectively. Enrichment of soil organic matter in ^{13}C with increasing depth from the surface of a soil is a common phenomenon and is usually attributed to two processes. Firstly, in the last 200 years the $\delta^{13}C$ of atmospheric CO_2 has decreased from -6.5 ‰ (Leuenberger *et al.*, 1992) to ~ -8.5 ‰ (Hemming *et al.*, 2005) due to the input of anthropogenic CO_2 with low $\delta^{13}C$ values (~ -27 ‰). As soil organic matter is formed directly from plant input and the $\delta^{13}C$ of plant tissue is strongly influenced by the $\delta^{13}C$ value of atmospheric CO_2 (Farquhar *et al.*, 1982), a decrease in the $\delta^{13}C$ value of plant material and therefore soil organic matter would be expected over the last 200 years.

Secondly, studies have shown that decomposer organisms such as microbes, fungi (Gleixner *et al.*, 1993) and invertebrates (De Niro & Epstein, 1978) fractionate carbon isotopes in soil, during decomposition. For example, De Niro and Epstein (1978) found that whole body tissue of earthworms fed an isotopically controlled diet were enriched in ^{13}C by ~ 1 ‰. Both the aforementioned studies did not measure the $\delta^{13}C$ of respired CO_2 from decomposer organisms directly, but it was hypothesised that it would have been more depleted in ^{13}C than the carbon substrate it was evolved from. However, direct evidence for fractionation during decomposition was provided by Nakamura *et al.* (1990) who found that respired CO_2 produced during microbial decomposition was between 0.9 and 1.8 ‰ more depleted relative to the soil. In this way, the potential for residual soil organic carbon to become enriched in ^{13}C over time, clearly exists (Boutton, 1996).

In addition to an investigation into the $\delta^{13}C$ variation of bulk peat, an assessment of spatial variation of the ^{14}C content in the top 16 cm of the peat profile was performed. The ^{14}C

variation between cores can be explained, in part, by differences in peat accumulation rates over the period of the radiocarbon bomb spike. In addition, variation in the ^{14}C content between depth increments can be attributed to rapid changes in atmospheric ^{14}C content over the 50-year period of the bomb spike. For example, least variation in ^{14}C content between cores was observed in the surface (0-4 cm) layer of peat (Figure 5.7, LHS). The surface 4 cm represents the most recent carbon accumulation, with vegetation assimilating carbon when atmospheric radiocarbon levels were decreasing relatively slowly, i.e. over the last ~10-20 years (Levin & Kromer, 2004).

Similarly, within most of the 12-16 cm layer samples, pre-bomb ^{14}C concentrations were measured, and although these 4 cm slices of peat could have been accumulating for a considerable time (i.e. several decades), the variation in ^{14}C content between sites was small due to relatively slow variations in the ^{14}C content of the atmosphere during the pre-bomb period. However, samples from the 4-8 cm and 8-12 cm layers, mainly cover the period when atmospheric bomb ^{14}C levels were highest and undergoing the most rapid changes. Thus, the variation in the 4-8 and 8-12 cm layers between cores is likely to be partly due to the layers being comprised of slightly differing contributions of pre-bomb and bomb-peak carbon as a result of different peat accumulation rates.

Peat accumulation rates are clearly an important factor contributing to the differences in the ^{14}C profiles. In particular, core 'ecosystem' 3 was distinct from the other profiles in that bomb ^{14}C was evident even in the deepest (12-16 cm) layer. There are a number of possible explanations for this observation, such as a higher rate of peat accumulation (i.e. height increase) at this location. Alternatively, if plot 'ecosystem' 3 had undergone less compaction compared to the other coring locations, then one might expect a deeper penetration of bomb carbon with depth. As the Hard Hill site has been subject to light grazing the possibility arises that varying degrees of compaction may have occurred resulting in the different pattern in ^{14}C content found in core 'ecosystem' 3.

Peat bulk density values for 'ecosystem' 3 were consistently lower at most depths relative to the other sampling locations (Table 5.2), suggesting that variation in density may be part of the explanation. This is illustrated in Figure 5.15 where the ^{14}C content of each profile is plotted against cumulative carbon (from the surface); this plot removes variations caused by differences in bulk density and shows that, in terms of carbon accumulation, the ^{14}C profile of 'ecosystem' 3 is more similar to the other profiles.

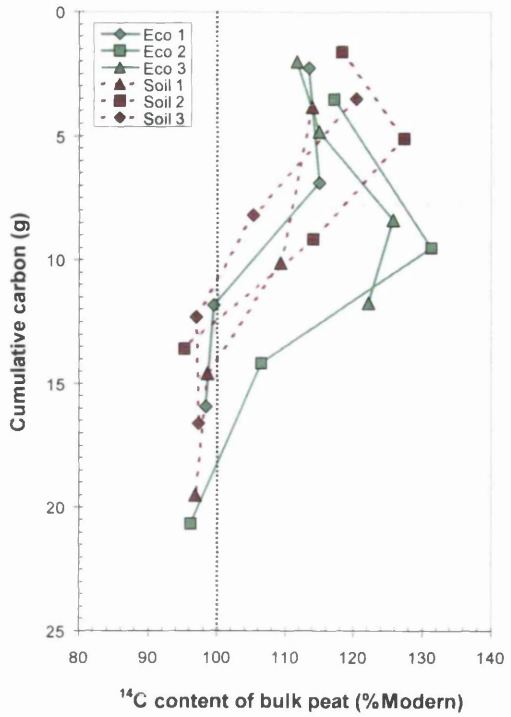

Figure 5.15 - Profiles of cumulative carbon versus depth of treatment cores removed from the Hard Hill study site. Eco = plots where peatland vegetation was left intact. Soil = plots where the peatland vegetation was removed.

The presence of bomb radiocarbon in each of the six profiles is evidence that peat accumulation has at least been occurring in the surface layer of this blanket bog over the last 50 years. By using the layer containing the depth where ^{14}C concentrations first exceed 100 %Modern as a chronological reference point common to all plots, recent carbon accumulation was estimated for each of the locations where treatment cores were removed. The use of this reference layer has limitations; for example, the samples were not subjected to chemical pretreatment because, from a carbon cycling point of view, it was necessary to determine the ^{14}C content all carbon fractions that contribute to respiration within each treatment plot. However, certain components in peat are known to be mobile e.g. fulvic acids (Shore *et al.*, 1995) and evidence for transport of modern carbon to depth by *Eriophorum vaginatum* (Kilian *et al.*, 2000) and root channels (Barber *et al.*, 2000) has been demonstrated.

Therefore the assertion that the 100 %Modern layer represents ~AD 1955 should be treated with some caution. Despite this, the main aim was to use the 100 %Modern reference layer to compare across the six treatment plots, and therefore, since vegetation cover was relatively homogeneous, it could be assumed that all cores would have been similarly affected by any migration of peat components or the introduction of modern carbon to depth.

No clear differences or patterns were found in the profiles of radiocarbon content or carbon accumulation under the two treatments ('ecosystem and 'soil'). However, it is notable that the two highest carbon accumulation rates (Table 5.3) were found to have taken place in cores under the 'ecosystem' treatment. Since fastest decay occurs in the first few years following senescence (Clymo *et al.*, 1998), it is possible that the higher carbon accumulation rates in the 'ecosystem' plots reflects the continued input of new organic matter from plants over the last two years; due to vegetation removal, no new plant inputs entered the 'soil' plots over this period.

Our assessment of peat and carbon accumulation rates was hindered by the very coarse resolution of our sampling interval (i.e. 4 cm depth increments). Thus only maximum and minimum estimates for these rates are reported, which in some cases, cover a large range (Table 5.3). However, the approach adopted offered a useful means for the broad assessment of variation in peat accumulation and carbon accumulation across this small area of blanket bog at the Hard Hill site. It should be noted however, that estimates for peat accumulation and carbon accumulation rate only cover peat formed over the last ~50 years and therefore, since much of the peat is still within the acrotelm and decaying relatively rapidly under aerobic conditions, our values are on average higher than estimates for long-term deep peat accumulation reported elsewhere (Borren *et al.*, 2004; Turunen *et al.*, 2002).

5.4.3 Isotopic signature of DOC

Dissolved organic carbon was extracted from one of the 16 cm cores under each of the two experimental treatments to investigate the contribution (if any) to respired CO_2. DOC has been demonstrated in a number of studies to be a significant source of labile carbon for substrate utilisation during microbial gas production (Charman *et al.*, 1994). In addition, the origin of DOC was to be investigated and from that an attempt was made to deduce whether there was any significant movement of DOC within the peat profile at the Hard Hill experimental site.

$\delta^{13}C$ analysis of DOC (Table 5.4; Figure 5.9) revealed that DOC became progressively enriched in ^{13}C under both treatments for all depths except one (the $\delta^{13}C$ value of DOC from the 'ecosystem' treatment remained the same at 8-12 cm as in the increment directly above (-27.1 ‰)). One possible explanation for this could be the introduction of recently fixed carbon, e.g. root exudates, to depth within the 8-12 cm increment. For example, in bogs, the rooting depth of *Calluna vulgaris* is confined to shallow depths above the water

table, the average rooting depth being ~ 10 cm (Gimingham, 1960), although roots have been known to reach 18 cm (Boggie *et al.*, 1958).

Penetration of roots to depth could account for the fact that the 8-12 cm depth increment retains the same $\delta^{13}C$ value as the 4-8 cm increment above. Furthermore, vegetation is known to allocate substantially more recently fixed carbon to above ground biomass at the start of the growing season and progressively more below ground towards the end of the season (Wallén, 1983). No significant differences in $\delta^{13}C$ values were found between the two treatments within the top 8 cm of the profile. However, at 8-12 and 12-16 cm the 'soil' treatment was significantly more enriched at > 2 σ than the 'ecosystem' treatment. Again, one reason for this could be due to allocation of recently fixed carbon (and hence more depleted in ^{13}C) below ground in the 'ecosystem' treatment. Olrud and Christensen (2004) demonstrated that at the beginning of the growing season in a subarctic mire, the majority of carbon assimilated was allocated above ground. However, the reverse was found to be the case in August and September and it was suggested that this could be interpreted as increased root exudation.

Figure 5.16 illustrates the $\delta^{13}C$ of DOC from the two treatments relative to the surrounding

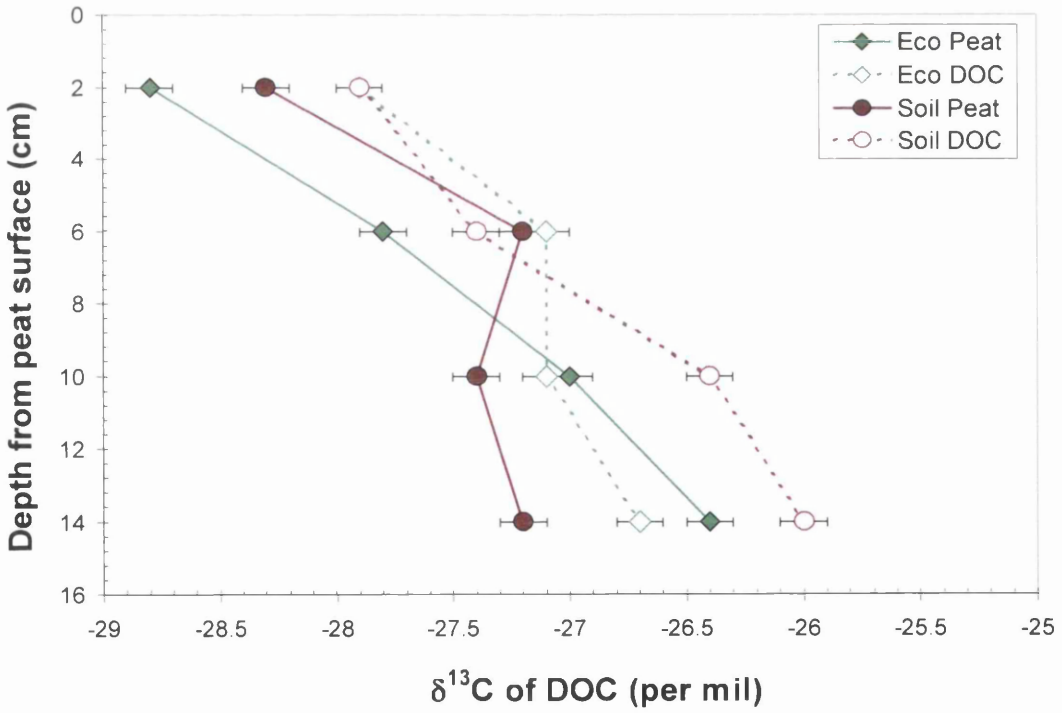

Figure 5.16 - $\delta^{13}C$ values for DOC and bulk peat from which it was extracted. n = 1 for each data point. Error bars are ± 1 σ (standard deviation - analytical error).

bulk peat from which it was extracted. Significant differences in $\delta^{13}C$ were apparent when comparing the bulk peat and the DOC for each treatment but not throughout the entire profile. For example, within the top 8 cm of the profile, 'ecosystem' DOC was significantly enriched in ^{13}C relative to the bulk peat from which it was extracted. However this was not true for the bottom 8 cm of the 'ecosystem' profile, where both DOC and bulk peat had the same $\delta^{13}C$ value within 1 σ. Conversely, DOC extracted from the top 8 cm of the 'soil' treatment had statistically the same $\delta^{13}C$ values as the bulk peat. However, DOC from the bottom 8 cm of the 'soil' treatment was significantly more enriched in ^{13}C than the bulk peat at 2 σ.

Figure 5.17 illustrates the ^{14}C content of DOC and the surrounding bulk peat from which it

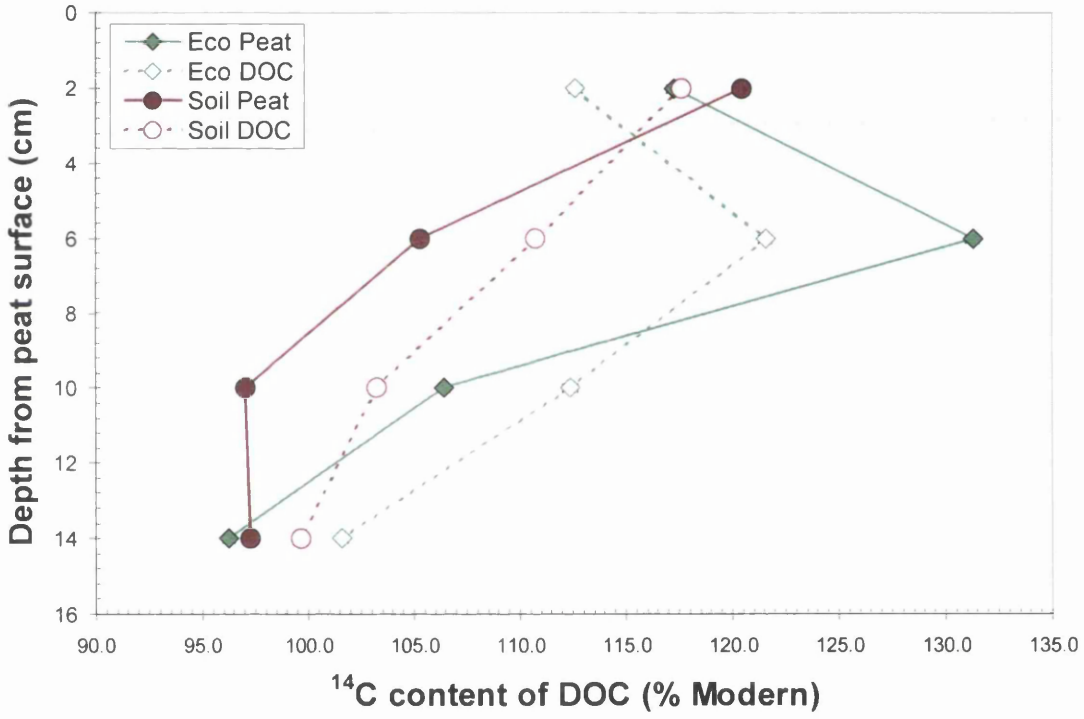

Figure 5.17 - ^{14}C of DOC and the bulk peat from which it was extracted. n = 1 for each data point. Error bars are ± 1 σ (standard deviation - analytical error).

was extracted. DOC is significantly depleted in ^{14}C at > 2 σ relative to the surrounding peat for the surface 8 cm under the 'ecosystem' treatment and the reverse is true for the bottom 8 cm. The radiocarbon content of DOC for the 'ecosystem' treatment was significantly enriched at > 2 σ relative to the 'soil' treatment for all depths with the exception of the surface 4 cm where DOC for the 'soil' treatment was significantly enriched relative to DOC from the 'ecosystem' treatment.

The surface 4 cm of the 'ecosystem' treatment could be more depleted in radiocarbon relative to the 'soil' treatment due to the fact that this treatment had had 2 years worth of litter added to it whereas the 'soil' treatment had not. However, this was inevitable as the collars for treatment chambers were inserted well in advance in order to minimise disturbance effects. In addition, the time between setting up the treatment plots and sampling, allowed for plant roots and other faster cycling carbon pools produced by plants, to decompose within the 'soil' plots. Litter recently added to the 'ecosystem' plots would be depleted in ^{14}C relative to the surface of the 'soil' treatment plot due to the fact that the litter would have been growing in an atmosphere more depleted in radiocarbon. In addition, fresh litter is rapidly decomposed by the soil microbiota, thus leading to the production of DOC more depleted in ^{14}C. Under the 'soil' treatment DOC is significantly enriched (at > 2 σ) in ^{14}C in all but the top 4 cm. Thus, no clear pattern in the ^{14}C content of DOC with depth emerges.

Figure 5.18 shows the relationship between the ^{14}C content of the eight 4 cm increments of

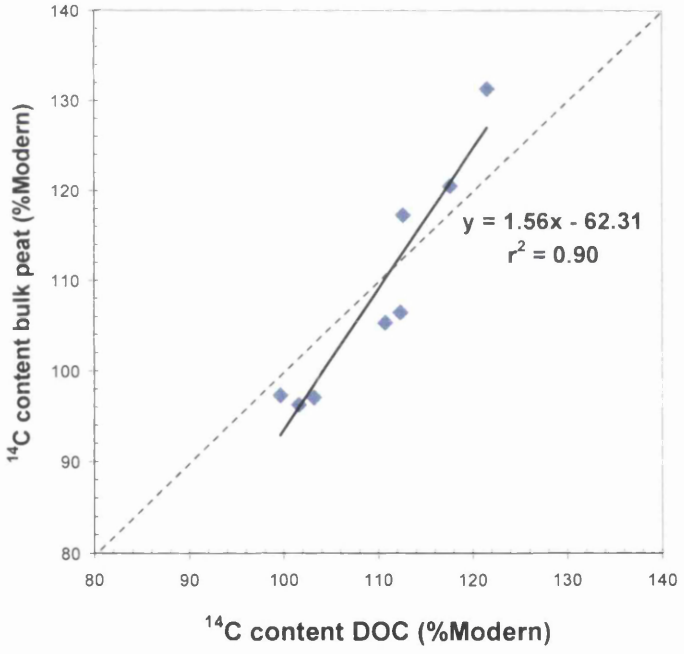

Figure 5.18 – shows the relationship between the ^{14}C content of eight 4 cm increments of bulk peat and the ^{14}C content of DOC extracted from the same increments of peat.

bulk peat plotted against the ^{14}C content of the DOC extracted from the same depth increments. The plot shows that there is a strong correlation between both the ^{14}C content of the bulk peat and the ^{14}C content of the DOC, which is highly significant ($P < 0.01$). This indicates that the bulk peat in each layer contributes a significant amount of ^{14}C to the DOC within the same layer. However, not all the ^{14}C in the DOC is likely to be derived entirely from the bulk peat, as the relationship is not 1:1.

5.4.3.1 Conceptual modelling of the ^{14}C content of DOC

A number of possibilities exist as to the source of ^{14}C present in the DOC extracted from each of the 4 cm increments of bulk peat. Four conceptual models are presented here as to possible processes/mechanisms of DOC production that could explain the ^{14}C concentration of DOC extracted from each depth increment of peat. Every 4 cm increment of peat illustrated in each of the models that is marked with an asterisk (*) indicates a layer in which the proposed model or mechanism of DOC formation is not feasible.

The first mechanism, mentioned in the last section, is that DOC is produced entirely *in situ*. Figure 5.19 illustrates a model of *in situ* production of DOC for both experimental

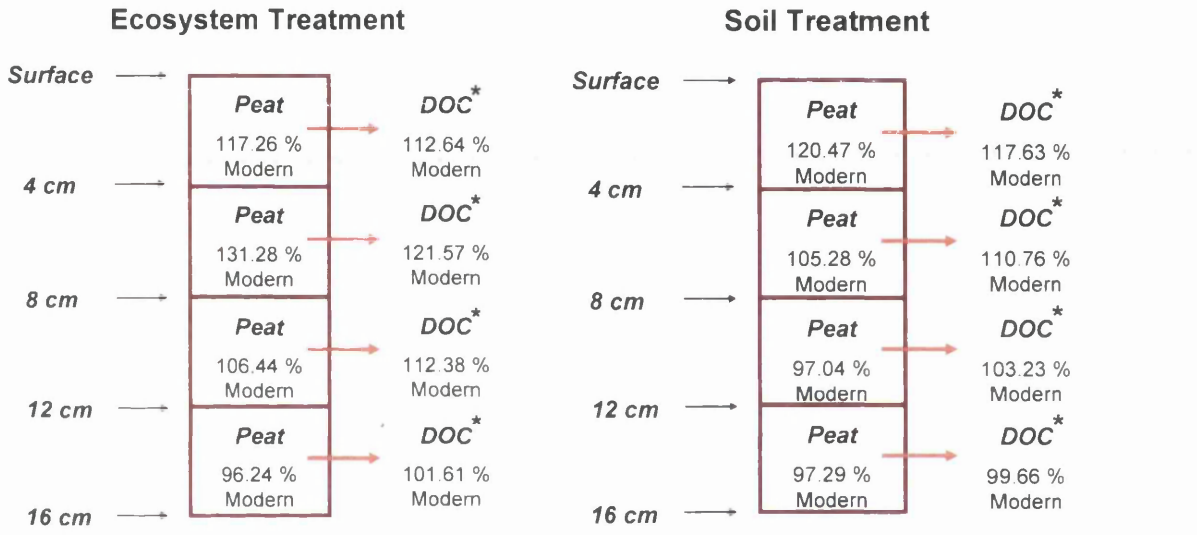

Figure 5.19 – Schematic illustration of the ^{14}C content of bulk peat and extracted DOC at each 4 cm depth in the profile for each of the two experimental treatments. The model illustrates the possibility the DOC being produced entirely *in situ*.

treatments. If all the ^{14}C present in the DOC was produced *in situ* then the ^{14}C concentration of DOC throughout the profile should reflect the ^{14}C concentration of the bulk peat. However, the ^{14}C concentration of DOC extracted from the surface 16 cm of peat is either depleted or enriched in radiocarbon (by $>$ or $<$ 2 σ), relative to the surrounding bulk peat, for both treatments. This model confirms what is deduced from the plot in Figure 5.18, further demonstrating that the relationship between the ^{14}C content of DOC and the ^{14}C content of the surrounding bulk peat is not 1:1.

The previous model assumes that an equal amount of DOC is produced throughout the depth of the entire 4 cm increment. In fact it is quite likely that there is proportionately more DOC produced from the top 1-2 cm of each increment, as this is where decomposition has occurred for the least amount of time. Hence, it is also likely that there

will be a greater proportion of DOC produced from the top part of each depth increment of bulk peat, than from the bottom. This mechanism is illustrated for both experimental treatments in Figure 5.20. The larger arrows represent the fact that proportionately, most of

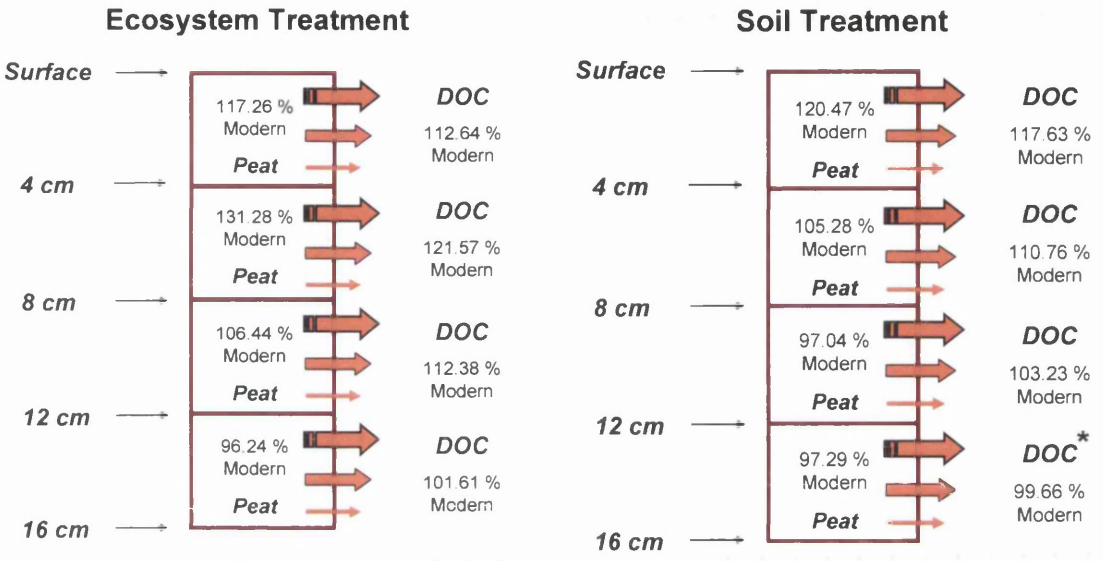

Figure 5.20 - Schematic illustration of the ^{14}C content of bulk peat and extracted DOC at each 4 cm depth in the profile for each of the two experimental treatments. The model illustrates *in situ* production of DOC and in addition, that proportionally more of the *in situ* DOC produced, comes from the top of each 4 cm depth increment.

the DOC produced within each depth increment is being released from the top of the increment, which has had less time to decompose and hence will contribute more DOC to the overall amount of DOC being released from each depth.

Application of this model to the 'ecosystem' treatment in Figure 5.20, demonstrates that the model fits the observations at all depths. The top of the 0-4 cm increment will have a ^{14}C concentration that is more depleted than the mean ^{14}C content of the bulk peat due to incorporation of recent plant litter (and hence more depleted in ^{14}C). The ^{14}C content of the DOC reflects this. Moving down to the 4-8 cm increment, we do not know for sure whether the top of this 4 cm increment is pre or post bomb peak (1963), therefore the top of this layer could be less enriched than the mean bulk peat value (131.28 %Modern). The DOC ^{14}C concentration in this instance again reflects this scenario.

The ^{14}C concentration of the DOC produced within the bottom 8 cm of the profile is more enriched than the mean ^{14}C concentration of the bulk peat. This could reflect the fact that at around 8 cm we are now at a depth in the profile where the peat was formed before the maximum peak in bomb ^{14}C occurred and therefore the top of each 4 cm increment would be more enriched in ^{14}C than the mean bulk peat ^{14}C value. If more carbon is being decomposed and added to the DOC pool from the top part of each increment then the ^{14}C

in the DOC will be more enriched than the mean value for the bulk peat, which is what we observe.

If we apply the model featured in Figure 5.20 to the DOC extracted from the 'soil' profile we see that for the top 12 cm, the conceptual model works. The ^{14}C content of the DOC from the 0-4 cm increment reflects the fact that the top of this increment will be more depleted in ^{14}C due to the addition of litter that is depleted in ^{14}C. DOC from the 4-8 and 8-12 cm increments is more enriched than the bulk peat. This reflects the fact that the top of each increment will be more enriched in ^{14}C than the mean ^{14}C value for the bulk peat. However, moving down to the 12-16 cm depth increment, we find that the ^{14}C content of the DOC is more enriched than the ^{14}C content of the bulk peat in the layer above. The ^{14}C content present in the DOC could not have arisen from the bulk peat, no matter what proportion of the DOC is produced in the top part of this depth increment. Therefore this model does not adequately describe the ^{14}C content of DOC throughout the entire 16 cm profile.

An alternative mechanism to DOC being produced entirely *in situ*, is to postulate that there is a certain contribution from another source of carbon in addition to that produced by the surrounding peat. Plant litter on the surface of each peat profile could contribute a significant amount of carbon to the DOC pool at each depth, as this source contains one of the most labile carbon inputs to the profile. Furthermore, plant root exudates will also contribute a labile and easily decomposed source of carbon to depth (Chimner & Cooper, 2003). In the third model presented (Figure 5.21), both litter and root exudate pools contribute modern carbon (derived from the contemporary atmosphere) to DOC throughout the entire profile of both treatments (illustrating relatively fast downward movement of DOC). Thus, the DOC extracted from each depth, would have a ^{14}C concentration that lies between the ^{14}C concentration of the bulk peat and the ^{14}C concentration of recent plant litter that had accumulated on the peat surface and/or recent carbon released as exudates in the rhizosphere of peatland vegetation.

The ^{14}C content of litter depicted in the 'soil' treatment (~ 107.5 %Modern) has a value approximately that of the atmosphere two years previous. This was calculated by adding 0.4 %Modern (Levin & Hesshaimer, 2000) per year, for each of the two years that litter had not been added to the top of the 'soil' profile, to the mean ^{14}C content of the atmosphere measured on August and September 2005. The concentration of ^{14}C in the DOC would therefore depend on how much each of both the bulk peat and plant litter would individually contribute to the DOC pool.

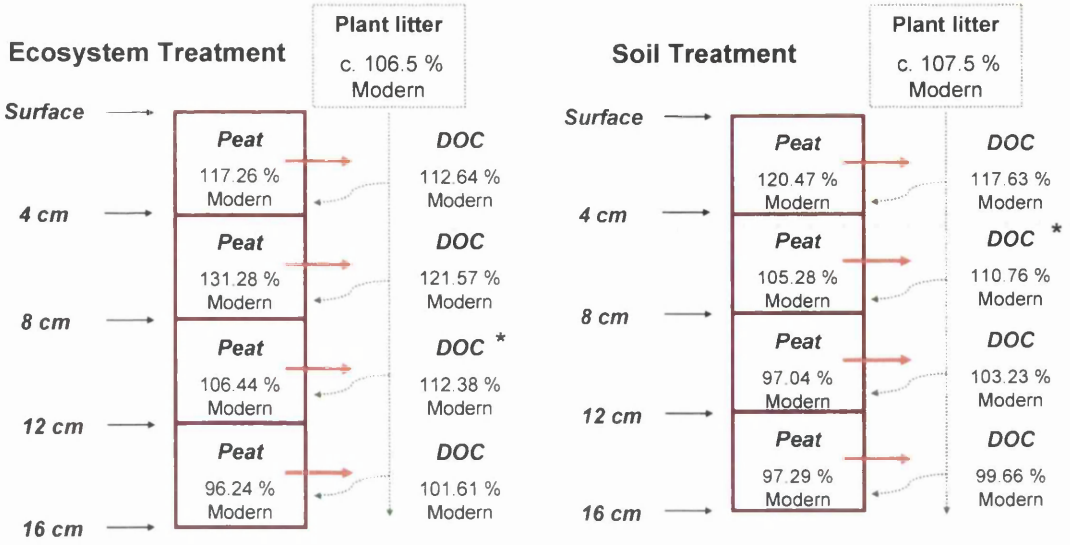

Figure 5.21 – Schematic illustration of the ^{14}C content of bulk peat and extracted DOC at each 4 cm depth in the profile for each of the two experimental treatments. The model illustrates the possibility of recent plant litter being a major source of carbon to the DOC throughout the profile.

If we look at the model featured in the left of Figure 5.21 that represents the 'ecosystem' treatment we see that for the top 8 cm of the profile, the DOC has a ^{14}C concentration that falls between the bulk peat and recent plant litter. However, at the 8-12 cm depth increment the measured DOC is enriched in radiocarbon relative to the surrounding bulk peat and to possible litter inputs, and so for this particular depth increment the model fails. If we apply the model to the profile of the 'soil' treatment then we can see that for the top 4 cm of the profile the ^{14}C concentration of the DOC has a value between the radiocarbon concentration of the bulk peat and the plant litter. However, at 4-8 cm, DOC is enriched relative to the bulk peat and possible litter contributions and therefore the model does not replicate the findings at this point.

A fourth mechanism that could explain the ^{14}C concentration of DOC extracted from the experimental peat cores, is downward transport of DOC within the profile. This model is illustrated in Figure 5.22, and postulates relatively slow downward movement of DOC, for both experimental treatments. The model demonstrates that for each depth in the profile there is a contribution from DOC present in the layer directly above in the profile, to the main DOC pool produced *in situ* from the surrounding peat. For the surface 4 cm, this would mean contributions to the DOC pool from accumulated plant litter, which is assumed to have the same ^{14}C concentration as the litter itself. Therefore, this model should show that the ^{14}C concentration of DOC within each 4 cm increment of the profile has a value that lies between the ^{14}C concentration of the bulk peat (from which the majority of the DOC is produced) and the ^{14}C concentration of the DOC in the layer of peat directly above.

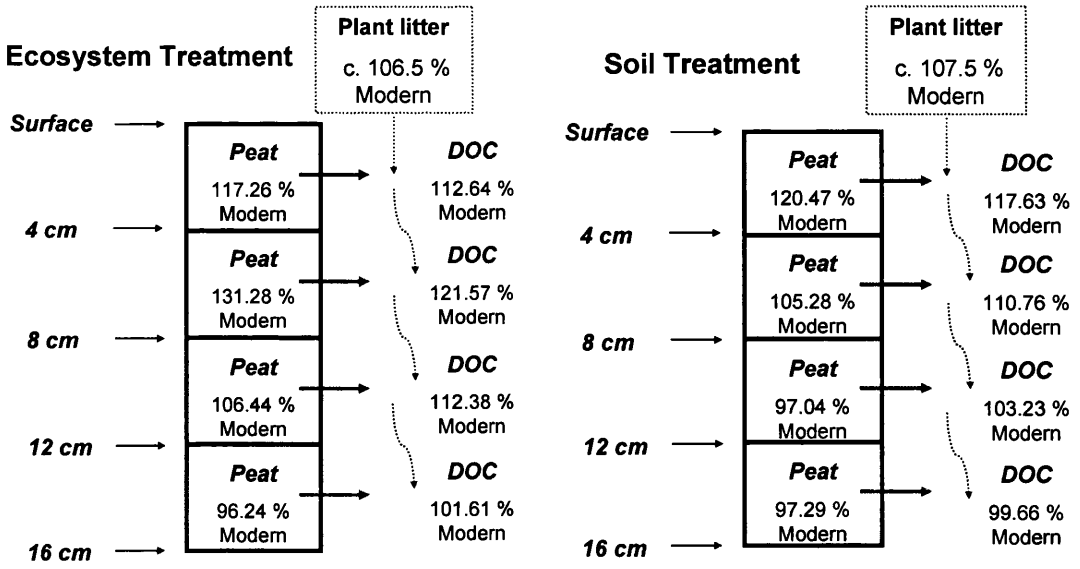

Figure 5.22 - Schematic illustration of the ^{14}C content of bulk peat and extracted DOC at each 4 cm depth in the profile for each of the two experimental treatments. The model illustrates the slow downward movement of DOC throughout the profile.

The model in Figure 5.22, demonstrates that relatively slow downward movement of DOC could explain the ^{14}C concentration of DOC extracted from the surrounding bulk peat at all depths. DOC from each 4 cm increment in the profile, under both treatments, retains a ^{14}C signature that lies between the radiocarbon concentration of the bulk peat from which it was extracted and the ^{14}C concentration of DOC produced in the layer directly above it in the profile. Downward transport of DOC has been postulated in a number of studies investigating the age of DOC in deep peat (Aravena *et al.*, 1993; Charman *et al.*, 1999; Chasar *et al.*, 2000). These models provide a useful means by which to envisage the major processes at work within the peat profile; however, other processes may be taking place, but are not distinguishable.

It should also be mentioned that another mechanism of DOC transport that can take place is a reversal of the hydrostatic head, which would result in transport of DOC upwards within the peat profile. If this transport mechanism were to have taken place within the profile, then we would expect DOC extracted from the 12-16 cm increments of both experimental treatments to be older, and hence have less radiocarbon, than the surrounding bulk peat. However, we see from Figure 5.22 that the ^{14}C content of the DOC for both treatments is actually enriched relative to the surrounding peat. Therefore although this mechanism might have occurred, the predominant direction of movement appears to be downward.

5.4.4 Flux of respired CO_2 from treatment plots

Respired CO_2 was captured using the static flux chamber method (Heikkinen *et al.*, 2002; Nykänen *et al.*, 2003). Fluxes of CO_2 were significantly higher under the 'ecosystem' treatment relative to the 'soil' treatment in both August and September. The largest mean flux measured was ~157 mg C m^{-2} h^{-1} (3.8 g C m^{-2} d^{-1}) in September. A similar but smaller value (119 mg C m^{-2} h^{-1}) was measured from incubated peat monoliths dominated by *Eriophorum vaginatum* removed from a Swedish peatland (Strom *et al.*, 2005). Fluxes measured emanating from a Finnish ombrotrophic low sedge bog (Silvola *et al.*, 1996) were slightly higher (178 mg C m^{-2} h^{-1}) than those measured at the Hard Hill site.

CO_2 fluxes were found to be greater from both treatments in September when compared to those measured in August, but were not significantly greater. Soil temperature at the site was 11.5 °C in both August and September and so was not considered to be a factor in differences in flux rates produced within the 'soil' treatment plots, or to have an effect on the soil contribution to respired CO_2 in the 'ecosystem' plots. A regression analysis was performed to investigate whether differences in CO_2 fluxes were caused by variation in water table depths. No significant effect of water table was found for either of the two experimental treatments with the 'soil' treatment having an r^2 value of 0.01 ($P < 0.95$) and the 'ecosystem' treatment having an r^2 value of 0.39 ($P < 0.95$).

Despite the fact these results are not significant, other studies such as Silvola *et al.* (1996) and Chimner *et al.* (2003) also measured higher CO_2 fluxes at lower water table levels that were not statistically significant. This may be due to a certain amount of inertia operating in the acrotelm. Furthermore, Blodau and Moore (2003) in a study of carbon dynamics under fluctuating water tables stated that the response of carbon cycling may depend not just on mean water table depth but also on the frequency of water table fluctuation. Moreover, Blodau and Moore (2003) also stated that this phenomenon (water table fluctuation frequency) could account for the lack of correlation between trace gas fluxes and environmental variables found in investigative field studies.

'Soil' respiration was found to contribute ~ 38 % of total ecosystem respiration in both August and September. In some forests, soil respiration has been shown to contribute between 30-80 % of total ecosystem respiration (Davidson *et al.*, 2006b). The contribution of 'soil' respiration was found to be greater in May 2005 (Chapter 3), although a direct comparison with 'ecosystem' respiration was not possible as no mean flux was acquired for this treatment. However, in May 2005, 'soil' respiration was found to be 50 % of the

'no shrubs' treatment and 45 % of the 'no monocots' treatment (although it should be remembered that there was only one reliable measurement for this treatment). The larger contribution of 'soil' respiration in May could be due to the fact that mean air temperature during sampling was lower than it was in August and September, thus reducing the rate of photosynthesis by all plant species.

Fluxes in May, August and September suggested that soil respiration contributed between 38 and 45 % of total ecosystem respiration. By difference it could then be calculated that plant respiration contributes between 55 and 62 % to total ecosystem respiration. However, this inference makes the assumption that soil respiration is the same when plants are present.

5.4.5 $\delta^{13}C$ and ^{14}C signatures of soil respired CO_2

The $\delta^{13}C$ values for the bulk peat within the top 4 cm of the profile under the 'soil' treatment had a mean value of -28.1 ± 1.0 ‰ with the 4-8 cm increment being slightly more (but not significant) enriched in ^{13}C at -27.6 ± 1.0 ‰. The $\delta^{13}C$ of respired CO_2 from the 'soil' plots reflected these values; having a mean value of -27.4 ± 0.4 ‰ in August and -27.3 ± 0.6 ‰ in September and values for both months are statistically identical at 1 σ to the $\delta^{13}C$ value of bulk peat in the top 8 cm of the profile. Because the $\delta^{13}C$ value of respired CO_2 is statistically identical at 1 σ to the $\delta^{13}C$ value of the bulk peat, it is possible that the biospheric system measured at the Hard Hill site may in fact be at steady state. Steady state is reached when the $\delta^{13}C$ of the flux reaches that of production, as constrained by mass balance (Amundson *et al.*, 1998). This phenomenon has been proposed by a number of workers (Amundson *et al.*, 1998; Dörr & Münnich, 1980).

'Soil' respiration was significantly enriched in ^{14}C relative to 'ecosystem' respiration in both August (by ~ 8 %Modern) and September (by ~ 9 %Modern) of 2005. In addition 'soil' respiration was enriched in ^{14}C relative to the contemporary atmosphere in both August and September of 2005 by ~ 8 and 10 %Modern respectively. The values obtained for 'soil' respiration would suggest that there must be a source with a considerable amount of bomb ^{14}C that is being utilised by the heterotrophic population for decomposition. Two sources existing in the peat profile that would have been available for decomposition were soil organic matter and DOC, both of which were found to contain bomb ^{14}C (Figure 5.7 and 5.8 respectively). Both these sources were enriched in ^{14}C (> 100 %Modern) within the top 8 cm of the profile.

On comparison of the ^{14}C content of CO_2 produced by the 'soil' treatment plots with the atmospheric $^{14}CO_2$ record (Levin & Kromer, 2004), the enrichment of between 115 and 116 %Modern suggests that 'soil' respiration had a mean age of ~ 15 years relative to the time of original fixation from the atmosphere (Figure 5.23). This makes the simplifying

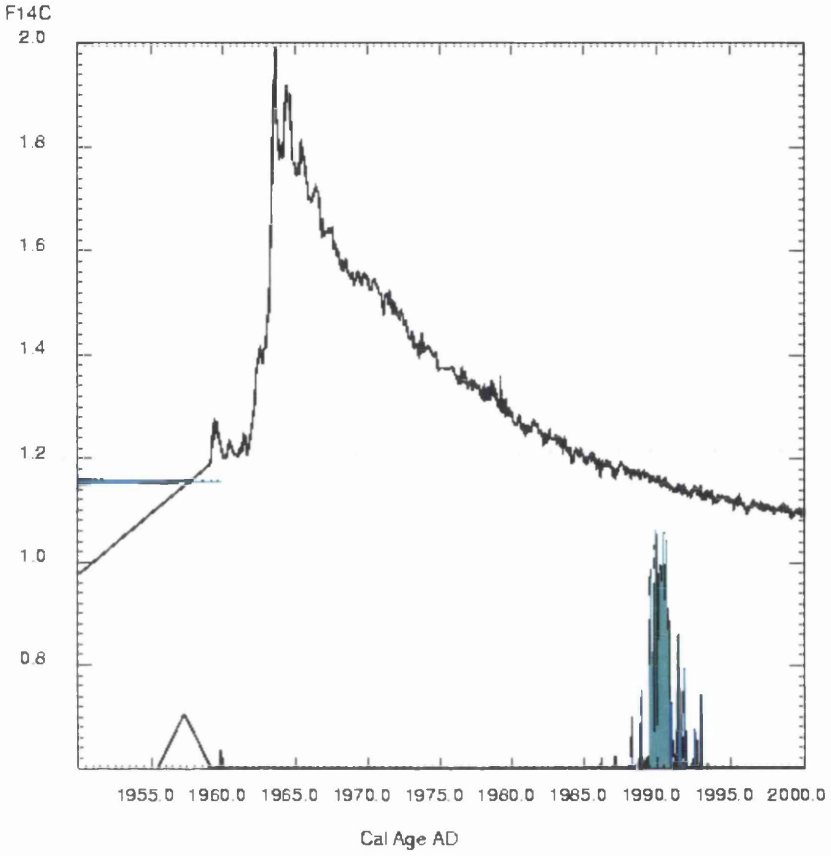

Figure 5.23 – Calibration of 115.5 %Modern (expressed as Fraction Modern) using CALIBomb (http://calib.qub.ac.uk/CALIBomb/frameset.html) based on the Levin & Kromer, (2004) data set. One σ error ranges from July 1989 to July 1991. Two σ error would include the range June 1955 to December 1959, also shown.

assumption that all of the CO_2 respired from the 'soil' treatment plots was derived from carbon fixed since the peak in atmospheric ^{14}C in 1963 (based on an error of 1 σ). It is evident from the ^{14}C signatures of both the bulk peat and DOC in the 'soil' profile that the majority of respired CO_2 for both August and September is likely to have been produced in the top 4 cm of the profile (in addition, the average water table depth for the 3 'soil' plots between the two sampling dates was 3.7 cm below the peatland surface). This provides further evidence for the hypothesis that most of the decomposition occurs above the level of the water table.

Since in September 'soil' respiration was significantly enriched in ^{14}C relative to 'soil' respiration in August, a regression of the ^{14}C content of respired CO_2 versus water table depth was performed (Figure 5.14). The regression showed that the ^{14}C content of 'soil' respiration was not significantly affected by water table depth. However, much spatial variation exists in the ^{14}C content of individual peat profiles and also in carbon accumulation rates (section 5.4.2). Furthermore, there was considerable variation in water table heights within individual treatment plots, possibly due to differences in compaction or in the vertical accumulation rate of peat between plots. Therefore data points plotted in Figure 5.14 are not a comparison of replicated plots having exactly the same characteristics.

However, when comparing the ^{14}C content of respired CO_2 from 'soil' plots in August and then again from the same plots in September, there is a direct comparison of the same treatment plots (having all the same characteristics), but with different water table depths. On doing this it was found that the mean ^{14}C content of 'soil' respired CO_2 in September was significantly enriched (at $> 2\ \sigma$) to that produced from the same plots in August (Figure 5.12). Furthermore, 'soil' plot 3 produced CO_2 that was the most enriched in ^{14}C relative to 'soil' plots 1 and 2 in both August and September. The CO_2 produced by 'soil' plot 3 was not significantly enriched in ^{14}C relative to the remaining two 'soil' plots, but it was found to have the lowest water table depth on both sampling occasions.

The mean depth of the water table within the 3 'soil' plots was 1.8 cm below the peatland surface in August, whilst in September the water table was nearly 4 cm lower at -5.6 cm. The results suggest that the depth of the water table (and hence the concentration of ^{14}C available in the profile for aerobic decomposition) influenced the amount of radiocarbon that was present in 'soil' respired CO_2 and that the greater the amount of the peat profile containing bomb ^{14}C that was exposed to aerobic decomposition, the greater the amount of ^{14}C that was contained in 'soil' respired CO_2. In addition, fluxes from the 'soil' plots in September were higher (although not significantly so) than in August, suggesting further that the greater depth of peat in the profile that is exposed to aerobic conditions, the more carbon substrate is available for utilisation by microbes. The fact that respiration rates are not significantly higher in September may be attributed to water table fluctuation frequency (Blodau & Moore, 2003), as mentioned previously.

5.4.6 Isotopic (^{13}C and ^{14}C) signature of plant respired CO_2

The $\delta^{13}C$ of respired CO_2 from the 'ecosystem' plots ranged between -20.8 ‰ in August and -23.2 ‰ in September. As 'soil' respiration was -27.4 ‰ for both months, the $\delta^{13}C$ values obtained for 'ecosystem' respiration indicate that plant respired CO_2 must contain a source of carbon that is enriched in the heavy stable isotope, or that the contribution from 'soil' respiration is small. The ^{14}C content of 'ecosystem' respiration (~ 107 %Modern in August and September) was identical at 1 σ to the ^{14}C content of the contemporary atmosphere in August and September 2005. Since 'ecosystem' respiration is made up of both plant and soil respiration, it was immediately apparent that either plant respired CO_2 contained a depleted source of radiocarbon, or, that 'soil' respiration contribution to total 'ecosystem' respiration was extremely small.

The ^{14}C concentrations (mean) of respired CO_2 for both treatments were entered into a mass balance equation (equation 3) along with mean fluxes for each treatment, in order to calculate the ^{14}C signature of plant respired CO_2. The flux of plant respiration was calculated by deducting the 'soil' flux from the 'ecosystem' flux (the assumption being that soil respiration in the 'ecosystem' plot was the same as that measured in the 'soil' plots). The calculated ^{14}C signature for plant respiration in August was 101.95 %Modern and for September 100.84 %Modern. Mass balance was also applied to the $\delta^{13}C$ values for respired CO_2 from both treatments and the calculated stable isotopic signature of plant respired CO_2 for August was -20.8 ‰ and for September -23.2 ‰.

It was deemed unlikely that peatland vegetation would respire CO_2 with a ^{14}C signature of between 100.84 and 101.95 %Modern, as this would mean that plants were respiring carbon that was > 50 years old. Therefore, it was considered that the two-component model (one component being soil respiration and the other plant respiration) approach was inappropriate. One assumption in the two-component model is that the soil respiration flux (in the 'ecosystem' plots) is the same as it was when plants are removed ('soil' plots). This assumption is likely to be an oversimplification. When plants are present, they will transport recently fixed carbon to depth (Schuur & Trumbore, 2006), which will be exuded by roots and easily decomposed by the heterotrophic population. Furthermore, studies have shown that the ^{14}C content of soil CO_2 at high respiration rates in the summer, becomes close to that of the ^{14}C content of the atmosphere (Dörr & Münnich, 1986). Dörr & Münnich (1986) attributed this phenomenon to the influence of root respiration (and by inference the allocation of recently fixed carbon below ground).

It is clear from the two-component box model mass balance approach that the calculated ^{14}C signature of plant respiration is incorrect. Therefore, instead, if we assume that plant respiration has a signature similar to that of the contemporary atmosphere (106.98 %Modern in August and 106.00 %Modern in September), as also done by Gaudinski *et al.* (2000), we can then calculate the fraction that plant respiration contributes to 'ecosystem' respiration. Using the values measured for the ^{14}C content of 'ecosystem' respiration and 'soil' respiration we can enter them into the following set of equations postulated to describe the dynamic ecosystem under investigation:

$$\mathbf{F_T = F_P + F_S} \qquad \mathbf{(4)}$$

where F_T is the total 'ecosystem' respiration flux, F_P is the plant respiration flux and F_S is the 'soil' respiration flux. Adding isotope mass balance to equation 4, we get:

$$\mathbf{\delta_T F_T = \delta_P F_P + \delta_S F_S} \qquad \mathbf{(5)}$$

where δ is the stable carbon isotopic signature of CO_2 and

$$\mathbf{\Delta_T F_T = \Delta_P F_P + \Delta_S F_S} \qquad \mathbf{(6)}$$

where Δ is the radiocarbon content of respired CO_2 (note that this equation is the same as equation 2). We can also express equation 4 as:

$$\mathbf{F_T/F_T = F_P/F_T + F_S/F_T}$$

$$\mathbf{1 = f_T = f_P + f_S}$$

where f is the fraction that each pool contributes to the total respiration flux. The fraction of the soil component, f_S is then,

$$\mathbf{f_S = (1 - f_P)} \qquad \mathbf{(7)}$$

where f_P is equal to the fraction that is plant respiration and $(1 - f_P)$ is equal to the fraction that is soil respiration. Substituting for f_S in equation 6 using equation 7 gives:

$$\mathbf{\Delta_T = \Delta_P f_P + \Delta_S (1 - f_P)} \qquad \mathbf{(8)}$$

Using the values (^{14}C) for August as an example and substituting into equation 8 we get:

$$\mathbf{106.95 = 106.98 \times f_P + 114.94 \times (1 - f_P)}$$

$$106.95 = 106.98f_P + 114.94 - 114.94f_P$$

$$f_P = 7.99/7.96$$

$$f_P = 1.00$$

Therefore using this method, plant respiration is estimated to contribute 100 % of total ecosystem respiration and therefore, 'soil' respiration does not contribute to total 'ecosystem' respiration at all. Similarly when substituting the ^{14}C content of 'ecosystem', 'soil' and 'plant' (atmospheric CO_2) respiration for September we find that 'plant' and 'soil' respiration each contribute 94.7 and 5.3 % respectively, of total ecosystem respiration. As the fraction calculated for soil respiration was far less than the fluxes actually measured within the 'soil' plots (38 % of 'ecosystem' respiration), it was considered that the two-box model approach was inadequate to describe respiration fluxes within the peatland ecosystem at the Hard Hill site.

It was then postulated that there might be a third contribution to 'ecosystem' respiration that was mediated by the presence of plants. Assuming that there were three potential contributions to the overall 'ecosystem' respiration flux: plant respiration (flux F_P, Δ_P δ_P), soil respiration (flux F_S, Δ_S δ_S) and an additional flux produced by the presence of plants (flux F_R, Δ_R δ_R), we can apply mass balance to the entire (total) system, i.e. (flux F_T, Δ_T δ_T), followed by isotope balance, as follows:

$$F_T = F_P + F_S + F_R \quad (9)$$

where F is the flux that each pool contributes.

$$\delta_T F_T = \delta_P F_P + \delta_S F_S + \delta_R F_R \quad (10)$$

where δ is the stable isotopic signature of CO_2.

$$\Delta_T F_T = \Delta_P F_P + \Delta_S F_S + \Delta_R F_R \quad (11)$$

where Δ is the radiocarbon content of respired CO_2. We can also express equation 9 as:

$$F_T/F_T = F_P/F_T + F_S/F_T + F_R/F_T$$

$$1 = f_T = f_P + f_S + f_R$$

where f is the fraction that each pool contributes to the total respiration flux. The fraction of the third component, f_R is then,

$$f_R = (1 - f_P - f_S) \quad (12)$$

substituting for f_R in equations 10 and 11 using equation 12 gives:

$$\delta_T = \delta_P f_P + \delta_S f_S + \delta_R(1 - f_P - f_S)$$

$$\delta_T = \delta_P f_P + \delta_S f_S + \delta_R - \delta_R f_P - \delta_R f_S$$

$$\delta_T = f_P(\delta_P - \delta_R) + f_S(\delta_S - \delta_R) + \delta_R \quad (13)$$

and:

$$\Delta_T = \Delta_P f_P + \Delta_S f_S + \Delta_R(1 - f_P - f_S)$$

$$\Delta_T = \Delta_P f_P + \Delta_S f_S + \Delta_R - \Delta_R f_P - \Delta_R f_S$$

$$\Delta_T = f_P(\Delta_P - \Delta_R) + \Delta_R + f_S(\Delta_S - \Delta_R) \quad (14)$$

We have measured the values for Δ_T, Δ_S, δ_T and δ_S but we must make some assumptions about Δ_P and δ_P as they were not measured directly. First, we assume that Δ_P has the same ^{14}C content as the contemporary atmosphere (Gaudinski *et al.*, 2000; Schuur & Trumbore, 2006) on the same date that Δ_S and Δ_T were measured in August and September of 2005. In addition, a value of -27 ‰ is assumed for the $\delta^{13}C$ of plant respiration (Gaudinski *et al.*, 2000). The chosen values for δ_P and Δ_P and the measured values are substituted into equation 13, again using the August measurements as an example:

$$-20.8 = f_P(-27 - \delta_R) + 0.38(-27 - \delta_R) + \delta_R$$

$$-20.8 = f_P(-27 - \delta_R) - 10.26 + 0.62\delta_R$$

therefore,

$$f_P = (10.54 + 0.62\delta_R) / (27 + \delta_R) \quad (15)$$

Substituting the numerical values for ^{14}C for August into equation 14 gives:

$$106.95 = f_P(106.98 - \Delta_R) + 0.38(114.94 - \Delta_R) + \Delta_R$$

$$106.95 = f_P(106.98 - \Delta_R) + 43.68 + 0.62\Delta_R \quad (16)$$

therefore, substituting equation 15 for f_P in 16 gives:

$$106.95 = 43.68 + 0.62\Delta_R + ((10.54 + 0.62\delta_R) / (27 + \delta_R))(106.98 - \Delta_R) \quad (17)$$

The only unknowns in equation 17 are δ_R and Δ_R, the stable carbon and radiocarbon signatures of the postulated third respiration pool, the two quantities that we require. Although we cannot derive unique values from 17, we can model the locus of pairs (δ_R, Δ_R) that satisfy 17. Calculated pairs of Δ_R and δ_R that satisfy 17 for August and September are shown in Figures 5.24 and 5.25 respectively. Calculated points in both plots are

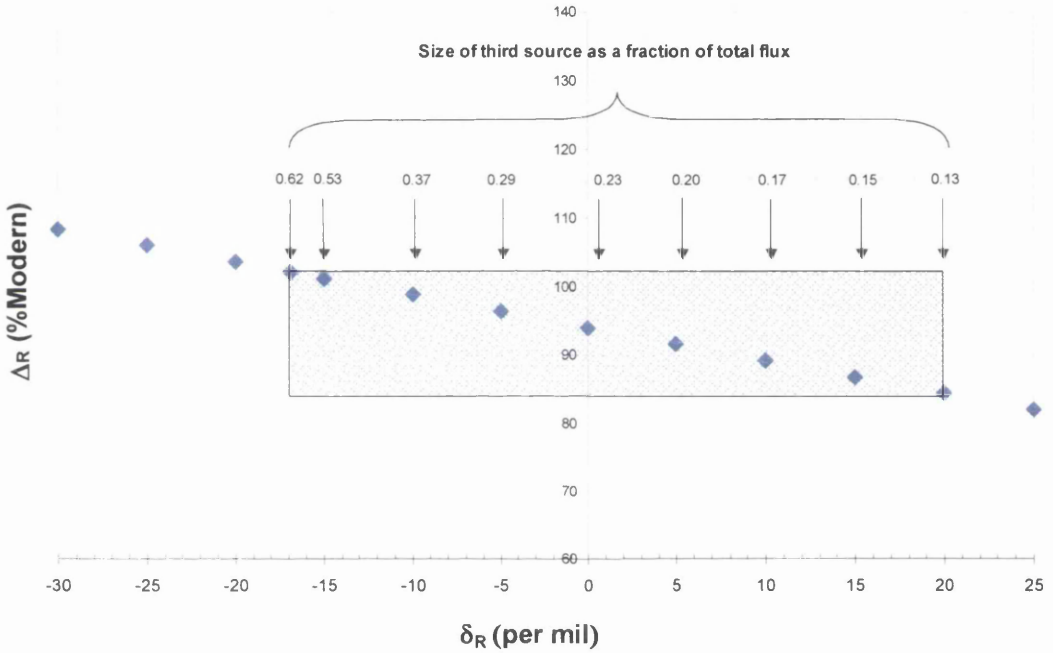

Figure 5.24 – Plot illustrating values for a possible third source (δ_R and Δ_R) that fit the model predicted by equation 17 for the August sampling. Only values within the shaded area are possible based on the fact that the flux of the third source must be a fraction < 0.62 of the total flux and in addition is unlikely to have a $\delta^{13}C$ value greater than +20 ‰.

constrained by the fact that the fraction of CO_2 contributed by the third pool to the total unlikely to have a $\delta^{13}C$ value greater than +20 ‰ (Strapoc *et al.*, 2006).

Figure 5.24 demonstrates that the postulated third source of carbon could contribute between 13 to 62 % of the total 'ecosystem' respiration flux. Similarly, substituting the $\delta^{13}C$ and ^{14}C contents for respiration fluxes (both measured and assumed) in September into equation 17, we see from Figure 5.25 that the third pool/contribution to the 'ecosystem' respired carbon flux could contribute between 8 and 62 % of the total flux. Before we can begin to attempt to determine both the size and the isotopic (^{13}C and ^{14}C)

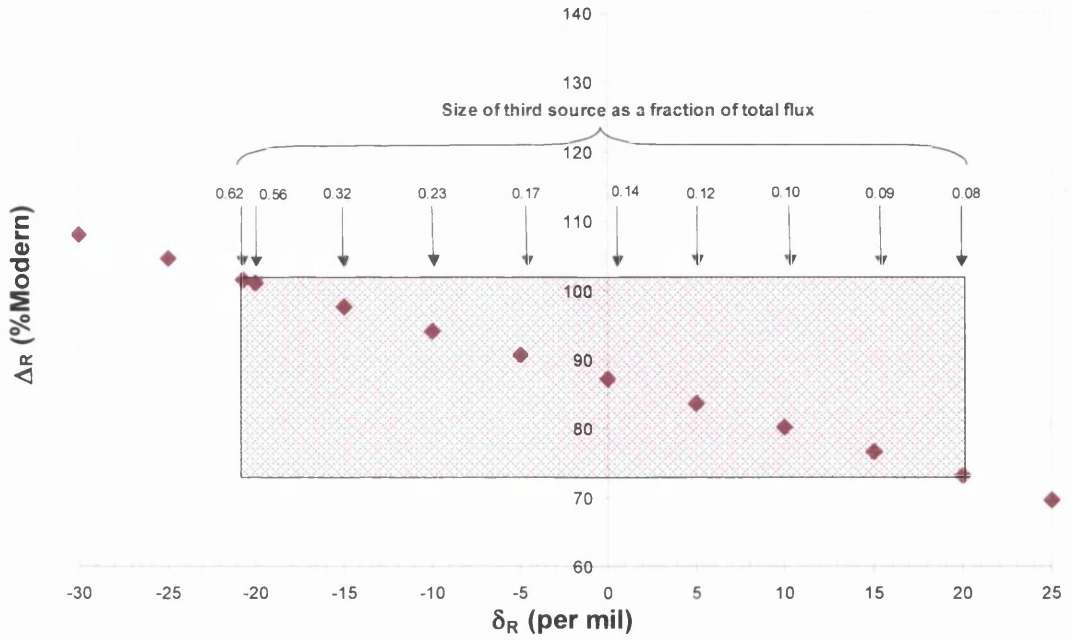

Figure 5.25 - Plot illustrating values for a possible third source (δ_R and Δ_R) that fit the model predicted by equation 17 for the September sampling. Only values within the shaded area are possible based on the fact that the flux of the third source must be a fraction of < 0.62 of the total flux and in addition is unlikely to have a $\delta^{13}C$ value greater than +20 ‰.

composition of the third pool of carbon we must present a plausible and realistic suggestion as to the source of the third carbon pool. Peatland vegetation holds the key to the possible third pool of carbon, as it is when vegetation is present that the derived values from the two box model are either not consistent with what was measured (flux rates) or seem unrealistic (plants respiring pre-bomb carbon).

It is well established in the literature that certain peatland plants, in particular vascular plants such as grasses and sedges (e.g. *Eriophorum, Carex* and *Juncus*), serve as conduits for the transport of methane from depth, to the atmosphere (Chanton & Whiting, 1995; Chanton *et al.*, 2002; Chanton *et al.*, 2005; Marinier *et al.*, 2004; Rinnan *et al.*, 2003; Schutz *et al.*, 1991; Shannon *et al.*, 1996; Strom *et al.*, 2005; Verville *et al.*, 1998; Watson *et al.*, 1997). Furthermore, it has also been shown that this transport mechanism (as opposed to ebullition or diffusion through the water column) is responsible for up to 90 % of the methane flux from peatlands (Shannon *et al.*, 1996). In contrast, ebullition is a more important mechanism for CH_4 release from lakes, estuaries and swamps and accounts for ≥ 50 % of the total surface emission from the Amazonian floodplain (Chanton & Whiting, 1995). Interestingly, Schutz & Seiler (1989) and Schutz *et al.* (1989) showed that methane transport in a rice paddy shifted from > 90 % release *via* ebullition to > 90 % release *via* plant transport as the rice matured.

Evidence from these studies suggests that in the absence of plants, or at least in the absence of a reasonable sized plant tiller (Marinier *et al.* (2004) found that clipping fresh leaves from *Eriophorum vaginatum* tussocks reduced methane emissions by up to 79 %), ebullition is the dominant release mechanism for CH_4 produced under anaerobic conditions within a peatland/wetland profile. However, when vascular plants are present, they facilitate a continual diffusion of CH_4 from depth (along a concentration gradient), to the atmosphere. This plant-mediated release of CH_4 from depth thus prevents any pressure build-up caused by CH_4 that would otherwise only escape when the pressure is large enough to create 'breakthrough', followed by release to the atmosphere *via* the ebullition process. If, as is the case, that vascular plants are a well documented and accepted mechanism of CH_4 transport from depth in peatlands, then plant mediated transport of CO_2 produced at depth, may also be an important pathway for CO_2 release to the atmosphere.

For example, Koncalová *et al.* (1988) demonstrated that pore waters rich in CO_2 can cause gas flow from plant roots to the atmosphere *via* non-through-flow convection, in addition to facilitating O_2 transport to the roots, through gas-transporting tissues called aerenchyma (the conduit effect), contained within vascular plants. The development of aerenchymateous tissue in vascular plants is thought to have arisen due to soil anoxia, and provides the submerged parts of plants with oxygen. Transfer of O_2 to depth and its subsequent consumption is known to cause pressure deficits of up to 20 % (the concentration of O_2 in the atmosphere) in the root zone, again leading to gas flow from roots to the atmosphere (Raskin & Kende, 1983; 1985).

In a study of peat-forming wetland methane emissions, Joabsson *et al.* (1999) found that the entrance of CH_4 to plant root aerenchyma is facilitated by the diffusion gradient that exists between the atmosphere and the peat. The importance of the presence of plant roots of higher plants as a mechanism of significant gas transfer from peatlands has been demonstrated in a number of studies (Sundh *et al.*, 1994; Thomas *et al.*, 1995). Indeed, Thomas *et al.* (1996) stated that the path of least resistance for gas diffusion from water-logged peat was the extensive lacunal systems in the leaves, roots and rhizomes of a number of monocotyledonous species. In addition, Chimner & Cooper (2003) state that the majority of soil CH_4 and soil CO_2 in saturated soils is transported to the atmosphere *via* plants, as opposed to the processes of diffusion up through the water column or ebullition.

Furthermore, in a review paper, Joabsson *et al.* (1999) maintain that one mechanism of bulk transport of gases from peat, thermo-osmosis, results in the flushing of 'methane and other gases accumulated in the root zone' to the atmosphere. Whilst the majority of the

aforementioned studies have been concerned with methane, it is conceivable that the same mechanism that transports methane from deep peat to the atmosphere (*via* aerenchyma) is also an important route for CO_2 release. For example, *Eriophorum vaginatum*, the dominant monocotyledon vascular plant at the Hard Hill experimental site, can produce roots that penetrate to 1 m (Heal *et al.*, 1978) and sometimes even 1.5 m into the peat profile. This being the case, it is probable that old carbon at depth, that has been mineralised to produce CO_2 (in addition to CH_4 production), could be transported to the atmosphere *via* this type of vascular plant.

However, unless this source is quite sizeable, concomitant $\delta^{13}C$ values must be a great deal more enriched than those found in the surrounding bulk peat (see Figures 5.24 and 5.25). For example, the three-box model featured in Figure 5.24 predicts that for August, a third source of carbon having a $\delta^{13}C$ value that ranges between -5 and + 10 ‰, the associated ^{14}C contents of this source would be between 96.4 and 89.2 %Modern and would contribute between 17 and 29 % of total 'ecosystem' respiration respectively. Similarly, in September, for a third source of carbon having $\delta^{13}C$ values that range again between -5 and +10 ‰, the three-box model featured in Figure 5.25 predicts that the associated ^{14}C content of a source with this range in $\delta^{13}C$ would be between 80.2 and 90.6 %Modern and would have to contribute between 10 and 17 % respectively of the total 'ecosystem' respiration flux.

The predicted radiocarbon age of the CO_2 produced by the third source is easily possible. For example, radiocarbon data for the base of the peat (236-242 and 258-264 cm) at nearby Shaft Hill (Garnett, unpublished data: SRR-6613 and SR-6614) shows that at these depths the bulk peat has a ^{14}C content of between 45.10 %Modern (6396 ± 46 years) and 44.46 %Modern (6511 ± 50 years). But, is it possible that the third source could contain CO_2 that is sufficiently enriched in ^{13}C as to produce positive $\delta^{13}C$ values? Interestingly, enriched $\delta^{13}C$ values for CO_2 at depth in peat profiles have been measured. For example, Charman *et al.* (1999) measured $\delta^{13}C$ values for deep carbon gases in an English raised mire and found CO_2 that had $\delta^{13}C$ values that were particularly enriched in ^{13}C with values up to +7.1 ‰ at depths of 2.3 to 2.5 m. Furthermore, Bryant *et al.* (2006) and Clymo & Bryant (in prep.), in a study of the carbon isotopic signatures of deep peat gases in a Scottish raised peat bog recorded $\delta^{13}C$ values for CO_2 of between +4.0 ‰ and +10.0 ‰ at depths of 1.5 to 6 m. Both these studies suggest that the ^{13}C-enriched CO_2 was probably produced during methanogenesis (producing CH_4 that is depleted in ^{13}C), for example, during acetate fermentation (Bryant *et al.*, 2006; Clymo & Bryant, in prep.).

Therefore, the range of ^{14}C concentrations predicted by our models of locus pairs are completely realistic. Likewise the range of $\delta^{13}C$ values for CO_2 respired by the third source are also realistic as studies by Clymo & Bryant (in prep.) and Charman *et al.* (1999) have demonstrated. Therefore, the fraction of CO_2 that a third pool could realistically contribute to total 'ecosystem' flux would be ~ 10-20 %. If this is indeed the case, then CO_2 released in this way could be enriched in ^{13}C whilst at the same time being depleted in ^{14}C, being derived by fermentation within deeper (older) peat.

In addition, the accumulation rate of the acrotelm of the blanket bog at Moor House has been estimated at 450 g m^{-2} yr^{-1} (Clymo, 1984). Moreover, the rate of input to the catotelm from the acrotelm is about 10 % of primary productivity (Clymo, 1983; Schimel, 1995b; Tolonen *et al.*, 1992). According to Clymo (1984), the rate of organic matter input to the catotelm (in most of the cases where data exist) is about 50 g m^{-2} yr^{-1}. If we make the assumption that net carbon accumulation is close to zero in the catotelm (i.e. that the peat has reached its limit of growth), the rate of input to the catotelm from the acrotelm must be balanced by an output from the catotelm to the acrotelm of ~ 50 g m^{-2} yr^{-1} (as both methane and CO_2, and assuming loss *via* DOC is minimal). Studies have shown (Popp *et al.*, 2000; Strom *et al.*, 2005) that between 90 and 99 % of methane is oxidised to CO_2 by methanotrophs before leaving the peatland surface. Therefore, we can assume that the loss of carbon from the blanket bog at Moor House is approximately 50 g m^{-2} yr^{-1} and is lost mostly in the form of CO_2.

A further assumption can be made, which is that the vast majority of catotelm CO_2 lost from the peatland is mediated by plants, as loss by diffusion is considered minimal and ebullition is a more important mechanism of loss in flooded environments such as salt marshes, swamps and rice paddies (Chanton & Whiting, 1995). Therefore the postulated third pool of carbon would be equal to the loss of CO_2 from the catotelm mediated by plants (catotelm CO_2) and would be according to Clymo (1984) ~ 50 g m^{-2} yr^{-1}. This flux expressed as a fraction of the loss of carbon from the acrotelm (NPP minus what makes it into the catotelm, is 400 g m^{-2} yr^{-1}) is 12.5 %.

From the three-box models featured in Figures 5.23 and 5.24 we can estimate that when plants are present, the contribution to total 'ecosystem' flux, from catotelm CO_2 (mediated by plants) would be in the region of ~20 %. This would then mean that the total 'soil' respiration contribution to 'ecosystem' respiration would be ~58 % (38 % that was measured in the 'soil' plots and ~20 % catotelm CO_2 mediated by the presence of plants). Plant-mediated catotelm CO_2 would therefore contribute a relatively large fraction of total

'soil' respiration (~34 %), just over twice that calculated (for catotelm CO_2) using the data from Clymo (1984). This is not surprising, as the estimate calculated for the catotelm CO_2 contribution using the Clymo (1984) data is an annual estimate. The estimate calculated here is based on rates measured during the growing season months of August and September when plant respiration rates are possibly at their highest due to warmer air temperatures and increased soil aeration.

Furthermore, gas fluxes released from depth are likely to be larger in August and September, as it is towards the end of the growing season when plants transport most of their carbon below ground, increasing root density throughout the summer (Christensen *et al.*, 2000). Moreover, the three-box model predicted a larger contribution of catotelm CO_2 to total 'ecosystem' CO_2 during high water table sampling (Figure 5.23) than at lower water table sampling (September). As the peat would be more anoxic at higher water table levels, the possibility arises that the larger contribution from CO_2 produced at depth would be caused by the greater need of plant mediated transport of O_2 to depth, and hence subsequent increased gas flushing from the root zone.

Therefore, with this knowledge and the results of the three-box model, it is suggested that the release of catotelm CO_2 from depth (which is both depleted in ^{14}C and enriched in ^{13}C), like CH_4, mediated by the aerenchymateous tissue of plants, is taking place. Furthermore, this third pool may be a significant source of CO_2 to the atmosphere at the site studied.

5.5 Conclusion

An assessment of the ^{14}C content of the peat surface layers at the Hard Hill site was made and the results show that there was considerable variation in ^{14}C content of the 0-16 cm profile of this area of upland blanket bog. Radiocarbon concentrations ranged from 95 to 130 %Modern, with the largest range in variation occurring in the 4-12 cm part of the peat profile. This was attributed to both rapid changes in atmospheric radiocarbon content and differences in peat accumulation and carbon accumulation rates. Despite limitations imposed by the coarse sampling resolution (4 cm increments), the results show that there was greater variation in peat accumulation rates (depth increase) across the site than in rates of carbon accumulation over the last ~50 years.

DOC extracted from the same surface layers of peat also demonstrated much variation in radiocarbon content. It was shown that the source of radiocarbon contained in the DOC was supplied mainly by the bulk peat as concentrations of both were strongly correlated (r^2

= 0.90). However, this relationship was not 1:1 and conceptual modelling demonstrated that the most likely additional source to the DOC pool was gradual downward movement of DOC produced higher up in the profile.

The contribution of 'soil' respiration to total ecosystem respiration was found to be ~ 40 % of total ecosystem respiration, having a mean age of 15 years relative to the time of original fixation from the atmosphere. Despite the wide variation in the radiocarbon content of both the bulk peat and DOC, soil respiration maintained a relatively small range in radiocarbon signatures (between 114.59 and 116.25 %Modern). It was assumed that plant respiration had an isotopic signature similar to that of CO_2 in the contemporary atmosphere (Schuur & Trumbore, 2006) as it could not be measured directly. Mass balance subsequently revealed that there had to be a source other than 'soil' and 'plant' respiration contributing to total ecosystem respiration. Modelling of locus pairs demonstrated that this source was both depleted in radiocarbon and enriched in the heavy carbon isotope ^{13}C and could contribute a sizeable amount of CO_2 (perhaps 20 %) to the atmosphere, possibly varying with water table depth.

Peatland vegetation was characterised and found to have the same ^{14}C content as the contemporary atmosphere. It was expected that some peatland vegetation species, bryophytes in particular, might provide evidence of re-fixation/recycling of soil-respired CO_2, but this was not detected. However, as the ^{14}C content of 'ecosystem' respiration (which included a contribution from a third pool at depth) was statistically indistinguishable from the contemporary atmosphere, it is likely that this could be the reason that recycling was not detected, even though it is likely taking place as demonstrated by other studies (Garnett & Billett, In press; Jungner *et al.*, 1995; Turetsky & Wieder, 1999). This has implications for palaeoecological studies that use plant macrofossils (in particular *Sphagnum* spp.) for constructing radiocarbon chronologies of peat bogs. For example, if *Sphagnum* growing on the surface of a bog in pre-bomb times fixed older soil respired carbon, released from both the catotelm and the acrotelm, it acquired a depleted ^{14}C signature, which when subsequently ^{14}C dated, could appear older than its true age.

Further studies are needed to examine the contribution of a third source (plant mediated catotelm CO_2) to total 'ecosystem' respiration. One possibility could be the use of a system that transported gas contained in peat at depth, to the atmosphere, without plants being present; perhaps a type of artificial plant (e.g. installation of many lengths of narrow gauge tubing into plant-free peat). An alternative experiment might be to grow vascular plants

such as *Eriophorum*, *Juncus* and *Carex* in mediums with distinctly different isotopic signatures but under similar temperature, moisture and lighting conditions in order that the isotopic signature of emitted CO_2 be compared. Alternatively, the aforementioned monocotyledon vascular plants could be grown again under the same abiotic conditions and in a growth medium with the same isotopic signature but grown in atmospheres containing CO_2 of contrasting isotopic signature (labelling approach).

6 Discussion

The Earth's terrestrial biosphere contains approximately three times as much carbon (2190 Gt) as is currently resident in the atmosphere (Schimel, 1995a). Therefore any small shift in the balance of carbon stored in these ecosystems has the potential to have a considerable impact on the CO_2 loading of the atmosphere and on subsequent associated changes in climate. Climatic drivers are the primary regulators of both plant and soil carbon storage and release. Therefore it is vital to understand what effect these drivers will have on production and decomposition rates of vegetation and soil components within terrestrial ecosystems. Moreover, long-term changes in abiotic variables can lead to permanent changes in the vegetative composition of an ecosystem, thus exacting a further influence on peatland carbon cycling. This is particularly important as plant species composition can both directly and indirectly affect ecosystem carbon cycling. Northern peatlands, in particular, are at greatest risk to predicted changes in climate, as climate disturbance is expected to be greatest at these latitudes. Therefore, it is these ecosystems in particular that are at greatest risk of an alteration in carbon storage (IPCC, 2001).

Consequently, the objective of this study was to investigate fluxes of respired CO_2, (both primary and isotopic) emanating from a peatland (blanket bog) ecosystem under a number of vegetation manipulation treatments. The effects of climatic drivers, such as moisture and temperature, on peatland CO_2 fluxes were also studied. The isotopic signature of respired CO_2 (both ^{13}C and ^{14}C) produced within a number of ecosystems is becoming more widely used, as characterisation of such fluxes is regarded as an important and powerful tool in carbon cycling studies (Gaudinski *et al.*, 2000; Trumbore, 2000). Moreover, these fluxes can provide much valuable information regarding not just source but also the age of sources used by biological systems that produce CO_2 within these ecosystems. However, in order to obtain enough CO_2 for both stable and radiocarbon analysis, either a large volume of air must be collected or the CO_2 must be concentrated into or onto a suitable absorbent or adsorbent. Advances in the measurement of radiocarbon (i.e. AMS) have meant that capture of just a few ml of CO_2 can yield a radiocarbon analysis. Currently, the minimum volume of CO_2 required for routine radiocarbon analysis is about 1 ml.

Traditional methods of CO_2 capture in the field have in the past been quite unwieldy (e.g. the transport of several large evacuated flasks to a remote field location) or even potentially hazardous (the use of liquid N_2 or alkaline solutions such as NaOH). There was a need therefore, to develop a system that could capture CO_2 in the field at remote

locations, quickly and easily with potential hazards either minimised or eliminated. In this thesis study a sampling system was developed that can capture CO_2, using a material that presented the minimum of physical caveats, both in transport and use (Chapter 2). The material chosen was molecular sieve Type 13X (a synthetic zeolite). This material had been utilised in the past for carbon isotope studies (Gaudinski *et al.*, 2000; Koarashi *et al.*, 2002), but had not been stringently tested with the use of internationally calibrated isotopic standards, with particular regard to radiocarbon. Developments were made to an original molecular sieve cartridge design (Bol & Harkness, 1995) and these cartridges were incorporated into a sampling system that was robust and lightweight (see Figure 2.2).

A thorough testing programme was undertaken, with the alternate application of stable isotopic standards (^{13}C) of widely varying isotopic values (~ -27.0 ‰ to ~ +1.8 ‰). After it was demonstrated that a number of stable carbon isotopic standards could be sequentially applied and removed from two different molecular sieve cartridges and yield results that were within 2 σ analytical error, a testing programme was formulated for radiocarbon analysis. Results showed that the sampling system developed in Chapter 2 trapped CO_2 for radiocarbon analysis without fractionation, contamination or hysteresis (Hardie *et al.*, 2005).

Before use of the developed molecular sieve sampling system in the field, a preliminary study was performed, using Exetainers, to investigate primary CO_2 fluxes and the stable isotopic signature of respired CO_2 produced by a vegetation manipulation experiment that was set up by Sue Ward in 2003 (Ward, 2006). This experiment consisted of a number of different vegetation manipulation treatments, and was established to ascertain the effect that different vegetation types had on peatland ecosystem carbon cycling. It was thought that in measuring the natural abundance stable carbon isotopic signature of the primary fluxes, the individual sources that contribute to total 'ecosystem' respiration might be distinguished (Chapter 3).

Methodological difficulties meant that only three treatments could realistically be compared; these were the 'soil' treatment, the 'no monocots' treatment and the 'no shrubs' treatment. Results showed that respiration fluxes were greatest in the vegetated plots with fluxes produced by the 'soil' treatment measuring ~ 50 % of the 'no shrubs' treatment and 45 % of the 'no monocots' treatment. No differences were found in the stable isotopic signature of respired CO_2 produced by the three treatments. This may have been due to the fact that either there were no differences between the different treatments or that differences were too small to detect using the Keeling plot/Exetainer approach.

However, assuming there were differences in the isotopic signature of respired CO_2, they may not have been detected for a number of possible reasons including: relatively small sample size and the fact that $\delta^{13}C$ values estimated using the Keeling plot technique are a number of units of per mil away from actual measured values, possibly leading to large extrapolation errors. In addition, respired CO_2 from treatment plots was captured in specially designed and tested peatland respiration chambers (Ward, 2006). Whilst these chambers were perfectly adequate for CO_2 collection without loss of sample, the siting of chamber collars that housed the respiration chambers proved to have drawbacks.

This study revealed, that if chamber collars were not sunk to a depth of at least 8-10 cm, the integrity of respiration samples was compromised. The main treatments to be affected were ones that contained shrub roots. For example, it was evident from both the concentration and the stable carbon isotopic signature of CO_2 collected from the 'no moss' and the 'ecosystem' treatments that respired CO_2 was lost from all ten chambers. Similar differences have been reported by other workers; for example, Davidson *et al.* (2002), in a review of the reduction of chamber artefacts and biases suggested that chamber collars be inserted to a depth of 9 cm when measuring fluxes emanating from forest soils.

Loss of sample from some chambers was deduced by the fact that CO_2 contained within aliquots of headspace gas removed from treatment chambers, for the most part, demonstrated little deviation in either concentration or $\delta^{13}C$ value to that of the contemporary atmosphere. Conversely, CO_2 collected during a time series from the 'no shrubs' and the 'soil' treatments demonstrated both a monotonic increase in CO_2 concentration and a monotonic decrease in the $\delta^{13}C$ value of respired CO_2 for 90 % of the 'soil' chambers and 100 % of the 'no shrubs' chambers. This demonstrated that chamber collars for these treatments were making a good seal with the peatland surface (probably due to the fact that they were not affected by laterally growing shrub roots), thus preserving the integrity of respired CO_2 collected in treatment chambers.

It is vitally important to determine individually, the responses of both plant and soil respiration to total ecosystem respiration, because soil carbon feedback to climate change is expected to outstrip carbon gains *via* photosynthesis. Loss of soil carbon in the form of CO_2 has the potential to add greatly to the CO_2 loading of the atmosphere and further exacerbate climate change by creating a positive feedback (IPCC, 2001). Moreover, it has been suggested that increases in soil respiration will exceed NPP by 25-50 % (Raich & Potter, 1995). As soil carbon cycling is less well understood than above ground carbon cycling, an incubation study was performed to examine the effects of abiotic variables

(both individually and interactively) on peatland soil carbon fluxes, primary and isotopic (Chapter 4).

The experimental design considered three variables: temperature (5, 10 and 15 °C), soil moisture content (50 and 100 % field capacity) and substrate quality (using 3 different depths in the peat profile as an analogue for substrate quality; 0-10, 10-20 and 20-30 cm). Results from the incubation study (Chapter 4) demonstrated that abiotic parameters such as temperature, soil moisture and substrate quality all have an important influence on soil decomposition rates and hence respired CO_2 fluxes. CO_2 fluxes were significantly greater (under identical temperature and moisture regimes) from incubated cores removed from the surface 10 cm of the peatland profile, relative to cores extracted from 10-20 and 20-30 cm depths. This is attributed to the presence of a greater amount of more labile soil organic matter (SOM) in the surface 10 cm of the peatland profile.

In addition to substrate quality, temperature was also found to increase soil respiration rates. Results showed that soil organic matter decomposition increased for every 5 °C step increase in temperature, under both moisture treatments, with most of these increases being significant at 2 σ_e (see Figure 4.9). This finding is contrary to results obtained by Giardina & Ryan (2000) and Liski *et al.* (2000) who suggested that soil organic matter decomposition was tolerant of temperature increase. However, this finding confirms theoretical predictions such as those offered by Bosatta & Ågren (1999).

The influence of soil moisture on soil decomposition was found to be less clear-cut than temperature effects. For example, reduced soil moisture (50 % field capacity) significantly increased respiration fluxes in the top 10 cm of the peat profile when incubated at 10 and 15 °C relative to those cores incubated at 100 % field capacity. Conversely, however, at lower depths in the profile, reduced soil moisture content caused soil respiration rates at 5 and 15 °C to be significantly higher.

Crucially, this experiment demonstrated the importance of examining the effects of abiotic factors, not just in isolation but also, interactively. The results of the incubation study demonstrated that decomposition of older more recalcitrant soil organic matter was more sensitive to temperature increase than more labile soil organic matter, when combined with the interactive effect of reduced soil moisture content. For example, mean Q_{10} values obtained for the 10-20 and 20-30 cm depths, incubated at 50 % soil moisture content, were significantly higher at 2 σ_e than those obtained for the 0-10 cm depth. The mean Q_{10} value for the 0-10 cm depth increment under the 50 % moisture treatment was 3.3 ± 0.3, whereas

for the 10-20 and 20-30 cm depth increments the Q_{10} values were 5.3 ± 1.1 and 9.7 ± 2.7 respectively, thus demonstrating that fluxes produced by the 20-30 cm depth increment were almost 3 times as sensitive to temperature increase when combined with reduced soil moisture, than decomposition occurring within the surface 10 cm.

The incubation study also involved an investigation into the stable isotopic ($\delta^{13}C$) signature of respired CO_2 under the three different treatments using firstly a method that incorporated the use of Exetainers, and secondly the use of the molecular sieve sampling system (MS^3) developed in Chapter 2. Initial results using the Exetainer technique revealed that the $\delta^{13}C$ values of respired CO_2 reflected the stable isotopic signature of soil organic matter and also that there were no statistically significant differences in the $\delta^{13}C$ values of respired CO_2 produced by the various treatments. This was partially attributed to propagation of error incorporated into mass balance calculations. Errors were found to be particularly large for treatments where relatively small volumes of respired CO_2 were produced (e.g. see Figure 4.10).

This problem was partially circumvented by extending the incubation time for treatment cores where respiration rates were slow (e.g. 5 °C and 50 % moisture content). Subsequent incubations revealed that only respired CO_2 produced by the 20-30 cm depth increment under the combined treatments of 15 °C and 50 % field moisture could be statistically distinguished at 2 σ_e from respired CO_2 produced by the 10-20 and 0-10 cm depth cores. Respired CO_2 produced by the 20-30 cm depth cores was enriched in ^{13}C relative to that produced at depths higher in the profile. This result again reflects the higher $\delta^{13}C$ values of soil organic matter with depth (see Table 4.1) but also suggests that the microbial population may have been accessing different carbon sources at this depth.

The use of MS^3 to characterise the stable isotopic signature of respired CO_2 produced by the incubation study revealed that at 15 °C, either different sources of carbon were being accessed by the microbial populations at the three different depths in the profile or that isotopic fractionation was occurring during decomposition. The $\delta^{13}C$ values of respired CO_2 were statistically distinguishable (> 2 σ_e) at all depths under the 15 °C treatment, and in addition demonstrated an enrichment in ^{13}C with increasing depth from the surface. However at 5 °C only CO_2 produced by the 0-10 cm depth was distinguishable statistically from that produced at lower depths in the peatland profile. The use of radiocarbon in this experiment may reveal more clearly whether, at increasing depth in the profile, different sources of carbon are being accessed during decomposition or whether an isotopic

fractionation effect is taking place. Furthermore, it has been successfully demonstrated in Chapter 4 that enough CO_2 can be collected from an incubation experiment for radiocarbon analysis by the use of MS^3.

The experiments undertaken in Chapters 3 and 4 attempted to distinguish different sources of carbon being respired by various components of a peatland ecosystem and also investigated the interactive effects of abiotic drivers on these sources *via* stable carbon isotope analysis. The final experiment (Chapter 5) aimed to distinguish sources of respired carbon using 'bomb' produced radiocarbon as a tracer in an *in situ* field study by firstly characterising the radiocarbon signature of respired CO_2 from two treatments ('soil' and 'ecosystem'). All possible sources that could contribute to the radiocarbon signature of respired CO_2 (i.e. plant tissue, dissolved organic carbon, bulk peat and the contemporary atmosphere) were characterised. A further objective was to attempt to partition 'ecosystem' respired CO_2 into its constituent components of plant and soil respired CO_2.

Results showed that peatland vegetation had a radiocarbon signature similar to that of the contemporary atmosphere in which they were growing (~ 106-107 %Modern). Cores of bulk peat removed from the top 16 cm of the peatland profile demonstrated a wide range of radiocarbon concentration from pre-bomb (~ 95 %Modern) to post-bomb with maximum ^{14}C enrichment reaching ~ 130 %Modern in any one 4 cm depth increment. Peat accumulation rates were calculated using a specified reference point (the lowest depth increment in each peat profile which contained bomb ^{14}C) and ranged from 0.08 to > 0.32 cm yr^{-1}. The ranges in peat accumulation rates are quite wide, but primarily the investigation centred on sources that contribute to 'ecosystem' and 'soil' respiration. Had the investigation not had that central theme, one cm depth increments would have been selected to better constrain peat accumulation rates.

The ^{14}C content of DOC was similar to that of bulk peat but with a slightly smaller range (~100 to ~122 %Modern). A plot of ^{14}C content of bulk peat versus the ^{14}C content of DOC (Figure 5.18) demonstrated a strong linear relationship with an r^2 value of 0.90 ($P > 0.99$). This plot showed that that the majority of ^{14}C contained in DOC (extracted from each 4 cm depth increment) was derived from the surrounding bulk peat. However, as the relationship was not 1:1, a modelling approach was utilised to elucidate other possible sources of ^{14}C that contribute to the DOC pool. Conceptual modelling of the data suggested that there was an additional contribution from DOC produced within the layer directly above in the profile (or plant litter when considering the surface 4 cm). This evidence supports the interpretation that gradual downward movement of DOC is taking place within the profile

at the experimental site as has been suggested in other peatland studies, e.g. Charman *et al.* (1994; 1999).

Respired CO_2 produced by both 'soil' and 'ecosystem' plots was characterised as to ^{14}C content, with results initially proving to be rather enigmatic. 'Soil' respired CO_2 captured from the three 'soil' plots had a mean ^{14}C signature of 114.94 ± 0.30 %Modern in August and 116.02 ± 0.20 %Modern in September. These results showed that there was a considerable amount of 'bomb' radiocarbon present in CO_2 produced by these plots, presumably from the decomposition of soil organic carbon containing ^{14}C produced by thermonuclear weapons testing. On comparison with the atmospheric $^{14}CO_2$ record (Levin & Kromer, 2004) these results indicated that the mean age of respired CO_2 produced by the 'soil' plots is about 15 years, relative to time of fixation. In addition, these results were extremely reproducible despite considerable variation in the height of the water table.

Respired CO_2 collected from the 'ecosystem' plots had an entirely different ^{14}C signature to the 'soil' plots, with mean ^{14}C concentrations for the former ranging from 106.95 ± 0.41 %Modern in August to 106.53 ± 0.17 %Modern in September. Results for the 'ecosystem' plots from both August and September were statistically indistinguishable from the ^{14}C content of the contemporary atmosphere. On initial inspection this might not appear unusual, as one would expect that the radiocarbon content of plant respired CO_2 would be similar to that of the atmosphere from which it was fixed. However, as 'ecosystem' respiration is identical to the atmosphere in ^{14}C concentration, this would indicate that the contribution to ecosystem respiration from soil is negligible (deduced purely from ^{14}C isotope mass balance).

Isotope mass balance was applied to the respiration results using a two end member approach; the ^{14}C signature of plant respiration was calculated and found to be between ~ 101 and 102 %Modern. This was considered unlikely, as it would have meant that plants were respiring carbon that was greater than 50 years old. Despite an extensive literature search, it would appear that the ^{14}C signature of plant respiration has not been directly measured. However, the ^{14}C signature of plant respiration is generally assumed to be similar to that of the contemporary atmosphere (Trumbore, 2000). Therefore, a three-component model approach was applied to the respiration results. This approach implied the existence of a third source of CO_2 (in addition to plant and soil) that contributes to total ecosystem respiration. This third source, was estimated to contribute ~ 20 % of total ecosystem respiration and was calculated to have an enriched stable carbon isotopic

signature of between ~ -5 and +10 ‰ with a corresponding ^{14}C signature of between ~ 80 and 96 %Modern.

It was postulated that the origin of this third source was deep peat. Peat gases produced at depth, *via* acetate fermentation, have been shown to produce CO_2 with positive $\delta^{13}C$ values of up to +10 ‰ (Bryant *et al.*, 2006; Charman *et al.*, 1999; Clymo & Bryant, in prep.). Furthermore, radiocarbon analyses of the base of the peat (~2.5 m) at nearby Shaft Hill (Garnett, unpublished data) have shown the peat to have a ^{14}C signature in the region of 45 %Modern (~ 6414 years). Therefore it was deemed very likely that gases produced at depth in the peat profile at the Hard Hill experimental site could have the required ^{14}C signature predicted by the three-component model.

The mechanism of transport for CO_2 produced at depth (termed here 'plant mediated catotelm CO_2') was postulated to be the same mechanism that transports methane from depth, i.e. facilitated by the aerenchymateous tissue of plants, a mechanism that has been shown to transport in excess of 90 % of methane release from peatlands (Shannon *et al.*, 1996). Modelling of results in this investigation showed that plant mediated catotelm CO_2 could contribute ~ 20 % of ecosystem respired CO_2.

To our knowledge this process has never been demonstrated before and could have considerable implications for carbon release from peatlands in the face of climate change. For example, Verville *et al.* (1998) demonstrated that sedge removal reduced CO_2 flux by up to 50 % and CH_4 flux by up to 60 %. In addition, Verville *et al.* (1998) also found that when compared to manipulation of soil and air temperatures, changes in vegetation species composition had the greater effect on peatland CO_2 efflux. The results from this thesis investigation add further evidence to the study by Verville *et al.* (1998) and a number of other studies, e.g. (Strom *et al.*, 2005), that changes in species composition, brought about by changes in climate, have the potential to impact on carbon cycling in peatlands (Verville *et al.*, 1998).

6.1 Suggestions for future research

6.1.1 Methodological improvements for field studies

All scientific studies are not without caveats in some shape or form, and therefore quite often a trade-off is necessary. For example, a compromise that is regularly made during the analysis of many samples measured by chromatography is one of reduced sample

resolution for an increase in sample throughput or *vice-versa*. Carbon cycling studies, particularly in peatlands are no different; however, trade-offs made will depend on exactly what is being measured. For example, in Chapter 3 partitioning of the stable isotope signature of respired CO_2 produced by different components of a peatland ecosystem was attempted. Methodological problems meant that of five treatments that were to have the stable carbon isotope composition of respired CO_2 characterised, only three could realistically be compared (however it should be remembered that only one replicate from the 'no monocots' treatment satisfied the flux criterion).

The main concern for attempting this type of measurement in the future is the presence of shrub roots underneath chamber collars. If chamber collars are not inserted to sufficient depth in the peat profile then loss of sample may occur. Conversely, if chamber collars are sunk too deep, this can result in the senescence of peatland vegetation, thus calling into question how representative of the entire ecosystem the vegetation contained within the chamber collar is. It is suggested that a number of trial runs on basic flux measurements be performed in the field to check that each chamber is not subject to loss of sample. Collars could then be moved or adjusted until sample integrity is preserved, and only then should isotopic analyses be performed on collected respiration samples.

The use of Exetainers is a very quick and easy method by which to measure respiration fluxes. However when combined with the Keeling plot approach to characterise the stable isotopic signature of CO_2 this technique does not have the required precision to partition sources with small differences in $\delta^{13}C$ values. However, it may be possible to improve estimates of the $\delta^{13}C$ values of source CO_2 if respiration chambers are first scrubbed of atmospheric CO_2. Even if there is a small amount of atmospheric CO_2 left in chambers after scrubbing, the $\delta^{13}C$ value of CO_2 in the chambers will reflect mainly the ecosystem itself, thus reducing the extrapolation error associated with the Keeling plot technique. This additional step may improve the error on the extrapolated intercept and hence the accuracy of $\delta^{13}C$ values obtained for source respired CO_2.

6.1.2 Methodological improvements for laboratory based studies

It was found during the course of Chapter 4, that increasing the incubation time of cores that produced small fluxes greatly reduced the error on calculated stable isotopic signatures of respired CO_2. However, even with increased incubation times, the stable isotopic signature of respired CO_2 produced by cores extracted from the surface 10 cm could not be

resolved from that produced by depths lower in the profile under 100 % field capacity conditions. Scrubbing of chambers before removal of CO_2 from respiration chambers could also be applied to incubation experiments. The comparison of the two sampling techniques (MS^3 versus Exetainers and isotope mass balance) demonstrated that the deployment of MS^3 in conjunction with chamber scrubbing allowed the $\delta^{13}C$ values of CO_2 produced by the surface 10 cm (under 100 % field capacity conditions) to be statistically distinguished from CO_2 produced by the two lower depths (10-20 and 20-30 cm) in the peat profile.

Bulk peat from the two lower depths had $\delta^{13}C$ values that were statistically identical at 1 σ, and therefore it is not too surprising that partitioning of the stable isotopic signature of CO_2 produced from the bulk peat could not be distinguished. MS^3 was successfully used to collect CO_2 from the incubation experiment in Chapter 4 to characterise the $\delta^{13}C$ of respired CO_2. It is suggested that radiocarbon analysis of respired CO_2 produced by incubation experiments may provide a more revealing insight into pools of carbon in the soil that are being accessed by the soil microbiota.

6.1.3 Future field research

One of the key findings of this thesis was the demonstration of a third source (plant mediated catotelm CO_2) of CO_2 that contributes to total ecosystem respiration. However, further verification of this source is required. The comparison of plots in the field where vegetation has been removed ('soil') and where vegetation is left intact ('ecosystem'), similar to those established for experimental work in Chapters 3 and 5, is required. There are a number of options for experimental work on these plots including the use of some type of artificial plant (anything that will facilitate the transport of CO_2 from depth to the atmosphere) and isotope labelling approaches. The two labelling approaches suggested here are either, one of a labelled atmosphere in which to grow peatland plants (e.g. ^{14}C free air), and comparing respired CO_2 produced in these plots with respired CO_2 produced by vegetation that has been grown in an unlabelled atmosphere. Alternatively, placing a ^{14}C labelled substrate such as glucose into the soil within the root zone of grasses and sedges may help to establish definitively the plant mediated transport of CO_2 from depth to the atmosphere.

In addition to the above, similar research (i.e. the characterisation of 'soil' and 'ecosystem' respiration) should be carried out at different peatland sites, both fen and moor, in order to establish variations both in the contribution and isotopic signature of plant mediated catotelm CO_2. A natural extension to this research would be to characterise the isotopic

signature of respiration, using MS^3, in a number of other ecosystems such as boreal forest, Arctic tundra and grassland sites.

6.2 Conclusions

The main findings from this thesis investigation are as follows:

1. A portable sampling system was developed (MS^3) incorporating zeolite molecular sieve, which can capture CO_2 for stable and radiocarbon analysis without contamination, fractionation or hysteresis. The sampling system and its application in studies of respiration and carbon cycling, both *in situ* and *ex situ*, has the potential to be applied in a wide range of ecosystems, and has already been successfully used for the capture of CO_2 evaded from peatland streams (Billett *et al.*, 2006). Furthermore, unlike traditional methods of capture (e.g. NaOH), MS^3 can be used to collect CO_2 from remote areas of the world such as the Arctic or Antarctic. Once captured on MSCs, samples may then be transported *via* aeroplane, all over the world for AMS analysis. This would not be the case for samples of CO_2 trapped in liquid N_2 or alkaline solutions such as NaOH.

2. The use of stable carbon isotopes as a technique for partitioning respired CO_2 emitted by different components of an ecosystem containing vegetation species utilising only a single photosynthetic pathway has limited use, particularly when the method of collection is *via* Exetainers. The reasons for this are mainly methodological. For example, the presence of shrub roots under chamber collars can lead to loss of sample. In addition, extrapolation of the linear regression of data presented in a Keeling plot may lead to large errors in the intercept, and hence in the interpretation of $\delta^{13}C$ values of source respiration. The shrub root problem will be an inherent one for all peatland flux studies that use the static sampling chamber technique. Careful placement of chamber collars may reduce or eliminate problems with shrub roots; however in this thesis careful site selection was performed, but did not eliminate problems with a large number of chambers.

3. Temperature was found to significantly increase fluxes of CO_2 from incubated cores removed from 3 different depths in the peat profile (0-10, 10-20 and 20-30 cm), with one exception on day 34 (10-20 cm) which exhibited higher flux rates than on the remaining sampling dates. Decreased moisture (from 100 to 50 % field capacity) was found to significantly increase respiration fluxes from the surface 10

cm of the peat profile. However this was not true for depths lower in the profile, where reduced moisture decreased respiration fluxes. Stable carbon isotope analyses used in conjunction with the Exetainer technique failed to distinguish sources of respired CO_2 produced by different depths in the peat profile. The use of MS^3 to determine the $\delta^{13}C$ values of CO_2 respired produced from different depths in the profile allowed sources of CO_2 to be statistically distinguished at 15 °C but not at 5 °C. It is suggested radiocarbon may be a more powerful isotopic tool in this regard.

4. Radiocarbon analysis of both 'soil' and 'ecosystem' respiration in the field was successfully characterised by the use of MS^3. Modelling demonstrated there to be a third source of CO_2, produced within the deep peat, which contributes to total ecosystem respiration. Plant mediated catotelm CO_2 is estimated to contribute up to ~ 20 % to total ecosystem CO_2 flux. To the best of our knowledge, this is the first time that the process of release of plant mediated catotelm CO_2 to the atmosphere has been observed (made possible by the successful development of MS^3) and has potentially significant implications for carbon cycling within peatland ecosystems.

Appendix i

Testing the use of septum capped vials for analysis of carbon dioxide concentration

Several methods for collecting CO_2 have been developed for soil respiration studies. A method of CO_2 collection that has become popular recently is injection into small (3 ml – 12 ml) screw cap (containing butyl rubber septa) soda-glass/borosilicate glass vials after withdrawal from a chamber placed over the soil. To test how Exetainers performed at maintaining the concentration of a standard gas, one hundred and twenty, 3 ml Exetainers were evacuated to 10^{-1} mbar and filled with 5 ml of a standard gas (541 ppm, BOC Edwards, UK). Half of the Exetainers were stored in the laboratory at 20 °C. The other 60 Exetainers were stored at 5 °C for 24 hours, followed by storage at 20 °C for the remainder of the test period. Storage at 5 °C for 24 hours was carried out in order to investigate whether any pressure effects might occur when sampling in the field (e.g. when carrying out a diurnal sampling). Both sets of 60 Exetainers were analysed at 12 time points (5 replicates per time point) over a period of 51 days, by gas chromatography.

Figure A1.1 illustrates the concentration of CO_2 measured in Exetainers stored at 20 °C

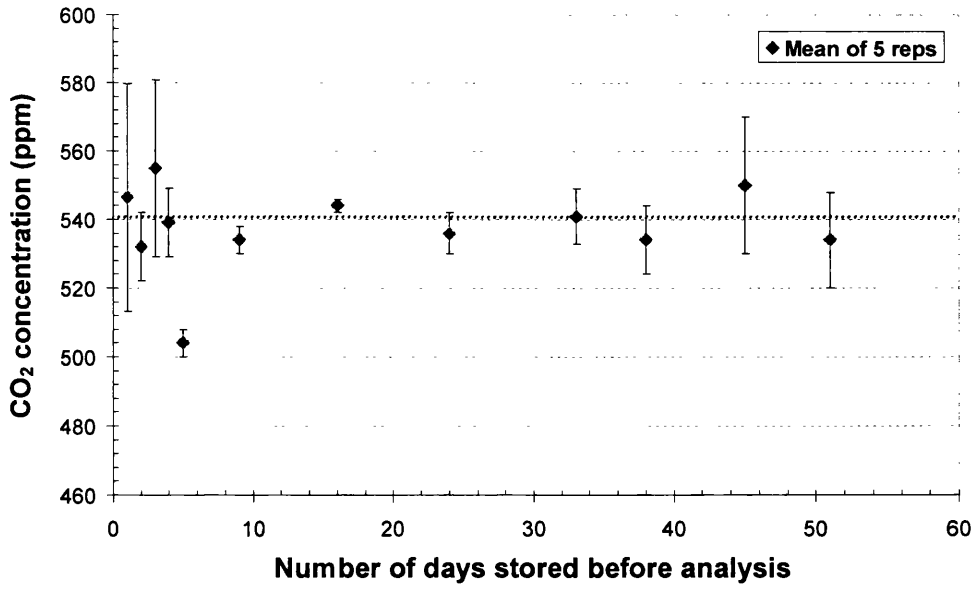

Figure A1.1 – Changes in CO_2 concentration of the 541 ppm standard over the course of the storage period. Storage temperature was 20 °C for the entire 51-day test. The dotted line denotes the concentration of the CO_2 standard. Error bars are 2 standard deviations.

over the course of the test period. The plot shows that the mean CO_2 concentration for each time point stored over the 51-day period is within 10 ppm of the standard, except on two occasions; days 3 and 5. Mean CO_2 concentrations are statistically the same at 2 σ for all days, with the one exception of day 5. Figure A1.2 shows how CO_2 concentration varies

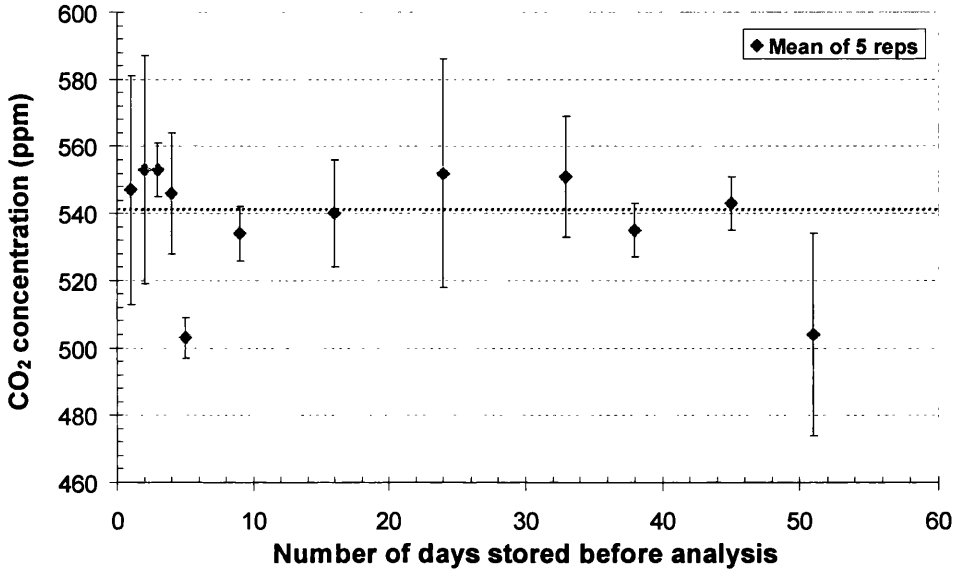

Figure A1.2 – Changes in CO_2 concentration of the 541 ppm standard over the course of the storage period. Exetainers stored at 5 °C for the first 24 hours and subsequently at 20 °C for the remainder of the 51-day test. The dotted line denotes the concentration of the CO_2 standard. Error bars are 2 standard deviations.

with storage time for Exetainers stored at 5°C for the first 24 hours, followed by storage at 20 °C for the remainder of the test period. The larger error bars on sampling points in this plot indicate greater variability in the CO_2 concentration relative to those in Figure A1.2. Mean CO_2 concentrations are within 11 ppm of the standard concentration for all time points except those on days 5 and 51. The CO_2 concentration for all time points are statistically indistinguishable from the standard concentration except for that measured on days 5 and 51.

The results from both storage treatments indicate that Exetainers are suitable for storing CO_2 for up to a period of 45 days without any significant change in CO_2 concentration. However, vials stored for 51 days that were kept at 5°C for the first 24 hours showed a significant deviation in concentration from the standard. This finding suggests that storage of sample vials at 5 °C or less for 24 hours or more may lead to loss of sample. It is suggested therefore that all CO_2 samples that are collected and stored in Exetainers be stored at temperatures close to those occurring at the time of filling. In addition, it is

recommended that samples meant for CO_2 analysis are stored for a period of no longer than 45 days before analysis, with a time period of not more than 30 days being preferable.

Appendix ii

Methane fluxes for field experiment performed in May 2005

In addition to the CO_2 fluxes measured during the course of the experiment performed in Chapter 3, CH_4 fluxes were also recorded and were as follows:

'Soil' treatment:

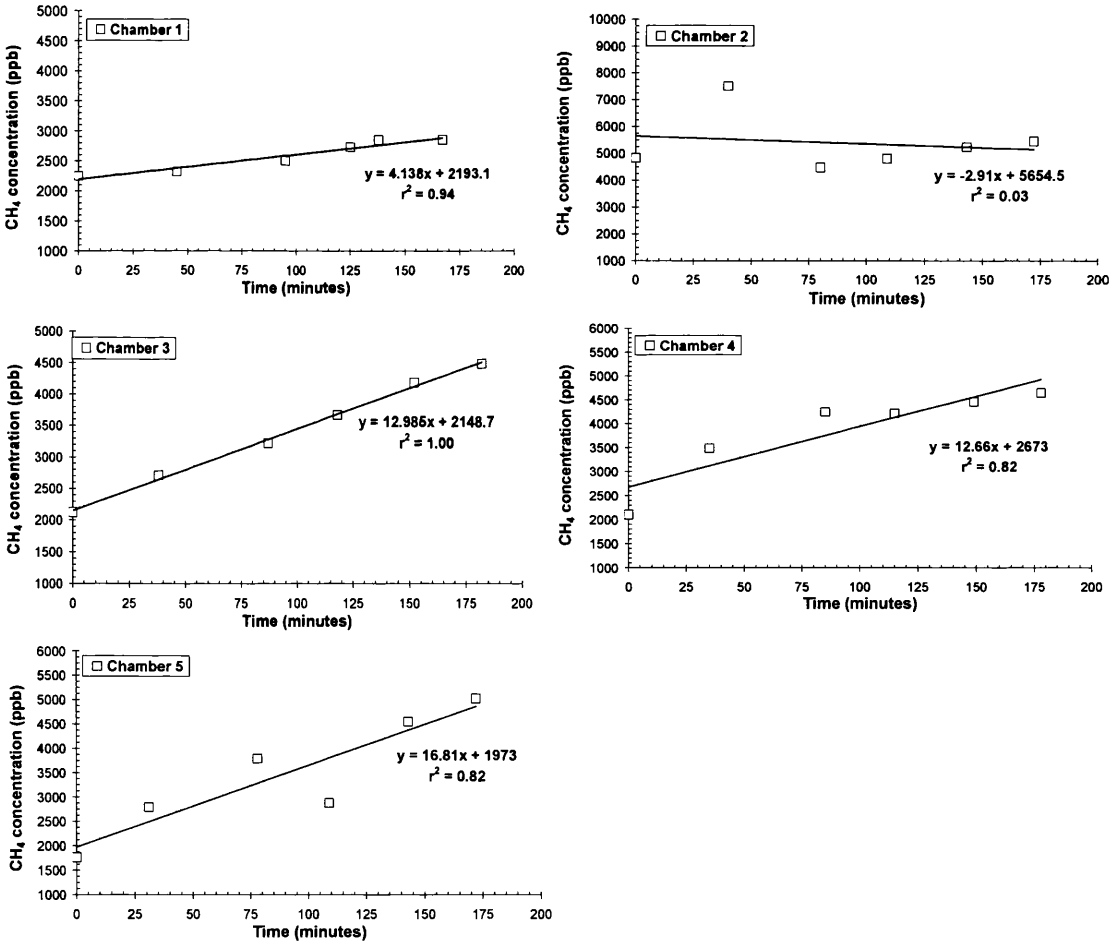

Figure A2.1 – CH_4 concentration for five replicate treatments in which all the peatland vegetation had been removed (i.e. soil respiration).

'Ecosystem' treatment:

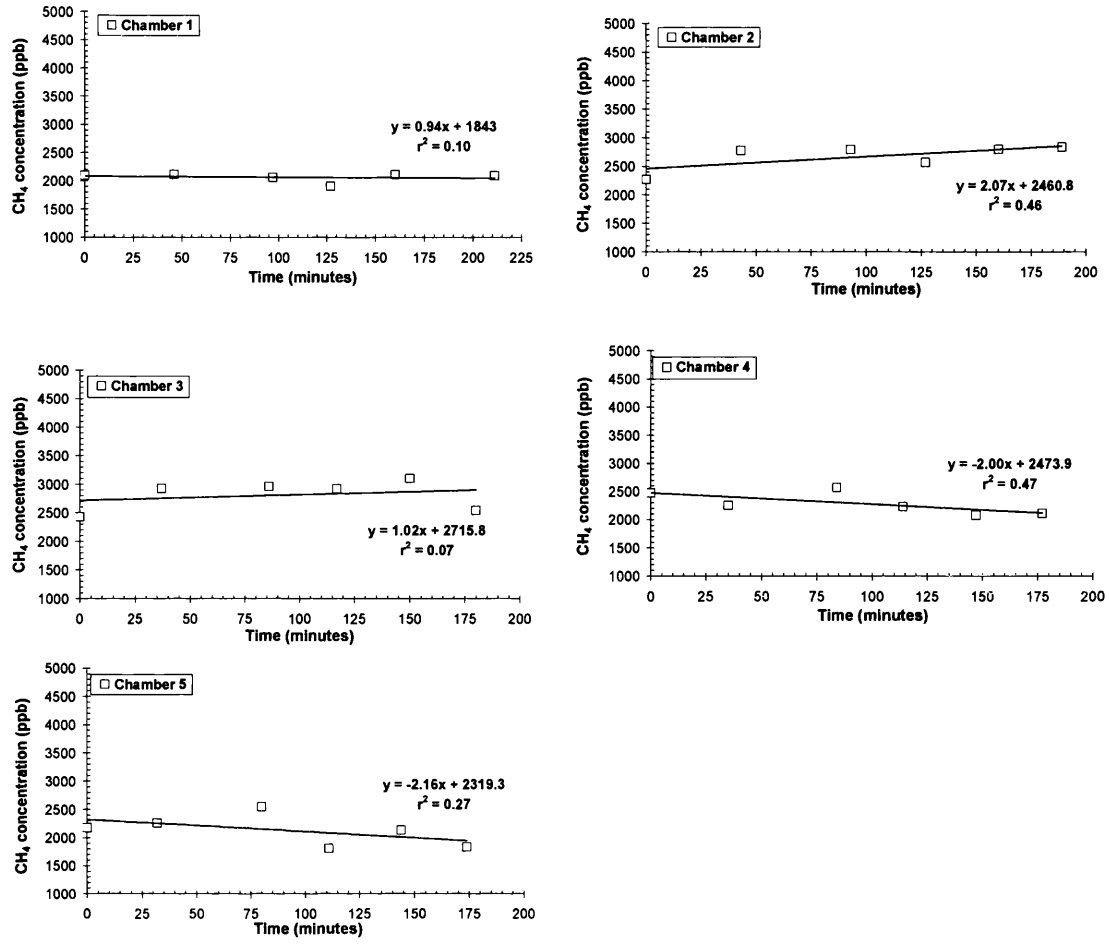

Figure A2.2 – CH_4 concentration within five replicate treatments containing the 'ecosystem' treatment (all peatland vegetation was left intact).

'No shrubs' treatment:

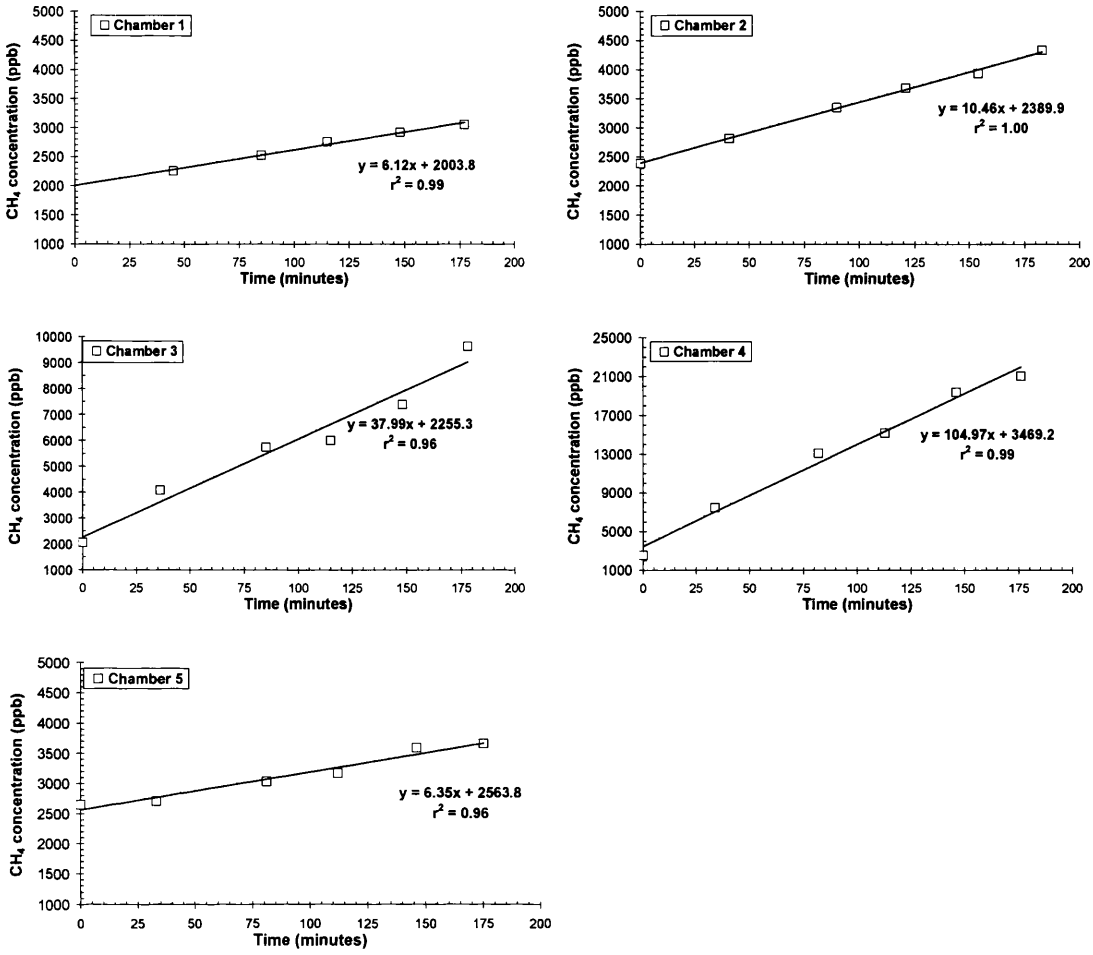

Figure A2.3 – CH_4 concentration within chambers containing the 'no shrubs' treatment over a six point time series.

'No monocots' treatment:

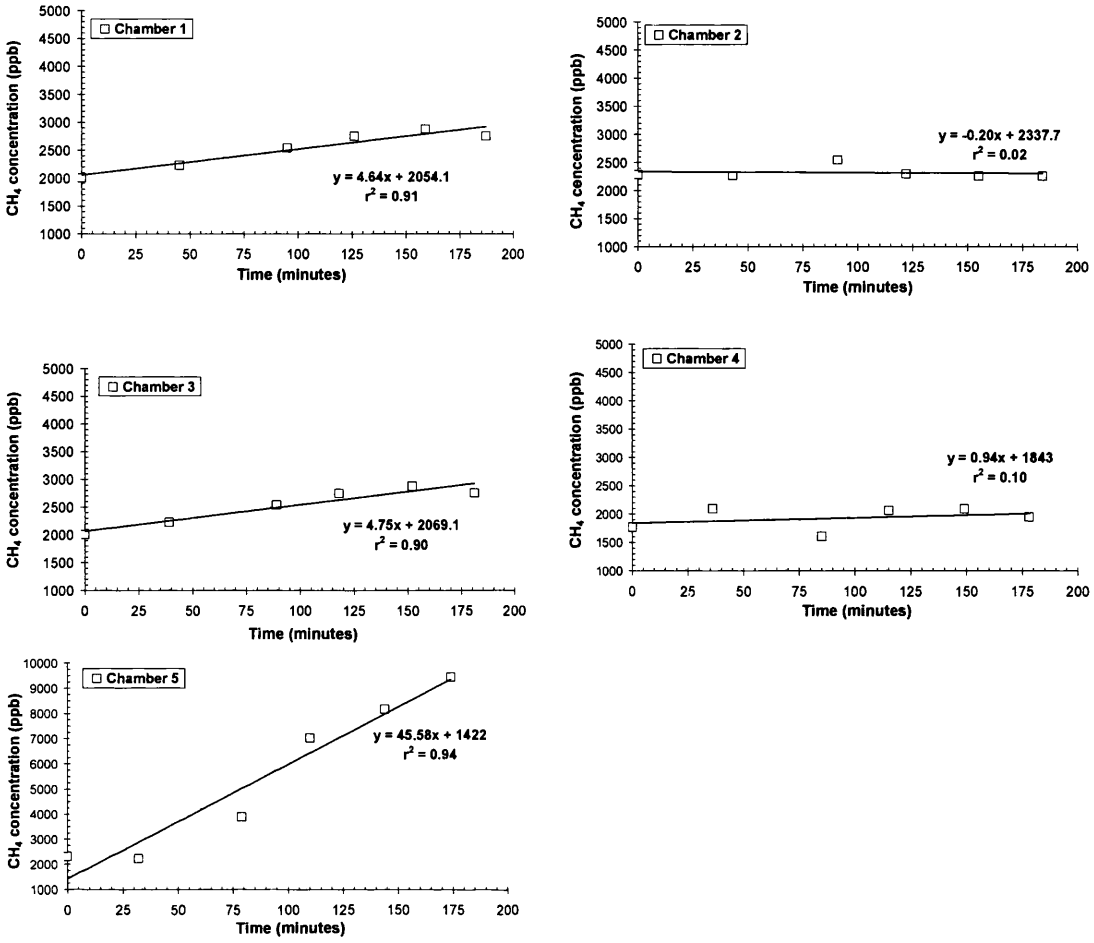

Figure A2.4 – CH_4 concentration within five chambers in which all the monocots had been removed.

'No moss' treatment:

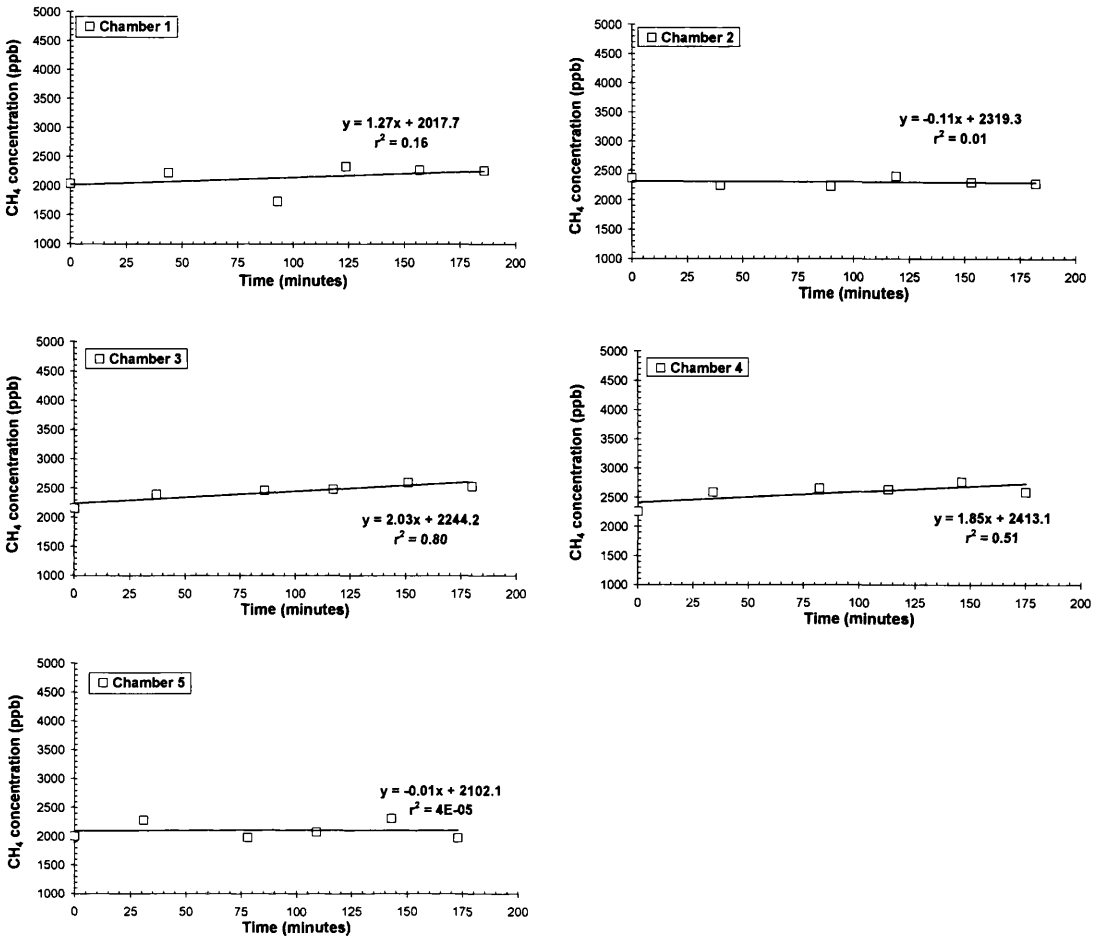

Figure A2.5 – CH_4 concentration within five respiration chambers in which all the bryophytes had been removed.

Appendix iii

Temperature data recorded during field experiment performed in May 2005

The graph displayed in Figure A3.1 illustrates temperatures recorded in the field during collection of data for Chapter 3.

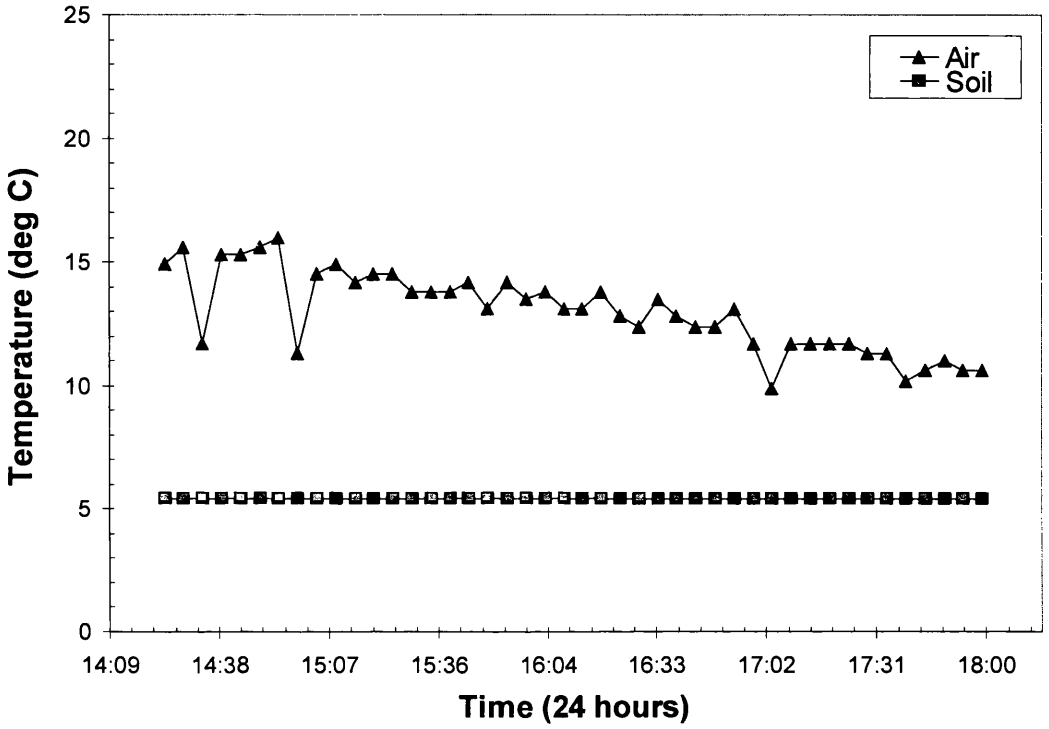

Figure A3.1 - Temperature data recorded for the atmosphere and soil during the Keeling plot time series, sampled in May 2005.

Appendix iv

Linearity test for respiration collected from incubated cores

Three surface cores held at 15 °C and 100 % field capacity were incubated in closed microcosms for a period of 3 days to establish a period over which respiration was linear. Figure A4.1 illustrates the linear regressions performed on respiration data.

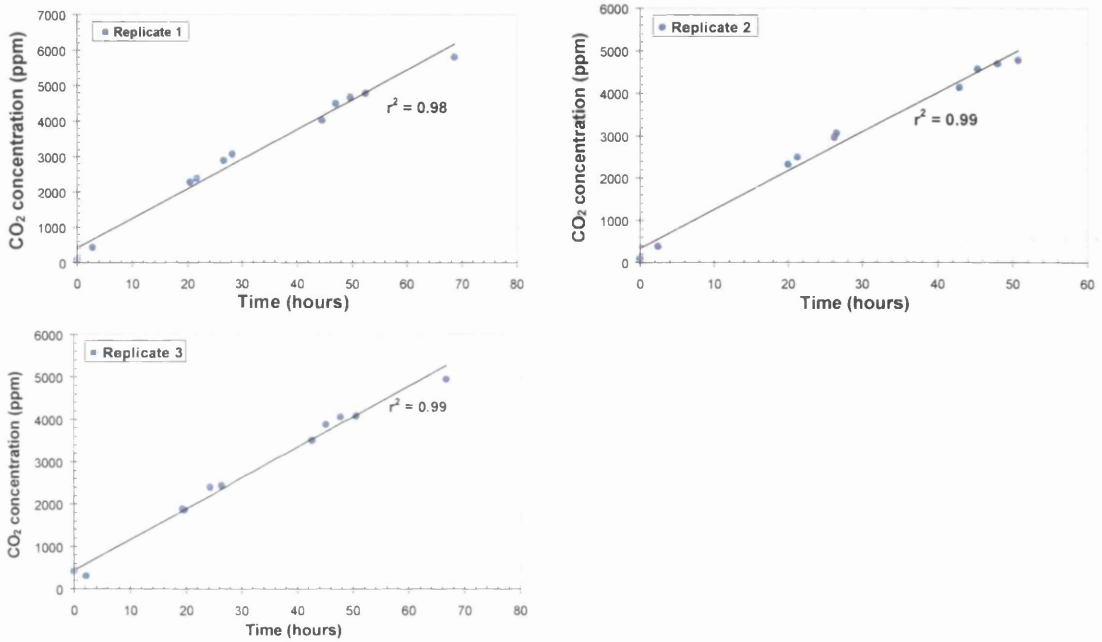

Figure A4.1– Plots illustrate respired CO_2 collected from three cores over a 2-3 day incubation period. Respiration was collected from cores incubated at 15 °C and 100 % field capacity.

r^2 values obtained were 0.99 for < 5000 ppm and 0.98 < 5500 ppm ($P > 0.99$) for plots of accumulated respiration.

Concentration and $\delta^{13}C$ data for CO_2 respired during soil incubation experiment

There now follows a number of tables containing all data acquired for the incubation experiment in Chapter 4 on days 34, 42, 84 and 116.

Day 34

Depth (cm)	5 deg C % Moisture/ Rep	CO_2 flux per day	10 deg C % Moisture/ Rep	CO_2 flux per day	15 deg C % Moisture/ Rep	CO_2 flux per day
0-10	5°C – 100% -1	25.4	10°C – 100% - 1	26.6	15°C – 100% -1	99.5
0-10	5°C – 100% - 2	22.0	10°C – 100% - 2	39.2	15°C – 100% -2	58.8
0-10	5°C – 100%- 3	24.9	10°C – 100%- 3	50.0	15°C – 100%-3	92.2
0-10	5°C – 100% -4	23.4	10°C – 100% -4	38.5	15°C – 100% -4	88.2
0-10	5°C – 100% -5	17.4	10°C – 100% -5	47.5	15°C – 100% -5	76.6
	Mean	**22.6**	**Mean**	**40.4**	**Mean**	**83.1**
	St Dev	**3.2**	**St Dev**	**9.2**	**St Dev**	**14.2**
10-20	**5°C – 100% -1**	25.7	**10°C – 100% - 1**	27.5	**15°C – 100% -1**	47.9
10-20	**5°C – 100% -2**	23.6	**10°C – 100% - 2**	26.3	**15°C – 100% -2**	50.3
10-20	**5°C – 100%-3**	13.5	**10°C – 100%- 3**	19.0	**15°C – 100%-3**	35.7
10-20	**5°C – 100% -4**	18.8	**10°C – 100% -4**	22.6	**15°C – 100% -4**	21.1
10-20	**5°C – 100% -5**	15.5	**10°C – 100% -5**	16.3	**15°C – 100% -5**	57.1
		19.4	**Mean**	**22.3**	**Mean**	**42.4**
	St Dev	**5.2**	**St Dev**	**4.8**	**St Dev**	**14.2**
20-30	5°C – 100% -1	5.2	10°C – 100% - 1	19.6	15°C – 100% -1	32.3
20-30	5°C – 100% - 2	9.6	10°C – 100% - 2	16.7	15°C – 100% -2	37.2
20-30	5°C – 100%- 3	8.1	10°C – 100%- 3	19.0	15°C – 100%-3	36.9
20-30	5°C – 100% -4	10.2	10°C – 100% -4	17.7	15°C – 100% -4	25.2
20-30	5°C – 100% -5	4.5	10°C – 100% -5	11.5	15°C – 100% -5	26.8
	Mean	**7.5**	**Mean**	**16.9**	**Mean**	**31.7**
	St Dev	**2.6**	**St Dev**	**3.2**	**St Dev**	**5.0**
0-10	**5°C – 50% -1**	20.5	**10°C – 50% -1**	54.3	**15°C – 50% -1**	128.0
0-10	**5°C – 50% -2**	24.2	**10°C – 50% -2**	52.0	**15°C – 50% -2**	119.2
0-10	**5°C – 50%-3**	16.6	**10°C – 50%-3**	51.5	**15°C – 50%-3**	121.2
0-10	**5°C – 50% -4**	18.2	**10°C – 50% -4**	53.6	**15°C – 50% -4**	94.3
0-10	**5°C – 50% -5**	26.6	**10°C – 50% -5**	53.0	**15°C – 50% -5**	85.8
		21.2	**Mean**	**52.9**	**Mean**	**109.7**
	St Dev	**4.2**	**St Dev**	**1.2**	**St Dev**	**16.5**
10-20	5°C – 50% -1	4.3	10°C – 50% -1	24.6	15°C – 50% -1	30.3
10-20	5°C – 50% -2	-	10°C – 50% -2	21.5	15°C – 50% -2	33.0
10-20	5°C – 50%-3	1.9	10°C – 50%-3	23.2	15°C – 50%-3	33.3
10-20	5°C – 50% -4	4.1	10°C – 50% -4	15.3	15°C – 50% -4	32.3
10-20	5°C – 50% -5	5.3	10°C – 50% -5	16.6	15°C – 50% -5	57.9
	Mean	**3.9**	**Mean**	**20.2**	**Mean**	**37.4**
	St Dev	**1.4**	**St Dev**	**4.1**	**St Dev**	**10.3**
20-30	**5°C – 50% -1**	1.2	**10°C – 50% -1**	4.4	**15°C – 50% -1**	26.5
20-30	**5°C – 50% -2**	-	**10°C – 50% -2**	20.0	**15°C – 50% -2**	33.5
20-30	**5°C – 50%-3**	2.8	**10°C – 50%-3**	10.1	**15°C – 50%-3**	27.3
20-30	**5°C – 50% -4**	1.3	**10°C – 50% -4**	7.7	**15°C – 50% -4**	26.3
20-30	**5°C – 50% -5**	-	**10°C – 50% -5**	7.7	**15°C – 50% -5**	24.8
	Mean	**1.75**	**Mean**	**10.0**	**Mean**	**27.7**
	St Dev	**0.9**	**St Dev**	**5.9**	**St Dev**	**3.0**

A4.2 - Flux data for each individual peat core on day 34 of the incubation. Fluxes are given in mg CO_2-C g $soil^{-1}$ d^{-1}.

Day 41

Depth (cm)	5 deg C % Moisture/ Rep	CO_2 flux per day	10 deg C % Moisture/ Rep	CO_2 flux per day	15 deg C % Moisture/ Rep	CO_2 flux per day
0-10	5°C – 100% -1	21.8	10°C – 100% - 1	29.5	15°C – 100% -1	62.9
0-10	5°C – 100% - 2	25.3	10°C – 100% - 2	43.0	15°C – 100% -2	67.8
0-10	5°C – 100%- 3	29.6	10°C – 100%- 3	50.0	15°C – 100%-3	84.9
0-10	5°C – 100% -4	20.4	10°C – 100% -4	42.5	15°C – 100% -4	75.1
0-10	5°C – 100% -5	22.5	10°C – 100% -5	52.3	15°C – 100% -5	63.1
	Mean	**23.9**	**Mean**	**43.5**	**Mean**	**70.8**
	St Dev	**3.7**	**St Dev**	**8.9**	**St Dev**	**9.3**
10-20	**5°C – 100% -1**	27.8	**10°C – 100% - 1**	24.9	**15°C – 100% -1**	48.0
10-20	**5°C – 100% -2**	9.1	**10°C – 100% - 2**	25.3	**15°C – 100% -2**	45.3
10-20	**5°C – 100%-3**	11.4	**10°C – 100%- 3**	18.9	**15°C – 100%-3**	38.7
10-20	**5°C – 100% -4**	15.6	**10°C – 100% -4**	21.2	**15°C – 100% -4**	32.6
10-20	**5°C – 100% -5**	8.6	**10°C – 100% -5**	15.9	**15°C – 100% -5**	55.2
	Mean	**14.5**	**Mean**	**21.3**	**Mean**	**44.0**
	St Dev	**7.9**	**St Dev**	**4.0**	**St Dev**	**8.7**
20-30	5°C – 100% -1	8.7	10°C – 100% - 1	16.2	15°C – 100% -1	34.9
20-30	5°C – 100% - 2	12.6	10°C – 100% - 2	13.3	15°C – 100% -2	35.7
20-30	5°C – 100%- 3	8.9	10°C – 100%- 3	15.2	15°C – 100%-3	26.3
20-30	5°C – 100% -4	10.5	10°C – 100% -4	16.7	15°C – 100% -4	25.2
20-30	5°C – 100% -5	5.3	10°C – 100% -5	9.5	15°C – 100% -5	26.4
	Mean	**9.2**	**Mean**	**14.2**	**Mean**	**29.7**
	St Dev	**2.7**	**St Dev**	**2.9**	**St Dev**	**5.2**
0-10	**5°C – 50% -1**	15.6	**10°C – 50% -1**	54.8	**15°C – 50% -1**	113.7
0-10	**5°C – 50% -2**	28.0	**10°C – 50% -2**	48.7	**15°C – 50% -2**	101.1
0-10	**5°C – 50%-3**	16.8	**10°C – 50%-3**	52.0	**15°C – 50%-3**	96.5
0-10	**5°C – 50% -4**	20.5	**10°C – 50% -4**	51.1	**15°C – 50% -4**	70.2
0-10	**5°C – 50% -5**	26.0	**10°C – 50% -5**	54.7	**15°C – 50% -5**	76.9
	Mean	**21.4**	**Mean**	**52.2**	**Mean**	**91.7**
	St Dev	**5.5**	**St Dev**	**2.6**	**St Dev**	**17.9**
10-20	5°C – 50% -1	5.3	10°C – 50% -1	25.2	15°C – 50% -1	20.7
10-20	5°C – 50% -2	6.6	10°C – 50% -2	17.4	15°C – 50% -2	20.9
10-20	5°C – 50%-3	4.7	10°C – 50%-3	22.5	15°C – 50%-3	18.6
10-20	5°C – 50% -4	4.3	10°C – 50% -4	11.3	15°C – 50% -4	20.6
10-20	5°C – 50% -5	3.7	10°C – 50% -5	15.6	15°C – 50% -5	43.2
	Mean	**4.9**	**Mean**	**18.4**	**Mean**	**24.8**
	St Dev	**1.13**	**St Dev**	**5.5**	**St Dev**	**10.3**
20-30	**5°C – 50% -1**	3.0	**10°C – 50% -1**	8.1	**15°C – 50% -1**	18.5
20-30	**5°C – 50% -2**	2.0	**10°C – 50% -2**	9.6	**15°C – 50% -2**	22.6
20-30	**5°C – 50%-3**	3.7	**10°C – 50%-3**	9.4	**15°C – 50%-3**	18.9
20-30	**5°C – 50% -4**	1.7	**10°C – 50% -4**	7.2	**15°C – 50% -4**	16.1
20-30	**5°C – 50% -5**	2.7	**10°C – 50% -5**	9.4	**15°C – 50% -5**	16.1
	Mean	**2.6**	**Mean**	**8.7**	**Mean**	**18.4**
	St Dev	**0.82**	**St Dev**	**1.06**	**St Dev**	**2.7**

A4.3 - Flux data for each individual peat core on day 41 of the incubation. Fluxes are given in mg CO_2-C g soil^{-1} d^{-1}.

Day 41

	5 deg C		10 deg C		15 deg C	
Depth (cm)	**% Moisture/ Rep**	**$\delta^{13}C$**	**% Moisture/ Rep**	**$\delta^{13}C$**	**% Moisture/ Rep**	**$\delta^{13}C$**
0-10	5°C – 100% -1	-35.3	10°C – 100% -1	-27.5	15°C – 100% -1	-23.3
0-10	5°C – 100% - 2	-28.1	10°C – 100% -2	-25.6	15°C – 100% -2	-23.9
0-10	5°C – 100%- 3	-26.8	10°C – 100%-3	-24.3	15°C – 100%-3	-22.8
0-10	5°C – 100% -4	-33.8	10°C – 100% -4	-24.7	15°C – 100% -4	-25.5
0-10	5°C – 100% -5	-24.9	10°C – 100% -5	-22.5	15°C – 100% -5	-24.8
	Mean	**-29.8**	**Mean**	**-24.9**	**Mean**	**-24.1**
	St Dev	**4.5**	**St Dev**	**1.9**	**St Dev**	**1.1**
10-20	**5°C – 100% -1**	-22.1	**10°C – 100% -1**	-24.9	**15°C – 100% -1**	-22.6
10-20	**5°C – 100% -2**	-34.5	**10°C – 100% -2**	-23.5	**15°C – 100% -2**	-18.7
10-20	**5°C – 100%-3**	-30.4	**10°C – 100%-3**	-29.1	**15°C – 100%-3**	-25.1
10-20	**5°C – 100% -4**	-23.8	**10°C – 100% -4**	-24.4	**15°C – 100% -4**	-26.6
10-20	**5°C – 100% -5**	-22.6	**10°C – 100% -5**	-29.1	**15°C – 100% -5**	-28.1
	Mean	**-26.7**	**Mean**	**-26.2**	**Mean**	**-24.2**
	St Dev	**5.5**	**St Dev**	**2.7**	**St Dev**	**3.7**
20-30	5°C – 100% -1	-28.4	10°C – 100% -1	-25.4	15°C – 100% -1	-25.6
20-30	5°C – 100% -2	-21.8	10°C – 100% -2	-28.9	15°C – 100% -2	-26.7
20-30	5°C – 100%-3	-17.8	10°C – 100%-3	-26.3	15°C – 100%-3	-22.0
20-30	5°C – 100% -4	-17.6	10°C – 100% -4	-25.5	15°C – 100% -4	-22.3
20-30	5°C – 100% -5	-	10°C – 100% -5	-31.2	15°C – 100% -5	-25.6
	Mean	**-21.4**	**Mean**	**-27.5**	**Mean**	**-24.4**
	St Dev	**5.0**	**St Dev**	**2.5**	**St Dev**	**2.1**
0-10	**5°C – 50% -1**	-18.3	**10°C – 50% -1**	-26.4	**15°C – 50% - 1**	-27.4
0-10	**5°C – 50% -2**	-22.7	**10°C – 50% -2**	-26.3	**15°C – 50% - 2**	-28.1
0-10	**5°C – 50%-3**	-19.5	**10°C – 50%-3**	-24.7	**15°C – 50%- 3**	-28.2
0-10	**5°C – 50% -4**	-21.9	**10°C – 50% -4**	-27.6	**15°C – 50% - 4**	-27.5
0-10	**5°C – 50% -5**	-22.7	**10°C – 50% -5**	-26.0	**15°C – 50% - 5**	-27.4
	Mean	**-21.0**	**Mean**	**-26.2**	**Mean**	**-27.7**
	St Dev	**2.0**	**St Dev**	**1.0**	**St Dev**	**0.4**
10-20	5°C – 50% -1	-17.9	10°C – 50% -1	-23.8	15°C – 50% -1	-28.2
10-20	5°C – 50% -2	-19.9	10°C – 50% -2	-27.0	15°C – 50% -2	-29.8
10-20	5°C – 50%-3	-19.0	10°C – 50%-3	-24.9	15°C – 50%-3	-31.3
10-20	5°C – 50% -4	-33.9	10°C – 50% -4	-23.5	15°C – 50% -4	-28.5
10-20	5°C – 50% -5	-19.0	10°C – 50% -5	-27.3	15°C – 50% -5	-28.5
	Mean	**-21.9**	**Mean**	**-25.3**	**Mean**	**-29.2**
	St Dev	**6.7**	**St Dev**	**1.8**	**St Dev**	**1.3**
20-30	**5°C – 50% -1**	-12.9	**10°C – 50% -1**	-25.2	**15°C – 50% -1**	-29.5
20-30	**5°C – 50% -2**	-14.4	**10°C – 50% -2**	-	**15°C – 50% -2**	-28.0
20-30	**5°C – 50%-3**	-39.4	**10°C – 50%-3**	-24.5	**15°C – 50%-3**	-27.3
20-30	**5°C – 50% -4**	-3.1	**10°C – 50% -4**	-32.2	**15°C – 50% -4**	-31.1
20-30	**5°C – 50% -5**	-13.1	**10°C – 50% -5**	-20.6	**15°C – 50% -5**	-28.6
	Mean	**-16.6**	**Mean**	**-25.6**	**Mean**	**-28.9**
	St Dev	**13.5**	**St Dev**	**4.9**	**St Dev**	**1.5**

A4.4 - Calculated stable carbon isotopic signature (per mil) of source CO_2 for each individual core.

Day 84

Depth (cm)	5 deg C % Moisture/ Rep	CO_2 flux per day	10 deg C % Moisture/ Rep	CO_2 flux per day	15 deg C % Moisture/ Rep	CO_2 flux per day
0-10	5°C – 100% -1	24.1	10°C – 100% - 1	25.4	15°C – 100% -1	57.6
0-10	5°C – 100% - 2	25.1	10°C – 100% - 2	35.4	15°C – 100% -2	58.1
0-10	5°C – 100%- 3	25.3	10°C – 100%- 3	40.5	15°C – 100%-3	72.4
0-10	5°C – 100% -4	25.1	10°C – 100% -4	35.9	15°C – 100% -4	68.4
0-10	5°C – 100% -5	15.4	10°C – 100% -5	57.6	15°C – 100% -5	43.8
	Mean	**23.0**	**Mean**	**38.9**	**Mean**	**60.1**
	St Dev	**3.8**	**St Dev**	**10.6**	**St Dev**	**10.0**
10-20	**5°C – 100% -1**	13.6	**10°C – 100% - 1**	26.4	**15°C – 100% -1**	44.8
10-20	**5°C – 100% -2**	10.3	**10°C – 100% - 2**	23.4	**15°C – 100% -2**	37.1
10-20	**5°C – 100%-3**	8.2	**10°C – 100%- 3**	19.9	**15°C – 100%-3**	27.0
10-20	**5°C – 100% -4**	16.5	**10°C – 100% -4**	19.8	**15°C – 100% -4**	24.5
10-20	**5°C – 100% -5**	11.8	**10°C – 100% -5**	8.1	**15°C – 100% -5**	48.7
	Mean	**12.1**	**Mean**	**19.5**	**Mean**	**36.4**
	St Dev	**3.2**	**St Dev**	**6.2**	**St Dev**	**9.5**
20-30	5°C – 100% -1	10.0	10°C – 100% - 1	18.6	15°C – 100% -1	37.1
20-30	5°C – 100% - 2	10.4	10°C – 100% - 2	14.1	15°C – 100% -2	34.5
20-30	5°C – 100%- 3	10.7	10°C – 100%- 3	18.0	15°C – 100%-3	30.2
20-30	5°C – 100% -4	-	10°C – 100% -4	21.5	15°C – 100% -4	24.4
20-30	5°C – 100% -5	6.9	10°C – 100% -5	11.0	15°C – 100% -5	23.9
	Mean	**9.5**	**Mean**	**16.6**	**Mean**	**30.0**
	St Dev	**1.77**	**St Dev**	**3.7**	**St Dev**	**5.3**
0-10	**5°C – 50% -1**	30.1	**10°C – 50% -1**	62.2	**15°C – 50% -1**	115.8
0-10	**5°C – 50% -2**	31.1	**10°C – 50% -2**	67.7	**15°C – 50% -2**	107.0
0-10	**5°C – 50%-3**	20.7	**10°C – 50%-3**	63.8	**15°C – 50%-3**	104.1
0-10	**5°C – 50% -4**	20.7	**10°C – 50% -4**	62.0	**15°C – 50% -4**	72.3
0-10	**5°C – 50% -5**	26.2	**10°C – 50% -5**	65.6	**15°C – 50% -5**	75.4
	Mean	**25.8**	**Mean**	**64.3**	**Mean**	**94.9**
	St Dev	**4.4**	**St Dev**	**2.2**	**St Dev**	**17.6**
10-20	5°C – 50% -1	5.8	10°C – 50% -1	32.7	15°C – 50% -1	26.2
10-20	5°C – 50% -2	7.0	10°C – 50% -2	24.5	15°C – 50% -2	27.3
10-20	5°C – 50%-3	5.1	10°C – 50%-3	25.4	15°C – 50%-3	30.5
10-20	5°C – 50% -4	7.8	10°C – 50% -4	14.6	15°C – 50% -4	44.9
10-20	5°C – 50% -5	7.0	10°C – 50% -5	18.1	15°C – 50% -5	58.5
	Mean	**6.5**	**Mean**	**23.1**	**Mean**	**37.5**
	St Dev	**1.0**	**St Dev**	**6.3**	**St Dev**	**13.9**
20-30	**5°C – 50% -1**	2.3	**10°C – 50% -1**	12.4	**15°C – 50% -1**	20.4
20-30	**5°C – 50% -2**	0.2	**10°C – 50% -2**	13.8	**15°C – 50% -2**	29.7
20-30	**5°C – 50%-3**	3.7	**10°C – 50%-3**	16.0	**15°C – 50%-3**	25.9
20-30	**5°C – 50% -4**	1.5	**10°C – 50% -4**	13.9	**15°C – 50% -4**	27.4
20-30	**5°C – 50% -5**	0.8	**10°C – 50% -5**	14.3	**15°C – 50% -5**	23.9
	Mean	**1.7**	**Mean**	**14.1**	**Mean**	**25.5**
	St Dev	**1.4**	**St Dev**	**1.2**	**St Dev**	**3.6**

A4.5 - Flux data for each individual peat core on day 84 of the incubation. Fluxes are given in mg CO_2-C g $soil^{-1}$ d^{-1}.

Day 84

	5 deg C		10 deg C		15 deg C	
Depth (cm)	**% Moisture/ Rep**	**$\delta^{13}C$**	**% Moisture/ Rep**	**$\delta^{13}C$**	**% Moisture/ Rep**	**$\delta^{13}C$**
0-10	5°C – 100% -1	-27.66	10°C – 100% -1	-22.3	15°C – 100% -1	-24.8
0-10	5°C – 100% - 2	-24.89	10°C – 100% -2	-24.7	15°C – 100% -2	-24.9
0-10	5°C – 100%- 3	-27.23	10°C – 100%-3	-25.7	15°C – 100%-3	-25.2
0-10	5°C – 100% -4	-27.23	10°C – 100% -4	-27.0	15°C – 100% -4	-25.8
0-10	5°C – 100% -5	-28.18	10°C – 100% -5	-24.7	15°C – 100% -5	-25.8
	Mean	**-27.03**	**Mean**	**-24.89**	**Mean**	**-25.31**
	St Dev	**1.26**	**St Dev**	**1.54**	**St Dev**	**0.43**
10-20	**5°C – 100% -1**	-26.15	**10°C – 100% -1**	-25.3	**15°C – 100% -1**	-25.7
10-20	**5°C – 100% -2**	-26.49	**10°C – 100% -2**	-25.3	**15°C – 100% -2**	-25.9
10-20	**5°C – 100%-3**	-26.74	**10°C – 100%-3**	-25.3	**15°C – 100%-3**	-21.0
10-20	**5°C – 100% -4**	-25.32	**10°C – 100% -4**	-23.1	**15°C – 100% -4**	-22.1
10-20	**5°C – 100% -5**	-28.09	**10°C – 100% -5**	-	**15°C – 100% -5**	-25.1
	Mean	**-26.56**	**Mean**	**-24.76**	**Mean**	**-23.96**
	St Dev	**1.01**	**St Dev**	**1.10**	**St Dev**	**2.23**
20-30	5°C – 100% -1	-25.76	10°C – 100% -1	-22.8	15°C – 100% -1	-22.7
20-30	5°C – 100% -2	-19.63	10°C – 100% -2	-25.1	15°C – 100% -2	-23.4
20-30	5°C – 100%-3	-18.90	10°C – 100%-3	-22.9	15°C – 100%-3	-23.3
20-30	5°C – 100% -4	-18.81	10°C – 100% -4	-23.7	15°C – 100% -4	-25.8
20-30	5°C – 100% -5	-24.61	10°C – 100% -5	-29.3	15°C – 100% -5	-24.2
	Mean	**-21.54**	**Mean**	**-24.75**	**Mean**	**-23.90**
	St Dev	**3.37**	**St Dev**	**2.70**	**St Dev**	**1.18**
0-10	**5°C – 50% -1**	-23.51	**10°C – 50% -1**	-26.1	**15°C – 50% - 1**	-26.64
0-10	**5°C – 50% -2**	-25.32	**10°C – 50% -2**	-26.0	**15°C – 50% - 2**	-27.31
0-10	**5°C – 50%-3**	-26.24	**10°C – 50%-3**	-25.2	**15°C – 50%- 3**	-26.71
0-10	**5°C – 50% -4**	-26.99	**10°C – 50% -4**	-26.0	**15°C – 50% - 4**	-27.94
0-10	**5°C – 50% -5**	-25.21	**10°C – 50% -5**	-28.0	**15°C – 50% - 5**	-27.77
	Mean	**-25.45**	**Mean**	**-26.25**	**Mean**	**-27.27**
	St Dev	**1.31**	**St Dev**	**0.94**	**St Dev**	**0.53**
10-20	5°C – 50% -1	-28.26	10°C – 50% -1	-27.0	15°C – 50% -1	-26.66
10-20	5°C – 50% -2	-25.86	10°C – 50% -2	-28.4	15°C – 50% -2	-26.42
10-20	5°C – 50%-3	-25.36	10°C – 50%-3	-25.7	15°C – 50%-3	-26.08
10-20	5°C – 50% -4	-29.39	10°C – 50% -4	-31.8	15°C – 50% -4	-27.22
10-20	5°C – 50% -5	-24.91	10°C – 50% -5	-31.0	15°C – 50% -5	-26.86
	Mean	**-26.76**	**Mean**	**-28.79**	**Mean**	**-26.65**
	St Dev	**1.96**	**St Dev**	**2.60**	**St Dev**	**0.43**
20-30	**5°C – 50% -1**	-38.41	**10°C – 50% -1**	-23.3	**15°C – 50% -1**	-25.09
20-30	**5°C – 50% -2**	-406.74	**10°C – 50% -2**	-31.0	**15°C – 50% -2**	-22.81
20-30	**5°C – 50%-3**	-11.85	**10°C – 50%-3**	-24.9	**15°C – 50%-3**	-23.24
20-30	**5°C – 50% -4**	14.25	**10°C – 50% -4**	-28.2	**15°C – 50% -4**	-26.29
20-30	**5°C – 50% -5**	-99.19	**10°C – 50% -5**	-24.0	**15°C – 50% -5**	-25.68
	Mean	**-108.39**	**Mean**	**-26.30**	**Mean**	**-24.62**
	St Dev	**172.01**	**St Dev**	**3.23**	**St Dev**	**1.53**

A4.6 - Calculated stable carbon isotopic signature (per mil) of source CO_2 for each individual core.

Day 116

Depth (cm)	5 deg C % Moisture/ Rep	CO_2 flux per day	10 deg C % Moisture/ Rep	CO_2 flux per day	15 deg C % Moisture/ Rep	CO_2 flux per day
0-10	5°C – 100% -1	22.4	10°C – 100% - 1	23.4	15°C – 100% -1	95.5
0-10	5°C – 100% - 2	21.6	10°C – 100% - 2	34.3	15°C – 100% -2	73.8
0-10	5°C – 100%- 3	22.8	10°C – 100%- 3	41.6	15°C – 100%-3	91.6
0-10	5°C – 100% -4	23.9	10°C – 100% -4	35.6	15°C – 100% -4	84.5
0-10	5°C – 100% -5	13.8	10°C – 100% -5	41.4	15°C – 100% -5	53.9
	Mean	**20.9**	**Mean**	**35.2**	**Mean**	**79.9**
	St Dev	**4.0**	**St Dev**	**7.4**	**St Dev**	**16.7**
10-20	**5°C – 100% -1**	11.9	**10°C – 100% - 1**	22.2	**15°C – 100% -1**	62.6
10-20	**5°C – 100% -2**	11.0	**10°C – 100% - 2**	22.1	**15°C – 100% -2**	43.4
10-20	**5°C – 100%-3**	8.1	**10°C – 100%- 3**	19.3	**15°C – 100%-3**	24.3
10-20	**5°C – 100% -4**	10.6	**10°C – 100% -4**	20.0	**15°C – 100% -4**	25.6
10-20	**5°C – 100% -5**	10.6	**10°C – 100% -5**	14.8	**15°C – 100% -5**	58.5
	Mean	**10.4**	**Mean**	**19.7**	**Mean**	**42.9**
	St Dev	**1.4**	**St Dev**	**3.0**	**St Dev**	**17.9**
20-30	5°C – 100% -1	8.7	10°C – 100% - 1	15.8	15°C – 100% -1	34.6
20-30	5°C – 100% - 2	6.4	10°C – 100% - 2	10.8	15°C – 100% -2	29.2
20-30	5°C – 100%- 3	9.0	10°C – 100%- 3	14.4	15°C – 100%-3	28.1
20-30	5°C – 100% -4	3.4	10°C – 100% -4	21.1	15°C – 100% -4	35.2
20-30	5°C – 100% -5	5.9	10°C – 100% -5	8.9	15°C – 100% -5	21.8
	Mean	**6.7**	**Mean**	**14.2**	**Mean**	**29.8**
	St Dev	**2.3**	**St Dev**	**4.7**	**St Dev**	**5.5**
0-10	**5°C – 50% -1**	29.0	**10°C – 50% -1**	54.9	**15°C – 50% -1**	125.3
0-10	**5°C – 50% -2**	32.6	**10°C – 50% -2**	61.2	**15°C – 50% -2**	107.9
0-10	**5°C – 50%-3**	21.4	**10°C – 50%-3**	59.9	**15°C – 50%-3**	106.5
0-10	**5°C – 50% -4**	22.9	**10°C – 50% -4**	59.5	**15°C – 50% -4**	75.5
0-10	**5°C – 50% -5**	25.0	**10°C – 50% -5**	61.5	**15°C – 50% -5**	78.3
	Mean	**26.2**	**Mean**	**59.4**	**Mean**	**98.7**
	St Dev	**4.6**	**St Dev**	**2.7**	**St Dev**	**21.2**
10-20	5°C – 50% -1	6.4	10°C – 50% -1	29.5	15°C – 50% -1	29.9
10-20	5°C – 50% -2	7.6	10°C – 50% -2	24.1	15°C – 50% -2	31.9
10-20	5°C – 50%-3	6.0	10°C – 50%-3	24.7	15°C – 50%-3	30.6
10-20	5°C – 50% -4	9.0	10°C – 50% -4	16.7	15°C – 50% -4	35.6
10-20	5°C – 50% -5	8.2	10°C – 50% -5	22.0	15°C – 50% -5	60.7
	Mean	**7.4**	**Mean**	**23.4**	**Mean**	**37.7**
	St Dev	**1.2**	**St Dev**	**4.6**	**St Dev**	**13.0**
20-30	**5°C – 50% -1**	5.2	**10°C – 50% -1**	16.4	**15°C – 50% -1**	23.4
20-30	**5°C – 50% -2**	4.4	**10°C – 50% -2**	18.7	**15°C – 50% -2**	25.5
20-30	**5°C – 50%-3**	6.4	**10°C – 50%-3**	18.0	**15°C – 50%-3**	24.1
20-30	**5°C – 50% -4**	4.9	**10°C – 50% -4**	15.0	**15°C – 50% -4**	26.1
20-30	**5°C – 50% -5**	5.0	**10°C – 50% -5**	12.8	**15°C – 50% -5**	32.0
	Mean	**5.2**	**Mean**	**16.2**	**Mean**	**26.2**
	St Dev	**0.7**	**St Dev**	**2.4**	**St Dev**	**3.4**

A4.7 - Flux data for each individual peat core on day 116 of the incubation. Fluxes are given in mg CO_2-C g $soil^{-1}$ d^{-1}.

Day 116

	5 deg C		10 deg C		15 deg C	
Depth (cm)	**% Moisture/ Rep**	**$\delta^{13}C$**	**% Moisture/ Rep**	**$\delta^{13}C$**	**% Moisture/ Rep**	**$\delta^{13}C$**
0-10	5°C – 100% -1	-26.4	10°C – 100% -1	-23.0	15°C – 100% -1	-25.5
0-10	5°C – 100% - 2	-27.4	10°C – 100% -2	-25.9	15°C – 100% -2	-25.9
0-10	5°C – 100%- 3	-26.6	10°C – 100%-3	-27.0	15°C – 100%-3	-26.4
0-10	5°C – 100% -4	-27.7	10°C – 100% -4	-26.4	15°C – 100% -4	-25.1
0-10	5°C – 100% -5	-26.7	10°C – 100% -5	-26.6	15°C – 100% -5	-26.1
	Mean	**-27.0**	**Mean**	**-25.8**	**Mean**	**-25.8**
	St Dev	**0.6**	**St Dev**	**1.6**	**St Dev**	**0.5**
10-20	**5°C – 100% -1**	-24.7	**10°C – 100% -1**	-26.9	**15°C – 100% -1**	-25.7
10-20	**5°C – 100% -2**	-25.7	**10°C – 100% -2**	-24.9	**15°C – 100% -2**	-26.6
10-20	**5°C – 100%-3**	-27.5	**10°C – 100%-3**	-26.2	**15°C – 100%-3**	-26.4
10-20	**5°C – 100% -4**	-26.7	**10°C – 100% -4**	-26.2	**15°C – 100% -4**	-26.0
10-20	**5°C – 100% -5**	-26.6	**10°C – 100% -5**	-25.5	**15°C – 100% -5**	-26.0
	Mean	**-26.3**	**Mean**	**-25.9**	**Mean**	**-26.1**
	St Dev	**1.1**	**St Dev**	**0.7**	**St Dev**	**0.3**
20-30	5°C – 100% -1	-26.4	10°C – 100% -1	-24.1	15°C – 100% -1	-25.5
20-30	5°C – 100% -2	-28.1	10°C – 100% -2	-26.7	15°C – 100% -2	-24.3
20-30	5°C – 100%-3	-27.0	10°C – 100%-3	-24.7	15°C – 100%-3	-25.1
20-30	5°C – 100% -4	-27.9	10°C – 100% -4	-26.4	15°C – 100% -4	-26.0
20-30	5°C – 100% -5	-26.4	10°C – 100% -5	-26.5	15°C – 100% -5	-25.9
	Mean	**-27.2**	**Mean**	**-25.7**	**Mean**	**-25.4**
	St Dev	**0.8**	**St Dev**	**1.2**	**St Dev**	**0.7**
0-10	**5°C – 50% -1**	-26.8	**10°C – 50% -1**	-27.4	**15°C – 50% - 1**	-27.4
0-10	**5°C – 50% -2**	-29.4	**10°C – 50% -2**	-25.5	**15°C – 50% - 2**	-27.6
0-10	**5°C – 50%-3**	-27.9	**10°C – 50%-3**	-26.6	**15°C – 50%- 3**	-28.2
0-10	**5°C – 50% -4**	-27.6	**10°C – 50% -4**	-27.0	**15°C – 50% - 4**	-27.8
0-10	**5°C – 50% -5**	-25.6	**10°C – 50% -5**	-27.9	**15°C – 50% - 5**	-27.2
	Mean	**-27.5**	**Mean**	**-26.9**	**Mean**	**-27.6**
	St Dev	**1.4**	**St Dev**	**0.9**	**St Dev**	**0.4**
10-20	5°C – 50% -1	-25.8	10°C – 50% -1	-27.7	15°C – 50% -1	-27.0
10-20	5°C – 50% -2	-24.8	10°C – 50% -2	-26.1	15°C – 50% -2	-27.6
10-20	5°C – 50%-3	-27.9	10°C – 50%-3	-27.6	15°C – 50%-3	-26.3
10-20	5°C – 50% -4	-26.2	10°C – 50% -4	-26.0	15°C – 50% -4	-26.9
10-20	5°C – 50% -5	-27.1	10°C – 50% -5	-28.2	15°C – 50% -5	-27.4
	Mean	**-26.4**	**Mean**	**-27.1**	**Mean**	**-27.0**
	St Dev	**1.2**	**St Dev**	**1.0**	**St Dev**	**0.5**
20-30	**5°C – 50% -1**	-22.8	**10°C – 50% -1**	-21.2	**15°C – 50% -1**	-25.6
20-30	**5°C – 50% -2**	-24.0	**10°C – 50% -2**	-24.2	**15°C – 50% -2**	-25.2
20-30	**5°C – 50%-3**	-23.6	**10°C – 50%-3**	-24.1	**15°C – 50%-3**	-26.8
20-30	**5°C – 50% -4**	-30.0	**10°C – 50% -4**	-28.6	**15°C – 50% -4**	-24.9
20-30	**5°C – 50% -5**	-	**10°C – 50% -5**	-24.8	**15°C – 50% -5**	-25.9
	Mean	**-25.1**	**Mean**	**-24.6**	**Mean**	**-25.7**
	St Dev	**3.3**	**St Dev**	**2.6**	**St Dev**	**0.7**

A4.8 - Calculated stable carbon isotopic signature (per mil) of source CO_2 for each individual core.

References

Aerts, R. (1997). Climate, leaf litter chemistry and leaf litter decomposition in terrestrial ecosystems: a triangular relationship. *Oikos* **79**, 439-449.

Ågren, G. I., Bosatta, E. & Balesdent, J. (1996). Isotope discrimination during decomposition of organic matter: a theoretical analysis. *Soil Science Society of America Journal* **60**, 1121-1126.

Alm, J., Schulman, L., Walden, J., Nykänen, H., Martikainen, P. J. & Silvola, J. (1999). Carbon balance of a boreal bog during a year with an exceptionally dry summer. *Ecology* **80**, 161-174.

Amundson, R., Stern, L., Baisden, T. & Wang, Y. (1998). The isotopic composition of soil and soil-respired CO_2. *Geoderma* **82**, 83-114.

Anderson, E. C., Libby, W. F., Weinhouse, S., Reid, A. F., Kirshenbaum, A. D. & Grosse, A. V. (1947). Natural radiocarbon from cosmic radiation. *Physical Review* **72**, 931-936.

Andres, R. J., Marland, G., Boden, T. & Bischof, S. (2000). Carbon Dioxide Emission from Fossil Fuel Consumption and Cement Manufacture, 1751-1991, and an Estimate of their Isotopic Composition and Latitudinal Distribution. In *The Carbon Cycle*, pp. 53-62. Edited by T. M. L. Wigley & S. Schimel. Cambridge, UK: Cambridge University Press.

Andrews, J. A., Matamala, R., Westover, K. M. & Schlesinger, W. H. (2000). Temperature effects on the diversity of soil heterotrophs and the $\delta^{13}C$ of soil-respired CO_2. *Soil Biology & Biochemistry* **32**, 699-706.

Aravena, R., Warner, B. G., Charman, D. J., Belyea, L. R., Mathur, S. P. & Dinel, H. (1993). Carbon isotopic composition of deep carbon gases in an ombrogenous peatland, northwestern Ontario, Canada. *Radiocarbon* **35**, 271-276.

Arrhenius, S. (1896). On the influence of carbonic acid in the air upon the temperature of the ground. *Philosophical Magazine and Journal of Science* **41**, 237-276.

Avery, B. W. (1980). Soil Classification for England and Wales (Higher Categories). In *Soil Survey*. Harpenden: Rothamsted Experimental Station.

Bakwin, P. S., Tans, P. P., White, J. W. C. & Andres, R. J. (1998). Determination of the isotopic ($^{13}C/^{12}C$) discrimination by terrestrial biology from a global network of observations. *Global Biogeochemical Cycles* **12**, 555-562.

Baldocchi, D. D., Hicks, B. B. & Meyers, T. P. (1988). Measuring biosphere-atmosphere exchanges of biologically related gases with micrometeorological methods. *Ecology* **69**, 1331-1340.

Barber, K., Dumayne-Peaty, L., Hughes, P., Mauquoy, D. & Scaife, R. (1998). Replicability and variability of the recent macrofossil and proxy-climate record from raised bogs: field stratigraphy and macrofossil data from Bolton Fell Moss and Walton Moss, Cumbria, England. *Journal of Quaternary Science* **13**, 515-528.

Barber, K. E., Maddy, D., Rose, N., Stevenson, A. C., Stoneman, R. & Thompson, R. (2000). Replicated proxy-climate signals over the last 2000 yr from two distant UK peat bogs: new evidence for regional palaeoclimate teleconnections. *Quaternary Science Reviews* **19**, 481-487.

Barrer, R. M. (1959). New selective sorbents: porous crystals as molecular filters. *British Chemical Engineering*, 267-279.

Barrer, R. M. (1978). *Zeolites and Clay Minerals as Sorbents and Molecular Sieves.* pp.547. New York: Academic Press.

Battle, M., Bender, M. L., Tans, P. P., White, J. W. C., Ellis, J. T., Conway, T. & Francey, R. J. (2000). Global carbon sinks and their variability inferred from atmospheric O_2 and $\delta^{13}C$. *Science* **287**, 2467-2470.

Bauer, J. E., Williams, P. M. & Druffel, E. R. M. (1992). Recovery of submilligram quantities of carbon dioxide from gas streams by molecular sieve for subsequent determination of isotopic (^{13}C and ^{14}C) natural abundances. *Analytical Chemistry* **64**, 824-827.

BDH (No date). *'Union Carbide' molecular sieves for selective adsorption*: BDH Chemicals Ltd.

Benner, R., Fogel, M. L., Sprague, E. K. & Hodson, R. E. (1987). Depletion of ^{13}C in lignin and its implications for stable carbon isotope studies. *Nature* **329**, 708-710.

Berg, B. (2000). Litter decomposition and organic matter turnover in northern forest soils. *Forest Ecology and Management* **133**, 13-22.

Bernoux, M., Cerri, C. C., Neill, C. & de Moraes, J. F. L. (1998). The use of stable carbon isotopes for estimating soil organic matter turnover rates. *Geoderma* **82**, 43-58.

Biasi, C., Rusalimova, O., Meyer, H., Kaiser, C., Wanek, W., Barsukov, P., Junger, H. & Richter, A. (2005). Temperature-dependent shift from labile to recalcitrant carbon sources of Arctic heterotrophs. *Rapid Communications in Mass Spectrometry* **19**, 1401-1408.

Billett, M. F., Garnett, M. H. & Hardie, S. M. L. (2006). A direct method to measure $^{14}CO_2$ lost by evasion from surface waters. *Radiocarbon* **48**, 61-68.

Bingeman, C. W., Varner, J. E. & Martin, W. P. (1953). The effect of the addition of organic materials on the decomposition of an organic soil. *Soil Science America Proceedings* **29**, 692-696.

Blodau, C. & Moore, T. R. (2003). Experimental response of peatland carbon dynamics to a water table fluctuation. *Aquatic Sciences* **65**, 47-62.

Boggie, R., Hunter, R. F. & Knight, A. H. (1958). Studies of the root development of plants in the field using radioactive-tracers. *Journal of Ecology* **46**, 621-639.

Bol, R., Bolger, T., Cully, R. & Little, D. (2003). Recalcitrant soil organic materials mineralize more efficiently at higher temperatures. *Journal of Plant Nutrition & Soil Science-Zeitschrift Fur Pflanzenernahrung Und Bodenkunde* **166**, 300-307.

Bol, R. A. & Harkness, D. D. (1995). The use of zeolite molecular sieves for trapping low concentrations of CO_2 from environmental atmospheres. *Radiocarbon* **37**, 643-647.

Bol, R. A., Harkness, D. D., Huang, Y. & Howard, D. M. (1999). The influence of soil processes on carbon isotope distribution and turnover in the British uplands. *European Journal of Soil Science* **50**, 41-51.

Boone, R. D., Nadelhoffer, K. J., Canary, J. D. & Kaye, J. P. (1998). Roots exert a strong influence on the temperature sensitivity of soil respiration. *Nature* **396**, 570-572.

Borren, W., Bleuten, W. & Lapshina, E. D. (2004). Holocene peat and carbon accumulation rates in the southern taiga of western Siberia. *Quaternary Research* **61**, 42-51.

Bosatta, E. & Ågren, G. I. (1999). Soil organic matter quality interpreted thermodynamically. *Soil Biology & Biochemistry* **31**, 1889-1891.

Boutton, T. W. (1991a). Stable Carbon Isotope Ratios of Natural Materials: II. Atmospheric, Terrestrial, Marine and Freshwater Environments. In *Carbon Isotope Techniques*, pp. 173-186. Edited by D. C. Coleman & B. Fry. San Diego: Academic Press Inc.

Boutton, T. W. (1991b). Stable Carbon Isotope Ratios of Natural Materials: I. Sample Preparation and Mass Spectrometric Analysis. In *Carbon Isotope Techniques*, pp. 155-172. Edited by D. C. Coleman & B. Fry. San Diego: Academic Press Inc.

Boutton, T. W. (1996). Stable Carbon Isotope Ratios of Soil Organic Matter and their Use as Indicators of Vegetation and Climate Change. In *Mass Spectrometry of Soils*, pp. 517. Edited by T. W. Boutton & S.-I. Yamasaki. New York: Marcel Dekker Inc.

Bowden, R. D., Newkirk, K. M. & Rullo, G. M. (1998). Carbon dioxide and methane fluxes by a forest soil under laboratory-controlled moisture and temperature conditions. *Soil Biology & Biochemistry* **30**, 1591-1597.

Breck, D. W. (1974). *Zeolite Molecular Sieves.* pp.771. New York: John Wiley & Sons Inc.

Breon, F. M. (2006). Climate - how do aerosols affect cloudiness and climate? *Science* **313**, 623-624.

Briones, M. J. I., Ineson, P. & Piearce, T. G. (1997). Effects of climate change on soil fauna; Responses of enchytraeids, Diptera larvae and tardigrades in a transplant experiment. *Applied Soil Ecology* **6**, 117-134.

Briones, M. J. I. & Ineson, P. (2002). Use of ^{14}C carbon dating to determine feeding behaviour of enchytraeids. *Soil Biology & Biochemistry* **34**, 881-884.

Briones, M. J. I., Poskitt, J. & Ostle, N. (2004). Influence of warming and enchytraeid activities on soil CO_2 and CH_4 fluxes. *Soil Biology & Biochemistry* **36**, 1851-1859.

Bryant, C. B., Clymo, R. S. & Murray, C. (2006). Carbon isotopes in peat, dissolved organic carbon, CO_2 and CH_4 in a raised peat bog, SW Scotland. In *Abstracts: 19th International Radiocarbon Conference*. Oxford, U.K.

Byrne, K. A. & Kiely, G. (2006). Partitioning of respiration in an intensively managed grassland. *Plant & Soil* **282**, 281-289.

Cao, M. K. & Woodward, F. I. (1998). Dynamic responses of terrestrial ecosystem carbon cycling to global climate change. *Nature* **393**, 249-252.

Carbolite (No date). Range of Tube furnaces: Carbolite, UK.

Carroll, D. M., Hartnup, R. & Jarvis, R. A. (1979). Soils of south and west Yorkshire. In *Lawes Agricultural Trust/Soil Survey of England and Wales*. Harpenden.

Cerling, T. E., Solomon, D. K., Quade, J. & Bowman, J. R. (1991). On the isotopic composition of carbon in soil carbon dioxide. *Geochimica et Cosmochimica Acta* **55**, 3403-3405.

Chanton, J. P. & Whiting, G. J. (1995). Trace Gas Exchange in Freshwater and Coastal Marine Environments: Ebullition and Transport by Plants. In *Biogenic Trace Gases: Measuring Emissions from Soil and Water*, pp. 98-125. Edited by P. A. Matson & R. C. Harriss. Oxford: Blackwell Science Ltd.

Chanton, J. P., Arkebauer, T. J., Harden, H. S. & Verma, S. B. (2002). Diel variation in lacunal CH_4 and CO_2 concentration and $\delta^{13}C$ in *Phragmites australis*. *Biogeochemistry* **59**, 287-301.

Chanton, J. P., Chasar, L. C., Glasser, P. & Siegel, D. (2005). Carbon and Hydrogen Isotopic Effects in Microbial Methane from Terrestrial Environments. In *Stable Isotopes and Biosphere-Atmosphere Interactions*, pp. 85-105. Edited by L. B. Flanagan, J. R. Ehleringer & D. E. Pataki. Amsterdam: Elsevier Academic Press.

Chapman, S. J. & Thurlow, M. (1996). The influence of climate on CO_2 and CH_4 emissions from organic soils. *Agricultural & Forest Meteorology* **79**, 205-217.

Chapman, S. J. & Thurlow, M. (1998). Peat respiration at low temperatures. *Soil Biology & Biochemistry* **30**, 1013-1021.

Charman, D. J., Aravena, R. & Warner, B. G. (1994). Carbon dynamics in a forested peatland in north-eastern Ontario, Canada. *Journal of Ecology* **82**, 55-62.

Charman, D. J., Aravena, R., Bryant, C. L. & Harkness, D. D. (1999). Carbon isotopes in peat, DOC, CO_2, and CH_4 in a Holocene peatland on Dartmoor, southwest England. *Geology* **27**, 539-542.

Chasar, L. S., Chanton, J. P., Glaser, P. H., Siegel, D. I. & Rivers, J. S. (2000). Radiocarbon and stable carbon isotopic evidence for transport and transformation of dissolved organic carbon, dissolved inorganic carbon, and CH_4 in a northern Minnesota peatland. *Global Biogeochemical Cycles* **14**, 1095-1108.

Chimner, R. A. & Cooper, D. J. (2003). Influence of water table levels on CO_2 emissions in a Colorado subalpine fen: an *in situ* microcosm study. *Soil Biology & Biochemistry* **35**, 345-351.

Christensen, T. R., Friborg, T., Sommerkorn, M., Kaplan, J., Illeris, L., Soegaard, H., Nordstroem, C. & Jonasson, S. (2000). Trace gas exchange in a high-arctic valley 1. Variations in CO_2 and CH_4 flux between tundra vegetation types. *Global Biogeochemical Cycles* **14**, 701-713.

Ciais, P., Tans, P. P., White, J. W. C. & other authors (1995). Partitioning of ocean and land uptake of CO_2 as inferred by $\delta^{13}C$ measurements from the NOAA Climate Monitoring and Diagnostics Laboratory Global Air Sampling Network. *Journal of Geophysical Research-Atmospheres* **100**, 5051-5070.

Ciais, P., Denning, A. S., Tans, P. P., Berry, J. A., Randall, D. A., Collatz, G. J., Sellers, P. J., White, J. W. C., Trolier, M., Meijer, H. A. J., Francey, R. J., Monfray, P. & Heimann, M. (1997). A three-dimensional synthesis study of $\delta^{18}O$ in atmospheric CO_2 1. Surface fluxes. *Journal of Geophysical Research-Atmospheres* **102**, 5857-5872.

Clymo, R. S. (1983). Peat. In *Mires, Swamp, Bog, Fen and Moor*, pp. 159-222. Edited by A. J. P. Gore. Amsterdam: Elsevier Scientific Publishing Company.

Clymo, R. S. (1984). The limits to peat bog growth. *Philosophical Transactions of the Royal Society of London Series B-Biological Sciences* **303**, 605-654.

Clymo, R. S., Turunen, J. & Tolonen, K. (1998). Carbon accumulation in peatland. *Oikos* **81**, 368-388.

Clymo, R. S. & Bryant, C. L. (in prep.). Carbon isotopes in peat, dissolved organic carbon, CO_2 and CH_4 in a raised peat bog, SW Scotland.

Coleman, D. C. & Fry, B. (1991). *Carbon Isotope Techniques*. pp. 274. San Diego: Academic Press Inc.

Coleman, J. S., McConnaughay, K. D. M. & Bazzaz, F. A. (1993). Elevated CO_2 and plant nitrogen use - is reduced tissue nitrogen concentration size dependent? *Oecologia* **93**, 195-200.

Conway, V. M. & Millar, A. (1960). The hydrology of some small peat-covered catchments in the northern Pennines. *Journal of the Institute of Water Engineers* **14**, 415-424.

Cox, P. M., Betts, R. A., Jones, C. D., Spall, S. A. & Totterdell, I. J. (2000). Acceleration of global warming due to carbon-cycle feedbacks in a coupled climate model. *Nature* **408**, 184-187.

Craig, H. (1953). The geochemistry of the stable carbon isotopes. *Geochimica et Cosmochimica Acta* **3**, 53-92.

Craig, H. (1957). Isotopic standards for carbon and oxygen and correction factors for mass-spectrometric analysis of carbon dioxide. *Geochimica et Cosmochimica Acta* **12**, 133-149.

Craine, J. M., Wedin, D. A. & Chapin, F. S. (1998). Predominance of ecophysiological controls on soil CO_2 flux in a Minnesota grassland. *Plant & Soil* **207**, 77-86.

Cui, Y., Kita, H. & Okamoto, K. (2003). Preparation and gas separation properties of zeolite T membrane. *Chemical Communications*, 2154-2155.

Cuttle, S. P. & Malcolm, D. C. (1979). Corer for taking undisturbed peat samples. *Plant & Soil* **51**, 297-300.

Dale, V. H. (1997). The relationship between land-use change and climate change. *Ecological Applications* **7**, 753-769.

Davidon, G. R. (1995). The stable isotopic composition and measurement of carbon in soil CO_2. *Geochimica et Cosmochimica Acta* **59**, 2485-2489.

Davidson, E. A., Trumbore, S. E. & Amundson, R. (2000). Biogeochemistry - soil warming and organic carbon content. *Nature* **408**, 789-790.

Davidson, E. A., Savage, K., Verchot, L. V. & Navarro, R. (2002). Minimizing artifacts and biases in chamber-based measurements of soil respiration. *Agricultural & Forest Meteorology* **113**, 21-37.

Davidson, E. A. & Janssens, I. A. (2006). Temperature sensitivity of soil carbon decomposition and feedbacks to climate change. *Nature* **440**, 165-173.

Davidson, E. A., Janssens, I. A. & Luo, Y. Q. (2006a). On the variability of respiration in terrestrial ecosystems: moving beyond Q_{10}. *Global Change Biology* **12**, 154-164.

Davidson, E. A., Richardson, A. D., Savage, K. E. & Hollinger, D. Y. (2006b). A distinct seasonal pattern of the ratio of soil respiration to total ecosystem respiration in a spruce-dominated forest. *Global Change Biology* **12**, 230-239.

Dawson, T. E., Mambelli, S., Plamboeck, A. H., Templer, P. H. & Tu, K. P. (2002). Stable isotopes in plant ecology. *Annual Review of Ecology & Systematics* **33**, 507-559.

De Niro, M. J. & Epstein, S. (1978). Influence of diet on distribution of carbon isotopes in animals. *Geochimica et Cosmochimica Acta* **42**, 495-506.

De Vries, H. (1958). Variation in concentration of radiocarbon with time and location on Earth. *Proceedings of the Koninklijke Nederlandse Academie van Wetenschappen Series B: Physical Sciences* **61**, 94-102.

Dioumaeva, I., Trumbore, S., Schuur, E. A. G., Goulden, M. L., Litvak, M. & Hirsch, A. I. (2002). Decomposition of peat from upland boreal forest: temperature dependence and sources of respired carbon. *Journal of Geophysical Research-Atmospheres* **108**, art. no.-8222.

Dixon, R. K., Brown, S., Houghton, R. A., Solomon, A. M., Trexler, M. C. & Wisniewski, J. (1994). Carbon pools and flux of global forest ecosystems. *Science* **263**, 185-190.

Dörr, H. & Münnich, K. O. (1980). Carbon-14 and carbon-13 in soil CO_2. *Radiocarbon* **22**, 909-918.

Dörr, H. & Münnich, K. O. (1986). Annual variations of the ^{14}C content of soil CO_2. *Radiocarbon* **28**, 338-345.

Dörr, H. & Münnich, K. O. (1987). Annual variations in soil respiration in selected areas of the temperate zone. *Tellus B* **39**, 114-121.

Dyer, A. (1988). *An Introduction to Zeolite Molecular Sieves.* pp.149. Chichester: J. Wiley & Sons.

Eddy, A., Welch, D. & Rawes, M. (1969). The vegetation of the Moor House National Nature Reserve in the Northern Pennines, England. *Vegetatio* **16**, 239-284.

Ehleringer, J. R., Buchmann, N. & Flanagan, L. B. (2000). Carbon isotope ratios in belowground carbon cycle processes. *Ecological Applications* **10**, 412-422.

Eliasson, P. E., McMurtrie, R. E., Pepper, D. A., Stromgren, M., Linder, S. & Ågren, G. I. (2005). The response of heterotrophic CO_2 flux to soil warming. *Global Change Biology* **11**, 167-181.

Evans, M. G., Burt, T. P., Holden, J. & Adamson, J. K. (1999). Runoff generation and water table fluctuations in blanket peat: evidence from UK data spanning the dry summer of 1995. *Journal of Hydrology* **221**, 141-160.

Falkowski, P., Scholes, R. J., Boyle, E., Canadell, J., Canfield, D., Elser, J., Gruber, N., Hibbard, K., Hogberg, P., Linder, S., Mackenzie, F. T., Moore, B., Pedersen, T., Rosenthal, Y., Seitzinger, S., Smetacek, V., & Steffen, W. (2000). The global carbon cycle: a test of our knowledge of Earth as a system. *Science* **290**, 291-296.

Falkowski, P. G., Barber, R. T. & Smetacek, V. (1998). Biogeochemical controls and feedbacks on ocean primary production. *Science* **281**, 200-206.

Fang, C. & Moncrieff, J. B. (2001). The dependence of soil CO_2 efflux on temperature. *Soil Biology & Biochemistry* **33**, 155-165.

Fang, C. M., Smith, P., Moncrieff, J. B. & Smith, J. U. (2005). Similar response of labile and resistant soil organic matter pools to changes in temperature. *Nature* **433**, 57-59.

Farquhar, G. D., O' Leary, M. H. & Berry, J. A. (1982). On the relationship between carbon isotope discrimination and the inter-cellular carbon dioxide concentration in leaves. *Australian Journal of Plant Physiology* **9**, 121-137.

Fessenden, J. E. & Ehleringer, J. R. (2003). Temporal variation in $\delta^{13}C$ of ecosystem respiration in the Pacific Northwest: links to moisture stress. *Oecologia* **136**, 129-136.

Fierer, N., Allen, A. S., Schimel, J. P. & Holden, P. A. (2003). Controls on microbial CO_2 production: a comparison of surface and subsurface soil horizons. *Global Change Biology* **9**, 1322-1332.

Fifield, L. K. (1999). Accelerator mass spectrometry and its applications. *Reports on Progress in Physics* **62**, 1223-1274.

Fitter, A. H., Self, G. K., Brown, T. K., Bogie, D. S., Graves, J. D., Benham, D. & Ineson, P. (1999). Root production and turnover in an upland grassland subjected to artificial soil warming respond to radiation flux and nutrients, not temperature. *Oecologia* **120**, 575-581.

Flanagan, L. B. & Ehleringer, A. R. (1998). Ecosystem-atmosphere CO_2 exchange: interpreting signals of change using stable isotope ratios. *Trends in Ecology & Evolution* **13**, 10-14.

Flanigen, E. M. (1991). Zeolites and Molecular Sieves an Historical Perspective. In *Introduction to Zeolite Science and Practice*, pp. 13-34. Edited by H. van Bekkum, E. M. Flanigen & J. C. Jansen. Amsterdam: Elsevier Science Publishers B.V.

Fontaine, S., Mariotti, A. & Abbadie, L. (2003). The priming effect of organic matter: a question of microbial competition? *Soil Biology & Biochemistry* **35**, 837-843.

Forrest, G. I. & Smith, R. A. H. (1975). The productivity of a range of blanket bog vegetation types in the northern Pennines. *Journal of Ecology* **63**, 173-202.

Freeman, S., Xu, S., Schnabel, C., Dougans, A., Tait, A., Kitchen, R., Klody, G., Loger, R., Pollock, T., Schroeder, J., & Sundquist, M. (2004). Initial measurements with the SUERC accelerator mass spectrometer. *Nuclear Instruments & Methods in Physics Research Section B-Beam Interactions with Materials & Atoms* **223-24**, 195-198.

Fuglestvedt, J. S., Berntsen, T. K., Isaksen, I. S. A., Mao, H. T., Liang, X. Z. & Wang, W. C. (1999). Climatic forcing of nitrogen oxides through changes in tropospheric ozone and methane; global 3D model studies. *Atmospheric Environment* **33**, 961-977.

Fung, I., Field, C. B., Berry, J. A., Thompson, M. V., Randerson, J. T., Malmstrom, C. M., Vitousek, P. M., Collatz, G. J., Sellers, P. J., Randall, D. A., Denning, A. S., Badeck, F. & John, J. (1997). Carbon 13 exchanges between the atmosphere and biosphere. *Global Biogeochemical Cycles* **11**, 507-533.

Gainey, P. L. (1919). Parallel formation of carbon dioxide, ammonia and nitrate in soil. *Soil Science* **7**, 293-311.

Galimov, E. M. (1985). *The Biological Fractionation of Isotopes.* pp. 261. New York: Academic Press.

Garnett, M. H. (1998). Carbon storage in Pennine moorland and response to change. PhD thesis: University of Newcastle-Upon-Tyne. pp.302.

Garnett, M. H., Ineson, P. & Stevenson, A. C. (2000). Effects of burning and grazing on carbon sequestration in a Pennine blanket bog, UK. *Holocene* **10**, 729-736.

Garnett, M. H., Ineson, P., Stevenson, A. C. & Howard, D. C. (2001). Terrestrial organic carbon storage in a British moorland. *Global Change Biology* **7**, 375-388.

Garnett, M. H. & Stevenson, A. C. (2004). Testing the use of bomb radiocarbon to date the surface layers of blanket peat. *Radiocarbon* **46**, 841-851.

Garnett, M. H. & Billett, M. F. (In press). Do riparian plants fix CO_2 lost by evasion from surface waters? An investigation using carbon isotopes. *Radiocarbon.*

Gaudinski, J. B., Trumbore, S. E., Davidson, E. A. & Zheng, S. H. (2000). Soil carbon cycling in a temperate forest: radiocarbon-based estimates of residence times, sequestration rates and partitioning of fluxes. *Biogeochemistry* **51**, 33-69.

Gest, H. (2004). Samuel Ruben's contributions to research on photosynthesis and bacterial metabolism with radioactive carbon. *Photosynthesis Research* **80**, 77-83.

Ghashghaie, J., Duranceau, M., Badeck, F. W., Cornic, G., Adeline, M. T. & Deleens, E. (2001). $\delta^{13}C$ of CO_2 respired in the dark in relation to $\delta^{13}C$ of leaf metabolites: comparison between *Nicotiana sylvestris* and *Helianthus annuus* under drought. *Plant Cell & Environment* **24**, 505-515.

Ghashghaie, J., Badeck, F. W., Lanigan, G., Nogues, S., Tcherkez, G., Deleens, E., Cornic, G. & Griffiths, H. (2003). Carbon isotope fractionation during dark respiration and photorespiration in C_3 plants. *Phytochemistry Reviews* **2**, 145-161.

Giardina, C. P. & Ryan, M. G. (2000). Evidence that decomposition rates of organic carbon in mineral soil do not vary with temperature. *Nature* **404**, 858-861.

Gill, R. A., Polley, H. W., Johnson, H. B., Anderson, L. J., Maherali, H. & Jackson, R. B. (2002). Nonlinear grassland responses to past and future atmospheric CO_2. *Nature* **417**, 279-282.

Gimingham, C. H. (1960). Biological flora of the British Isles: *Calluna vulgaris* (L) Hull. *Journal of Ecology* **48**, 455-483.

Glasstone, S. & Dolan, P. J. (1977). The Effects of Nuclear Weapons, pp. 653. Washington, D.C.: U.S. Department of Defense & U.S. Department of Energy.

Gleixner, G., Danier, H. J., Werner, R. A. & Schmidt, H. L. (1993). Correlations between the ^{13}C content of primary and secondary plant-products in different cell compartments and that in decomposing basidiomycetes. *Plant Physiology* **102**, 1287-1290.

Godwin, H. (1962). Half-life of radiocarbon. *Nature* **195**, 984.

Gonfiantini, R. (1984). Stable Isotope Reference Samples for Geochemical and Hydrological Investigations, pp. 77. Vienna: Report Adv. Group Meeting.

Gorham, E. (1991). Northern peatlands - role in the carbon cycle and probable responses to climatic warming. *Ecological Applications* **1**, 182-195.

Goudriaan, J. (1992). Biosphere structure, carbon sequestering potential and the atmospheric ^{14}C carbon record. *Journal of Experimental Botany* **43**, 1111-1119.

Grace, J. & Rayment, M. (2000). Respiration in the balance. *Nature* **404**, 819-820.

Grace, J., Lloyd, J., McIntyre, J., Miranda, A. C., Meir, P., Miranda, H. S., Nobre, C., Moncrieff, J., Massheder, J., Malhi, Y., Wright, I. & Gash, J. (1995). Carbon-dioxide uptake by an undisturbed tropical rain-forest in southwest Amazonia, 1992 to 1993. *Science* **270**, 778-780.

Gu, L. H., Post, W. M. & King, A. W. (2004). Fast labile carbon turnover obscures sensitivity of heterotrophic respiration from soil to temperature: a model analysis. *Global Biogeochemical Cycles* **18**, art. no. GB1022

Gulliksen, S. & Scott, M. (1995). Report of the TIRI workshop, Saturday 13th August 1994. *Radiocarbon* **37**, 820-821.

Hanson, P. J., Edwards, N. T., Garten, C. T. & Andrews, J. A. (2000). Separating root and soil microbial contributions to soil respiration: a review of methods and observations. *Biogeochemistry* **48**, 115-146.

Hardie, S. M. L., Garnett, M. H., Fallick, A. E., Rowland, A. P. & Ostle, N. J. (2005). Carbon dioxide capture using a zeolite molecular sieve sampling system for isotopic studies (^{13}C and ^{14}C) of respiration. *Radiocarbon* **47**, 441-451.

Harkness, D. D., Harrison, A. F. & Bacon, P. J. (1986). The temporal distribution of bomb ^{14}C in a forest soil. *Radiocarbon* **28**, 328-337.

Harrison, A. F. & Harkness, D. D. (1994). Carbon Sequestration by Soils in the UK. In *Department of the Environment Report*, pp. 109-134: Institute of Terrestrial Ecology.

Harrison, A. F., Harkness, D. D., Rowland, A. P., Garnett, J. S. & Bacon, P. J. (2000). Chapter 11. Annual Carbon and Nitrogen Fluxes Along a European Forest Transect Determined Using ^{14}C-bomb. In *Carbon and Nitrogen Cycling in European Forest Ecosystems*, pp. 237-256. Edited by E.-D. Schulze. Heidelberg: Springer Verlag.

Harrison, K. G. (1996). Using bulk soil radiocarbon measurements to estimate soil organic matter turnover times: implications for atmospheric CO_2 levels. *Radiocarbon* **38**, 181-190.

Harvey, L. D. D. (2000). *Global warming: the hard science*: Pearson Education Limited, U.K. pp.336.

Haywood, J. & Boucher, O. (2000). Estimates of the direct and indirect radiative forcing due to tropospheric aerosols: a review. *Reviews of Geophysics* **38**, 513-543.

Heal, O. W., Latter, P. M. & Howson, G. (1978). A Study of the Rates of Decomposition of Organic Matter. In *Production Ecology of British Moorlands and Montane Grasslands*, pp. 136-159. Edited by O. W. Heal & D. F. Perkins. Berlin: Springer-Verlag.

Heal, O. W. & Smith, R. A. H. (1978). Introduction and Site Description. In *Production Ecology of British Moorlands and Montane Grasslands*, pp. 3-16. Edited by O. W. Heal & D. F. Perkins. Berlin: Springer-Verlag.

Heikkinen, J. E. P., Elsakov, V. & Martikainen, P. J. (2002). Carbon dioxide and methane dynamics and annual carbon balance in tundra wetland in NE Europe, Russia. *Global Biogeochemical Cycles* **16**, art. no.-1115.

Hemming, D., Yakir, D., Ambus, P., Aurela, M., Besson, C., Black, K., Buchmann, N., Burlett, R., Cescatti, A., Clement, R., Gross, P., Granier, A., Grunwald, T., Havrankova, K., Janous, D., Janssens, I. A., Knohl, A., Ostner, B. K., Kowalski, A., Laurila, T., Mata, C., Marcolla, B., Matteucci, G., Moncrieff, J., Moors, E. J., Osborne, B., Pereira, J. S., Pihlatie, M., Pilegaard, K., Ponti, F., Rosova, Z., Rossi, F., Scartazza,A., & Vesala, T. (2005). Pan-European $\delta^{13}C$ values of air and organic matter from forest ecosystems. *Global Change Biology* **11**, 1065-1093.

Hobbs, R. J. & Gimingham, C. H. (1987). Vegetation, fire and herbivore interactions in heathland. *Advances in Ecological Research* **16**, 87-173.

Holton, J. R., Haynes, P. H., McIntyre, M. E., Douglass, A. R., Rood, R. B. & Pfister, L. (1995). Stratosphere-troposphere exchange. *Reviews of Geophysics* **33**, 403-439.

Houghton, J. (1997). *Global Warming: the complete briefing*, 2nd edn. pp. 382. Cambridge, United Kingdom: Cambridge University Press.

Hua, Q. & Barbetti, M. (2004). Review of tropospheric bomb ^{14}C data for carbon cycle modeling and age calibration purposes. *Radiocarbon* **46**, 1273-1298.

Idso, S. B. & Kimball, B. A. (1993). Tree growth in carbon dioxide enriched air and its implications for global carbon cycling and maximum levels of atmospheric CO_2. *Global Biogeochemical Cycles* **7**, 537-555.

Illeris, L., Christensen, T. R. & Mastepanov, M. (2004). Moisture effects on temperature sensitivity of CO_2 exchange in a subarctic heath ecosystem. *Biogeochemistry* **70**, 315-330.

Ineson, P., Cotrufo, M. F., Bol, R., Harkness, D. D. & Blum, H. (1996). Quantification of soil carbon inputs under elevated CO_2: C_3 plants in a C_4 soil. *Plant & Soil* **187**, 345-350.

Ineson, P., Taylor, K., Harrison, A. F., Poskitt, J., Benham, D. G., Tipping, E. & Woof, C. (1998). Effects of climate change on nitrogen dynamics in upland soils. 1. A transplant approach. *Global Change Biology* **4**, 143-152.

Ingram, H. A. P. (1978). Soil layers in mires - function and terminology. *Journal of Soil Science* **29**, 224-227.

IPCC (2001). *Climate Change 2001: the Scientific Basis*, pp. 881. Edited by J. T. Houghton & D. Yihui. Cambridge: Cambridge University Press.

Janssens, I. A., Kowalski, A. S., Longdoz, B. & Ceulemans, R. (2000). Assessing forest soil CO_2 efflux: an in situ comparison of four techniques. *Tree Physiology* **20**, 23-32.

Jenkinson, D. S., Adams, D. E. & Wild, A. (1991). Model estimates of CO_2 emissions from soil in response to global warming. *Nature* **351**, 304-306.

Jenkinson, D. S., Harkness, D. D., Vance, E. D., Adams, D. E. & Harrison, A. F. (1992). Calculating net primary production and annual input of organic-matter to soil from the amount and radiocarbon content of soil organic-matter. *Soil Biology & Biochemistry* **24**, 295-308.

Joabsson, A., Christensen, T. R. & Wallen, B. (1999). Vascular plant controls on methane emissions from northern peatforming wetlands. *Trends in Ecology & Evolution* **14**, 385-388.

Johnson, D., Booth, R. E., Whiteley, A. S., Bailey, M. J., Read, D. J., Grime, J. P. & Leake, J. R. (2003). Plant community composition affects the biomass, activity and diversity of microorganisms in limestone grassland soil. *European Journal of Soil Science* **54**, 671-677.

Jungner, H., Sonninen, E., Possnert, G. & Tolonen, K. (1995). Use of bomb-produced ^{14}C to evaluate the amount of CO_2 emanating from two peat bogs in Finland. *Radiocarbon* **37**, 567-573.

Karlsson, H. R. (2002). The Use of Molecular Sieves in Stable Isotope Analysis. In *Handbook of Stable Isotope Analytical Techniques - Volume 1*. Edited by P. A. De Groot. Amsterdam: Elsevier.

Kasting, J. F., Toon, O. B. & Pollack, J. B. (1988). How climate evolved on the terrestrial planets. *Scientific American* **258**, 90-97.

Katterer, T., Reichstein, M., Andren, O. & Lomander, A. (1998). Temperature dependence of organic matter decomposition: a critical review using literature data analyzed with different models. *Biology & Fertility of Soils* **27**, 258-262.

Kaufman, Y. J. & Koren, I. (2006). Smoke and pollution aerosol effect on cloud cover. *Science* **313**, 655-658.

Keeling, C. D. (1958). The concentration and isotopic abundances of atmospheric carbon dioxide in rural areas. *Geochimica et Cosmochimica Acta* **13**, 322-334.

Keeling, C. D. & Whorf, T. P. (2002). Atmospheric CO_2 Records from Sites in the SIO Air Sampling Network. In *Trends: a Compendium of Data on Global Change*: Carbon Dioxide Information Analysis Center, Oak Ridge National Laboratory, U.S. Department of Energy, Oak Ridge, Tenn., U.S.A.

Kilian, M. R., van Geel, B. & van der Plicht, J. (2000). ^{14}C AMS wiggle matching of raised bog deposits and models of peat accumulation. *Quaternary Science Reviews* **19**, 1011-1033.

Kirschbaum, M. U. F. (1995). The temperature-dependence of soil organic-matter decomposition, and the effect of global warming on soil organic-C storage. *Soil Biology & Biochemistry* **27**, 753-760.

Kirschbaum, M. U. F. (2000). Will changes in soil organic carbon act as a positive or negative feedback on global warming? *Biogeochemistry* **48**, 21-51.

Kirschbaum, M. U. F. (2004). Soil respiration under prolonged soil warming: are rate reductions caused by acclimation or substrate loss? *Global Change Biology* **10**, 1870-1877.

Kirschbaum, M. U. F. (2006). The temperature dependence of organic-matter decomposition - still a topic of debate. *Soil Biology & Biochemistry* **38**, 2510-2518.

Knorr, W., Prentice, I. C., House, J. I. & Holland, E. A. (2005). Long-term sensitivity of soil carbon turnover to warming. *Nature* **433**, 298-301.

Koarashi, J., Amano, H., Andoh, M., Iida, T. & Moriizumi, J. (2002). Estimation of (CO_2)-^{14}C flux at soil-atmosphere interface and distribution of ^{14}C in forest ecosystem. *Journal of Environmental Radioactivity* **60**, 249-261.

Kohlmaier, G. H., Janecek, A. & Kindermann, J. (1990). Positive and Negative Feedback Loops Within the Vegetation/Soil System in Response to a CO_2 Greenhouse Warming. In *Soils and the Greenhouse Effect*, pp. 415-422. Edited by A. F. Bouwman. Chichester: Wiley.

Koncalová, H., Pokorny, J. & Kvet, J. (1988). Root ventilation in *Carex gracilis* Curt. - diffusion or mass flow? *Aquatic Botany* **30**, 149-155.

Kuzyakov, Y. (2006). Sources of CO_2 efflux from soil and review of partitioning methods. *Soil Biology & Biochemistry* **38**, 425-448.

Ladyman, S. J. & Harkness, D. D. (1980). Carbon isotope measurement as an index of soil development. *Radiocarbon* **22**, 885-891.

Lai, C. T., Ehleringer, J. R., Tans, P., Wofsy, S. C., Urbanski, S. P. & Hollinger, D. Y. (2004). Estimating photosynthetic ^{13}C discrimination in terrestrial CO_2 exchange from canopy to regional scales. *Global Biogeochemical Cycles* **18**, art. no. GB1041

Latter, P. M., Cragg, J. B. & Heal, O. W. (1967). Comparative studies on the microbiology of four moorland soils in the northern Pennines. *Journal of Ecology* **55**, 445-464.

Leifeld, J. & Fuhrer, J. (2005). The temperature response of CO_2 production from bulk soils and soil fractions is related to soil organic matter quality. *Biogeochemistry* **75**, 433-453.

Leuenberger, M., Siegenthaler, U. & Langway, C. C. (1992). Carbon isotope composition of atmospheric CO_2 during the last ice-age from an Antarctic ice core. *Nature* **357**, 488-490.

Levin, I. & Hesshaimer, V. (2000). Radiocarbon - a unique tracer of global carbon cycle dynamics. *Radiocarbon* **42**, 69-80.

Levin, I. & Kromer, B. (2004). The tropospheric $^{14}CO_2$ level in mid latitudes of the Northern Hemisphere (1959-2003). *Radiocarbon* **46**, 1261-1272.

Libby, W. F. (1946). Atmospheric helium three and radiocarbon from cosmic radiation. *Physical Review* **69**, 671-672.

Libby, W. F. (1960). Radiocarbon dating: Nobel lecture.

Lin, G. H. & Ehleringer, J. R. (1997). Carbon isotopic fractionation does not occur during dark respiration in C_3 and C_4 plants. *Plant Physiology* **114**, 391-394.

Lindroth, A., Grelle, A. & Moren, A. S. (1998). Long-term measurements of boreal forest carbon balance reveal large temperature sensitivity. *Global Change Biology* **4**, 443-450.

Lingenfelter, R. E. (1963). Production of carbon-14 by cosmic ray neutrons. *Reviews of Geophysics* **1**, 35-55.

Liski, J., Ilvesniemi, H., Mäkelä, A. & Westman, C. J. (1999). CO_2 emissions from soil in response to climatic warming are overestimated - the decomposition of old soil organic matter is tolerant of temperature. *Ambio* **28**, 171-174.

Liski, J., Ilvesniemi, H., Mäkelä, A. & Westman, C. J. (2000). Temperature dependence of old soil organic matter. *Ambio* **29**, 56.

Lloyd, J. & Farquhar, G. D. (1994). ^{13}C discrimination during CO_2 assimilation by the terrestrial biosphere. *Oecologia* **99**, 201-215.

Lloyd, J. & Taylor, J. A. (1994). On the temperature-dependence of soil respiration. *Functional Ecology* **8**, 315-323.

Löhnis, F. (1926). Nitrogen availability of green manures. *Soil Science* **22**, 253-290.

Longdoz, B., Yernaux, M. & Aubinet, M. (2000). Soil CO_2 efflux measurements in a mixed forest: impact of chamber disturbances, spatial variability and seasonal evolution. *Global Change Biology* **6**, 907-917.

Luo, Y. Q., Wan, S. Q., Hui, D. F. & Wallace, L. L. (2001). Acclimatization of soil respiration to warming in a tall grass prairie. *Nature* **413**, 622-625.

Mack, M. C., Schuur, E. A. G., Bret-Harte, M. S., Shaver, G. R. & Chapin, F. S. (2004). Ecosystem carbon storage in Arctic tundra reduced by long-term nutrient fertilization. *Nature* **431**, 440-443.

Malhi, Y., Nobre, A. D., Grace, J., Kruijt, B., Pereira, M. G. P., Culf, A. & Scott, S. (1998). Carbon dioxide transfer over a Central Amazonian rain forest. *Journal of Geophysical Research-Atmospheres* **103**, 31593-31612.

Manley, G. (1936). The climate of the northern Pennines the coldest part of England. *Quarterly Journal of the Royal Meteorological Society* **62**, 103-115.

RADIOCARBON, Vol 47, Nr 3, 2005, p 441–451 © 2005 by the Arizona Board of Regents on behalf of the University of Arizona

CARBON DIOXIDE CAPTURE USING A ZEOLITE MOLECULAR SIEVE SAMPLING SYSTEM FOR ISOTOPIC STUDIES (^{13}C AND ^{14}C) OF RESPIRATION

S M L Hardie[1,2,3] • M H Garnett[1] • A E Fallick[4] • A P Rowland[2] • N J Ostle[2]

ABSTRACT. A method for collecting an isotopically representative sample of CO_2 from an air stream using a zeolite molecular sieve is described. A robust sampling system was designed and developed for use in the field that includes reusable molecular sieve cartridges, a lightweight pump, and a portable infrared gas analyzer (IRGA). The system was tested using international isotopic standards (^{13}C and ^{14}C). Results showed that CO_2 could be trapped and recovered for both $\delta^{13}C$ and ^{14}C analysis by isotope ratio mass spectrometry (IRMS) and accelerator mass spectrometry (AMS), respectively, without any contamination, fractionation, or memory effect. The system was primarily designed for use in carbon isotope studies of ecosystem respiration, with potential for use in other applications that require CO_2 collection from air.

INTRODUCTION

The rapid increase in atmospheric CO_2 concentrations and concomitant rise in temperature observed in the last century have led to a need for a more accurate understanding of the link between the global carbon cycle and climate change (IPCC 2001). It is estimated that soils contain 1.6 Tt of carbon, a stock twice that found in the atmosphere and 3 times that of the terrestrial plant biomass (Schimel 1995). Both climate and land use are key regulators of ecosystem carbon stocks (Lindroth et al. 1998; Lloyd and Taylor 1994; Raich and Tufekcioglu 2000; Sanderman et al. 2003; Trumbore et al. 1996). Of particular importance in this respect is the balance between soil carbon sequestration and respiration that, if shifted, has the potential to contribute further to atmospheric CO_2 increases (Cox et al. 2000; Knorr et al. 2005; Mack et al. 2004).

Natural abundance carbon isotope tracers can be used as a means to better understand and predict how Earth's carbon reservoirs will respond to global change (climate, land use, pollution). Differences in the $\delta^{13}C$ signatures of C_3 and C_4 plants and derivative soil organic matter (SOM) have been used to examine rates of decomposition and turnover of SOM on time scales of 1 yr to hundreds of thousands of years (Balesdent and Mariotti 1996; Boutton 1996). Studies have also used radiocarbon analyses of bulk SOM to estimate rates of carbon cycling in a range of ecosystems (Harkness et al. 1986; Harrison 1996; Paul et al. 1997; Quideau et al. 2001; Richter et al. 1999). However, since SOM is composed of various pools of carbon cycling on different time scales (i.e. from hours to millennia), bulk measurements obscure the response of specific pools to both transient and long-term change. Furthermore, although measurements of ^{14}C in SOM have been used as a surrogate for soil respiration, Trumbore (2000) has suggested that this approach significantly underestimates CO_2 fluxes. Consequently, there is now considerable interest in the use of ecosystem and soil-respired CO_2 isotopic signatures to understand the role of environmental factors on the rate of organic matter decomposition and the magnitude and source of CO_2 fluxes.

Capture of CO_2 respired from soils for subsequent isotopic analysis has been achieved in the field using various methods, including cryogenic trapping, collection in evacuated flasks (e.g. Charman et al. 1999), and absorption in hydroxide solutions such as sodium hydroxide (e.g. Dörr and Münnich 1986). Each of these methods has its disadvantages, but common to all is the fact that they are impractical when used at remote locations in the field. For example, absorption of CO_2 in hydrox-

[1]NERC Radiocarbon Laboratory, Rankine Avenue, Scottish Enterprise Technology Park, East Kilbride, G75 0QF, United Kingdom.
[2]Centre for Ecology and Hydrology, Library Avenue, Bailrigg, Lancaster, LA1 4AP, United Kingdom.
[3]Corresponding author. Email: smlh@ceh.ac.uk.
[4]Scottish Universities Environmental Research Centre, Rankine Avenue, Scottish Enterprise Technology Park, East Kilbride, G75 0QF, United Kingdom.

ide solutions causes an isotopic fractionation effect (Keeling 1958), and the solutions are difficult to use in the field due to their caustic nature. Cryogenic trapping of CO_2 in the field using liquid nitrogen (b.p. –196 °C) is potentially hazardous and may result in the condensation of atmospheric O_2 (b.p. –183 °C). This may reduce the collection efficiency of CO_2 but more importantly could result in an explosive situation on recovery of CO_2 using a vacuum rig (Bauer 1992). A small number of studies have utilized zeolites (often referred to as molecular sieves) as an alternative method of CO_2 capture (Bauer et al. 1992; Bol and Harkness 1995; Gaudinski et al. 2000; Koarashi et al. 2002). The zeolite molecular sieve approach is easy to use and has none of the above disadvantages, thus making it ideal for field experiments and remote area research to determine the isotopic source of ecosystem and soil-respired CO_2. Furthermore, the molecular sieve material (synthetic faujasite) is reusable and can withstand temperatures of 500 °C almost indefinitely (Barrer 1959).

Zeolites

Zeolites are 3-dimensional crystalline aluminosilicates of the alkali and alkaline earth elements (commonly sodium, potassium, and calcium) represented by the empirical molecular formula:

$$M_{2/n}O \cdot Al_2O_3 \cdot xSiO_2 \cdot yH_2O$$

where n is the valence of the cation and x and y are integers. Zeolites are used in the petrochemical and petroleum refining industries as ion exchangers, adsorbents, and selective catalysts (Yang 1997). The characteristics of zeolites (dehydrated zeolites in particular) that are of interest when partitioning an analyte gas from a mixture of gases, such as the separation of CO_2 from air, include uniform molecular pore size, polarity, reversible and selective adsorption (different cationic forms of zeolite can lead to significant differences in the adsorption of a given gas), and adsorption capacity. Firstly, the 3-dimensional framework of the crystalline aluminosilicate structure created via the sharing of adjacent oxygen atoms by SiO_4 and AlO_4 tetrahedra (Breck 1974) contains a network of uniform molecular-sized pores (3–8 Å; Flanigen 1991). This feature gives zeolites their molecular sieving property as the porous structure allows selective admittance of molecules with diameters less than that of the pore window size, while those that are larger are sterically or kinetically hindered. Secondly, the isomorphous substitution of aluminium for silicon in the crystalline lattice structure of a zeolite lends it an overall net negative charge. This negative charge is neutralized by an electrochemical equivalent of cations (Barrer 1978) such as sodium, barium, and potassium. Consequently, zeolites have a high affinity for polar molecules such as H_2O and CO_2. Competitive adsorption is typically of the order $H_2O>CO_2>N_2>O_2$ (Breck 1974) at ambient temperature and pressure. The affinity of polar molecules like CO_2 for substituted zeolites is due to an interaction between the molecule and the zeolite. In the case of CO_2, it is the interaction of its quadrupole moment with the electric field of the zeolite (Cui et al. 2003), resulting in high adsorption of monolayer coverage (Siriwardane et al. 2001). Furthermore, the isotherms applicable to many zeolites follow classification "I" of IUPAC (International Union of Pure and Applied Chemistry) grouping, also known as the Langmuir type adsorption isotherm (Ruthven 1984). A crucial property possessed by zeolites is reversible sorption. Desorption of a gaseous adsorbate from zeolite can be effectively controlled by the application of adequate temperature or pressure (BDH, no date), otherwise a hysteretic effect may occur. Finally, zeolites possess a high adsorption capacity at ambient temperature and pressure, even at low adsorbate concentrations (BDH, no date).

Zeolites in Isotope Studies of CO_2

Zeolites that have been used in the partitioning of the trace gas CO_2 from carrier gas streams include molecular sieve type 4A (Koarashi et al. 2002), a sodium aluminosilicate with an effective pore

diameter of 4.2 Å, and type 13X (Bauer et al. 1992; Bol and Harkness 1995; Gaudinski et al. 2000), another sodium aluminosilicate with an effective pore diameter of 7.8 Å (Flanigen 1991). Bauer et al. (1992) used standards of known isotopic composition to test molecular sieve type 13X incorporated within a vacuum rig. The use of a single ^{13}C standard, however, precluded the detection of any isotopic memory effect. Two standards were used for ^{14}C, but any tests for memory effect were not reported.

Bol and Harkness (1995) carried out a method validation of their sampling system (incorporating molecular sieve type 13X) using the ^{13}C signal of atmospheric CO_2. While accounting for possible isotope fractionation, this method was not designed to detect any memory effect or indeed any contamination via atmospheric CO_2 leaking into the sampling system. Gaudinski et al. (2000) made a study of the ^{14}C content of soil respiration using molecular sieve type 13X but do not report testing of their sampling system. In another soil respiration study, Koarashi et al. (2002) used molecular sieve type 4A; tests were made for quantitative recovery but not for isotope fractionation or memory effect.

In this paper, we describe the development of a sampling system intended for ecosystem respiration studies that utilizes molecular sieve type 13X. In addition, a rigorous analytical testing program was executed by repeated measurement of authenticated laboratory standards (both $^{13}CO_2$ and $^{14}CO_2$) to enable the detection of any atmospheric contamination, isotopic fractionation, or memory effect.

EXPERIMENTAL

Sampling System Design

A closed-loop sampling system was designed (see Figures 1 and 2) for laboratory and field applications with elements similar to one described by Gaudinski et al. (2000). The sampling system incorporated the following components: a molecular sieve sampling cartridge (MSC), a CO_2 scrub, a bypass (to allow monitoring of CO_2 concentration before sampling), a water trap, a portable infrared gas analyzer (IRGA, PP Systems, UK), a sampling chamber, and a small battery-powered pump (AeroVironment Inc., USA).

The water trap, CO_2 scrubber, and sampling cartridges were made from quartz glass and based on an original design by Bol and Harkness (1995). Both ends of every cartridge were fitted with an auto-shutoff Quick Coupling™ (Colder Products Company, USA) attached with short lengths of PVC tubing (Tygon, Fisher Scientific, UK). WeLoc® clips (Scandinavia Direct, UK) were placed across the PVC tubing between each end of the cartridge and the Quick Couplings to control gas flow into the MSC during operation. All junctions were made using T-connectors (Kartell Plastics UK Ltd., UK).

The CO_2 scrubber cartridge was filled with ~14 g of soda lime (BDH laboratory supplies, UK) and the water trap (similar quartz cartridge) filled with a desiccant, regular $CaSO_4$, Lab Grade –10+20 Mesh (Alfa Aesar, Germany). A similar but smaller-bodied quartz cartridge was filled with 3–4 g of molecular sieve type 13X (1/16″ pellets, BDH Laboratory supplies, UK). The contents of all 3 cartridges were held in place with quartz wool. During the initial development of the sampling system, molecular sieve types 4A and 5A were tested before settling on the use of molecular sieve type 13X, the performance of which we discuss herein.

The sampling chamber (~5 L) used for the test program was constructed from PVC pipe and sealed at both ends with nitrile rubber (LRC Products Ltd, UK). The chamber was connected to the CO_2 sampling system via 2 Quick Couplings and nylon tubing (see Figure 2). Gas flow pathways within the sampling system were manipulated using WeLoc clips.

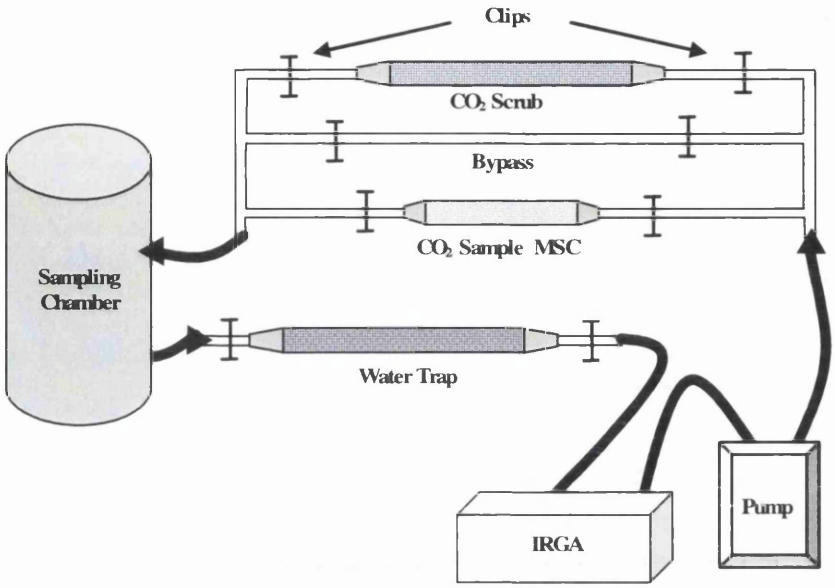

Figure 1 Schematic diagram of the molecular sieve sampling system. Gas flow pathways are manipulated by opening and closing the clips. Clips removed from the CO_2 scrub (soda lime) allow atmospheric CO_2 to be removed from within the sampling chamber. Removal of clips from the bypass allows CO_2 evolution inside the chamber to be monitored, thus ensuring that enough CO_2 has respired for ^{14}C analysis. Finally, clips are removed from the MSC to capture an isotopically representative sample of the CO_2 in the chamber. IRGA = infrared gas analyzer.

Figure 2 The molecular sieve sampling system in field operation. The chamber is for demonstration purposes only.

Molecular Sieve Cartridge Activation

To ensure that zeolite cartridges were free of contamination prior to sampling, MSCs were simultaneously heated to 500 °C using a tube furnace (Carbolite MTF 10/15, Carbolite, UK) and evacuated to 10^{-2} mbar (see Figure 3). A slush trap (consisting of dry ice and industrial methylated spirit) and a liquid nitrogen trap were used to aid desorption of any gases held on the zeolite. Each MSC was then allowed to cool to <30 °C and filled with high-purity N_2 gas to just above atmospheric pressure (~1100 mbar). We found that the new zeolite molecular sieve exhibited a small amount of hysteresis on first use (data not shown); therefore, fresh zeolite was first purged of all gases and then flushed with CO_2 in an air stream and repurged prior to sampling.

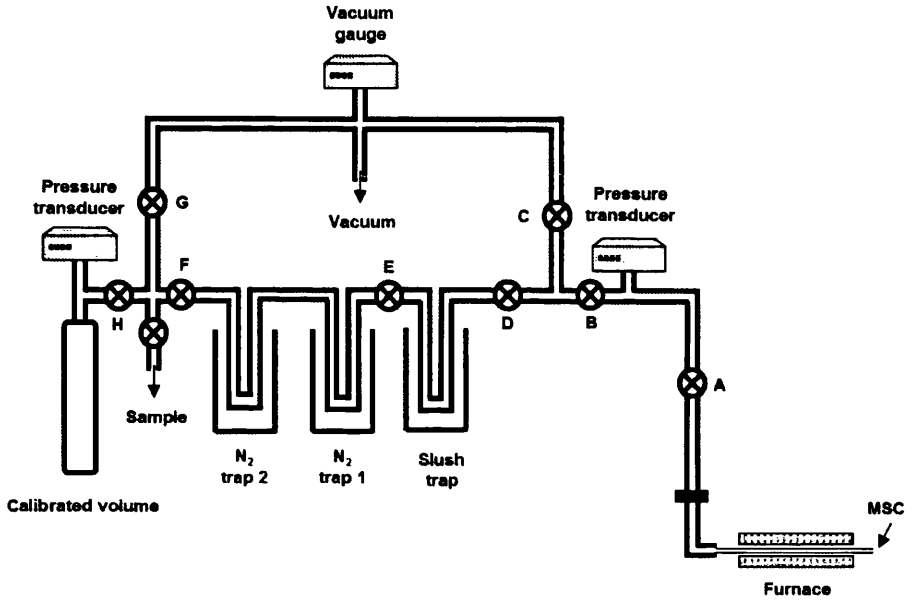

Figure 3 Schematic of the vacuum rig used in the desorption of CO_2 from the MSCs. Valves are labeled with capital letters.

CO_2 Sampling Procedure

A scored borosilicate glass tube containing a CO_2 standard was placed into the sampling chamber and positioned inside a cylindrical protrusion in one of the nitrile rubber seals. The sampling chamber atmosphere was then circulated by the pump (flow rate 500 mL min^{-1}) through the CO_2 scrubber cartridge and the CO_2 concentration monitored using the IRGA. The chamber was considered ready for testing when the CO_2 concentration had dropped below 10 ppm, whereupon the pathway through the CO_2 scrubber was closed and the pathway to the sample MSC was opened. This was considered acceptable for testing purposes because all standards were of a concentration greater than 1600 ppm CO_2 when released into the sampling chamber (i.e. the residual 10 ppm CO_2 accounted for <0.6% of the total).

The borosilicate glass tube containing a CO_2 standard was cracked within the sampling chamber, and the gas was pumped around the sampling system and through the MSC. The MSC was closed and sampling ceased when the sampling chamber CO_2 concentration had reduced to below 100 ppm.

Molecular Sieve Cartridge Desorption Procedure

The MSC was attached to the vacuum rig with the WeLoc clip still in place and dead space air removed by opening valves A, B, and C (see Figure 3) until 10^{-2} mbar was attained, whereupon all valves were closed. The MSC was then detached from the vacuum rig and the WeLoc clip removed from the front end of the cartridge to allow passage into the tube furnace. After insertion into the furnace, the clip was replaced and the MSC reattached to the rig. The vacuum rig was then pumped down to 10^{-2} mbar. A slush trap and 2 liquid N_2 traps were activated by raising the Dewar flasks around the borosilicate glass traps of the rig and valves A, B, D, and E opened. The MSC was then opened to the traps and the furnace temperature raised to 500 °C.

CO_2 was collected at 500 °C under static vacuum for 20 min after which valves F and G were opened and any non-condensables pumped away until a vacuum of 10^{-2} mbar was achieved in the MSC. All valves were then closed and the second nitrogen trap was removed and replaced with the slush trap. The CO_2 was transferred to the calibrated volume and the pressure of the expanded gas was measured using a pressure transducer (BOC Edwards, UK), allowing the volume of CO_2 recovered to be calculated. CO_2 was subsequently aliquoted into mass spectrometry tubes and $\delta^{13}C$ ratios analyzed by isotope ratio mass spectrometry (IRMS; dual inlet, VG Optima, UK). Further sub-samples of CO_2 were flame-sealed in borosilicate glass tubes, one of which was prepared as a graphite target (Slota et al. 1987) for ^{14}C measurement by accelerator mass spectrometry (AMS), by the 5MV tandem accelerator at the Scottish Universities Environmental Research Centre (SUERC), East Kilbride, UK (Freeman et al. 2004; Xu et al. 2004).

EXPERIMENTAL DESIGN

A total of 8 CO_2 standards were used in tests (ranging from 8 to 11 mL), 4 for each of the 2 MSCs used. The range of standard volumes chosen ensured sufficient CO_2 for AMS ^{14}C analysis, duplicate IRMS analysis, and also for a sub-sample to be archived. The CO_2 standards were prepared from materials with a wide range of $\delta^{13}C$ and ^{14}C isotopic signatures: Carbonate, Sucrose, and Barley mash (see Table 1). The range of $\delta^{13}C$ values from +1.8 to –26.8‰ allowed for stringent testing of the sampling system since the test covers a much greater range of values than would likely be encountered in the field. This also enabled a sensitive test for memory effect by alternating capture of standards (i.e. the difference between the Barley mash standard and the Carbonate standard for $\delta^{13}C$ analysis is 28.6‰).

Table 1 $\delta^{13}C$ and ^{14}C consensus values for isotopic standards used in the analytical testing program of the molecular sieve sampling system.

Standard material	$\delta^{13}C_{VPDB}$ ‰ (±0.1)	^{14}C concentration (% Modern ±1 σ)
Carbonate	+1.8	Background
Barley mash	–26.8	116.35 ± 0.0084 (Gulliksen and Scott 1995)
ANU Sucrose	–10.5	150.61 ± 0.11 (Rozanski et al. 1992)

The standards had natural abundance ^{14}C values ranging from 150.6% Modern (Sucrose) to background (Carbonate). A Sucrose standard following a Carbonate standard affects a difference of ~150% Modern and again allowed for a sensitive test of memory effect. Each of the 2 sets of standards were captured and recovered from both of the MSCs (1 and 2) sequentially. Table 2 illustrates the running order of the 4 standards with the previous standard applied to the 2 MSCs also given. All

values for ^{13}C are reported using the delta notation with $^{13}C/^{12}C$ variations relative to the international standard Vienna Pee Dee Belemnite (VPDB) as described by the following equation:

$$\delta^{13}C\,(‰) = \left[\frac{(^{13}C/^{12}C)_{Sample} - (^{13}C/^{12}C)_{VPDB}}{(^{13}C/^{12}C)_{VPDB}}\right] \times 1000$$

^{14}C data are reported as % Modern with samples being normalized to a $\delta^{13}C$ of –25‰ (Stuiver and Polach 1977).

Table 2 $\delta^{13}C$ and ^{14}C results for standard gases after adsorption and desorption from molecular sieve sampling cartridges 1 and 2 and subsequent recovery for analysis by IRMS and AMS. Numbers in brackets beside the run order identify which of the 2 MSCs were used. The $\delta^{13}C$ measurements are the mean of 2 replicate analyses.

Run order	Standard material	Publication code	$\delta^{13}C_{VPDB}$ (±0.1‰)	^{14}C concentration (% Modern ±1 σ)
Previous	Sucrose	—	—	—
1 (1)	Carbonate	SUERC-4181	+1.7	1.23 ± 0.02
2 (1)	Sucrose	SUERC-4182	–10.7	150.59 ± 0.44
3 (1)	Barley mash	SUERC-4183	–26.9	116.91 ± 0.36
4 (1)	Barley mash	SUERC-4187	–26.8	116.37 ± 0.27
Previous	Carbonate	—	—	—
1 (2)	Sucrose	SUERC-4188	–10.6	150.06 ± 0.41
2 (2)	Carbonate	SUERC-4189	+1.7	1.28 ± 0.02
3 (2)	Barley mash	SUERC-4191	–26.7	114.78 ± 0.28
4 (2)	Barley mash	SUERC-4192	–26.8	115.94 ± 0.36

RESULTS

During initial development of the molecular sieve sampling system, testing was undertaken at each stage using CO_2 standards of known volume and $\delta^{13}C$. These results are not presented but led to modifications to the design of the MSCs and the MSC activation and desorption procedures, which are described in the Discussion.

The results of the $\delta^{13}C$ and ^{14}C analysis of standards used to test the final design of the MSCs and procedures are displayed in Table 2. The table shows that all $\delta^{13}C$ results were within 2 σ of the consensus values of the standards. The ^{14}C concentrations of the 2 Carbonate standards (SUERC-4181 and -4189) were higher than the usual levels obtained at the laboratory for background standards (i.e. for blanks combusted in sealed quartz tubes or processed by acid hydrolysis) but were identical at 2 σ. The remaining standards were therefore background-corrected using the mean ^{14}C concentration of these 2 carbonates (1.25% Modern). With one exception, all results for the ^{14}C standards were within 2 σ of the consensus value.

DISCUSSION

Several studies have reported the use of a zeolite molecular sieve to capture CO_2 from air streams for isotope measurement (see Introduction). Of these, few present the results of tests used to verify their sampling methods. Through the development of our sampling system we made a number of changes to the original MSC design and operating procedures. Only when these changes were made did the

sampling system deliver quantitative trapping and recovery of CO_2 with preservation of isotopic integrity.

During the initial developmental stages of the sampling system, molecular sieve types 4A (pore window size 4.2 Å) and 5A (pore window size 4.9 Å; Dyer 1988) were tested for CO_2 capture before we settled on the use of molecular sieve type 13X (pore window size 7.8 Å). The kinetic diameter of CO_2 is 3.3 Å (Breck 1974), calculated from the minimum equilibrium dimension of 3.7 Å (as opposed to the Lennard-Jones approach), and so types 4A and 5A were deemed to have pore windows large enough to imbibe the CO_2 molecule. However, improved yields of CO_2 and $\delta^{13}C$ values that were much closer to the consensus values of the standards were obtained on initial testing of zeolite molecular sieve type 13X. Consequently, further testing of types 4A and 5A was abandoned.

Molecular sieve type 3A (effective pore diameter of 3 Å) was originally employed as a desiccant but was found to adsorb a small amount of CO_2 despite the fact that the kinetic diameter of this molecule is larger than the effective pore window size of the zeolite. This anomaly is due to 2 phenomena: 1) the oxygen framework of a zeolite is capable of being polarized (i.e. distorted); 2) both the zeolitic framework and the adsorbate molecule are continually vibrating under the influence of temperature, the net effect of which creates changes of ~0.4 Å in the size of the pore window (Dyer 1988). The combined effect of these processes is the adsorption of molecules of apparently larger diameter than that of the pore windows (measured crystallographically).

An important modification to the MSCs was to reduce the length of the section of quartz glass cartridge containing the zeolite molecular sieve material. Originally, this part of the MSC was the same length as the tube furnace used for desorption of CO_2 as based on the design of Bol and Harkness (1995). From their tests, Bol and Harkness (1995) reported mean recovery rates of only 88% of CO_2 (although they had other evidence suggesting greater recovery rates). However, with incomplete recovery of the sample, the risk of isotopic fractionation and memory effect remains. In the center of a tube furnace, there is a zone of uniform temperature (Carbolite, no date) that extends only to about 2.5 times the diameter of the tube measured from the outside of the furnace. Any area outside this central zone is likely to be at a lower temperature due to heat loss at the ends of the furnace. Only when the length of the main body of the MSC was reduced so that all the molecular sieve material was within the zone of uniform temperature did sample recoveries consistently reach ~100% and isotope results agree with consensus values. Prior to this modification, it is possible that some CO_2 that had been desorbed at 500 °C from within the zone of temperature uniformity was readsorbed onto cooler zeolite outside the zone. This was confirmed by moving the tube furnace backwards and forwards around the ends of the MSC while the MSC was attached to the vacuum rig during discharge. This movement resulted in an increase in pressure registered by the vacuum gauge.

In the procedure of Bol and Harkness (1995), MSCs were prepared by heating to 500 °C and evacuating to a best vacuum of 0.05 to 0.1 torr. We reduced this pressure to 10^{-2} mbar (0.0075 torr) for both activation and sample desorption. In this study, a higher vacuum ensured a sample recovery of >97% and an isotope signature consistent with the consensus value. The lower recoveries (~88%) observed by Bol and Harkness are therefore most likely due to incomplete desorption of CO_2 from the zeolite molecular sieve.

Another modification was the type of clips used to seal either end of the MSCs before and after sampling and to manipulate gas flows around the sampling system. The original design by Bol and Harkness (1995) utilized stainless steel Hoffman clips. These clips are relatively heavy, unwieldy to use, and require care to ensure that the tubing is sealed (plates of the Hoffman clip have to be paral-

lel). These were replaced with WeLoc clips, which are lighter; much easier to use, particularly in the field; and hold the required vacuum (10^{-2} mbar).

After all modifications were made, the sampling system was tested. Results are presented in Table 2. Since all ^{13}C results and all but one of the ^{14}C results of the standards recovered using the system fell within 2 σ of the consensus values, the results demonstrate that this sampling system collects isotopically representative samples of CO_2 from air streams.

The ^{14}C concentration of the Carbonate background standard was observed to be higher than the usual laboratory background (blank). This was not surprising given the greater number of potentially contaminating steps involved in the capture and desorption of the Carbonate standard (e.g. large surface areas of the molecular sieve material and the sampling system). It is possible that further modifications to the system could be made to provide a lower background value. However, current background levels are not considered to pose a particular limitation. First, the ^{14}C concentrations in the 2 background standards were statistically identical, suggesting a constant contribution that can be used to background-correct the other results. Secondly, the system is intended for the measurement of the ^{14}C concentration of ecosystem respiration, which is likely to be Modern (Gaudinski et al. 2000) and therefore little affected by variations in background.

We attribute a 1-σ error of ±0.1‰ to the IRMS measurement of $\delta^{13}C$. The $\delta^{13}C$ results were all within 2 σ of the consensus values, showing that the sampling system enabled capture, recovery, and analysis of a CO_2 sample without isotopic fractionation. For ^{14}C, there may be a suggestion of a memory effect in the results presented in Table 2 with, for example, the ^{14}C result for SUERC-4191 falling to the side of the previous standard applied to the MSC. However, there are also instances in the results that would not indicate any memory effect, e.g. the result for SUERC-4182 (150.59% Modern) is almost exactly the same as the consensus value (150.61% Modern), yet the previous standard on the MSC was a background standard (SUERC-4181).

The single result that fell outside the consensus value (SUERC-4191) could possibly be explained by a small amount of air contamination, assuming air would have a contemporary ^{14}C concentration of about 107% Modern (Levin and Kromer 2004). However, there are many examples in Table 2 that strongly suggest that they have not been contaminated with air. In the example of SUERC-4191, it is likely that the contamination would also have reflected a detectable shift in the $\delta^{13}C$ result due to the amount of air required (which was not the case). Consequently, since the results from the measurement of both ^{13}C and ^{14}C concentration, for a range of different standards, fell within 2-σ error of the consensus value (with the exception of one ^{14}C result), we believe that this molecular sieve sampling system provides a reliable method to collect isotopically representative samples of CO_2 from air streams.

CONCLUSIONS

A sampling system has been developed and tested for the collection of CO_2 from air. The system is easy to use, safe, portable, and suitable for use in the laboratory or at remote locations. Results from the measurement of standards collected using the system show that it can be used reliably to capture representative samples of CO_2 for isotopic studies. Although primarily designed for use in carbon isotope studies of soil and plant respiration, the system could be used for other applications that require CO_2 collection from air.

ACKNOWLEDGMENTS

We thank staff at the NERC Radiocarbon Laboratory for their assistance and support. We also thank the staff at the SUERC and the SUERC AMS for their contribution to this project. The authors acknowledge the NERC for providing ^{14}C support through allocation 1056.1003, and SMLH acknowledges the UK's Centre for Ecology and Hydrology for funding of a NERC studentship.

REFERENCES

Balesdent J, Mariotti A. 1996. Measurement of soil organic matter turnover using ^{13}C natural abundance. In: Boutton TW, Yamasaki S-I, editors. *Mass Spectrometry of Soils*. New York: Marcel Dekker Inc. p 83–112.

Barrer RM. 1959. New selective sorbents: porous crystals as molecular filters. *British Chemical Engineering* May Issue: 267–79.

Barrer RM. 1978. *Zeolites and Clay Minerals as Sorbents and Molecular Sieves*. New York: Academic Press. 497 p.

Bauer JE, Williams PM, Druffel ERM. 1992. Recovery of submilligram quantities of carbon dioxide from gas streams by molecular sieve for subsequent determination of isotopic (^{13}C and ^{14}C) natural abundances. *Analytical Chemistry* 64(7):824–7.

BDH. No date. 'Union Carbide' molecular sieves for selective adsorption. BDH Chemicals Ltd.

Bol RA, Harkness DD. 1995. The use of zeolite molecular sieves for trapping low concentrations of CO_2 from environmental atmospheres. *Radiocarbon* 37(2):643–7.

Boutton TW. 1996. Stable carbon isotope ratios of soil organic matter and their use as indicators of vegetation and climate change. In: Boutton TW, Yamasaki S-I, editors. *Mass Spectrometry of Soils*. New York: Marcel Dekker Inc. p 47–82.

Breck DW. 1974. *Zeolite Molecular Sieves: Structure, Chemistry and Use*. New York: John Wiley & Sons, Inc. 771 p.

Carbolite. No date. Range of tube furnaces. Carbolite, UK.

Charman DJ, Aravena R, Bryant CL, Harkness DD. 1999. Carbon isotopes in peat, DOC, CO_2, and CH_4 in a Holocene peatland on Dartmoor, southwest England. *Geology* 27(6):539–42.

Cox PM, Betts RA, Jones CD, Spall SA, Totterdell IJ. 2000. Acceleration of global warming due to carbon-cycle feedbacks in a coupled climate model. *Nature* 408(6809):184–7.

Cui Y, Kita H, Okamoto K. 2003. Preparation and gas separation properties of zeolite T membrane. *Chemical Communications* 17:2154–5.

Dörr H, Münnich KO. 1986. Annual variations of the ^{14}C content of soil CO_2. *Radiocarbon* 28(2A):338–45.

Dyer A. 1988. *An Introduction to Zeolite Molecular Sieves*. Chichester: J. Wiley & Sons. 149 p.

Flanigen EM. 1991. Zeolites and molecular sieves. An historical perspective. In: van Bekkum H, Flanigen EM, Jansen JC, editors. *Introduction to Zeolite Science and Practice*. Amsterdam: Elsevier Science Publishers B.V. p 13–34.

Freeman S, Xu S, Schnabel C, Dougans A, Tait A, Kitchen R, Klody G, Loger R, Pollock T, Schroeder J, Sundquist M. 2004. Initial measurements with the SUERC accelerator mass spectrometer. *Nuclear Instruments and Methods in Physics Research Section B* 223–24:195–8.

Gaudinski JB, Trumbore SE, Davidson EA, Zheng S. 2000. Soil carbon cycling in a temperate forest: radiocarbon-based estimates of residence times, sequestration rates and partitioning of fluxes. *Biogeochemistry* 51(1):33–69.

Gulliksen S, Scott M. 1995. Report of the TIRI workshop, Saturday 13 August 1994. *Radiocarbon* 37(2): 820–1.

Harkness DD, Harrison AF, Bacon PJ. 1986. The temporal distribution of "bomb" ^{14}C in a forest soil. *Radiocarbon* 28(2A):328–37.

Harrison KG. 1996. Using bulk soil radiocarbon measurements to estimate soil organic matter turnover times: implications for atmospheric CO_2 levels. *Radiocarbon* 38(2):181–90.

IPCC (Intergovernmental Panel on Climate Change). 2001. Houghton JT, Ding Y, Griggs DJ, Noguer M, van der Linden PJ, Dai X, Maskell K, Johnson CA, editors. *Climate Change 2001: The Scientific Basis*. Cambridge: Cambridge University Press. 892 p.

Keeling CD. 1958. The concentration and isotopic abundances of atmospheric carbon dioxide in rural areas. *Geochimica et Cosmochimica Acta* 13(4):322–34.

Knorr W, Prentice IC, House JI, Holland EA. 2005. Long-term sensitivity of soil carbon turnover to warming. *Nature* 433(7023):298–301.

Koarashi J, Amano H, Andoh M, Iida T, Moriizumi J. 2002. Estimation of $^{14}CO_2$ flux at soil-atmosphere interface and distribution of ^{14}C in forest ecosystem. *Journal of Environmental Radioactivity* 60(3):249–61.

Levin I, Kromer B. 2004. The tropospheric $^{14}CO_2$ level in mid-latitudes of the Northern Hemisphere (1959–2003). *Radiocarbon* 46(3):1261–72.

Lindroth A, Grelle A, Morén A-S. 1998. Long-term measurements of boreal forest carbon balance reveal large temperature sensitivity. *Global Change Biology* 4(4): 443–50.

Lloyd J, Taylor JA. 1994. On the temperature dependence of soil respiration. *Functional Ecology* 8(3): 315–23.

Mack MC, Schuur EAG, Bret-Harte MS, Shaver GR, Chapin FS III. 2004. Ecosystem carbon storage in arctic tundra reduced by long-term nutrient fertilization. *Nature* 431(7007):440–3.

Paul EA, Follett RF, Leavitt SW, Halvorson A, Peterson GA, Lyon DJ. 1997. Radiocarbon dating for determination of soil organic matter pool sizes and dynamics. *Soil Science Society of America Journal* 61(4):1058–67.

Quideau SA, Chadwick OA, Trumbore SE, Johnson-Maynard JL, Graham RC, Anderson MA. 2001. Vegetation control on soil organic matter dynamics. *Organic Geochemistry* 32(2):247–52.

Raich JW, Tufekcioglu A. 2000. Vegetation and soil respiration: correlations and controls. *Biogeochemistry* 48(1):71–90.

Richter DD, Markewitz D, Trumbore SE, Wells CG. 1999. Rapid accumulation and turnover of soil carbon in a re-establishing forest. *Nature* 400(6739):56–8.

Rozanski K, Stichler W, Gonfiantini R, Scott EM, Beukens RP, Kromer B, van der Plicht J. 1992. The IAEA ^{14}C Intercomparison Exercise 1990. *Radiocarbon* 34(3):506–19.

Ruthven D. 1984. *Principles of Adsorption and Adsorption Processes*. New York: John Wiley & Sons, Inc. 464 p.

Sanderman J, Amundson RG, Baldocchi DD. 2003. Application of eddy covariance measurements to the temperature dependence of soil organic matter mean residence time. *Global Biogeochemical Cycles* 17(2): 1061.

Schimel DS. 1995. Terrestrial ecosystems and the carbon cycle. *Global Change Biology* 1(1):77–91.

Siriwardane RV, Shen M-S, Fisher EP, Poston JA. 2001. Adsorption of CO_2 on molecular sieves and activated carbon. *Energy and Fuels* 15(2):279–84.

Slota PJ, Jull AJT, Linick TW, Toolin LJ. 1987. Preparation of small samples for ^{14}C accelerator targets by catalytic reduction of CO. *Radiocarbon* 29(2):303–6.

Stuiver M, Polach HA. 1977. Discussion: reporting of ^{14}C data. *Radiocarbon* 19(3):355–63.

Trumbore S. 2000. Age of soil organic matter and soil respiration: radiocarbon constraints on belowground C dynamics. *Ecological Applications* 10(2):399–411.

Trumbore SE, Chadwick OA, Amundson R. 1996. Rapid exchange between soil carbon and atmospheric carbon dioxide driven by temperature change. *Science* 272(5260):393–6.

Xu S, Anderson R, Bryant C, Cook GT, Dougans A, Freeman S, Naysmith P, Schnabel C, Scott EM. 2004. Capabilities of the new SUERC 5MV AMS facility for ^{14}C dating. *Radiocarbon* 46(1):59–64.

Yang RT. 1997. *Gas Separation by Adsorption Processes*. Series on Chemical Engineering, Volume 1. London: Imperial College Press. 364 p.

RADIOCARBON, Vol 48, Nr 1, 2006, p 61–68 © 2006 by the Arizona Board of Regents on behalf of the University of Arizona

A DIRECT METHOD TO MEASURE $^{14}CO_2$ LOST BY EVASION FROM SURFACE WATERS

M F Billett[1] • M H Garnett[2] • S M L Hardie[2,3]

ABSTRACT. Recent methodological advances in the use of zeolite molecular sieves for measuring the isotopic signature of CO_2 have provided the opportunity to make direct measurements of $^{14}CO_2$ in various field situations. We linked a portable molecular sieve/pump/IRGA system to a floating chamber to demonstrate the potential of the method to quantify the isotopic signature ($\delta^{13}C$ and ^{14}C) of CO_2 lost by evasion (outgassing) from surface waters. The system, which was tested on a peatland stream in Scotland, involved 1) an initial period of scrubbing ambient CO_2 from the chamber, 2) a period of CO_2 build-up caused by surface water evasion, and 3) a final period of CO_2 collection by the molecular sieve cartridge. The field test at 2 different sites on the same drainage system suggested that the results were reproducible in terms of $\delta^{13}C$ and ^{14}C values. These represent the first direct measurements of the isotopic signature of CO_2 lost by evasion from water surfaces.

INTRODUCTION

Surface waters in parts of the world are potentially significant flux pathways for CO_2 transport to the atmosphere; this has raised interesting questions about the nature and origin of CO_2 in terrestrial aquatic systems. In the Amazon Basin, evasion of CO_2 from wetlands is thought to account for 0.5 Gt C yr^{-1} and may represent a significant proportion of the "missing" C in the global carbon cycle (Richey et al. 2002). Recent isotopic data have confirmed that the CO_2 is mainly derived from respiration of young (<5 yr) allochthonous organic matter (Mayorga et al. 2005); this highlights the important role that isotopes can play in establishing key terrestrial C pathways (Grace and Malhi 2002). Streams and lakes associated with northern peatlands are also typically supersaturated with CO_2 (Kling et al. 1991), which is almost wholly lost to the atmosphere by evasion. Initial measurements at 2 Scottish peatland sites (Hope et al. 2001; Billett et al. 2004) suggests that the flux is significant and may be comparable to other flux terms in the peatland C cycle.

The ease of collecting streamwater dissolved and particulate organic carbon (DOC and POC) samples coupled with the use of accelerator mass spectrometry (AMS) means that natural abundance ^{14}C data are providing a significant amount of information about the age of organic carbon in surface waters. These data suggest that most, but not all, DOC in streamwater is modern (post-bomb, ^{14}C-enriched) carbon (Schiff et al. 1997; Raymond and Bauer 2001a,b; Palmer et al. 2001). Older DOC with depleted ^{14}C values appear to be derived from catchments like the Hudson River characterized by a higher degree of disturbance of the soil C pool (Raymond and Bauer 2001a). Data for rivers draining into the North Atlantic suggest that POC is ^{14}C-depleted, with ^{14}C ages ranging from modern to 4763 BP (Raymond and Bauer 2001a).

In contrast to DOC and POC and with the exception of the work by Mayorga et al. (2005), relatively little is known about the origin of CO_2 in streams and rivers. Methodological constraints have restricted isotopic studies of streamwater CO_2, which have been based on an acidification step that converts all the dissolved inorganic carbon (DIC) to CO_2, which is then captured cryogenically. This indirect "gas stripping" method, based on a procedure developed for seawater (Kroopnick et al. 1970; Kroopnick 1974), has been used to study the ^{13}C composition of DIC in freshwaters and large river estuaries (Quay et al. 1992; Pawellek and Veizer 1994; Yang et al. 1996; Atekwana and Krishnamurthy 1998; Palmer et al. 2001). It has also been used to study $^{14}CO_2$ evolution from ^{14}C labeled

[1]Centre for Ecology and Hydrology, Bush Estate, Penicuik, Midlothian, EH26 0QB, United Kingdom.
[2]Natural Environment Research Council (NERC) Radiocarbon Laboratory, Rankine Avenue, Scottish Enterprise Technology Park, East Kilbride, G75 0QF, United Kingdom.
[3]Centre for Ecology and Hydrology, Library Avenue, Bailrigg, Lancaster, LA1 4AP, United Kingdom.

organic substrates (e.g. Taylor et al. 1981). A recent paper by Mayorga et al. (2005), which presents ^{14}C and ^{13}C isotopic composition data for CO_2, is based on IRMS and AMS analysis of cryogenically purified CO_2 stripped after acidification of preserved water samples. The main difficulty with this indirect "gas stripping" method is that the isotopic composition of CO_2 lost by evasion is calculated and makes a number of assumptions about equilibrium reactions involving the various forms of DIC in streamwater (HCO_3^-, CO_3^{2-}, free CO_2). The composition of DIC in freshwater is strongly pH dependent and is derived from a variety of sources, such as weathering, in-stream respiration of organic matter, soil inputs of CO_2, and atmospheric invasion of CO_2 (Wetzel 1983). There is a need to develop a direct method, which does not involve chemical manipulation of water samples, to both age and source the origin of CO_2 lost by evasion from water surfaces.

The method presented here uses a combination of a floating chamber and zeolite molecular sieves to trap sufficient CO_2 for AMS analysis. Molecular sieves have been used successfully to trap CO_2 (e.g. Bauer et al. 1992; Bol and Harkness 1995), and the method described below is based on a system designed and tested for portable use in the field (Hardie et al. 2005). The method was tested at 2 sites on Black Burn, a peatland stream draining Auchencorth Moss, located 17 km SW of Edinburgh (central Scotland). The catchment (335 ha) is the site of a major study of evasion from surface waters and is characterized at its outlet by low pH (mean 4.7), high TOC (mean 40.7 mg L^{-1}) drainage waters (Billett et al. 2004).

METHODS

Samples for the isotopic determination of CO_2 lost by evasion from surface waters were collected by linking a portable zeolite molecular sieve/pump/IRGA (infrared gas analyzer) system (Hardie et al. 2005) with a floating chamber (Figure 1). The latter consists of a 1-kg brown opaque injection molded polypropylene box supplied by H C Slingsby plc (UK), external dimensions 30.5 cm (length), 30.5 cm (width), and 15.2 cm (height). The base of the box (volume: 9464 cm^3; basal area: 728 cm^2) has a 1-cm-wide lip, making it both stable and easier to form an effective seal with the water surface. Four holes were drilled into "spines" at the corners of the box to enable it where necessary to be held in position at a specific location on the water surface. The sealed chamber has sufficient volume to float freely without any buoyancy aid. To maintain the seal between the chamber and the water surface, the base of the chamber is submerged 2–3 cm below the water level; this decreases the "effective volume" of the floating chamber to ~9000 cm^3. Two auto-shutoff Quick Couplings™ (Colder Products Company, USA) were fitted into holes drilled 10 cm from the opposite corners of the upper chamber surface to allow gas to be pumped in and out of the floating chamber.

Subsequent to the use of the above floating chamber, we have found that in higher flow and windier conditions (greater water turbulence) a more stable chamber is necessary to maintain an effective seal with the water surface. We have been successfully using a chamber (supplied by H C Slingsby plc) with a rectangular (rather than square) base with the following external dimensions: 45.5 cm (length), 30.5 cm (width), and 15.2 cm (height). The chamber has a volume of 15,400 cm^3 and a basal area of 1141 cm^2.

Gas transfer between the stream surface and the atmosphere is controlled by the difference in gas concentration and turbulence at the air-water interface (Liss and Slater 1974); the latter caused by factors such as wind shear or, more importantly, streambed roughness and gradient. Locating the floating chamber close to zones of natural (or man-made) turbulence will selectively sample areas of the stream surface with high rates of degassing, and increase the amount of CO_2 available for trapping by the molecular sieve.

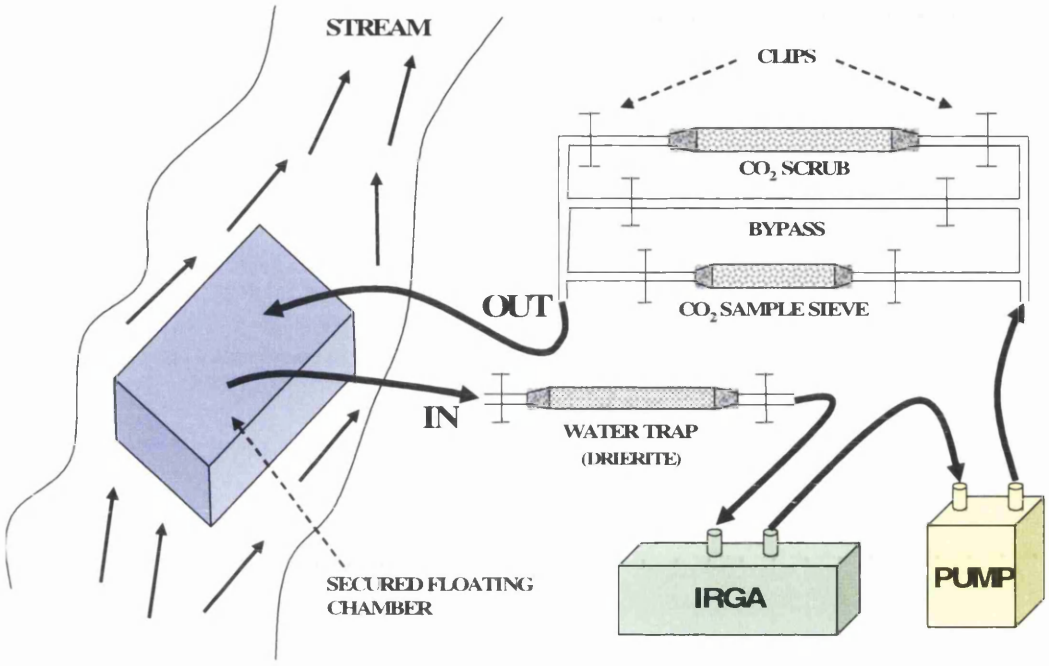

Figure 1 Schematic diagram to show the attachment of the floating chamber with the molecular sieve sampling system in the field.

The floating chamber is connected to a closed-loop sampling system, which first scrubs atmospheric CO_2 from the chamber, allows it to build up in the chamber, and then traps CO_2 lost by evasion from the water surface using a zeolite molecular sieve cartridge containing a type 13X molecular sieve (BDH, UK) (Figure 1). Initially, air from the chamber is drawn through a water trap (drierite; Alfa Aesar, Germany) into a portable IRGA (PP Systems, UK) and then out via a lightweight pump (flow rate ~600 mL min^{-1}) through a soda lime CO_2 scrub cartridge before re-entering the floating chamber through the second auto-shutoff coupling. A series of *T* pieces and WeLoc® clips (Scandinavia Direct, UK) allow the CO_2 scrub to be isolated after 30 min during which time 2 chamber volumes of air (18 L) have circulated through the system. CO_2 is then allowed to build up in the chamber as the air passes through an inert bypass cartridge; the rate of build-up can be continuously monitored by the inline IRGA. After a sufficient period of CO_2 build-up in the chamber (a function of the evasion rate), the zeolite molecular sieve cartridge is switched inline and the CO_2 trapped. The sampling time is a function of the rate of CO_2 build-up inside the chamber.

To test reproducibility and CO_2 recovery rates, the whole system was field tested on 13 August 2004 at Black Burn. Duplicate samples were collected from 2 sites (5 and 5A) located 750 m apart on the main stream channel (Figure 2). Evasion rates have been measured on 3 occasions at 5 different points along the main stream channel between January–August 2005 as part of a wider program of measurements in UK peatland streams. These results are presented to show how the $^{13}C/^{14}C$ "test" sites fit into the overall downstream spatial patterns in CO_2 evasion rates along Black Burn.

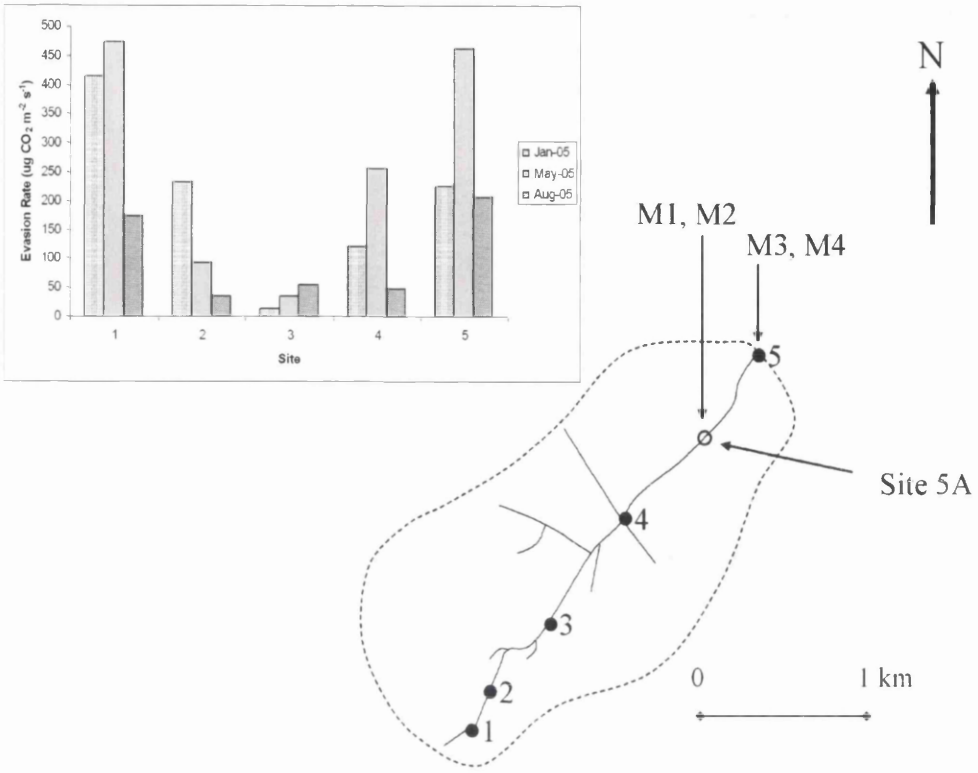

Figure 2 Location of the 2 sampling sites (5 and 5A) within the Auchencorth catchment and the variation in evasion rates along the length of Black Burn.

RESULTS

Evasion rates on the main stream channel at Auchencorth Moss varied from 14 to 475 μg CO_2 m^{-2} s^{-1}, with the lowest values occurring in the central part of the catchment where the stream is deep and slow flowing (Figure 2). Downstream trends exhibit significant and consistent spatial variation on different sampling occasions, temporal variation being strongly related to stream flow.

Figure 3 illustrates the changes in CO_2 concentrations occurring during the collection of the 4 "test" samples and demonstrates the 3 stages in the procedure: scrubbing, CO_2 build-up, and sampling. At both sites, CO_2 was scrubbed from the system for 30 min, sufficient time to allow 2 chamber volumes to be circulated through the system. At Site 5A, scrubbing was related to an increase in CO_2 concentrations because CO_2 was evaded from the stream surface faster than it was removed by the soda lime trap. At Site 5, CO_2 concentrations decreased because the evasion rate was lower. Following scrubbing, the rate of CO_2 increase can be used to calculate the evasion rate (knowing the chamber volume and surface area). This was significantly higher at Site 5A (Table 1), with chamber CO_2 concentrations reaching 1055 and 1155 ppmv within 10 min after the start of the build-up period.

We aimed to trap ~10 mL of CO_2 for each sample to provide sufficient material for AMS ^{14}C analysis, ^{13}C measurement, and to archive a sub-sample. Since previous tests have shown that the molecular sieve cartridges strip all the CO_2 from the airstream (Hardie et al. 2005), the amount of time to collect the required CO_2 was determined from the pump rate and chamber CO_2 concentration. For example, in the case of sample M1, the CO_2 concentration after CO_2 build-up was ~1000 ppmv;

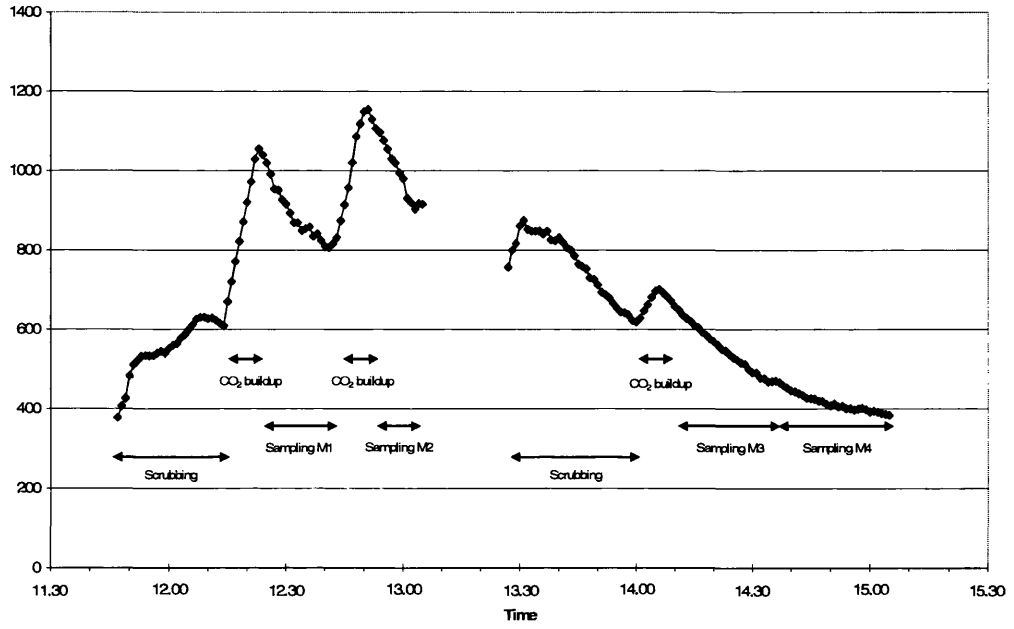

Figure 3 Temporal changes in CO_2 concentration during scrubbing, build-up, and sampling of CO_2 during the testing of the method.

Table 1 Isotopic data and evasion rates at the 2 test sites.

Lab code (SUERC-)	Sample identifier	Site	^{14}C enrichment (% Modern ±1 σ)	Conventional ^{14}C age (yr BP ±1 σ)	$\delta^{13}C_{VPDB}$‰ (±0.1)	CO_2 recovered (mL)	CO_2 evasion rate (μg CO_2 $m^{-2}s^{-1}$)
5930	M1	5A	83.44 ± 0.30	1454 ± 29	−21.0	9.9	203
5933	M2	5A	83.56 ± 0.30	1443 ± 29	−21.1	8.6	147
5934	M3	5	89.94 ± 0.29	852 ± 26	−21.0	8.2	60
5937	M4	5	88.76 ± 0.29	958 ± 26	−21.6	6.5	nd

therefore, at a pump rate of ~600 mL min^{-1}, approximately 0.6 mL min^{-1} CO_2 would be sampled, and so the total required sampling time was ~17 min. However, due to CO_2 trapping on the molecular sieve, the CO_2 concentration in the chamber progressively decreased (Figure 3) and a slightly longer sampling time was required; for sample M1 we collected a total of 9.9 mL CO_2 in 18 min. The higher chamber CO_2 concentration for sample M2 permitted a shorter sampling time (12 min), but since the evasion rates were lower at Site 5, CO_2 collection in cartridges M3 and M4 took longer (30 min on both occasions).

The molecular sieve cartridges containing the sample require no special storage and were returned to the NERC Radiocarbon Laboratory for processing. The CO_2 was collected from each sieve cartridge by heating (500 °C) and cryogenically collecting the CO_2 released on a purpose-built vacuum rig (full details of the method are provided by Hardie et al. 2005). A sub-sample of the CO_2 was graphitized using Fe-Zn reduction and underwent ^{14}C measurement on the 5MV AMS at the Scottish Universities Environmental Research Centre (Xu et al. 2004). A further sub-sample was analyzed for ^{13}C concentration using the NERC Radiocarbon Laboratory's IRMS (VG Optima, UK).

^{13}C concentrations are reported using the delta notation with $^{13}C/^{12}C$ variations relative to the international standard Vienna Pee Dee Belemnite (VPDB), described by the following equation:

$$\delta^{13}C\ (‰) = (^{13}C/^{12}C)_{Sample} - (^{13}C/^{12}C)_{VPDB} \times 1000(^{13}C/^{12}C)_{VPDB}$$

^{14}C results were expressed as % Modern and conventional ^{14}C age, having been normalized to a $\delta^{13}C$ of –25‰ (Stuiver and Polach 1977).

Table 1 shows that between 6.5 and 9.9 mL of CO_2 was recovered from the molecular sieve cartridges for the 4 test samples. The replicate samples from Site 5A (M1 and M2) had identical (<1 σ) ^{14}C ages and ^{13}C concentrations; however, there was a slight difference between the replicates (M3 and M4) from Site 5. The 2-σ ranges for both the ^{14}C and ^{13}C values just failed to overlap. The ^{14}C age of the evaded CO_2 differed far more between the 2 sampling locations; the mean age for samples from Site 5A was ~1450 BP, whereas 750 m downstream at Site 5 the age of the CO_2 was 500 to 600 yr younger.

DISCUSSION AND CONCLUSIONS

While floating chambers have been extensively used to measure gas release rates from lakes, estuaries, rivers, and streams (e.g. MacIntyre et al. 1995; Richey et al. 2002; Borges et al. 2004), the recent development and testing of a portable field system using zeolite molecular sieve cartridges (Hardie et al. 2005) has provided the opportunity to make a methodological step in the isotopic analysis of CO_2 lost by evasion from water surfaces. This avoids the need for sample acidification and can be carried out entirely in the field. The direct collection and analysis of CO_2 outgassed from the water surface allows this flux to be largely disconnected from the other components of dissolved inorganic carbon in streamwater. This is one of the main problems associated with indirect methods, in which the isotopic composition of CO_2 gas in equilibrium with DIC can be calculated assuming that a steady state or quasi-steady state exists between evaded CO_2 and CO_2 produced by within-stream production (Mayorga et al. 2005). Although a dynamic equilibrium exists between HCO_3^-, CO_3^{2-}, and free CO_2 in streamwater of low pH and high DOC (such as that characteristic of peatland drainage systems), most of the DIC is present in the form of free CO_2 (Wetzel 1983). A method that avoids chemical manipulation of the carbonate system and does not makes assumptions about equilibrium kinetics is therefore preferable and more likely to provide isotopic data that directly links CO_2 lost by evasion to its sources. The method may also be applied to a range of biogeochemically different aquatic environments, including high pH systems where carbonate dissolution is an important component of the equilibrium dynamics of DIC.

The data presented in Table 1 lists the first direct measured values of $\delta^{13}C$ and ^{14}C of CO_2 lost by evasion from water surfaces. The data demonstrate the reproducibility of the method; despite the replicates from Site 5 just failing to overlap at 2 σ, the other set of replicates had identical ^{13}C and ^{14}C contents at the <1-σ level. A possible reason for the small difference in the carbon isotope contents of the replicates from Site 5 could be due to inadequate scrubbing of the chamber prior to allowing the CO_2 to build up. This would result in a small component of atmospheric CO_2 contributing to the first samples in each pair of replicates from the 2 sites (i.e. M1 and M3). Given a pump rate of 600 mL min^{-1} and assuming complete removal of the CO_2 from the gas stream, we calculated that scrubbing the equivalent of 2 chamber volumes would leave an estimated ~0.40 mL of atmospheric CO_2 in the chamber (assuming the chamber had an initial atmospheric CO_2 concentration of 380 ppm). Using mass balance and assuming an atmospheric ^{14}C concentration of ~107% Modern (Levin and Kromer 2004) and ^{13}C of –9‰, we can correct the first replicate of each of the 2 sets of samples for this possible source of contamination. For sample M1, the correction resulted in a

slightly older ^{14}C age (1550 ± 29 BP) and a shift in the ^{13}C value to –21.5‰; however, the results remain identical (at <2 σ) to those of the replicate M2. When the results for M3 are corrected for this small amount of contamination, the new results (^{14}C age of 930 ± 26 BP and ^{13}C of –21.6‰) become identical to the replicate (M4) at the <1-σ level. Consequently, we consider that a greater amount of chamber air should be scrubbed prior to the CO_2 build-up stage, and recommend a minimum of the equivalent of 5 volumes be scrubbed. Although this would lead to a longer scrubbing period in the field, this can be reduced by using a pump with a flow rate greater than 600 mL min^{-1}.

Interestingly, the ^{14}C results suggest that the CO_2 is relatively old. This implies that the CO_2 is either derived from deep (old) peat or that it contains the signature of carbonates that are known to occur in thin bands beneath the peat bog. Peat has been accumulating at Auchencorth Moss since the end of the last ice age (~10,000 BP) and reaches up to 10 m in thickness. The possibility that the CO_2 is derived from the peat is also supported by the $\delta^{13}C$ values, which are all very similar and consistent with an allochthonous, soil-derived source for CO_2. The values also fall in the middle of the range of values (–17.2 to –25.2‰) reported for soil atmosphere CO_2 samples collected from deep peat and riparian soil in the Brocky Burn catchment, NE Scotland (Palmer et al. 2001). Clearly, more data are required to investigate this further; the main aim here is to present the method rather than to hypothesize further about the origins of CO_2 lost by evasion from peatland surface waters.

In conclusion, the ability to ^{14}C date CO_2 lost by evasion from surface waters and in other atmospheric samples using zeolite molecular sieves linked to a suitable collection system has the potential to improve our understanding of the C cycle; specifically, the technique is able to identify different sources of ^{14}C-enriched or depleted atmospheric CO_2. The direct method also removes some of the uncertainty associated with the indirect "gas stripping" method. Isotopic analysis of CO_2 clearly has the potential to provide answers to key questions about the cycling of C in the terrestrial environment.

ACKNOWLEDGMENTS

MFB acknowledges the support of NERC through an Advanced Research Fellowship and SMLH thanks the UK's Centre for Ecology and Hydrology for funding a NERC studentship. We also acknowledge the NERC for providing ^{14}C support.

REFERENCES

Atekwana EA, Krishnamurthy RV. 1998. Seasonal variations of dissolved inorganic carbon and $\delta^{13}C$ of surface waters: applications of a modified gas evolution technique. *Journal of Hydrology* 205:265–78.

Bauer JE, Williams PM, Druffel ERM. 1992. Recovery of submilligram quantities of carbon dioxide from gas streams by molecular-sieve for subsequent determination of isotopic (C-13 and C-14) natural abundances. *Analytical Chemistry* 64(7):824–7.

Billett MF, Palmer SM, Hope D, Deacon C, Storeton-West R, Hargreaves KJ, Flechard C, Fowler D. 2004. Linking land-atmosphere-stream carbon fluxes. *Global Biogeochemical Cycles* 18, GB1024, doi:10.1029/2003GB002058.

Bol RA, Harkness DD. 1995. The use of zeolite molecular sieves for trapping low concentrations of CO_2 from environmental atmospheres. *Radiocarbon* 37(2):643–7.

Borges AV, Delille B, Schiettecatte LS, Gazeau F, Abril A, Frankignoulle M. 2004. Gas transfer velocities of CO_2 in three European estuaries (Randers Fjord, Scheldt and Thames). *Limnology and Oceanography* 49:1630–41.

Grace J, Malhi Y. 2002. Carbon dioxide goes with the flow. *Nature* 416:594–5.

Hardie SML, Garnett MH, Fallick AE, Rowland AP, Ostle NJ. 2005. Carbon dioxide capture using a zeolite molecular sieve sampling system for isotopic studies (^{13}C and ^{14}C) of respiration. *Radiocarbon* 47(3):441–51.

Hope D, Palmer SM, Billett MF, Dawson JJC. 2001. Carbon dioxide and methane evasion from a temperate peatland stream. *Limnology and Oceanography* 46:847–57.

Kling GW, Kipphut GW, Miller MC. 1991. Arctic streams and lakes as gas conduits to the atmosphere:

implications for tundra carbon budgets. *Science* 251: 298–301.

Kroopnick P. 1974. The dissolved O_2-CO_2-^{13}C system in the eastern equatorial Pacific. *Deep-Sea Research* 21: 211–7.

Kroopnick P, Deuser WG, Craig H. 1970. Carbon-13 measurements on dissolved inorganic carbon at the North Pacific (1969) GEOSECS station. *Journal of Geophysical Research* 75:7668–71.

Levin I, Kromer B. 2004. The tropospheric $^{14}CO_2$ level in mid-latitudes of the Northern Hemisphere (1959–2003). *Radiocarbon* 46(3):1261–72.

Liss PS, Slater PG. 1974. Flux of gases across the air-sea interface. *Nature* 247:181–4.

MacIntyre S, Wanninkhof R, Chanton JP. 1995. Trace gas exchange across the air-water interface in freshwater and coastal marine environments. In: Matson PA, Harriss RC, editors. *Biogenic Trace Gases: Measuring Emissions From Soil and Water*. Oxford: Blackwell Science Ltd. p 52–97.

Mayorga E, Aufdenkampe AK, Masiello CA, Krusche AV, Hedges JI, Quay PD, Richey JE, Brown TA. 2005. Young organic matter as a source of carbon dioxide outgassing from Amazonian rivers. *Nature* 436:538–41.

Palmer SM, Hope D, Billett MF, Dawson JJC, Bryant CL. 2001. Sources of organic and inorganic carbon in a headwater stream: evidence from carbon isotope studies. *Biogeochemistry* 52:321–38.

Pawellek F, Veizer J. 1994. Carbon cycle in the upper Danube and its tributaries: $\delta^{13}C_{DIC}$ constraints. *Israel Journal of Earth Sciences* 43:187–94.

Quay PD, Wilbur DO, Richey JE, Hedges JI, Devol AH. 1992. Carbon cycling in the Amazon River: implications from the ^{13}C compositions of particles and solutes. *Limnology and Oceanography* 37:857–71.

Raymond PA, Bauer JE. 2001a. Riverine export of aged terrestrial organic matter to the North Atlantic Ocean. *Nature* 409:497–500.

Raymond PA, Bauer JE. 2001b. Use of ^{14}C and ^{13}C natural abundances for evaluating riverine, estuarine, and coastal DOC and POC sources and cycling: a review and synthesis. *Organic Geochemistry* 32:469–85.

Richey JE, Melack JM, Aufdenkampe AK, Ballester VM, Hess LL. 2002. Outgassing from Amazonian rivers and wetlands as a large tropical source of atmospheric CO_2. *Nature* 416:617–20.

Schiff SL, Aravena R, Trumbore SE, Hinton MJ, Elgood R, Dillon PJ. 1997. Export of DOC from forested catchments on the Precambrian Shield of central Ontario: clues from ^{13}C and ^{14}C. *Biogeochemistry* 36:43–65.

Stuiver M, Polach HA. 1977. Discussion: reporting of ^{14}C data. *Radiocarbon* 19(3):355–63.

Taylor CD, Ljungdahl PO, Molongoski. 1981. Technique for simultaneous determination of (^{35}S) sulfide and (^{14}C) carbon dioxide in anaerobic aqueous samples. *Applied and Environmental Microbiology* 41:822–5.

Wetzel RG. 1983. *Limnology*. 2nd edition. New York: Saunders College Publishing. 860 p.

Xu S, Anderson R, Bryant C, Cook GT, Dougans A, Freeman S, Naysmith P, Schnabel C, Scott EM. 2004. Capabilities of the new SUERC 5MV AMS facility for ^{14}C dating. *Radiocarbon* 46(1):59–64.

Yang C, Telmer K, Veizer J. 1996. Chemical dynamics of the "St Lawrence" riverine system: δD_{H2O}, $\delta^{18}O_{H2O}$, $\delta^{13}C_{DIC}$, $\delta^{34}S_{sulfate}$, and dissolved $^{87}Sr/^{86}Sr$. *Geochimica et Cosmochimica Acta* 60:851–66.

Radiocarbon, In press, September 2006

Spatial variability of bomb-^{14}C in an upland peat bog

S.M.L. Hardie[1,2], M.H. Garnett[1], A.E. Fallick[3], A.P. Rowland[2] and N.J. Ostle[2]

[1] NERC Radiocarbon Laboratory, Rankine Avenue, Scottish Enterprise Technology Park, East Kilbride, G75 0QF, UK

[2] Centre for Ecology and Hydrology, Library Avenue, Bailrigg, Lancaster, LA1 4AP, UK

[3] Scottish Universities Environmental Research Centre, Rankine Avenue, Scottish Enterprise Technology Park, East Kilbride, G75 0QF, UK

Abstract

As part of a study investigating the carbon balance of a blanket bog we made an assessment of the spatial variation of radiocarbon concentrations in the surface layers of a small area of peatland in the north of England. The peat depth at which bomb-^{14}C content was highest varied considerably between cores sampled from across the site. At several sampling locations ^{14}C levels >100 %Modern were confined to the surface 8 cm, whereas bomb-^{14}C was evident at one site, located only metres away, to a depth of at least 12-16 cm. Using the layer where ^{14}C levels first exceeded 100 %Modern as a chronological reference layer, we estimated the carbon accumulation rate over the last 50 years for the surface peat at each site (range ~20 to ~125 g C m^2 yr^{-1}). Our results show that although carbon accumulation over the last 50 years was similar across the site, variation in the depth to which bomb-^{14}C was evident, implied considerable variation in vertical peat growth rate.

Introduction

Globally, soils contain ~1600 Gt of carbon, more than twice the amount currently resident in the atmosphere (Schimel 1995). Despite covering only ~3 % of the land surface, peatlands (subarctic and boreal) contain ~455 Gt of carbon and are one of the largest and most important stocks of soil carbon on Earth (Gorham 1991). There is considerable potential for global and local changes in climate, N deposition rates, CO_2 concentrations, invasive species and landuse to alter the net carbon balance of these ecosystems. This could result in the net transfer of large quantities of carbon to the atmosphere, thus contributing further to the current atmospheric CO_2 loading (IPCC 2001). Indeed, it has been suggested that in the UK organic soils including peatlands have already lost as much as 10 % C in the past 30 years (Bellamy et al. 2005). The study of peatland carbon stocks and fluxes is therefore necessary to determine whether they are sequestering or releasing carbon. One of the biggest challenges in terrestrial carbon cycle research, is to source and partition net carbon fluxes. Methods are many and varied and have been reviewed in detail by Hanson et al. (2000). Natural abundance isotopic (^{13}C and ^{14}C) techniques, in particular, offer a useful, non intrusive, means of tracing carbon flow through ecosystems.

Thermonuclear weapons testing during the 1950s and 60s resulted in a rapid injection of ^{14}C to the atmosphere, almost doubling the natural radiocarbon abundance. The incorporation of bomb-^{14}C *via* photosynthesis into the Earth's biosphere, has provided a valuable tool for studies of carbon cycling in the atmosphere and in terrestrial and marine environments (Levin & Hesshaimer 2000). Researchers have used ^{14}C to estimate soil organic matter turnover in forests (Harkness & Harrison 1989), grasslands (Masiello et al. 2004), tropical soils (Trumbore 1993), agricultural soils (Jenkinson et al. 1992) and in peatlands (Borren et al. 2004). More recently the carbon isotopic signature of ecosystem respiration has been used to investigate the CO_2 'sink-source' function of soils (Schuur & Trumbore 2006; Trumbore et al. 2006; Dioumaeva et al. 2002; Wang et al. 2000). However, one of the issues with using natural abundance or bomb-^{14}C tracers in soils is the spatial variability attributable to differences in both biotic (plant productivity, decomposition rates, inputs and community structure) and abiotic factors (hydrology, climate, chemical and physical parameters).

Few studies of peatland carbon dynamics have investigated the spatial variation in ^{14}C content and accumulation rates in surface organic matter layers (Charman et al. 1999), largely due to the prohibitive costs of radiocarbon analysis. In palaeoecological studies it is common for ^{14}C values of material obtained from a single peat core to be taken as representative of the entire peatland; Barber et al. (1998) provide one of the few investigations of spatial variability in peat palaeoecological records. However, peat growth (i.e. rate of depth increase) and carbon accumulation rates in peat are known to be greatly affected by a range of biotic and abiotic factors which themselves may vary over short distances and in time (Clymo et al. 1998).

Here we present the results of an investigation into spatial variation in the ^{14}C concentration of peat surface layers in an upland ombrotrophic bog. We also report estimated rates of recent carbon accumulation derived from these ^{14}C values.

Methods

Site Description

Moor House National Nature Reserve (UK National Grid ref. NY70 30) was chosen as the study site, being an area of blanket bog moorland considered to be representative of British upland terrain. It is an area of high carbon storage (Garnett et al. 2001) and has been intensively studied in the past (http://www.ecn.ac.uk/Publications.htm). Peat cores were taken from an experimental site within the Reserve, Hard Hill (NY735 335), an area characterised by gentle slopes with typical blanket bog/moorland vegetation. This particular site was chosen because plant species cover was homogeneous and because the site had not previously been used for experimental work (although the site has been and continues to be subject to grazing). Plant community composition at this site included *Sphagnum* spp., *Calluna vulgaris* and *Eriophorum vaginatum*. The average peat depth at this site was approximately 2 metres.

Peat Sampling

Samples were taken in August 2005 from a carbon dynamics experiment set up in September 2003 that included plant free plots (SOIL) and vegetated plots (VEG). These treatments were established to examine differences in soil carbon cycling attributable to the

presence of vegetation. Plots were circular with a diameter of 30 cm (area = 0.071 m^2) and each replicated plot was separated by between 2 to 5 metres. A total of 6 plots were investigated in the present study, 3 VEG and 3 SOIL, all of which were contained within an area of 57.5 m^2 (5.0 x 11.5 m). The vegetation in the SOIL plots was removed using secateurs, cutting as close to the peat surface as possible. Roots were left in place in order to minimise soil disturbance. After vegetation removal the SOIL plots were covered with a black cloth that allowed rain to percolate through but minimal light penetration. The plots were regularly tended and any new vegetation growth was removed. Peat samples were taken using a stainless steel corer (4.7 x 4.9 x 100 cm) designed to minimise compaction (Cuttle & Malcolm 1979). The corer was carefully removed from the peat profile and the top 16 cm of each core was cut into 4 cm increments. Samples were placed into labelled plastic bags and kept in a cool box until arrival at the NERC Radiocarbon Laboratory. Samples were stored at 4 °C until required for analysis.

Determination of total carbon and radiocarbon content

Each 4 cm increment of peat was placed in an evaporation dish, weighed and dried at 85 °C to a constant weight. Samples were homogenised by grinding to a powder using a pestle and mortar. Sub-samples were combusted with pure oxygen in a high-pressure combustion bomb. The resulting gas was cryogenically purified on a vacuum line until only CO_2 remained, and the total volume recovered was measured (allowing % carbon of the peat to be determined). An aliquot of CO_2 from each sample was prepared as a graphite target via an Fe/Zn reduction reaction (Slota et al. 1987) and analysed for ^{14}C by accelerator mass spectrometry (AMS) using the 5 MV tandem accelerator (Xu et al. 2004) at the AMS facility, Scottish Universities Environmental Research Centre (SUERC), East Kilbride, UK. A further CO_2 sub-sample was taken for $\delta^{13}C$ measurement by IRMS (dual inlet, VG Optima, Micromass, UK). All concentrations for ^{13}C are reported using the delta notation with $^{13}C/^{12}C$ variations relative to the international standard Vienna Pee Dee Belemnite (VPDB) (Craig 1957), as described by the following equation:

$$\delta^{13}C\ (‰) = \left[\frac{(^{13}C/^{12}C)_{Sample} - (^{13}C/^{12}C)_{VPDB}}{(^{13}C/^{12}C)_{VPDB}} \right] \times 1000$$

^{14}C data are expressed as %Modern with samples having been normalised to a $\delta^{13}C$ of -25 ‰ (Stuiver & Polach 1977).

Rates of peat accumulation were calculated for the different cores using the depth in the profiles where levels of ^{14}C first exceeded 100 %Modern as a chronological reference point. This fixed point represents the deepest layer that contains unequivocal evidence of bomb-^{14}C. Therefore we considered that peat formed when atmospheric ^{14}C levels first exceeded 100 %Modern (~AD 1955) was contained within this 4 cm layer. Annual peat growth rate (cm yr^{-1}) was calculated, by dividing the depth of the peat slice containing the 100 %Modern layer by 50 (number of years for peat growth between AD 1955 and the sampling date). Carbon accumulation rates (g m^{-2} yr^{-1}) were calculated using the same 100 %Modern reference layer, dividing the total carbon accumulated (g) above the reference layer by the 50 year accumulation period. Since a very coarse sampling resolution was used, only maximum and minimum values for both these rates were calculated. These were based on the range of depth and carbon mass values represented by the 4 cm slices of peat containing the reference layer.

Results

Our study was limited to the top 16 cm of the peat profile. A total of six cores were sampled and ^{14}C analyses were made on each of the 0-4, 4-8, 8-12 and 12-16 cm sections taken from each core (i.e. a total of 24 AMS ^{14}C analyses). Table 1 provides the carbon content (%), bulk density and carbon isotope results. Carbon content for all samples was around 45-50 %, typical for ombrotrophic blanket peat. Bulk density was also typical of upland peats (Clymo 1983) and ranged from ~0.04 g cm^{-3} to ~0.14 g cm^{-3}, with the lowest values occurring in surface samples. There were no significant differences in either carbon content (%) or bulk density between SOIL and VEG peat cores.

The profiles of radiocarbon content with depth (Figure 1) showed considerable variation between cores, despite their close proximity in the field. Radiocarbon concentrations ranged from ~95 to ~130 %Modern (Table 1), with evidence of both pre-bomb and post-bomb levels of ^{14}C in all 16 cm depth cores, except for one (post bomb ^{14}C was present throughout

the entire profile of core VEG 3, see Figure 1). In the other peat cores the lowest radiocarbon concentrations were found in the deepest (12-16 cm) layer.

The range in ^{14}C content of the peat was depth dependent. For example, the radiocarbon content in the surface layer varied only between ~110 and ~120 %Modern, whereas the 4-8 cm layer ranged from ~105 to ~130 %Modern. In the deepest layer, radiocarbon content in 5 of the 6 profiles ranged from ~95 to ~99 %Modern, although again, core VEG 3 was distinct, having a radiocarbon concentration of 122 %Modern at this depth. There were no obvious differences in the profile of radiocarbon content under the two different treatments (VEG and SOIL).

Table 2 presents the calculated values of peat growth rate (annual rate of depth increase in cm yr^{-1}) and carbon accumulation rate (g m^{-2} yr^{-1}). Peat growth rate ranged from ~0.08 to 0.24 cm yr^{-1} for most sites, although core VEG 3 had an average growth rate of more than 0.32 cm yr^{-1} above the reference layer. Due to the coarse 4 cm sampling resolution, the ranges of carbon accumulation rates for each core were large, and the overall range was ~20 to ~125 g C m^{-2} yr^{-1}. There were no significant differences between the two treatments for peat growth and carbon accumulation rate as ranges overlapped.

Discussion

We made an assessment of spatial variation of the ^{14}C content in the uppermost layers of peat profiles taken from an ombrotrophic blanket bog located in the north of England. The ^{14}C variation between cores can be explained, in part, by differences in peat growth rates over the period of the bomb-^{14}C spike. At the same time, rapid changes in atmospheric ^{14}C content over the 50 year period of the bomb spike would have contributed to variation in the ^{14}C content between depth increments. For example, least variation in ^{14}C content between cores was observed in the surface (0-4 cm) layer of peat. This peat represents the most recent carbon accumulation with vegetation assimilating carbon when atmospheric radiocarbon levels were decreasing relatively slowly, i.e. over the last ~10-20 years (Levin & Kromer 2004).

Pre-bomb-^{14}C concentrations were evident in the 12-16 cm layer of most of the cores despite the fact that these 4 cm slices of peat could have been accumulating over a considerable time (i.e. several decades). The small variation in ^{14}C content of the 12-16 cm layers is probably attributable to limited variations in the ^{14}C content of the atmosphere during the pre-bomb period. However, samples from the 4-8 cm and 8-12 cm layers, mainly cover the period when atmospheric bomb-^{14}C levels were highest and undergoing the most rapid changes. Thus, the variation in the 4-8 and 8-12 cm layers between cores is likely to be partly due to the layers being comprised of slightly differing contributions of pre-bomb and bomb-peak carbon as a result of different peat growth rates.

Peat growth rates are clearly an important factor contributing to the differences in the ^{14}C profiles. In particular, core VEG 3 was distinct from the other profiles in that bomb-^{14}C was evident even in the deepest (12-16 cm) layer. We can suggest several explanations for this observation such as a higher rate of peat growth (i.e. height increase) at this location. Alternatively, if plot VEG 3 had undergone less compaction compared to the other coring locations, then we would expect a deeper penetration of bomb carbon with depth. As this site had been subject to light grazing the possibility arises that varying degrees of compaction may have occurred and could be an explanation for the different pattern in ^{14}C content found in core VEG 3.

Peat bulk density values for VEG 3 were consistently lower at most depths than the other sampling locations (Table 1), suggesting that variation in density may be part of the explanation. This is illustrated in Figure 2 where the ^{14}C content of each profile is plotted against cumulative carbon (from the surface); this plot removes variations caused by differences in bulk density and shows that, in terms of carbon accumulation, the ^{14}C profile of VEG 3 is similar to the other profiles.

The presence of bomb radiocarbon in each of the six profiles is evidence that peat accumulation has at least been occurring in the surface layer of this blanket bog over the last 50 years (although due to decomposition of peat below these layers it is not possible to state whether the ecosystem still represents a net carbon sink). By using the layer containing the depth where ^{14}C concentrations first exceed 100 %Modern as a chronological reference point common to all plots, we estimated recent carbon accumulation at each of the sampling locations. The use of this reference layer has limitations; for example, our samples were not

subjected to chemical pretreatment because, from a carbon cycling point of view, we were interested in all carbon fractions that contribute to respiration. However, certain components in peat are known to be mobile e.g. fulvic acids (Shore et al. 1995) and evidence for transport of modern carbon to depth by *Eriophorum vaginatum* (Kilian et al. 2000) and root channels (Barber et al. 2000) has been demonstrated. Therefore our assertion that the 100 %Modern layer represents ~AD 1955 should be treated with some caution. Despite this, our main aim was to use the 100 %Modern reference layer to compare across all our coring points, and therefore, since vegetation cover was relatively homogeneous, it could be assumed that all cores would have been similarly affected by any migration of peat components or introduction of modern carbon to depth.

We found no clear differences in the profiles of radiocarbon content or carbon accumulation under the two treatments (VEG and SOIL). However, it is notable that the two highest carbon accumulation rates were found in the VEG treatment. Since fastest decay occurs in the first few years following senescence (Clymo 1998), it is possible that the higher carbon accumulation rates in the VEG plots reflects the continued input of new organic matter from plants over the last two years; due to vegetation removal, no new plant inputs entered the SOIL plots over this period.

Our assessment of the rates of peat growth and carbon accumulation was hindered by the very coarse resolution of our sampling intervals (i.e. 4 cm depth increments). Thus we only report maximum and minimum estimates for these rates, which in some cases cover a large range (Table 2). However, the approach adopted offered a useful means for the broad assessment of variations in peat growth and carbon accumulation across this small area of blanket bog. It should also be noted that our estimates for peat growth and carbon accumulation rate only cover peat formed over the last ~50 years and therefore, since much of the peat is still within the acrotelm and decaying relatively rapidly under aerobic conditions, our values are on average higher than estimates for long-term deep peat accumulation reported elsewhere (Borren et al. 2004; Turunen et al. 2002). Despite these limitations, our results show that there was greater variation in peat growth rates (depth increase) across the site than in rates of carbon accumulation over the last ~50 years.

Conclusions

The results of this study show that there is considerable variation in ^{14}C content of the 0-16 cm profile of this upland blanket bog (95-130 %Modern) with the largest range in variation occurring in the 4-12 cm part of the peat profile. This was attributed to both rapid changes in atmospheric radiocarbon content and differences in peat growth and C accumulation rates. It is therefore important that natural variability, both horizontal and vertical, in bomb-^{14}C concentrations is considered in any assessment of peatland carbon dynamics that uses bomb-^{14}C values as a tracer.

Acknowledgments

We thank staff at the NERC Radiocarbon Laboratory, SUERC and the SUERC AMS Facility. The authors acknowledge NERC for providing radiocarbon support through allocation 1133.0405 and SMLH acknowledges NERC for funding of a CEH studentship. SMLH thanks CEH Lancaster and Lancaster University colleagues, Angela Wakefield, Susan Ward and Simon Weldon. We are grateful to the reviewers whose comments led to improvements in the manuscript.

References

Barber, K., L. Dumayne-Peaty, P. Hughes, D. Mauquoy & R. Scaife, 1998. Replicability and variability of the recent macrofossil and proxy-climate record from raised bogs: field stratigraphy and macrofossil data from Bolton Fell Moss and Walton Moss, Cumbria, England. *Journal of Quaternary Science,* 13(6), 515-28.

Barber, K. E., D. Maddy, N. Rose, A. C. Stevenson, R. Stoneman & R. Thompson, 2000. Replicated proxy-climate signals over the last 2000 yr from two distant UK peat bogs: new evidence for regional palaeoclimate teleconnections. *Quaternary Science Reviews,* 19(6), 481-7.

Bellamy, P. H., P. J. Loveland, R. I. Bradley, R. M. Lark & G. J. D. Kirk, 2005. Carbon losses from all soils across England and Wales 1978-2003. *Nature,* 437(7056), 245-8.

Borren, W., W. Bleuten & E. D. Lapshina, 2004. Holocene peat and carbon accumulation rates in the southern taiga of Western Siberia. *Quaternary Research,* 61(1), 42-51.

Charman, D. J., R. Aravena, C. L. Bryant & D. D. Harkness, 1999. Carbon isotopes in peat, DOC, CO_2, and CH_4 in a Holocene peatland on Dartmoor, southwest England. *Geology,* 27(6), 539-42.

Clymo, R., (1983). Peat, in *Mires, Swamp, Bog, Fen and Moor*, ed. A. Gore Amsterdam: Elsevier Scientific Publishing Company, 159-222.

Clymo, R. S., J. Turunen & K. Tolonen, 1998. Carbon accumulation in peatland. *Oikos,* 81(2), 368-88.

Craig, H., 1957. Isotopic standards for carbon and oxygen and correction factors for mass-spectrometric analysis of carbon dioxide. *Geochimica et Cosmochimica Acta,* 12(1-2), 133-49.

Cuttle, S. P. & D. C. Malcolm, 1979. Corer for taking undisturbed peat samples. *Plant and Soil,* 51(2), 297-300.

Dioumaeva, I., S. Trumbore, E. A. G. Schuur, M. L. Goulden, M. Litvak & A. I. Hirsch, 2002. Decomposition of peat from upland boreal forest: Temperature dependence and sources of respired carbon. *Journal of Geophysical Research-Atmospheres,* 108(D3), art. no.-8222.

Garnett, M. H., P. Ineson, A. C. Stevenson & D. C. Howard, 2001. Terrestrial organic carbon storage in a British moorland. *Global Change Biology,* 7(4), 375-88.

Gorham, E., 1991. Northern peatlands - role in the carbon cycle and probable responses to climatic warming. *Ecological Applications,* 1(2), 182-95.

Hanson, P. J., N. T. Edwards, C. T. Garten & J. A. Andrews, 2000. Separating root and soil microbial contributions to soil respiration: A review of methods and observations. *Biogeochemistry,* 48(1), 115-46.

Harkness, D. D. & A. F. Harrison, 1989. The influence of afforestation on upland soils - the use of bomb C-14 enrichment as a quantitative tracer for changes in organic status. *Radiocarbon,* 31(3), 637-43.

IPCC, (2001). Climate Change 2001:The Scientific Basis, eds. J. T. Houghton & Y. Ding Cambridge: Cambridge University Press.

Jenkinson, D. S., D. D. Harkness, E. D. Vance, D. E. Adams & A. F. Harrison, 1992. Calculating net primary production and annual input of organic-matter to soil from the amount and radiocarbon content of soil organic-matter. *Soil Biology & Biochemistry,* 24(4), 295-308.

Kilian, M. R., B. van Geel & J. van der Plicht, 2000. C-14 AMS wiggle matching of raised bog deposits and models of peat accumulation. *Quaternary Science Reviews,* 19(10), 1011-33.

Levin, I. & V. Hesshaimer, 2000. Radiocarbon - A unique tracer of global carbon cycle dynamics. *Radiocarbon,* 42(1), 69-80.

Levin, I. & B. Kromer, 2004. The tropospheric $^{14}CO_2$ level in mid latitudes of the Northern Hemisphere (1959-2003). *Radiocarbon,* 46, 1261-72.

Masiello, C. A., O. A. Chadwick, J. Southon, M. S. Torn & J. W. Harden, 2004. Weathering controls on mechanisms of carbon storage in grassland soils. *Global Biogeochemical Cycles,* 18(4).

Schimel, D. S., 1995. Terrestrial ecosystems and the carbon-cycle. *Global Change Biology,* 1(1), 77-91.

Schuur, E. A. G. & S. E. Trumbore, 2006. Partitioning sources of soil respiration in boreal black spruce forest using radiocarbon. *Global Change Biology,* 12(2), 165-76.

Shore, J. S., D. D. Bartley & D. D. Harkness, 1995. Problems encountered with the C-14 dating of peat. *Quaternary Science Reviews,* 14(4), 373-83.

Slota, P. J., A. J. T. Jull, T. W. Linick & L. J. Toolin, 1987. Preparation of small samples for ^{14}C accelerator targets by catalytic reduction of CO. *Radiocarbon,* 29(2), 303-6.

Stuiver, M. & H. A. Polach, 1977. Discussion: reporting of ^{14}C data. *Radiocarbon,* 19(2), 355-63.

Trumbore, S., E. S. Da Costa, D. C. Nepstad, P. B. De Camargo, L. Martinelli, D. Ray, T. Restom & W. Silver, 2006. Dynamics of fine root carbon in Amazonian tropical ecosystems and the contribution of roots to soil respiration. *Global Change Biology,* 12(2), 217-29.

Trumbore, S. E., 1993. Comparison of carbon dynamics in tropical and temperate soils using radiocarbon measurements. *Global Biogeochemical Cycles,* 7(2), 275-90.

Turunen, J., E. Tomppo, K. Tolonen & A. Reinikainen, 2002. Estimating carbon accumulation rates of undrained mires in Finland - application to boreal and subarctic regions. *Holocene,* 12(1), 69-80.

Wang, Y., R. Amundson & X. F. Niu, 2000. Seasonal and altitudinal variation in decomposition of soil organic matter inferred from radiocarbon measurements of soil CO_2 flux. *Global Biogeochemical Cycles,* 14(1), 199-211.

Xu, S., R. Anderson, C. Bryant, G. T. Cook, A. Dougans, S. Freeman, P. Naysmith, C. Schnabel & E. M. Scott, 2004. Capabilities of the new SUERC 5 MV AMS facility for C-14 dating. *Radiocarbon,* 46(1), 59-64.

Table 1 Carbon isotope, bulk density and %carbon results. VEG = plots with intact vegetation. SOIL = plots cleared of vegetation

Sample identifier (Core - depth)	Publication Code (SUERC-)	Bulk density (g cm^{-3})	% carbon	$\delta^{13}C_{VPDB}$ (‰)	^{14}C %Modern (± 1 σ)
VEG 1 - 0-4 cm	9398	0.050	48.9	-29.8	113.48 ± 0.40
VEG 1 - 4-8 cm	9399	0.106	47.8	-28.5	115.05 ± 0.40
VEG 1 - 8-12 cm	9400	0.114	47.1	-25.9	99.50 ± 0.35
VEG 1 - 12-16 cm	9401	0.094	47.7	-26.6	98.42 ± 0.31
VEG 2 - 0-4 cm	8521	0.080	47.5	-28.8	116.50 ± 0.35
VEG 2 - 4-8 cm	8522	0.132	49.4	-27.8	130.42 ± 0.30
VEG 2 - 8-12 cm	8523	0.106	47.6	-27.0	105.75 ± 0.25
VEG 2 - 12-16 cm	8527	0.143	49.2	-26.4	95.62 ± 0.28
VEG 3 - 0-4 cm	9404	0.045	48.0	-30.2	111.74 ± 0.39
VEG 3 - 4-8 cm	9405	0.065	46.7	-28.6	114.98 ± 0.41
VEG 3 - 8-12 cm	9406	0.087	44.6	-26.9	125.80 ± 0.45
VEG 3 -12-16 cm	9407	0.076	48.1	-28.0	122.15 ± 0.43
SOIL 1 - 0-4 cm	9408	0.086	48.3	-29.2	113.98 ± 0.40
SOIL 1 - 4-8 cm	9409	0.138	49.6	-28.7	109.37 ± 0.33
SOIL 1 - 8-12 cm	9411	0.101	48.4	-27.6	98.61 ± 0.35
SOIL 1 - 12-16 cm	9414	0.107	49.7	-27.7	96.89 ± 0.34
SOIL 2 - 0-4 cm	9415	0.038	46.2	-28.0	118.40 ± 0.38
SOIL 2 - 4-8 cm	9416	0.079	48.3	-26.9	127.35 ± 0.45
SOIL 2 - 8-12 cm	9417	0.095	46.4	-28.3	114.05 ± 0.40
SOIL 2 - 12-16 cm	9418	0.101	47.8	-25.9	95.22 ± 0.33
SOIL 3 - 0-4 cm	8528	0.084	45.2	-28.3	119.68 ± 0.36
SOIL 3 - 4-8 cm	8529	0.109	46.6	-27.2	104.59 ± 0.31
SOIL 3 - 8-12 cm	8531	0.097	46.2	-27.4	96.41 ± 0.29
SOIL 3 - 12-16 cm	8532	0.096	48.9	-27.2	96.66 ± 0.25

Table 2 Calculated ranges of peat growth and carbon accumulation rate above the 100 %Modern layer (i.e. for the last ~50 years). VEG = plots with intact vegetation. SOIL = plots cleared of vegetation

Core identifier	**Depth containing the 100 %Modern reference layer (cm)**	**Peat growth rate (cm yr^{-1})**	**Carbon accumulation rate (g C m^{-2} yr^{-1})**
VEG 1	4-8	0.08-0.16	19.6-60.0
VEG 2	8-12	0.16-0.24	82.6-123.0
VEG 3	>16	>0.32	>72.6
SOIL 1	4-8	0.08-0.16	33.2-88.0
SOIL 2	8-12	0.16-0.24	44.6-79.8
SOIL 3	4-8	0.08-0.16	30.4-71.0

Figure Captions

Figure 1 Profiles of radiocarbon concentration in the surface peat at the Hard Hill study site. VEG = plots with intact vegetation. SOIL = plots cleared of vegetation

Figure 2 Profiles of cumulative carbon against depth at the Hard Hill study site. VEG = plots with intact vegetation. SOIL = plots cleared of vegetation

Figure 1

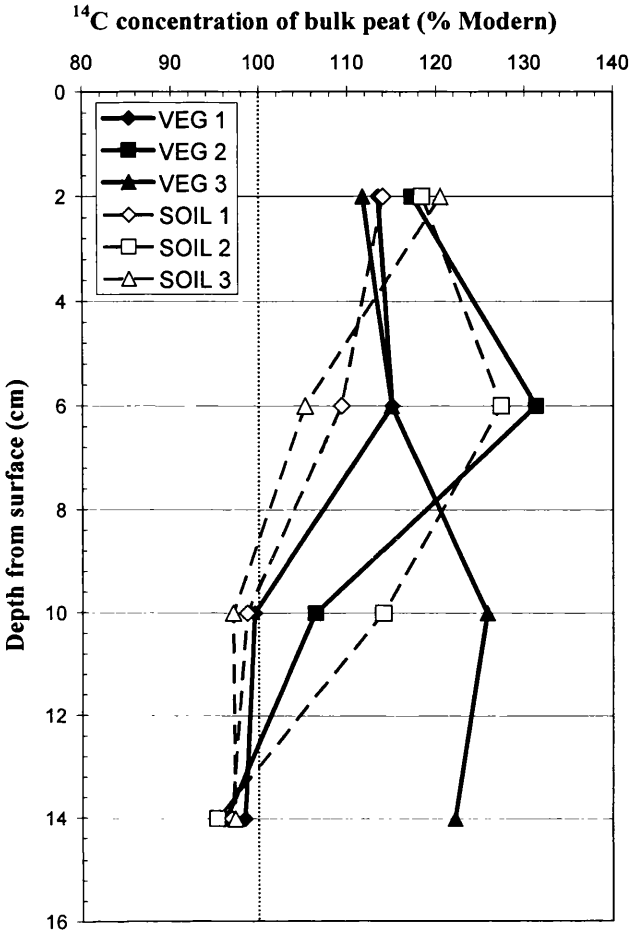
^{14}C concentration of bulk peat (% Modern)
80
90
100
110
120
130
140
0
2
4
6
8
10
12
14
16
Depth from surface (cm)
VEG 1
VEG 2
VEG 3
SOIL 1
SOIL 2
SOIL 3

Figure 2

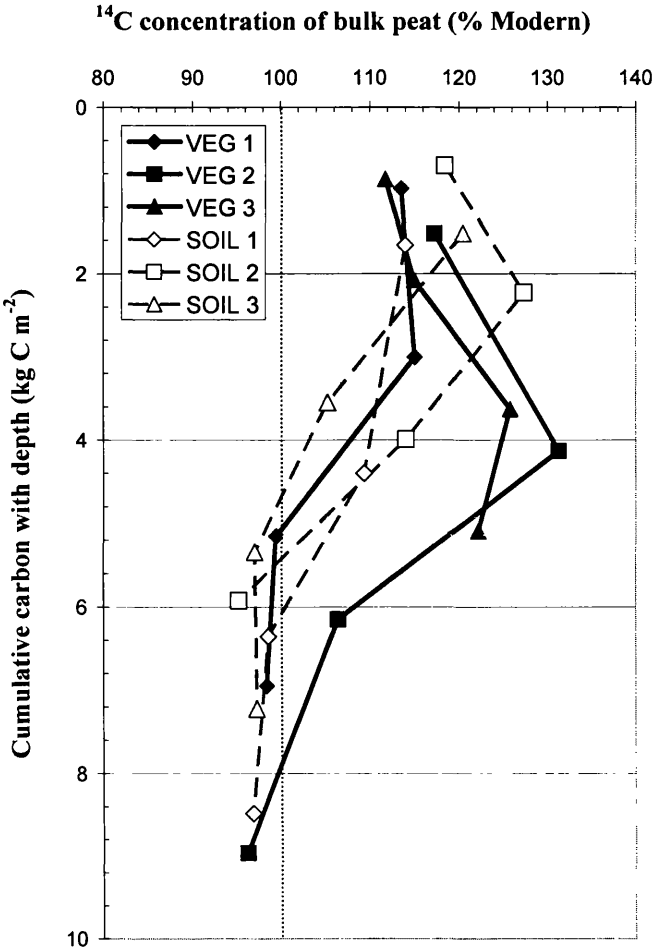

GLASGOW UNIVERSITY LIBRARY